Stem Cells International

Producing Stem Cell-Based Transplants for Future Therapeutic Purposes

Lead Guest Editor: Ivan Velasco
Guest Editors: Tilo Kunath, Veronica Ramos-Mejia, and Marco A. Velasco-Velazquez

Producing Stem Cell-Based Transplants for Future Therapeutic Purposes

Stem Cells International

Producing Stem Cell-Based Transplants for Future Therapeutic Purposes

Lead Guest Editor: Ivan Velasco
Guest Editors: Tilo Kunath and Veronica Ramos-Mejia

Copyright © 2017 Hindawi. All rights reserved.

This is a special issue published in "Stem Cells International." All articles are open access articles distributed under the Creative Commons Attribution License, which permits unrestricted use, distribution, and reproduction in any medium, provided the original work is properly cited.

Editorial Board

James Adjaye, Germany
Dominique Bonnet, UK
Daniel Bouvard, France
Silvia Brunelli, Italy
Bruce A. Bunnell, USA
Kevin D. Bunting, USA
Benedetta Bussolati, Italy
Yilin Cao, China
Pier Paolo Claudio, USA
Gerald A. Colvin, USA
Varda Deutsch, Israel
Leonard M. Eisenberg, USA
Tong-Chuan He, USA
Boon C. Heng, Hong Kong
Xiao J. Huang, China
Thomas Ichim, USA
Joseph Itskovitz-Eldor, Israel
Mark D. Kirk, USA
Valerie Kouskoff, UK
Andrzej Lange, Poland
Laura Lasagni, Italy
Renke Li, Canada
Tao-Sheng Li, Japan
Susan Liao, Singapore
Shinn-Zong Lin, Taiwan
Yupo Ma, USA
Giuseppe Mandraffino, Italy
Athanasios Mantalaris, UK
Eva Mezey, USA
Claudia Montero-Menei, France
Karim Nayernia, UK
Sue O'Shea, USA
Stefan Przyborski, UK
Bruno Pèault, USA
Peter J. Quesenberry, USA
Pranela Rameshwar, USA
Bernard A. J. Roelen, Netherlands
Peter Rubin, USA
Hannele T. Ruohola-Baker, USA
Benedetto Sacchetti, Italy
Ghasem Hosseini Salekdeh, Iran
Heinrich Sauer, Germany
Coralie Sengenes, France
Shimon Slavin, Israel
Shay Soker, USA
Giorgio Stassi, Italy
Ann Steele, USA
Alexander Storch, Germany
Corrado Tarella, Italy
Hung-Fat Tse, Hong Kong
Marc L. Turner, UK
Dominik Wolf, Austria
Qingzhong Xiao, UK
Zhaohui Ye, USA

Contents

Hindawi
Stem Cells International
Volume 2017, Article ID 9592302, 3 pages
https://doi.org/10.1155/2017/9592302

Editorial

Producing Stem Cell-Based Transplants for Future Therapeutic Purposes

Iván Velasco,[1,2] Tilo Kunath,[3] Verónica Ramos-Mejía,[4] and Marco A. Velasco-Velázquez[5,6]

[1]*Instituto de Fisiología Celular-Neurociencias, Universidad Nacional Autónoma de México, 04510 Ciudad de México, Mexico*
[2]*Laboratorio de Reprogramación Celular del IFC-UNAM, Instituto Nacional de Neurología y Neurocirugía "Manuel Velasco Suárez", 14269 Ciudad de México, Mexico*
[3]*University of Edinburgh, Edinburgh EH16 4UU, UK*
[4]*Centre for Genomics and Oncological Research (GENYO), 18016 Granada, Spain*
[5]*Departamento de Farmacología, Facultad de Medicina, Universidad Nacional Autónoma de México, 04510 Ciudad de México, Mexico*
[6]*Unidad Periférica de Investigación en Biomedicina Translacional, ISSSTE C.M.N. 20 de Noviembre, Facultad de Medicina, Universidad Nacional Autónoma de México, 03100 Ciudad de México, Mexico*

Correspondence should be addressed to Iván Velasco; ivelasco@ifc.unam.mx

Received 14 November 2017; Accepted 14 November 2017; Published 11 December 2017

Copyright © 2017 Iván Velasco et al. This is an open access article distributed under the Creative Commons Attribution License, which permits unrestricted use, distribution, and reproduction in any medium, provided the original work is properly cited.

Stem cells have been used in the clinic for very specific pathologies, but research has been conducted to develop new therapies for a wider range of human diseases. Currently, there is a great need for step-by-step investigations that consider all aspects related to cell therapy in disease-specific contexts. The objective of this special issue is to bring together timely reviews as well as original papers on different aspects related to the use of stem cells or their progeny in transplantation procedures that can positively modify degenerating or accidentally damaged tissues and organs. A considerable number of manuscripts were submitted, and after peer review, eight papers were published. The topics of these papers are diverse, including the generation of immortalized cells with inducible systems, the biological behavior of transit-amplifying cells, the expansion capacity of mesenchymal cells over hematopoietic cells, and the influence of growth factors in the maintenance of a differentiated phenotype. Regarding transplantation procedures, the non-immunogenic intrauterine grafting of muscle cells and cell replacement therapies for retinal degenerative conditions are reviewed. Evaluation scales to assess the effects of therapies including cells and biocompatible support agents after damage to the spinal cord are also discussed. Grafting of pluripotent stem cell products poses a risk for the development of teratomas; thus, several factors were studied to identify strategies to eliminate tumorigenic cells. We think that these papers cover several of the areas that are important for the proper handling of stem cells to become therapeutically relevant and suggest improvements on the evaluation after grafting of biological materials, which in the long term might lead to new therapeutic interventions.

The paper by K. An et al. presents a potentially relevant tool for the analysis of stem-cell based therapies in the field of pain therapy. First, they immortalized rat bone marrow mesenchymal stromal cells (BMSCs) by introducing the human telomerase reverse transcriptase (hTERT). Then, they introduced a tetracycline-inducible lentivirus delivery system to express the rat GAL gene into the immortalized rat BMSCs. The authors further characterized the phenotypic properties of these cells and confirmed their ability to produce GAL in a doxycycline-controlled manner. Finally, the authors advise that further studies are necessary to rule-out the possibility of transformation after long-term expansion of hTERT-BMSCs and to eliminate the leakiness of this inducible system.

The field of in utero transplantation (IUT) has, until recently, been focused on the hematopoietic system. The review by N. Chowdhury and A. Asakura comprehensively

describes the literature on in utero stem cell transplantation, covering hematopoietic applications as well as multiple other cell types and organ systems. The detection of genetic disorders in utero is now possible due to advances in cell-free fetal DNA diagnostics in maternal blood. This provides an opportunity for intervention and the application of in utero stem cell transplantation therapies. The authors explore the emerging area of IUTs for muscle disorders, in particular muscular dystrophies. Attempts to treat children with muscular dystrophy with muscle stem cell transplantations have failed partially due to the sheer number of cells needed to treat a patient. One solution outlined in detail by the authors is to treat the fetus in utero by transplantation of muscle stem cells.

Human adipose-derived stem cells (hASCs) are a source of differentiated cells that could be employed in regenerative medicine. A. E. Mortimer et al. examine the role of different stimuli in the *in vitro* maintenance of Schwann-like cells produced from hASCs. Authors found that basic fibroblast growth factor (FGF-2) was essential for the maintenance of the Schwann-like phenotype. In contrast, differentiation was partially preserved in absence of glial growth factor 2 (GGF-2), platelet-derived growth factor (PDGF), or forskolin. The lack of forskolin in the culture medium reduced mRNA and protein levels of brain-derived neurotrophic factor (BDNF), suggesting that an elevated cAMP concentration and the consequent CREB activation are required for BDNF expression. Finally, they identified that GGF-2 alone supports the expression of Krox20, a transcription factor indispensable for myelination. The evidence presented in this paper indicates that maintenance of the Schwann-like cells requires the synergistic activation of different signaling pathways.

The paper by O. Gordeeva and S. Khaydukov explores the differences in the differentiation potential between embryonic stem (ES) cells and embryonal carcinoma (EC) cells in a retinoic acid differentiation protocol. During differentiation, the ES cells lost pluripotency markers, such as *Oct4* and *Nanog*, more readily than EC cells and then gained some, but not all, differentiation markers with faster kinetics. In particular, *Activin A*, *BMP4*, *TGFβ1*, and *Nodal* were more highly expressed in differentiating ES cells when compared to EC cells. The addition of these TGFβ superfamily members as recombinant proteins to the differentiation conditions further enhanced loss of pluripotent markers and increase commitment to differentiated lineages. This also further reduced the tumorigenicity in teratoma assays. This work shows that activation of TGFβ signaling in ES cells can decrease their tumorigenicity and increase their safety profile for cell-based therapies.

The review by E. Rangel-Huerta and E. Maldonado describes the different biological properties of transit amplifying cells (TACs), early intermediates in tissue regeneration. With special focus on epidermal skin studies, they discuss important aspects of TACs such as gene expression profiles, division rates, asymmetric cell division, and environmental cues that may regulate their behavior. The authors propose that understanding TACs' biology is a key issue for their implementation in regenerative medicine.

Transplantation of stem cell-derived retinal pigmented epithelium (RPE) has already began in human clinical trials. However, there are no universally agreed upon animal models to assess the efficacy and safety of these therapies to treat these retinal degenerative conditions. The review by T.-C. Lin et al. systematically surveys all the animal models in use for this type of stem cell-based therapy. They cover mouse, rat, rabbit, dog, cat, pig, and nonhuman primate models of preclinical retinal degeneration. Since the therapies are using human cells, they discuss various methods to deal with immunosuppression in the animal models. A particularly novel one is the description of the crossing of immunodeficient nude rats (*Foxn1*-null) to the RCS rat that suffers from a progressive form of retinal degeneration. Although the larger animal models are useful for refining the surgical techniques, the rodent studies have the benefit of larger animal numbers and genetic manipulation to more closely model the human condition. A consensus on the most informative models of efficacy and safety for testing RPE cell products requires further exploration.

Spinal cord injury (SCI) is a common lesion in accidents, which cause disability in people; currently, there are no efficient therapeutic interventions in the clinic. The review paper by W. R. Kim et al. relates to the importance of having grading scales that are both easy to use and reproducible to assess the damage, as well as the recovery, on experimental animals subjected to SCI. The damage to this part of the central nervous system can have severe and long-lasting affections to the anatomy and the function of motor aspects that are greatly influenced by the extension and the anteroposterior position of the injury. After describing the most widely used animal models for SCI, a summary of the beneficial effects of stem cell grafting, either alone or combined with biomaterials, is presented. This section clearly shows that several types of cells, trophic factors, and polymers can all contribute to the correction of disturbed functions. The final part discusses the different scales to measure spinal cord function for rodents and nonhuman primates, highlighting its advantages and limitations.

Mesenchymal stromal cells are found in the bone marrow and contribute to the microenvironment that preserves hematopoietic stem cells *in vivo*. Mesenchymal stem/stromal cells (MSCs) have also been isolated from other sources such as adipose tissue, umbilical cord, and placenta. Hematopoietic stem and progenitor cells (HPCs) can be expanded or differentiated by coincubation with bone marrow MSCs *in vitro*. Perinatal sources of MSCs such as the umbilical cord and placenta are more accessible than the bone marrow aspirates. In the paper by G. R. Fajardo-Orduña et al., the ability of cord blood and placenta MSCs to expand HSCs was compared to the standard bone marrow MSCs. After immunophenotypic and functional characterization of the three types of MSCs, the expansion potential for primitive HSCs was tested without significant differences between the different MSCs. Also, the induction of myeloid colony forming units was very similar for bone marrow, umbilical cord, and placenta. These results suggest that MSCs from different origins might be used in the expansion of HSCs aimed to transplantation.

Acknowledgments

We thank all the authors who contributed to this special issue. Peer review for these papers would not be possible without the kind participation of expert referees, who provided criticism and constructive feedback.

Iván Velasco
Tilo Kunath
Verónica Ramos-Mejía
Marco A. Velasco-Velázquez

Hindawi
Stem Cells International
Volume 2017, Article ID 6061729, 9 pages
https://doi.org/10.1155/2017/6061729

Research Article

Human Mesenchymal Stem/Stromal Cells from Umbilical Cord Blood and Placenta Exhibit Similar Capacities to Promote Expansion of Hematopoietic Progenitor Cells In Vitro

Guadalupe R. Fajardo-Orduña,[1] Héctor Mayani,[2] Patricia Flores-Guzmán,[2] Eugenia Flores-Figueroa,[3] Erika Hernández-Estévez,[1] Marta Castro-Manrreza,[4] Patricia Piña-Sánchez,[5] Lourdes Arriaga-Pizano,[6] Alejandro Gómez-Delgado,[7] Alarcón-Santos Guadalupe,[7] Odette Balvanera-Ortíz,[8] and Juan J. Montesinos[1]

[1]*Mesenchymal Stem Cells Laboratory, Oncology Research Unit, Oncology Hospital, National Medical Center, IMSS, Mexico City, Mexico*
[2]*Hematopoietic Stem Cells Laboratory, Oncology Research Unit, Oncology Hospital, National Medical Center, IMSS, Mexico City, Mexico*
[3]*Niche and Hematopoietic Microenvironment Laboratory, Oncology Research Unit, Oncology Hospital, National Medical Center, IMSS, Mexico City, Mexico*
[4]*FES Zaragoza, National Autonomous University of Mexico, Mexico City, Mexico*
[5]*Molecular Oncology Laboratory, Oncology Research Unit, Oncology Hospital, National Medical Center, IMSS, Mexico City, Mexico*
[6]*Immunochemistry Research Unit, Specialties Hospital, National Medical Center "Siglo XXI", IMSS, Mexico City, Mexico*
[7]*Infectious and Parasitic Diseases, Medical Research Unit, Pediatric Hospital, National Medical Center, IMSS, Mexico City, Mexico*
[8]*Troncoso General Hospital, IMSS, Mexico City, Mexico*

Correspondence should be addressed to Juan J. Montesinos; montesinosster@gmail.com

Received 8 March 2017; Revised 28 June 2017; Accepted 10 September 2017; Published 9 November 2017

Academic Editor: Tilo Kunath

Copyright © 2017 Guadalupe R. Fajardo-Orduña et al. This is an open access article distributed under the Creative Commons Attribution License, which permits unrestricted use, distribution, and reproduction in any medium, provided the original work is properly cited.

Mesenchymal stem/stromal cells (MSCs) from bone marrow (BM) have been used in coculture systems as a feeder layer for promoting the expansion of hematopoietic progenitor cells (HPCs) for hematopoietic cell transplantation. Because BM has some drawbacks, umbilical cord blood (UCB) and placenta (PL) have been proposed as possible alternative sources of MSCs. However, MSCs from UCB and PL sources have not been compared to determine which of these cell populations has the best capacity of promoting hematopoietic expansion. In this study, MSCs from UCB and PL were cultured under the same conditions to compare their capacities to support the expansion of HPCs in vitro. MSCs were cocultured with $CD34^+CD38^-Lin^-$ HPCs in the presence or absence of early acting cytokines. HPC expansion was analyzed through quantification of colony-forming cells (CFCs), long-term culture-initiating cells (LTC-ICs), and $CD34^+CD38^-Lin^-$ cells. MSCs from UCB and PL have similar capacities to increase HPC expansion, and this capacity is similar to that presented by BM-MSCs. Here, we are the first to determine that MSCs from UCB and PL have similar capacities to promote HPC expansion; however, PL is a better alternative source because MSCs can be obtained from a higher proportion of samples.

1. Introduction

Mesenchymal stem/stromal cells (MSCs) are primitive cells that give rise to bone marrow (BM) stromal cells, which are responsible for supporting hematopoiesis [1, 2]. MSCs themselves also support hematopoiesis, as they form part of the niche of hematopoietic stem cells (HSCs) and provide the necessary conditions to regulate self-renewal, proliferation,

and differentiation [3–6]. Previous results from our group demonstrated the capacity to support hematopoiesis of BM-MSCs in vitro because these cells favor the expansion of hematopoietic progenitor cells (HPCs) from umbilical cord blood (UCB) [7]. HPCs obtained from UCB using ex vivo expansion systems have already been used clinically in patients undergoing hematopoietic cell transplant (HCT) [8]. Moreover, BM-MSCs have been applied in patients undergoing HCT, resulting in an increase in the graft size and faster hematopoietic recovery [6, 9–11]. Therefore, BM-MSCs are considered a serious candidate for improving HCT.

The main source of MSCs is BM; however, the use of BM has some drawbacks, as obtaining BM is an invasive procedure for the donor [12], and the number of MSCs and their capacities for proliferation and differentiation decrease with the age of the individual [13, 14]. Our research group has obtained MSCs from neonatal sources, such as umbilical cord blood (UCB) and the placenta (PL). It is noteworthy that the proportion of PL samples from which we were able to obtain MSCs was higher than that of UCB samples (100% and 11%, resp.) [15]. Moreover, for the two sources, we showed that their morphologies, immunophenotypes, and capacities for osteogenic and chondrogenic differentiation are similar to those of BM-MSCs [15] and that they have immunosuppression capacities [16, 17]. Other groups have shown that MSCs from UCB [18] and PL [19] have the capacity to support hematopoiesis in vitro but have not compared these cell types to determine which type has the best capacity for potential clinical application. In this study, we used the same coculture conditions to compare the capacities of MSCs from UCB and PL to support the in vitro expansion of HPCs from an enriched population of UCB $CD34^+CD38^-Lin^-$ cells. MSCs from BM were included as a control. Our results demonstrate that MSCs from UCB and PL have similar capacities to support HPC expansion, and this capacity is similar to that of BM-MSCs.

2. Materials and Methods

2.1. Collection and Culture of MSCs from BM, UCB, and PL. BM samples were obtained from hematologically healthy donors according to the Declaration of Helsinki and the Local Ethics Committee of Villacoapa Hospital, Mexican Institute for Social Security (IMSS). UCB and PL samples were collected according to the Declaration of Helsinki and the Local Ethics Committee of the Troncoso Hospital (IMSS, Mexico). MSCs from BM ($n = 6$), UCB ($n = 6$), and PL ($n = 6$) were obtained as we previously reported [16, 20]. Briefly, mononuclear cells (MNCs) were obtained from BM and UCB samples by density gradient centrifugation (specific gravity < 1.077 g/mL; GE Healthcare Bio-Sciences AB, Uppsala, Sweden). MNCs were seeded at a density of 0.2×10^6 cells/cm^2 in low glucose Dulbecco's modified Eagle's medium (Lg-DMEM; Gibco BRL, Rockville, MD, USA) supplemented with 10% fetal bovine serum (FBS; Gibco BRL), 4 mM l-glutamine, 100 U/mL of penicillin, 100 mg/mL of streptomycin, and 100 mg/mL of gentamicin (all reagents were obtained from Gibco BRL). Four days later, nonadherent cells were removed, and fresh medium was added. Upon reaching 80% confluence, adherent cells were detached with trypsin-EDTA (0.05% trypsin, 0.53 mM EDTA, Gibco BRL, Rockville, MD, USA) and were reseeded at a density of 2×10^3 cells/cm^2. MSCs from the second or third passage were used for the experiments. MNCs from PL were obtained by enzymatic digestion with trypsin-EDTA (Gibco BRL, Rockville, MD, USA) and were processed in the same way as those from BM and UCB.

2.2. Characterization of MSCs

2.2.1. Immunophenotype. Immunophenotypic analysis of MSCs was performed by flow cytometry [15, 20]. Monoclonal antibodies against CD14, CD31, CD34, CD45, CD105, HLA-DR (Caltag Laboratories, USA), CD73, and CD90 (Becton Dickinson/PharMingen, USA) conjugated with FITC (fluorescein isothiocyanate), PE (phycoerythrin), or APC (allophycocyanin) were used. Cells were acquired using a FACSCalibur (Becton Dickinson), and the data were analyzed with FlowJo 7.6.1 software (FlowJo LLC, Ashland, Oregon, USA).

2.2.2. Differentiation Capacity. Osteogenic and adipogenic differentiation was induced with Stem Cell Kits™ (STEMCELL Technologies Inc., Vancouver, BC, Canada), and chondrogenic differentiation was induced using chondrogenic differentiation medium (Cambrex Bio Science Walkersville Inc., Maryland, USA) supplemented with 10 ng/mL transforming growth factor beta (TGFβ; Cambrex). Differentiation capacities were determined using immunocytochemical stains, as we previously reported [16, 20].

2.3. $CD34^+CD38^-Lin^-$ Cell Enrichment. $CD34^+CD38^-Lin^-$ cells were enriched from UCB MNCs by negative selection using a StemStep™ kit (Stem Cell Technologies Inc., Vancouver, Canada) according to the manufacturer's instructions, as we previously reported [21].

2.4. Coculture of MSCs-HPCs. As we previously reported [20], MSC layers at 80% confluence were incubated with 0.3 μg/mL mitomycin C to inhibit cell growth. Ten thousand cells enriched in $CD34^+CD38^-Lin^-$ cells were seeded on MSC layers in 6-well plates (Corning Inc., Costar, New York, NY, USA) in Stem Line medium (Sigma-Aldrich, St. Louis, MO, USA) with or without the early acting cytokines thrombopoietin (TPO), Flt-3 ligand (FL), stem cell factor (SCF), and interleukin-6 (IL-6) at a concentration of 10 ng/mL (Peprotech, USA). In cultures in which MSC-HPC contact was inhibited, 0.4 μm Transwells (BD) were used. Cultures were taken on day 14, with a medium change on day 7.

2.5. Proliferation of Hematopoietic Cells. The total numbers of nucleated and viable cells from cultures and cocultures were determined with a hemocytometer using Turck's solution and trypan blue stain (Gibco), respectively [20].

2.6. Colony-Forming Cell (CFC) Assays. To determine the expansion of HPCs, the presence of CFCs was analyzed using methylcellulose assays (MethoCult™; STI), as we previously reported [20–22]. After 14 days of culture, CFCs were counted with the aid of an inverted microscope. CFCs were

classified as follows: erythroid colonies included committed erythroid progenitor cells or CFC-Es (erythrocyte colony-forming cells) and colonies derived from erythroid progenitor cells or BFC-Es (erythrocyte burst-forming cells), whereas myeloid colonies included CFC-granulocytes (CFC-Gs), CFC-monocytes (CFC-Ms), and CFC-GMs.

2.7. Quantification of $CD34^+CD38^-Lin^-$ Cells. To determine the expansion of primitive HPCs, the frequency of $CD34^+CD38^-Lin^-$ cells was analyzed by flow cytometry as we previously reported [20]. Briefly, a total of 1×10^5 MNCs were incubated with antibodies against CD34, CD38, CD14, CD16, CD19, CD41a, and CD71 conjugated with FITC, PE, or APC (Becton Dickinson). Cells were acquired using a FACSCalibur (Becton Dickinson), and the data were analyzed with FlowJo 7.6.1 software (FlowJo LLC).

2.8. Long-Term Culture-Initiating Cell (LTC-IC) Assays. Detection of primitive HPCs was performed using LTC-IC assays (pre-CFCs) based on the method described by Sutherland et al. and Miller et al. [23, 24], as we previously reported [7]. Briefly, after coculture with MSCs for 14 days, hematopoietic cells were cultured with the M210B4 stromal line as a feeder layer for 35 days. Subsequently, MNCs were harvested and seeded in cultures with methylcellulose for CFC quantification. A CFC/LTC-IC ratio of 8 : 1 [7, 24] was considered.

2.9. Statistical Analysis. The means ± SDs (standard deviations) or SEMs (standard errors of the mean) of the number of experiments conducted are reported. Student's *t*-test or one-way analysis of variance (ANOVA) and Kruskal-Wallis tests followed by Mann–Whitney *U* tests were employed using IBM SPSS Statistics 22 software. Statistical significance was considered when the p value was less than 0.05.

3. Results

3.1. Characterization of MSCs from BM, UCB, and PL. As we reported previously, MSCs from BM, UCB, and PL expressed marker characteristic of MSCs, such as CD105, CD73, and CD90. The expression of hematopoietic markers (CD14, CD34, and CD45) was not observed, and CD31 and HLA-DR were also absent (Supplementary Table 1 in Supplementary Material available online at https://doi.org/10.1155/2017/6061729). Osteogenic differentiation, as detected by von Kossa staining, and chondrogenic differentiation, as detected by Alcian blue, were similar in MSCs obtained from the three sources. Furthermore, although adipogenic differentiation was evident in MSCs from BM, no cells with adipocyte morphologies were observed in MSCs from UCB and PL. However, small positive spots were detected with oil red O staining in the cytoplasm of the MSCs (Supplementary Figure 1).

3.2. Enrichment of the $CD34^+CD38^-Lin^-$ Population. A mean of $136.2 \pm 63.3 \times 10^6$ MNCs was obtained from UCB samples ($n = 12$ with 58.6 ± 18.3 mL volume). After enrichment by negative selection, a mean of $0.7 \pm 0.54 \times 10^6$ MNCs ($0.54 \pm 0.33\%$ recovery) was obtained. Enrichment in $CD34^+CD38^-Lin^-$ cells corresponded to a mean of $46.9 \pm 24.7\%$.

3.3. MSCs from UCB and PL Increased Proliferation of the Population Enriched in $CD34^+CD38^-Lin^-$ Cells. We previously defined proliferation as the production of new cells from a cell population regardless of the type of cells produced [22]. Cultures of HPCs with or without MSCs from BM, UCB, and PL were analyzed (Figure 1(a): A, B, C, and D). The data are shown as the fold increases in cell number, which is defined as B/A (where the initial value is A, and the final value is B). On day 14, in cocultures with MSC-HPC contact and in the absence of cytokines, fold increases in the total number of hematopoietic cells of 3.8 ± 4, 8.4 ± 9.4, and 7.6 ± 9.2 were observed in the presence of MSCs from BM, UCB, and PL, respectively (Figure 1(b), A). Interestingly, when cytokines were added to the cocultures, significantly greater ($p < 0.05$) fold increases of 444 ± 230, 248 ± 171, and 221 ± 98 were observed in the presence of MSCs from BM, UCB, and PL, respectively, compared with cultures containing only cytokines (26 ± 18) or MSCs (Figure 1(b), A). No significant differences ($p < 0.05$) in proliferation in the presence of cytokines were detected between MSCs from the three sources.

We also analyzed the significance of MSC-HPC contact in the proliferation of hematopoietic cells by performing cocultures in the presence of a Transwell membrane to inhibit cell-cell contact. In cocultures of MSCs from the three sources on days 7 and 14, no increase in the total number of cells was observed (Figure 1(b), B). Interestingly, when cytokines were added to the cocultures, significantly greater ($p < 0.05$) fold increases of 184.25 ± 62.14, 120.29 ± 47.89, and 120.20 ± 29.55 were observed with MSCs from BM, UCB, and PL, respectively, compared with cultures only grown with cytokines (26.65 ± 18) or MSCs (Figure 1(b), B). The increase in the total number of cells was significantly greater ($p < 0.05$) in cocultures in which cell-cell contact was allowed compared with those without contact. Due to this finding, we performed HPC expansion experiments (CFC assays, quantification of $CD34^+CD38^-Lin^-$ cells, and LTC-IC assays) only in cocultures with MSC-HPC contact.

3.4. MSCs from UCB and PL Increase CFC Expansion. We previously defined cellular expansion as the production of cells that maintain specific characteristics of the population of cells from which they originated [22]. Thus, hematopoietic progenitor expansion has been evaluated by the increase in the number of myeloid (CFC-G, CFC-M, and CFC-GM) and erythroid colonies (CFC-E and BFC-E) (myeloid colonies, Figure 2(a): A and B; erythroid colonies, Figure 2(a): C and D). On day 14, in cocultures without cytokines and in the presence of MSCs from BM, UCB, and PL, slight fold increases of CFC-myeloids were observed in comparison with cultures without MSCs (Figure 2(b), A). Interestingly, when cytokines were added to the cocultures, the fold increase of CFC-myeloids was significantly greater ($p < 0.05$) compared with cultures containing only cytokines or only MSCs (Figure 2(b), A). In cocultures without cytokines and with MSCs from BM and UCB, the number of CFC-erythroids

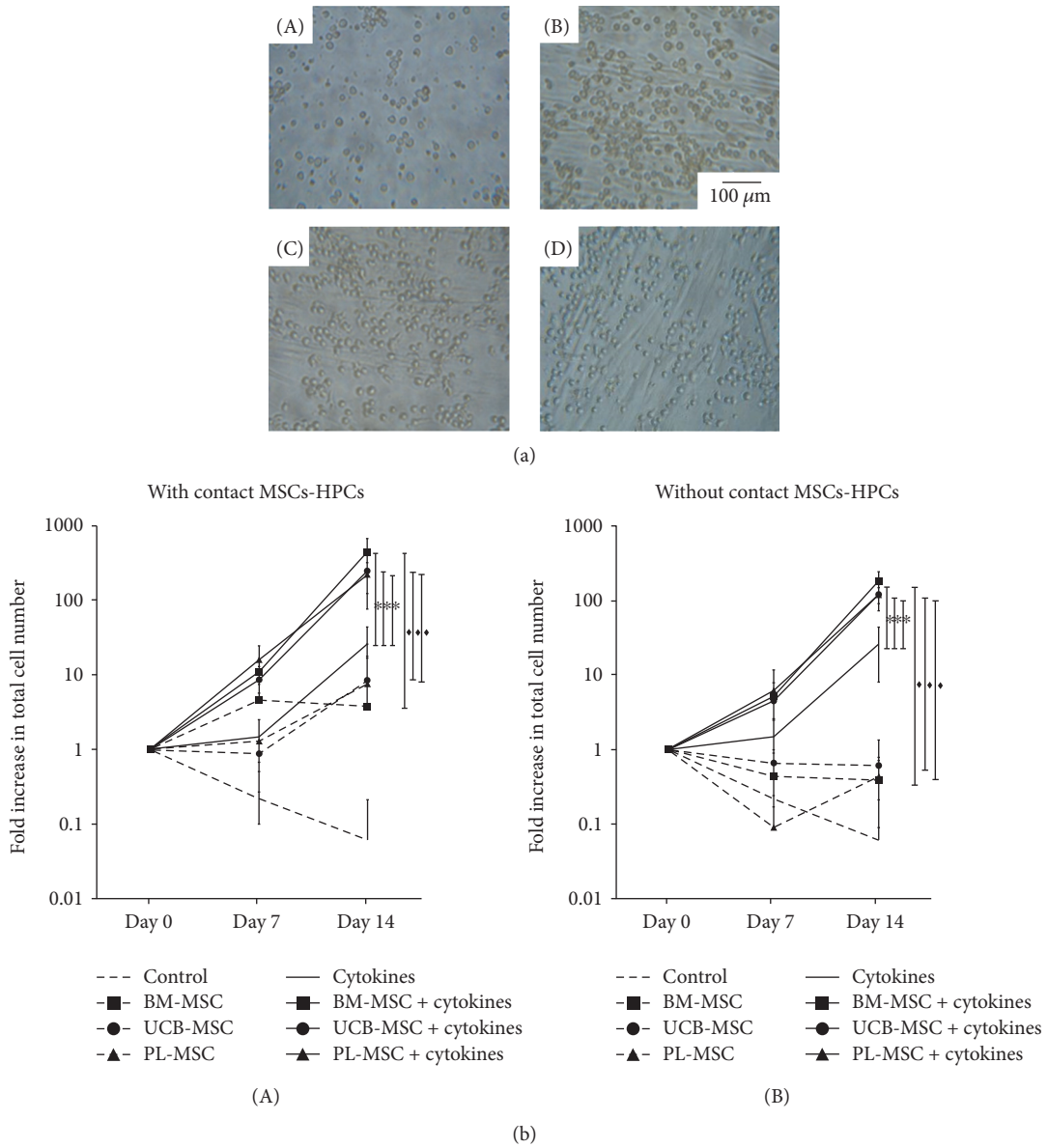

Figure 1: MSCs from UCB and PL increase proliferation of the population enriched in $CD34^+CD38^-Lin^-$ cells. (a) Representative culture of $CD34^+CD38^-Lin^-$ cells in the presence of cytokines (day 14): (A) without MSCs, (B) with BM-MSCs, (C) with UCB-MSCs, and (D) with PL-MSCs (magnification: 20x). (b) Kinetics of $CD34^+CD38^-Lin^-$ cell proliferation in the presence of MSCs and in the absence (dotted lines) or presence (solid lines) of cytokines. Cocultures were prepared in the presence (A) or absence (B) of cell-cell contact (MSCs-HPCs). Control without MSCs (no vignette); BM-MSCs (square); UCB-MSCs (circle); and PL-MSCs (triangle). Data are shown as the means ± SD for the fold increases in cell number (BM-MSCs: $n = 6$; UCB-MSCs: $n = 6$; and PL-MSCs $n = 6$). ∗ and ♦ indicate statistically significant differences, $p < 0.05$.

tended to increase in comparison with both cultures containing PL-MSCs and controls (Figure 2(b), B). When cytokines were added to cocultures, the fold increase of CFC-erythroids tended to increase compared with that of cultures containing only cytokines or only MSCs (Figure 2(b), B). No significant differences were detected in the number of myeloid and erythroid progenitors obtained in cocultures of MSCs from the three sources.

3.5. MSCs from UCB and PL Increase the Expansion of $CD34^+CD38^-Lin^-$ Cells. We then evaluated the increase in the percent and number of cells with the $CD34^+CD38^-Lin^-$ immunophenotype as another parameter to determine HPC expansion. For this experiment, cultures were generated with this population in the presence of cytokines and in the absence or presence of MSCs. On day 14 of culture, the percentages of $CD34^+CD38^-Lin^-$ cells increased by 18 ± 16%, 26 ± 30%, and 18 ± 20% in cultures with MSCs from BM, UCB, and PL, respectively, compared to those of cultures without MSCs (5.6 ± 3.3%), although these differences were not significant (Figure 3(a)). However, the fold increases in the number of $CD34^+CD38^-Lin^-$ cells of 146.88 ± 78.48,

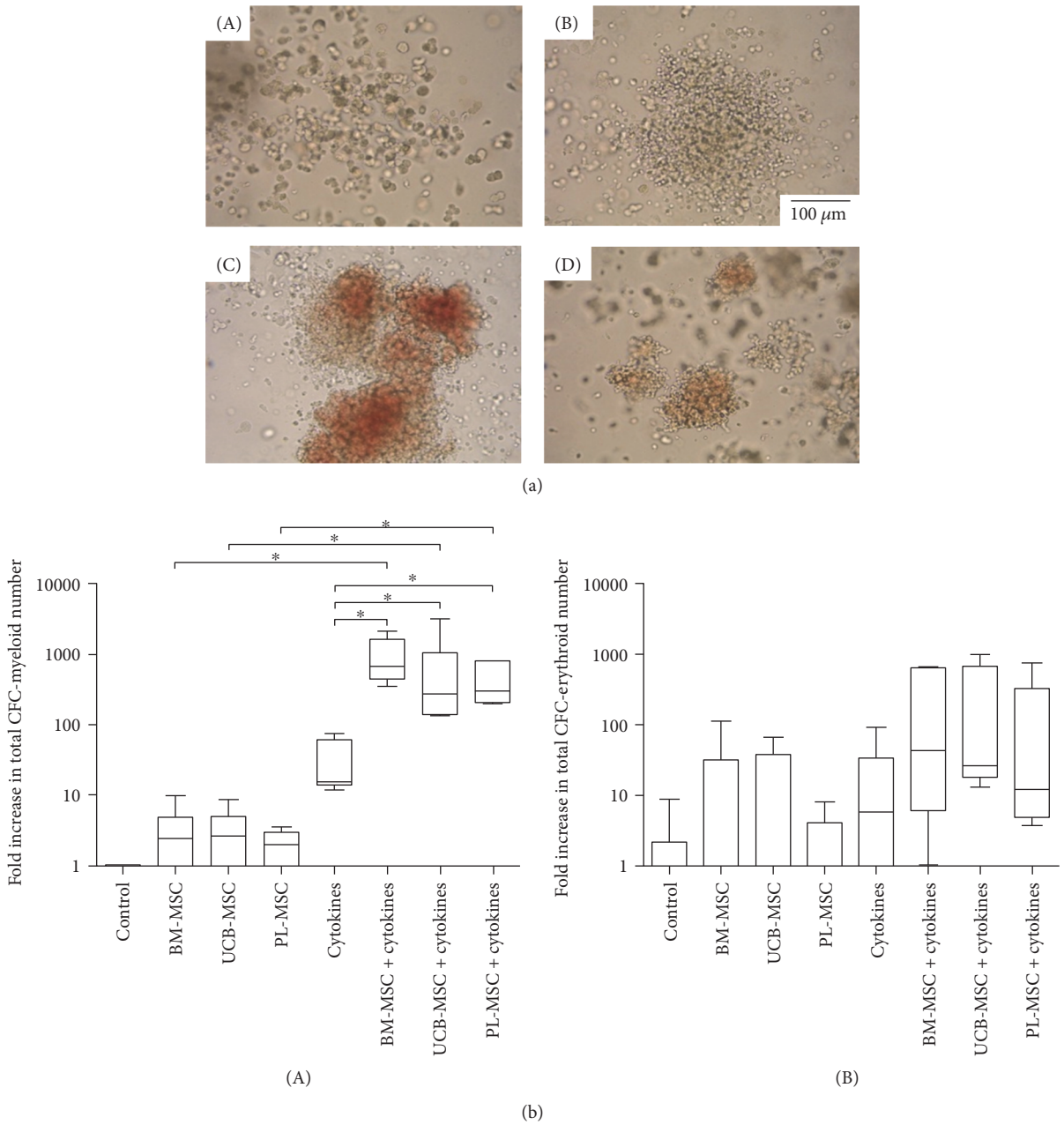

Figure 2: MSCs from UCB and PL increase CFC expansion of the population enriched in $CD34^+CD38^-Lin^-$ cells. (a) Photographs of colonies obtained on day 14 of culture: (A) CFC-monocytes, (B) CFC-granulocytes, (C) BFC-erythroids, and (D) CFC-erythroids (magnification: 20x). (b) Fold increases in the number of (A) CFC-myeloids and (B) BFC-erythroids and CFC-erythroids in cocultures in the absence and presence of cytokines. Data are shown as the fold increases in total CFC number (BM-MSCs: $n = 6$; UCB-MSCs: $n = 6$; and PL-MSCs $n = 6$). $*$ indicates a statistically significant difference, $p < 0.05$.

91.19 ± 35.73, and 31.59 ± 8 in cultures with MSCs from BM, UCB, and PL, respectively, were significantly greater ($p < 0.05$) than those of cultures without MSCs (3.50 ± 1.43; Figure 3(b)). No significant differences were detected between MSCs from the three sources. It should be noted that the percentage and number of cells with the $CD34^+CD38^-Lin^-$ immunophenotypes were not determined in the absence of cytokines due to the low cell numbers obtained in such cultures (data not shown).

3.6. MSCs from UCB and PL Favor LTC-IC Formation. We analyzed the effect of MSCs on the expansion of primitive HPCs with LTC-IC capacity in the presence of cytokines. The absolute values of LTC-IC obtained were 345 ± 10 on day 0 of culture; 41 ± 20 after 14 days of culture without MSCs; and 327 ± 203, 517 ± 365, and 113 ± 28 in the presence of BM-MSCs, UCB-MSCs, and PL-MSCs, respectively. On day 14 of culture, increases in the numbers of LTC-ICs were observed in some cultures containing MSCs

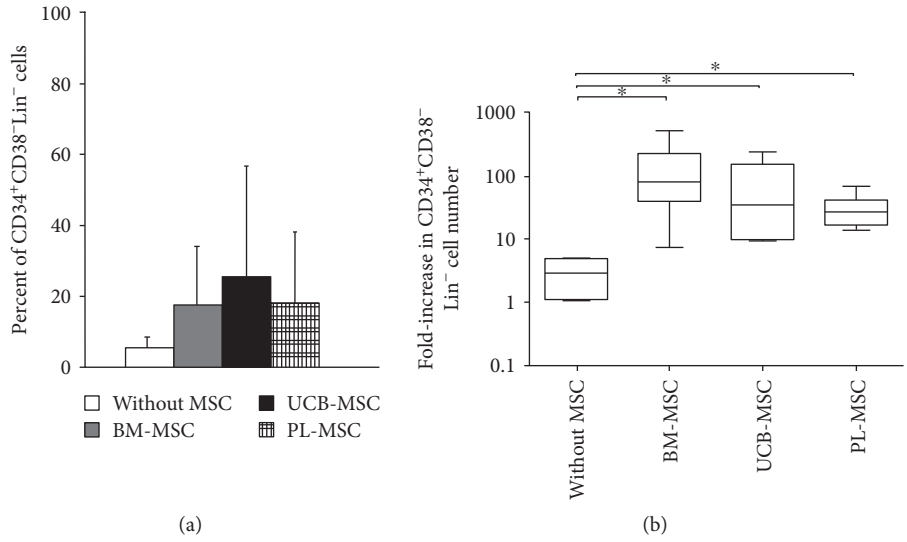

Figure 3: MSCs from UCB and PL increase expansion of the population enriched in $CD34^+CD38^-Lin^-$ cells. (a) Percent of $CD34^+CD38^-Lin^-$ cells in cocultures containing cytokines either without MSCs (white bar) or with BM-MSCs (gray bar), UCB-MSCs (black bar), and PL-MSCs (gridded bar). (b) Fold increases in the numbers of $CD34^+CD38^-Lin^-$ cells in cocultures containing cytokines in the presence of BM-MSCs, UCB-MSCs, and PL-MSCs. Cultures without MSCs and with cytokines were considered controls (without MSCs). Data are shown as the means ± SD for the percent and fold increases in cell number (BM-MSCs: $n = 6$; UCB-MSCs: $n = 6$; and PL-MSCs $n = 6$). ∗ indicates a statistically significant difference, $p < 0.05$.

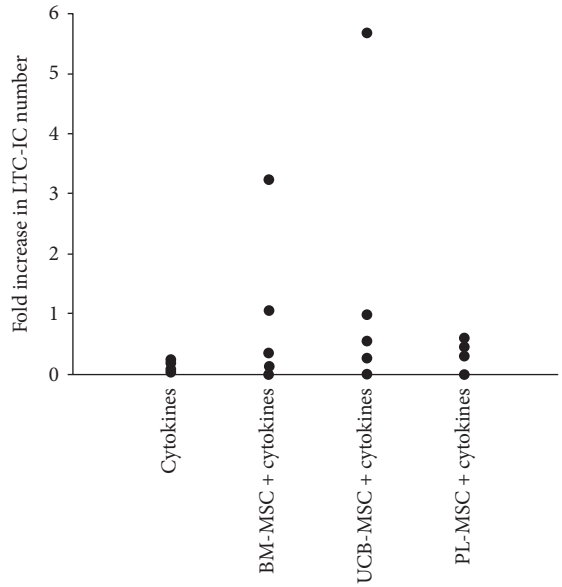

Figure 4: MSCs from UCB and PL favor the formation of LTC-ICs. Fold increases in the numbers of LTC-ICs on day 14 of culture. Cultures containing only cytokines were considered controls. Data are shown individually as independent experiments. Control, $n = 4$; BM-MSCs, $n = 5$; UCB-MSCs, $n = 5$; and PL-MSCs, $n = 4$.

from the three sources (Figure 4) compared to cultures with cytokines alone. The average fold increases of LTC-ICs with BM-MSCs, UCB-MSCs, and PL-MSCs were 0.95 ± 0.59, 1.5 ± 1.06, and 0.33 ± 0.08, respectively; compared with cultures containing only cytokines (0.12 ± 0.06), these values tended to be maintained (Figure 4).

4. Discussion

In this in vitro study, we used the same culture conditions to compare the capacities of UCB-MSCs and PL-MSCs to support hematopoiesis of a population enriched in $CD34^+CD38^-Lin^-$ cells obtained from UCB. MSCs from the two sources met the necessary immunophenotypic, osteogenic, and chondrogenic differentiation capacities according to criteria established by the ISCT [25]. However, as we have previously reported, MSCs from these two neonatal sources do not have the same adipogenic capacities as BM-MSCs, which may be related to the tendency of MSCs to form adipocytes in adulthood [16].

Few studies have been conducted to assess the in vitro hematological support capacities of UCB and PL. Such capacities have been evaluated separately in each source on populations enriched in $CD34^+$ cells [18, 19, 26, 27]. However, as we have shown previously, this hematopoietic population can be divided into $CD34^+CD38^+Lin^-$ and $CD34^+CD38^-Lin^-$ subpopulations, the latter of which has a greater potential for proliferation and expansion (because of their more primitive nature compared to the former subpopulation) [7, 21]. Therefore, we performed an in vitro analysis of the hematopoietic support capacity of MSCs from the two sources using the same culture conditions and a more primitive population enriched in $CD34^+CD38^-Lin^-$ cells. Importantly, we evaluated a primitive population that showed variable purity, which could influence the number of CFCs obtained. However, because the cell populations enriched in HPCs were cultured in the presence of MSCs from the two sources, which were established at the same time under the same culture conditions, such variations did not affect the potential of MSCs to provide hematopoietic support. Thus, we sought to determine which of the two

sources had the best in vitro hematopoietic support capacity in order to support their use in coculture systems as a feeder layer that promotes the expansion of HPCs, as these systems aim to obtain a sufficient number of cells to be used for hematopoietic cell transplantation.

MSCs from the two sources presented similar capacities to increase the number of hematopoietic cells under the same culture conditions. Similar results have been obtained in separate studies of UCB [18] and PL [19] in which populations enriched in $CD34^+$ cells were used, thus indicating that this capacity is maintained in populations with more primitive immunophenotypes. We observed a synergistic effect in which the capacity of MSCs from the two sources improved in the presence of early acting cytokines (SCF, TPO, FL, and IL-6), as we had previously reported for BM-MSCs [7] and as reported by other groups using other cytokines, such as fibroblast growth factor 1 and IL-3, in $CD34^+$ populations [18, 19, 27, 28]. In the presence of cytokines, MSCs from both sources showed similar capacities to increase proliferation. However, contrary to the effect that we observed on the population of $CD34^+CD38^-Lin^-$ cells, other groups have found that MSCs from UCB [18] and PL [19] have higher capacities than BM-MSCs to increase $CD34^+$ cell proliferation. This finding may be explained by the contributions of more mature populations in response to the effects of cytokines, which were added in higher concentrations than in our study.

Previous in vitro studies have analyzed the hematopoietic support capacities of MSCs from the two sources in cell contact cocultures [18, 19, 26, 27]; however, little is known about the significance of cell contact in that capacity. Our results demonstrate for the first time the significance of cell contact in terms of hematopoietic support of UCB-MSCs and PL-MSCs, as we observed that the increase in the number of hematopoietic cells was greater in cocultures with cell contact in both the absence and presence of cytokines. In this process, cell adhesion and extracellular matrix molecules may be involved, as N-cadherin, VCAM-I, ICAM-I, and ALCAM have been reported to be expressed by UCB-MSCs [13, 22]. Furthermore, ICAM-I, ALCAM, LFA-3, MCAM, fibronectin, and laminin have been shown to be expressed by PL-MSCs [15, 26, 29, 30]. All of these molecules are important in the adhesion, maintenance, and proliferation of primitive hematopoietic cells [6, 31–33]. Nonetheless, the observed increases in the number of hematopoietic cells in cocultures with UCB-MSCs and PL-MSCs without cell-cell contact may have been facilitated by the secretion of hematopoietic factors, such as SDF-1, IL-6, and granulocyte macrophage colony-stimulating factor (GM-CSF), by UCB-MSCs [26]. Moreover, UCB-MSCs express cytokine genes, such as TPO, SCF, FL, and macrophage colony-stimulating factor (M-CSF) [6, 18], whereas PL-MSCs produce SDF, IL-6, and SCF and express genes for FL [6, 19, 34]. Our laboratory is currently determining the expression profiles of extracellular matrix and hematopoietic molecules in our coculture system and their involvement in HPC expansion.

MSCs from the two sources showed the same in vitro capacity to increase the expansion of CFC-myeloids and CFC-erythroids, an effect that was synergistic in the presence of cytokines. Contrary to our results, it has been reported that PL-MSCs are more capable of increasing the expansion of CFCs when compared to BM-derived MSCs in the presence of cytokines [19]. This discrepancy might be explained by the different cytokines added to the cocultures and the differential response of the less primitive $CD34^+$ population of HPCs to those cytokines. Similarly, we observed a synergistic effect of MSCs in the presence of cytokines that increase the expansion of cells with the $CD34^+CD38^-Lin^-$ immunophenotype. There were no differences in the in vitro capacities of the MSCs from the two sources. Similar results have been reported for the effects of UCB-MSCs and BM-MSCs on the expansion of the primitive $CD34^+CD38^-$ population [26]; however, the same behavior was not observed with PL-MSCs compared with BM-MSCs on the $CD34^+$ population. This result may have been due to the greater potential showed by PL-MSCs to promote the expansion of the population [19, 34]. This finding supports the possible differential response in the hematopoietic expansion capacity of MSCs depending on the type of HPC population analyzed, which is important to consider in the clinical application of ex vivo HPC expansion.

We also observed that MSCs from the two sources tended to maintain the number of LTC-ICs in the presence of early acting cytokines compared with those cultured in the absence of MSCs, in which a progressive loss in the number of LTC-ICs was detected. Similar results have been reported for these capacities of UCB-MSCs and BM-MSCs, but those results were obtained in the absence of cytokines [26]. However, another study found that in the presence of cytokines, PL-MSCs have a greater capacity than BM-MSCs to increase the formation of LTC-ICs [19]. We demonstrated that MSCs from the two sources had similar in vitro capacities to maintain the number of LTC-ICs under the same culture conditions.

The in vitro hematopoietic support capacity of MSCs from neonatal sources makes them attractive therapeutic agents for HCT. However, evaluation of such capacity after expansion in clinical scale cultures (CSCs) is necessary for verification of their quality for cell therapy protocols. This step is important because, as we previously reported, BM-derived MSCs have decreased differentiation capacities toward the adipogenic, osteogenic, and chondrogenic lineages and a decreased ability to inhibit T cell proliferation even though they maintain their ability to support the proliferation and expansion of HPCs [20]. We are currently testing this hypothesis.

Notably, the immunosuppressive potential of MSCs derived from UCB and PL as alternative sources to BM is crucial due to the inflammatory and immunological role of BM-MSCs within the HSC niches. In a previous report, we compared MSCs from BM, UCB, and PL in terms of their immunosuppressive properties against lymphoid cell populations enriched in CD3+ T cells. Our results demonstrated that UCB-MSCs and, to a lesser extent, PL-MSCs have in vitro immunosuppressive potential [16].

Finally, although it is important to determine the in vitro hematopoietic support potential of UCB-MSCs and PL-MSCs, it is necessary to evaluate these capacities in animal models. These experiments are being planned for future studies.

5. Conclusion

This study demonstrates that UCB-MSCs and PL-MSCs have similar capacities to increase the proliferation and expansion of HPCs in terms of CFC production and the proportion of $CD34^{+}CD38^{-}Lin^{-}$ cells in vitro. Furthermore, MSCs from both sources showed a tendency toward the maintenance of LTC-ICs. Such capacities are similar to those presented by BM-MSCs. Additionally, for the two cell sources, cell-cell contact is important in the process of hematopoietic formation. To our knowledge, this is the first study to compare the hematopoietic support capacity of UCB-MSCs and PL-MSCs under identical culture conditions. Our results suggest that UCB-MSCs and PL-MSCs could be a good alternative to BM-MSCs in HCT. In addition, both sources could be used in ex vivo expansion protocols to increase the number of primitive HPCs from UCB for transplantation purposes. However, PL is a better alternative source than UCB because MSCs can be obtained from a higher proportion of PL samples than from UCB samples [15].

Additional Points

Highlights. Under the same culture conditions, MSCs from UCB and PL exhibit similar capacities to promote the expansion of UCB-HPCs in vitro. Feeder layers of MSCs from UCB and PL could be used for ex vivo expansion of UCB-HPCs for the purpose of hematopoietic cell transplantation. PL is a better alternative source of MSCs than UCB because MSCs can be obtained from a greater proportion of PL samples. MSCs from PL may be used as an alternative source to those from bone marrow for clinical applications, such as hematopoietic recovery in patients undergoing hematopoietic stem cell transplantation.

Conflicts of Interest

The authors declare that they have no competing financial interests.

Acknowledgments

Research in the authors' laboratory is supported by grants from the Mexican Institute of Social Security (IMSS, Grant nos. 062 and PRIO/10/010), México. The authors appreciate the contribution of the Thematic Network for Stem Cells and Regenerative Medicine in terms of financial support. Patricia Piña-Sánchez acknowledges the scholarship provided by the IMSS Foundation. The authors gratefully acknowledge the excellent technical assistance of Martina Flores Jiménez, Alarcón-Santos Guadalupe, and Juan de Dios Moreno Alvarez.

References

[1] M. E. Bernardo, A. M. Cometa, and F. Locatelli, "Mesenchymal stromal cells: a novel and effective strategy for facilitating engraftment and accelerating hematopoietic recovery after transplantation?," *Bone Marrow Transplantation*, vol. 47, pp. 323–329, 2012.

[2] A. Ehninger and A. Trumpp, "The bone marrow stem cell niche grows up: mesenchymal stem cells and macrophages move in," *The Journal of Experimental Medicine*, vol. 208, pp. 421–428, 2011.

[3] A. Nakamura-Ishizu and T. Suda, "Hematopoietic stem cell niche: an interplay among a repertoire of multiple functional niches," *Biochimica et Biophysica Acta (BBA) - General Subjects*, vol. 1830, pp. 2404–2409, 2013.

[4] S. J. Morrison and D. T. Scadden, "The bone marrow niche for haematopoietic stem cells," *Nature*, vol. 505, pp. 327–334, 2014.

[5] T. Nagasawa, Y. Omatsu, and T. Sugiyama, "Control of hematopoietic stem cells by the bone marrow stromal niche: the role of reticular cells," *Trends in Immunology*, vol. 32, pp. 315–320, 2011.

[6] G. R. Fajardo-Orduña, H. Mayani, and J. J. Montesinos, "Hematopoietic support capacity of mesenchymal stem cells: biology and clinical potential," *Archives of Medical Research*, vol. 46, pp. 589–596, 2015.

[7] P. Flores-Guzmán, E. Flores-Figueroa, J. J. Montesinos et al., "Individual and combined effects of mesenchymal stromal cells and recombinant stimulatory cytokines on the in vitro growth of primitive hematopoietic cells from human umbilical cord blood," *Cytotherapy*, vol. 11, pp. 886–896, 2009.

[8] M. de Lima, I. McNiece, S. N. Robinson et al., "Cord-blood engraftment with ex vivo mesenchymal-cell coculture," *The New England Journal of Medicine*, vol. 367, pp. 2305–2315, 2012.

[9] K. Le Blanc, H. Samuelsson, B. Gustafsson et al., "Transplantation of mesenchymal stem cells to enhance engraftment of hematopoietic stem cells," *Leukemia*, vol. 21, pp. 1733–1738, 2007.

[10] L. M. Ball, M. E. Bernardo, H. Roelofs et al., "Cotransplantation of ex vivo expanded mesenchymal stem cells accelerates lymphocyte recovery and may reduce the risk of graft failure in haploidentical hematopoietic stem-cell transplantation," *Blood*, vol. 110, pp. 2764–2767, 2007.

[11] H. Wang, H. Yan, Z. Wang, L. Zhu, J. Liu, and Z. Guo, "Cotransplantation of allogeneic mesenchymal and hematopoietic stem cells in children with aplastic anemia," *Pediatrics*, vol. 129, pp. e1612–e1615, 2012.

[12] K. H. Wu, C. Tsai, H. P. Wu, M. Sieber, C. T. Peng, and Y. H. Chao, "Human application of ex vivo expanded umbilical cord-derived mesenchymal stem cells: enhance hematopoiesis after cord blood transplantation," *Cell Transplantation*, vol. 22, pp. 2041–2051, 2013.

[13] Y. A. Romanov, V. A. Svintsitskaya, and V. N. Smirnov, "Searching for alternative sources of postnatal human mesenchymal stem cells: candidate MSC-like cells from umbilical cord," *Stem Cells*, vol. 21, pp. 105–110, 2003.

[14] I. Bellantuono, A. Aldahmash, and M. Kassem, "Aging of marrow stromal (skeletal) stem cells and their contribution to age-related bone loss," *Biochimica et Biophysica Acta (BBA) - Molecular Basis of Disease*, vol. 1792, pp. 364–370, 2009.

[15] J. J. Montesinos, E. Flores-Figueroa, S. Castillo-Medina et al., "Human mesenchymal stromal cells from adult and neonatal sources: comparative analysis of their morphology, immunophenotype, differentiation patterns and neural protein expression," *Cytotherapy*, vol. 11, pp. 163–176, 2009.

[16] M. E. Castro-Manrreza, H. Mayani, A. Monroy-García et al., "Human mesenchymal stromal cells from adult and neonatal sources: a comparative in vitro analysis of their immunosuppressive properties against T cells," *Stem Cells and Development*, vol. 23, pp. 1217–1232, 2014.

[17] M. E. Castro-Manrreza and J. J. Montesinos, "Immunoregulation by mesenchymal stem cells: biological aspects and clinical applications," *Journal of Immunology Research*, vol. 2015, Article ID 394917, 20 pages, 2015.

[18] Y. K. Jang, D. H. Jung, M. H. Jung et al., "Mesenchymal stem cells feeder layer from human umbilical cord blood for ex vivo expanded growth and proliferation of hematopoietic progenitor cells," *Annals of Hematology*, vol. 85, pp. 212–225, 2006.

[19] Y. Zhang, C. Li, X. Jiang et al., "Human placenta-derived mesenchymal progenitor cells support culture expansion of long-term culture-initiating cells from cord blood $CD34^+$ cells," *Experimental Hematology*, vol. 32, pp. 657–664, 2004.

[20] G. R. Fajardo-Orduña, H. Mayani, M. E. Castro-Manrreza et al., "Bone marrow mesenchymal stromal cells from clinical scale culture: in vitro evaluation of their differentiation, hematopoietic support, and immunosuppressive capacities," *Stem Cells and Development*, vol. 25, pp. 1299–1310, 2016.

[21] P. Flores-Guzmán, E. Flores-Figueroa, G. Martínez-Jaramillo, and H. Mayani, "*In vitro* characterization of two lineage-negative $CD34^+$ cell-enriched hematopoietic cell populations from human UC blood," *Cytotherapy*, vol. 7, pp. 334–344, 2005.

[22] P. Flores-Guzmán, M. Gutiérrez-Rodríguez, and H. Mayani, "*In vitro* proliferation, expansion, and differentiation of a $CD34^+$ cell-enriched hematopoietic cell population from human umbilical cord blood in response to recombinant cytokines," *Archives of Medical Research*, vol. 33, pp. 107–114, 2002.

[23] H. J. Sutherland and C. J. Eaves, "Long-term culture of human myeloid cells," in *Culture of Hematopoietic Cells*, R. I. Freshney, I. B. Pragnell and M. G. Freshney, Eds., pp. 139–162, Wiley-Liss, New York, NY, USA, 1994.

[24] C. L. Miller and C. J. Eaves, "Long-term culture-initiating cell assays for human and murine cells," *Methods in Molecular Medicine*, vol. 63, pp. 123–141, 2002.

[25] M. Dominici, K. Le Blanc, I. Mueller et al., "Minimal criteria for defining multipotent mesenchymal stromal cells. The International Society for Cellular Therapy position statement," *Cytotherapy*, vol. 8, pp. 315–317, 2006.

[26] W. Wagner, C. Roderburg, F. Wein et al., "Molecular and secretory profiles of human mesenchymal stromal cells and their abilities to maintain primitive hematopoietic progenitors," *Stem Cells*, vol. 25, pp. 2638–2647, 2007.

[27] N. Hayashi, K. Takahashi, Y. Abe, and I. Kashiwakura, "Placental/umbilical cord blood-derived mesenchymal stem cell-like stromal cells support hematopoietic recovery of X-irradiated human CD34+ cells," *Life Sciences*, vol. 84, pp. 598–605, 2009.

[28] T. Walenda, G. Bokermann, M. S. Ventura Ferreira et al., "Synergistic effects of growth factors and mesenchymal stromal cells for expansion of hematopoietic stem and progenitor cells," *Experimental Hematology*, vol. 39, pp. 617–628, 2011.

[29] G. A. Pilz, C. Ulrich, M. Ruh et al., "Human term placenta-derived mesenchymal stromal cells are less prone to osteogenic differentiation than bone marrow-derived mesenchymal stromal cells," *Stem Cells and Development*, vol. 20, pp. 635–646, 2011.

[30] B. Roson-Burgo, F. Sanchez-Guijo, C. Del Cañizo, and J. De Las Rivas, "Transcriptomic portrait of human mesenchymal stromal/stem cells isolated from bone marrow and placenta," *BMC Genomics*, vol. 15, p. 910, 2014.

[31] T. Li and Y. Wu, "Paracrine molecules of mesenchymal stem cells for hematopoietic stem cell niche," *Bone Marrow Research*, vol. 2011, Article ID 353878, 8 pages, 2011.

[32] A. Sittichokechaiwut, J. H. Edwards, A. M. Scutt, and G. C. Reilly, "Short bouts of mechanical loading are as effective as dexamethasone at inducing matrix production by human bone marrow mesenchymal stem cell," *European Cells and Materials*, vol. 20, pp. 45–57, 2010.

[33] E. Flores-Figueroa, J. J. Montesinos, and H. Mayani, "Células troncales mesenquimales: historia, biología y aplicación clínica," *Revista de Investigacion Clinica*, vol. 58, pp. 498–511, 2006.

[34] X. Luan, G. Li, G. Wang, F. Wang, and Y. Lin, "Human placenta-derived mesenchymal stem cells suppress T cell proliferation and support the culture expansion of cord blood $CD34^+$ cells: a comparison with human bone marrow-derived mesenchymal stem cells," *Tissue and Cell*, vol. 45, pp. 32–38, 2013.

Hindawi
Stem Cells International
Volume 2017, Article ID 5160261, 12 pages
https://doi.org/10.1155/2017/5160261

Review Article

Functional Test Scales for Evaluating Cell-Based Therapies in Animal Models of Spinal Cord Injury

Woon Ryoung Kim, Minjin Kang, Heejoo Park, Hyun-Joo Ham, Hyunji Lee, and Dongho Geum

Department of Biomedical Sciences, Korea University College of Medicine, Seoul 136-705, Republic of Korea

Correspondence should be addressed to Woon Ryoung Kim; wrkim@korea.ac.kr and Dongho Geum; geumd@korea.ac.kr

Received 5 April 2017; Revised 28 June 2017; Accepted 1 August 2017; Published 4 October 2017

Academic Editor: Ivan Velasco

Copyright © 2017 Woon Ryoung Kim et al. This is an open access article distributed under the Creative Commons Attribution License, which permits unrestricted use, distribution, and reproduction in any medium, provided the original work is properly cited.

Recently, spinal cord researchers have focused on multifaceted approaches for the treatment of spinal cord injury (SCI). However, as there is no cure for the deficits produced by SCI, various therapeutic strategies have been examined using animal models. Due to the lack of standardized functional assessment tools for use in such models, it is important to choose a suitable animal model and precise behavioral test when evaluating the efficacy of potential SCI treatments. In the present review, we discuss recent evidence regarding functional recovery in various animal models of SCI, summarize the representative models currently used, evaluate recent cell-based therapeutic approaches, and aim to identify the most precise and appropriate scales for functional assessment in such research.

1. Introduction

Spinal cord injury (SCI) is defined as damage to any spinal cord segment or nerve root. Such injuries often lead to permanent functional changes, such as paralysis or diminished muscle strength, movement, or sensation below the injured region. Thus, the pathological symptoms of SCI can vary depending on the site of injury and severity of the damage. As the annual incidence of SCI due to vehicular accidents or falls continues to increase worldwide [1, 2], the need to develop novel therapeutic strategies for SCI remains urgent in the field of spinal cord research. Due to the epidemiology and severity of SCI, various therapeutic techniques and biomaterials have been proposed [3, 4]. Most of these potential therapeutic agents are primarily tested in various animal models of SCI (e.g., rats, cats, dogs, and nonhuman primates) [5, 6]. In addition to the inherent advantages of animal models for evaluating the therapeutic effects of potential treatment strategies, such models are highly useful in assessing the degree of sensory/motor impairment following injury.

Among the four regions of the spinal cord (i.e., cervical, thoracic, lumbar, and sacral), the cervical and thoracic regions are most frequently studied in animal models of SCI. Injuries to the cervical spinal cord affect most of the body, including the arms and legs [1, 7], while those to the thoracic spinal cord and associated nerves result in trunk instability and abnormal movement of the lower extremities. In both rodents and primates, the anatomical locations of these regions allow for easy induction of SCI, analyses, and therapeutic manipulation involving cellular or biomaterial-based grafts. Based on the specific deficits observed, various behavioral tests have been developed to assess motor function and recovery following treatment in animal models of SCI [8–10].

The present review discusses recent evidence regarding functional testing in various animal models of SCI, the most suitable animal models for evaluating SCI, and current therapeutic challenges in SCI treatment. As several studies have highlighted the need for a well-developed, objective, and universal rating scale of functional impairments in rat models of SCI—such as the Basso, Beattie, and Bresnahan (BBB) scale [8–11]—we focused on suitable scales for assessing behavior, functional deficits, and therapeutic effects following a certain period of recovery or treatment.

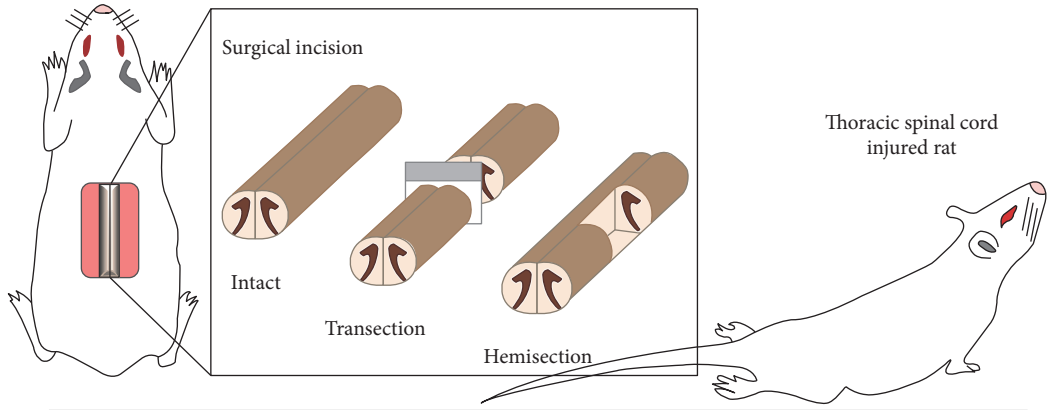

SCI animal model		Primary pathology	Motor neuron
Traumatic lesion	Contrusion	Spinal cord disruption	Axonal atrophy
	Compression		
	Traction		
	Laceration		
Sugical incision	Transection		
	Dorsal hemisection		
	Lateral hemisection		
Ischemic lesion	Vascular congestion		
	Aortic occlusion		
Drugs	Quisqualic acid	Cytotoxicity	Reduced
	Glutamate		
	N-Methylasparate		
	Kainic acid		
	Cuprizone	Partial demyelination	Axonal atrophy
	Lysolecithin		
Virus infection	TME Virus	Demyelination	
	MH Virus		

Figure 1: Development of animal models of spinal cord injury. (Upper illustration) methods for inducing spinal cord injury via surgical incision include transection and hemisection, both of which can be accomplished using a surgical knife (left). Hind limb paralysis following thoracic spinal cord injury in rats (right). (Lower table) animal models categorized by lesion method (left), the resulting primary pathology (middle), and final result of affected motor neurons (right).

2. Animal Models of Spinal Cord Injury

2.1. Traumatic Lesions. Since SCI frequently occurs following physical trauma (e.g., vehicular accident and falls), animal models of SCI are frequently developed using external stimuli such as dropped weight or clip compression (summarized in Figure 1). In animal models, traumatic SCIs are typically induced via contusion, compression, traction, or laceration. Among these, spinal contusion is most frequently utilized, as the size and severity of injury can be accurately adjusted and replicated using a well-defined weight-drop impactor [12]. The contusion method, which was first used to develop animal models of thoracic SCI, can cause severe damage and paralysis, which can be life-threatening when applied to the cervical region. Thus, hemicontusion is preferred for models of cervical SCI [13]. In clip compression models, the size and severity of damage can consistently be controlled by adjusting the time, forces, and angle of compression. Since compression can result in severe injury without transection, this method is advantageous for investigating variations in

recovery over time. Tractive SCI can be induced using a specialized spinal retractor, which allows the experimenter to control the length and duration of traction [14]. Such methods not only damage the structure of the spinal cord but also produce severe reductions in neuronal numbers. SCI via laceration results in severe irregular axonal damage, which mimics spinal injury due to a physical accident. Laceration is induced in animal models of SCI using the oscillating blade of a novel device known as the Vibraknife, which allows for precise control of the depth and size of the lesion without laminectomy [15].

2.2. Surgical Incision. Surgical incision is often utilized to develop models of SCI following penetrating injuries, such as knife wounds. Since the ends of the spine can be incised clearly and accurately using a blade, such models have been widely utilized in the investigation of neuronal regeneration and tissue engineering procedures (Figure 1, upper illustration). Since traumatic injuries do not completely sever the spinal cord, the transection method is more suitable for mimicking the symptoms of "complete" SCI, in which patients exhibit total and permanent loss of function below the injured site. Thus, the transection SCI model has been utilized to explore the function of each spinal segment and to evaluate functional and anatomical regeneration following complete transection [7, 16, 17]. In addition, partial transection via unilateral, dorsal, or ventral hemisection is highly useful in the investigation of therapeutic challenges such as transplantation. Both functional and anatomical alterations can be examined more precisely by comparing the ipsilateral and contralateral regions [18–20].

2.3. Ischemic Lesions. The spinal cord and spinal canal can be severely injured due to ischemia, which can be induced by either vascular congestion or aortic occlusion. Recent animal studies have frequently utilized photochemical ischemia to induce vascular congestion [21–23]. In this approach, following systemic injection of a dye such as Rose Bengal, spinal cord vessels are focally irradiated with an argon ion laser (560 nm). The ensuing photochemical reaction leads to vascular stasis without laminectomy, thereby resulting in tissue infarction and functional deficits. In contrast, aortic occlusion can easily be induced using an occlusion catheter [24], which allows for control of both the duration and severity of occlusion.

2.4. Drug-Induced Lesions. The primary advantage of a drug-induced model of SCI is that both tissue damage and functional deficits can be induced via local injection, without the need for laminectomy. Since both lesion area and functional outcomes are highly reproducible, the drug-induced SCI model has been widely utilized in this field of research. Local injection of excitotoxic drugs such as quisqualic acid, glutamate, N-methyl-D-aspartate, or kainic acid induces SCI via neuronal loss and subsequent inflammation [25]. Models of demyelination-induced SCI are also useful for evaluating the therapeutic effects of remyelination treatments. Drugs such as cuprizone and lysolecithin are frequently used to model multiple sclerosis [9], as these agents elicit partial demyelination when injected at specific sites in the spinal cord. In addition, animal models of demyelination-induced SCI can be developed using Theiler's murine encephalomyelitis virus and mouse hepatitis virus [26], allowing researchers to examine the efficacy of remyelination or Schwann cell grafting.

3. Therapeutic Approaches and Functional Recovery in Animal Models of Stem Cell Injury

As there is currently no cure for deficits induced via SCI, various therapeutic strategies have been investigated using animal models. Although the efficacy of cell grafting has been examined in several trials over the past several decades [4], the use of multifaceted therapeutic approaches involving novel biomaterials or cell-encapsulated scaffolds has recently increased (Figure 2(c)). Interestingly, accumulating evidence suggests that the integration of several cell types and combined biomaterials promotes regeneration and functional improvement following SCI [27–30]. A summary of the relevant findings is provided in Table 1.

3.1. Mesenchymal Stem Cells (MSCs)/Bone Marrow Stromal Cells (BMSCs). Since MSCs are easily obtained from autologous bone marrow or other sources, research regarding the use of MSC grafts or implantation of MSC-encapsulated scaffolds—which significantly reduce the immune response—has increased substantially in recent years. MSCs/BMSCs secrete significant levels of neurotrophic factors and can be transplanted via direct grafts, intravenously, or intrathecally. Recent evidence has suggested that these neurotrophic factors support CNS regeneration after injury. For example, direct infusion of neurotrophic factors such as brain-derived neurotrophic factor (BDNF) enhances neuronal survival and axonal growth in animal models of SCI [31, 32].

Fibrin, a representative fibrous protein that prevents blood clotting, is widely used to develop biopolymer scaffolds. Itosaka et al. [19] reported that, when BMSCs were supplied in conjunction with a fibrin matrix, model rats exhibited significant improvements in the recovery of neurological function, compared to when BMSCs were injected alone. In particular, remarkable improvements in motor function were observed (motor function test scale, BBB score = 15). The BBB scale is used to assess motor function, and BBB scores of 21 indicate complete recovery of motor function following injury. Additional studies have demonstrated that MSCs encapsulated with synthetic polymers (e.g., poly(lactic-co-glycolic acid) (PLGA) or N-(2-hydroxypropyl)-methacrylamide) attached to amino acid hydrogels (Arg-Gly-Asp (HPMA-RGD) hydrogels) can be implanted into the injured spinal cord cavity, resulting in increased tissue regeneration as well as significant improvements in functional recovery (BBB score = 10) [27, 33, 34]. During the first 1–6 months of recovery, structural scaffolds or hydrogels may promote tissue regeneration and functional improvement by assisting in the spread of healing factors within the damaged spinal cavity. Taken together, these results indicate that combined treatment involving cellular transplantation

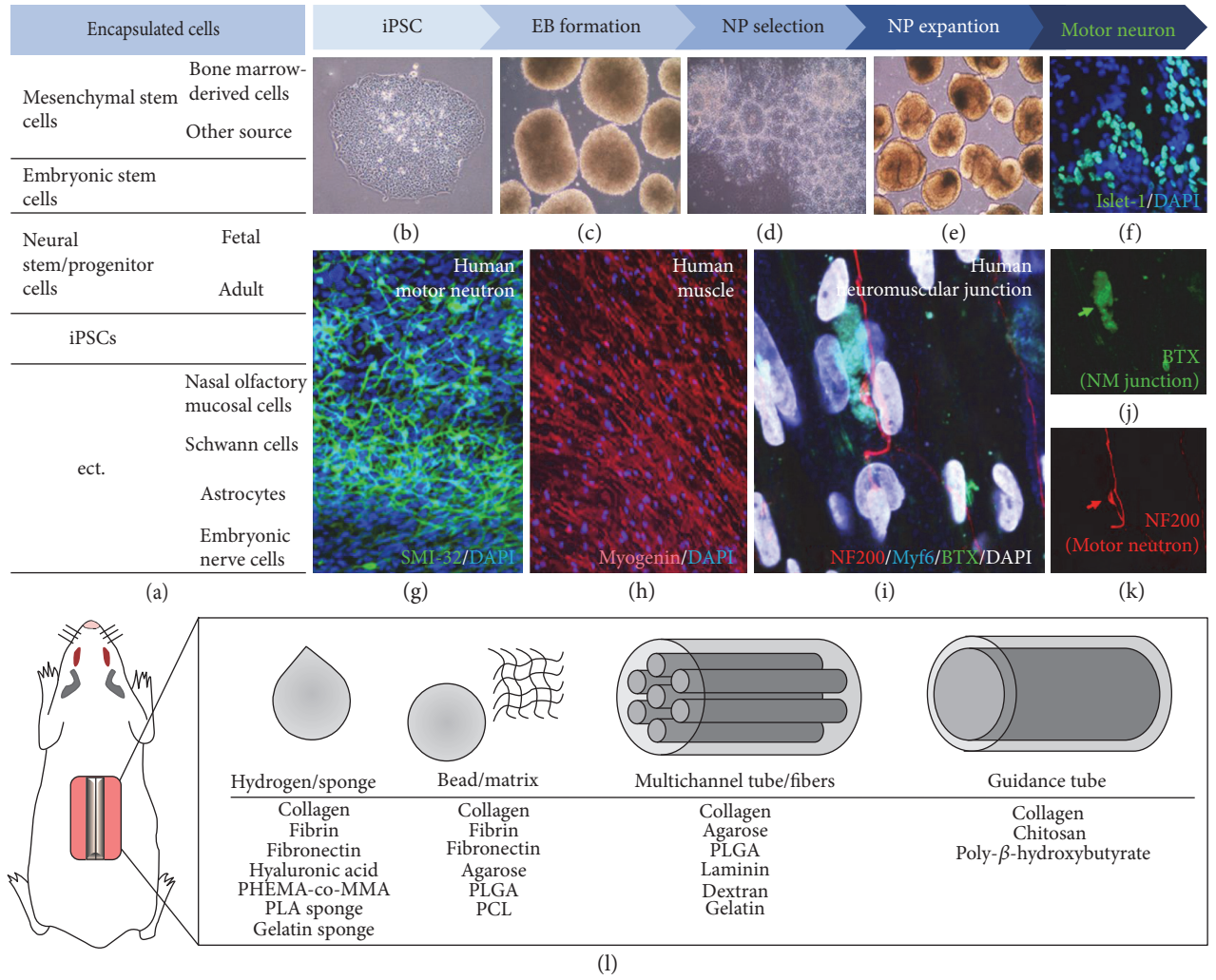

Figure 2: Multifaceted strategies for cell-based treatment. (a) List of cell types utilized in cell-based therapy for spinal cord injury. (b–k) Stem cell manipulation in various cell-based therapies. Induced pluripotent stem cells (iPSCs) can be generated from human somatic cells (b). Stem cells beginning to form embryoid body (c). Neural progenitors were isolated based on the neural rosette pattern and expanded in a culture dish (d, e). Following treatment with morphogenic agents, neural progenitors differentiate into many motor neurons (f, g). When motor neurons are cocultured with muscle fibers (h), the neuromuscular junction (i–k) can be detected on muscle fibers. (l) Scaffolds and biomaterials have developed for use in cell-based therapies. At a certain stage, stem cells can be transplanted alone or encapsulated in various scaffolds. PHEMA-co-MMA: poly(2-hydroxyethyl methacrylate-co-methyl methacrylate); PLA: polylactic acid; PLGA: poly(lactic-co-glycolic acid); PCL: polycaprolactone.

and biomaterial implants accelerates recovery from SCI, relative to the use of either treatment alone.

3.2. Neural Stem/Progenitor Cells (NSPCs). Various studies have investigated the role of NSPCs—which can differentiate into neurons, astrocytes, or oligodendrocytes—in neuronal regeneration following SCI [35]. Research has indicated that transplanted NSPCs may promote functional recovery via neuroregenerative processes (e.g., remyelination) [28]. In 2002, Teng and colleagues [29] reported that neural stem cells (NSCs) implanted into the injured thoracic spinal cord using a PLGA scaffold (NSC-PLGA) produced increases in the number of corticospinal tract fibers passing through the injury epicenter and significantly improved motor function 10 weeks after implantation (BBB score = 10). Theses finding are in accordance with those of Du and colleagues [30], who also demonstrated the therapeutic effects of NSC-PLGA on tissue regeneration and motor function (BBB score = 4). Surprisingly, therapeutic effects increased by over twofold (BBB score = 8.8) when levels of neurotrophin-3 and tyrosine receptor kinase C expression were increased in NSCs. Researchers have consistently demonstrated the therapeutic effects of NSC-PLGA in both rat and primate models of SCI. Pritchard and colleagues [31] reported similar levels of recovery following NSC-PLGA implantation in African green monkeys (Babu score = 15). The Babu scale is used to evaluate function in primates, and the maximum score of 67 points is considered an indicative of complete recovery. However, the use of NSCs does not guarantee improvements in

Table 1: Animal models of stem cell injury (SCI) and multifaceted approaches to cellular therapies.

Reference	SCI animal model			Materials for scaffold	Applied cells	Recovery time	Tests for motor function	Functional outcome	BBB score
ltosaka et al., 2009	Rat	T_8	Hemisection	Fibrin fibers	BMSC	4 weeks	BBB	Improved	15
Okuda, 2017		T_8	Transection	Cell sheet		4 weeks	BBB	Improved	5
Kang et al., 2011		T_{8-9}	Transection	PLGA scaffold	MSC	4 weeks	BBB	Improved	10
Yang, 2017		T_{9-10}	Transection	PLGA scaffold		4 weeks	BBB	Improved	7
Hejcl et al., 2010		T_{8-9}	Compression	HPMA-RGD hydrogel		35 weeks	BBB, plantar test	Improved	10
Hatami et al., 2009		T_{10}	Hemisection	Type1 collagen droplet	NSC	5 weeks	BBB	Improved	19
Nomura et al., 2008		T_8	Transection	Chitosan channels		12 weeks	BBB	No effect	9
Bozkurt et al., 2010		T_8	Compression			9 weeks	BBB	No effect	11
Teng et al., 2002		T_{9-10}	Hemisection	PLGA scaffold		10 weeks	BBB	Improved	10
Du et al., 2011		T_{9-10}	Transection			8 weeks	BBB, Incline test	Improved	9
Johnson et al., 2010		T_9	Hemisection	Fibrin scaffold		8 weeks	BBB, Grid walk	No effect	Data not shown
Ye, 2016		T_{10}	Contrusion	Self-assembling peptide nanofiber		5 weeks	BBB	Improved	12
Mothes, 2013		T_2	Compression	Hyaluronan-methy cellulose gel		9 weeks	BBB	No effect	12
Liu et al., 2015		T_{10}	Transection	PLGA scaffold	iNSC	10 weeks	BBB	Improved	14
				PLGA-PEG scaffold		10 weeks	BBB	Improved	17
Olson et al., 2009		T_{8-9}	Transection	PLGA scaffold		4 weeks	BBB	No effect	1
Wang et al., 2011		T_{10}	Transection	Gelform	SC	8 weeks	BBB, incline test	Improved	8
Hurtado et al., 2006		T_{9-10}	Transection	PDL tubular scaffold		6 weeks	BBB	No effect	7
Joosten et al., 2004		T_{7-9}	Transection	Collagen gel	Astrocyte	4 weeks	BBB, grid, catwalk	No effect	13
Rochkind et al., 2006		T_{7-8}	Transection	Dextran-gelatin tube	NOM, SCC	12 weeks	BBB	No effect	10
Zhang et al., 2016		T_9	Contrusion	Chitosan scaffold	hDPSC	4 weeks	BBB	Improved	12
Pritchard et al., 2010	Primate	T_9	Hemisection	PLGA scaffold	NSC	6 weeks	Babu scale	Improved	15
Nemati, 2013		C_5_L_1	Contrusion	Direct injection		49 weeks	Tarlov's scale	Improved	1.75

T: thoracic; C: cervical; L: lumbar; PLGA: poly(lactide-co-glycolide) acid; HPMA-RGD: N-(2-hydroxypropyl)-methacrylamide with attached amino acid sequences Arg-Gly-Asp; PDL: poly D-lactic acid; PLA: poly L-lactic acid; BMSC: bone marrow stromal cell; MSC: mesenchymal stem cells; NSC: neural stem cell; iNSC: induced neural stem cell; SC: Schwann cell; NOM: nasal olfactory mucosal cell; SCC: spinal cord cell; BBB: Basso, Beattie, and Bresnahan test scale.

therapeutic outcomes. Although application of a chitosan or fibrin channel filled with NSPCs to the SCI cavity promotes the survival of NSCs, such animals exhibit no improvements in functional deficits [32, 36, 37]. These results indicate that therapeutic effects are only maximized when NSCs are administered in conjunction with certain biomaterials and structural scaffolds, such as the NSC-PLGA scaffold.

3.3. Induced Pluripotent Stem Cells (iPSCs). Since iPSCs can be derived from somatic cells using reprogramming techniques, researchers have evaluated the utility of iPSCs in the treatment of various diseases. The use of iPSCs is advantageous in that these cells can be directed to develop into various cell types by modifying the differentiation protocol. NSCs can be induced via conversion from iPSCs (iPSC-NSCs) or via direct conversion of somatic cells (iNSCs). The embryoid body (EB) formation process can be used to generate NSCs from iPSCs (Figures 2(b) and 2(c)), following which therapeutic application of iPSC-NSCs is accomplished in a manner similar to that use for embryonic or adult NSCs, as described above (Figures 2(d) and 2(e)). Several reports

have indicated that direct transplantation of iPSC-NSCs elicits therapeutic effects in both rat and primate models of SCI [35, 38, 39]. Nutt and colleagues [39] demonstrated that intraspinal grafting of iPSC-NSCs results in successful integration and neuronal differentiation within the injured cervical segment. Similarly, the application of iPSC-derived EBs (Figure 2(c); i.e., the prior status to NSCs) on a 3D fibrin-based scaffold (or a mixture composed of iPSC-NSCs and hydrogel) promotes neuronal survival and differentiation. These results indicate that iPSC-NSCs combined with biomaterials promote repair following SCI [40, 41]. Further studies have revealed that iNSCs also promote neuronal and functional recovery in a rat model of SCI, with therapeutic effects similar to those of normal NSCs [42, 43]. Notably, the application of iNSCs within a PLGA or PLGA-polyethylene glycol (PEG) scaffold also promotes tissue regeneration and functional recovery. However, the therapeutic effect of the combined PLGA-PEG scaffold is greater than that of the PLGA scaffold [44]. Various studies have also reported that transplantation of Schwann cells [45–47], astrocytes [48], nasal olfactory mucosal cells [49], dental pulp stem cells [50], and spinal cord cells [49] in conjunction with biomaterials significantly enhances repair and recovery following SCI [51]. Taken together, these results suggest that the most appropriate combination of cells and biomaterials should be chosen to maximize tissue regeneration and promote recovery of functional deficits following SCI.

Despite recent advancements, a number of safety issues have been associated with the transplantation of nonterminally differentiated cells, as both stem cells and iPSCs may increase the risk of developing iatrogenic teratomas or tumors. To address this issue, researchers have investigated the effects of therapeutic strategies involving the transplantation of several somatic cell types, such as fully differentiated astrocytes, Schwann cells, olfactory ensheathing cells, and spinal cord cells. As the area and severity of damage following SCI due to contusion or transection vary, cell-based therapy is more frequently applied than gene therapy or treatment with drugs/neurotrophic factors. For cellular therapy to be clinically effective, the grafted cells should enable the regeneration of axons and functional replacement of lost cells. Although recent clinical trials have extensively investigated such strategies [52], the inherent risks of cell-based therapy highlight the need to develop drug- or biomaterial-based strategies (e.g., methylprednisolone) for promoting axonal regeneration.

4. Behavioral Test Scales to Evaluate Motor Function

As previously mentioned, various animal models have been utilized in SCI research. Animal models can be classified by species, lesion methods, and injured segments of the spinal cord. Moreover, there are multifaceted therapeutic approaches to SCI repair, such as stem cell transplantation, administration of neurotrophic factors, or cell-encapsulated scaffold grafting. Given the enormous diversity of factors, it is difficult to compare and interpret the results of these studies. Thus, the need for universal, objective indices of functional impairment/improvement remains critical. Moreover, when evaluating the effects of various therapeutic strategies, both anatomical and functional recovery must be considered. Indeed, anatomical recovery defined based on increases in neuronal number, axonal regeneration, and reduction of lesion size remains inadequate without concomitant functional recovery. Based on this consideration, we propose that assessments of functional recovery be based on a unified numerical scoring system for each model (rodent/primate) and lesion site (cervical/thoracic). The BBB and Babu scales represent such unified indices for rats and primates, respectively. Summaries of testing categories and scoring indices are provided in Tables 2 and 3, respectively.

4.1. Rodent Thoracic Spinal Cord Injury Model

4.1.1. BBB Scale. The BBB scale is a representative functional test administered following thoracic SCI injury [8, 11]. As mentioned previously, the development of thoracic SCI models is relatively easier and far less hazardous than the development of cervical models. In addition, rat models are more efficient than primate models due to the ease of operation and level of maintenance required in the animal facility. Thus, most SCI studies involve the use of rat models with injuries to the thoracic spinal cord. The BBB rating scale has long been utilized to assess thoracic SCI in rats. Thus, many studies report the BBB score only, which allows for sufficient estimation of the severity of functional impairments following injury. That is, the BBB scale functions as a unified index, allowing for straightforward evaluation and discussion of therapeutic effects. The BBB scale evaluates impairment based on locomotion in an open field, which allows researchers to observe voluntary movement, limb movement, trunk position, stepping patterns, and paw or tail position. Notably, scores can be evaluated at various stages of the recovery process: early, intermediate, and late phase after SCI. In the early phase, limb movements including hip, knee, ankle, and trunk positions are evaluated (BBB score = 0–8), followed by paw placement, stepping motion, and limb coordination in the intermediate phase (BBB score = 0–5). In the late phase, paw position—especially initial contact and lift-off behaviors—trunk instability, and tail position are used to evaluate the extent of functional recovery (BBB score = 0–8). A total maximum score of 21 points indicates normal function or complete recovery. However, as the BBB scale was developed to assess rat models of thoracic SCI (T_7–T_9) induced via contusion, there are several limitations regarding its general use in all rat models of SCI. In addition, rats may adapt to the open field environment, although this issue can be addressed by limiting testing time during rehabilitation.

4.1.2. Louisville Swimming Scale (LSS). The LSS was designed by Smith and colleagues [53] in 2006 for the assessment of hindlimb function during swimming. Although both the BBB and LSS can be used to assess impairments and recovery in rats with contusion-induced thoracic (T_9) SCI, the LSS possesses some unique advantages over the BBB scale. As previously mentioned, adaptation and rehabilitation can vary

Table 2: Rat models of spinal cord injury (SCI) and suitable test scales.

Target		Thoracic SCI							Cervical SCI				
Scale		BBB			LSS		CBS		Martinez				
Reference		Basso et al., 1995			Smith et al., 2006		Gale et al., 1985		Martinez et al., 2009				
	Recovery phase	Category I	Category II	Score	Swim ability	Score	Category	Score	Category	Forelimb	Score	Hindlimb	Score
	Early	Limb movement	Hip	0–2	HL movement	0–4	HL movement	0–45	Articular movement	Shoulder	0–2	Hip	0–2
			Knee	0–2	HL alternation	0–3	Toe spread	0–5		Elbow	0–2	Knee	0–2
			Ankle	0–2	FL dependency	0–4	Placing	0–5		Wrist	0–2	Ankle	0–2
		Trunk position	Side	0-1	Trunk instability	0–4	Withdrawal	0–15	Weight support	Stationary	0-1	Stationary	0-1
			Prop	0-1	Body angle	0–2	Righting	0–5		Active	0-1	Active	0-1
Category		Paw placement	Sweep	0–2			Inclined plane	0–15	Digit position		0–2		0–2
	Intermediate	Stepping	Dorsal	0-1			Hot plate	0–5	Paw placement at initial contact	Stepping	0–2	Stepping	0–2
			Plantar	0-1			Swim test	0–5					
		Limb coordination	Coordination	0-1									
		Paw position	Initial contact	0–3					Paw orientation during lift off	Stepping	0–2	Stepping	0–2
	Late		Lift off	0–3					Movement		0–2		0–2
		Trunk instability	Instability	0-1					Limb coordination		0–3		0–3
		Tail position	Up or down	0-1					Tail position		0-1		0-1
Maximum score (−normal)				21	(=normal)	17	(=severe)	100	Maximum score (=normal)		20		20

BBB: Basso, Beattie, and Bresnahan; LSS: Louisville swimming scale; CBS: combined behavioral score; HL: hindlimb; FL: Forelimb.

Table 3: Primate models of spinal cord injury (SCI) and suitable test scales.

Target	Thoracic SCI			Cervical SCI			
Scale	Babu			Nout			
Reference	Suresh Babu et al., 2000; bonnet monkey			Nout et al., 2012; rhesus monkeys			
Category 1	Category II	Category III	Score	Category I	Category II	Category III	Score
	Grasping		0–3			Forward movement	0–2
		Low speed	0–3			Number of limbs used	0–4
	Hopping	Medium speed	0–3		General	Number of perches reached	0–4
		High speed	0–3			Number of cups reached	0–5
Reflex	Righting		0–2			Truncal instability	0–2
	Extension withdrawal		0–2			Maximum score	17
	Pressure withdrawal		0–2			Extent of movements	0–8
	Pain withdrawal		0–2	Locomotion	Hind limb	Presence of weight support	0–3
	Placing		0–2			Presence of stepping	0–4
		Wide runway	0–5			Ability and extent of use of the hind limb	0–6
	Runways	Narrow beam 1	0–5			Maximum score	21
		Narrow beam II	0–5			Extent of movements	0–8
Runways		4 cm intervals	0–5		Forelimb	Presence of weight support	0–10
	Grid runways	5 cm intervals	0–5			Presence of stepping	0–4
		6 cm intervals	0–5			Ability and extent of use of the forelimb	0–6
		7 cm intervals	0–5			Maximum score	28
		Low speed	0–5			Posture of the animal during object manipulation	0–5
	Treadmill test	Medium speed				Use of the impaired hand for support and movement of the object	0–8
ect.		High speed		Hand function		Grasping method used	0–2
		Low degree	0–5			Extent of wrist and digit movements	0–6
	Inclined plane test	Medium degree				Maximum score	21
		High degree					
Maximum score (=normal)			67	Maximum score (=normal)			87

depending on the housing conditions of the injured animals. Thus, swimming tests can be used to provide a novel environment and avoid the influence of retraining effects, allowing for more accurate assessment of locomotor capability. The LSS evaluates function based on the following five categories: hindlimb movement (LSS score = 0–4), alternation (score = 0–3), forelimb dependency (score = 0–4), trunk instability, and body angle (score = 0–6). A total maximum score of 17 points indicates normal function. Together with the BBB scale, the LSS has become widely utilized for evaluating impairments and recovery following thoracic injury in rats. However, as immobility behaviors can be influenced by emotional states/depression [54], swimming ability should be measured within a limited period.

4.1.3. Combined Behavioral Score (CBS). Developed in 1984 by Gale and colleagues [55], the CBS is the oldest rating scale for the assessment of deficits following contusion-induced thoracic SCI (T_8). Function is assessed based on the following eight categories: hindlimb movement (CBS score = 0–45), toe spread and placement (score = 0–10), withdrawal reflexes following pain or pressure stimulation (score = 0–15), righting (score = 0–5), and maintenance of position on an inclined plane during increases in angle (beginning from 0°) (score = 0–15). In addition, somatosensory function is examined via the hot plate test, in which the latency to lick the forepaw and each hind paw when placed on a plate preheated to 50°C is scored (score = 0–5). Finally, in the swim test, the frequency of using the hindlimbs to swim and climb (score = 0–5) is recorded. A maximum CBS score of 100 points indicates severe paralysis in rats. However, as the range of CBS scores is quite wide, it is difficult to obtain consistent results from different observes. Due to these limitations, the ranges of scores in the more recently developed BBB and LSS are much narrower.

4.2. Rodent Cervical Spinal Cord Injury Model

4.2.1. Martinez's Scale. Since cervical SCI is potentially life-threatening, scales for functional assessment following thoracic SCI are more developed than those for cervical SCI. Currently, only one such scale has been designed for use in models of cervical SCI: Martinez's scale [56]. In 2009, Martinez and colleagues developed this rating scale to examine functional recovery following cervical (C_4) hemisection. The scale comprises eight categories that allow for separate evaluation of the forelimbs and hindlimbs: articular movement (score = 0–6), weight support pattern,

digit position, and paw placement during stepping (score = 0–10 for all). Limb coordination and tail position are also evaluated (score = 0–4). A total maximum score of 20 points indicates full functional recovery. As cervical SCI affects both the forelimbs and hindlimbs, Martinez's scale is suitable for the precise assessment of functional recovery in all affected limbs. The primary advantage of Martinez's scale is that this rating system can be used to assess functional recovery following either thoracic or cervical SCI in rats. As previously mentioned, although various rating scales have developed, each possesses a distinct array of limitations. To address such limitations, other behavioral tests such as the catwalk test [57], gait analysis [58], grid walk test [59], and incline test [60] have been used in conjunction with rating scales to enable more precise evaluation of therapeutic effects. As cervical SCI can affect both forelimb and hindlimb function, testing procedures and categories should be divided according to the limb in animal models of cervical SCI. As scores on this scale can also be influenced by retraining effects, animal movement should be video-recorded during short sessions, followed by separate assessments of forelimb and hindlimb function.

4.3. Primate Thoracic Spinal Cord Injury Model

4.3.1. Babu's Scale. The use of primate models in SCI research has recently increased. In 2002, Suresh Babu and colleagues [61] developed a rating scale designed to assess function in a primate model of thoracic SCI. Based on the CBS for rats, the modified scale was applied in Bonnet monkeys (*Macaca radiata*) following thoracic (T_{12}–L_1) hemisection. Babu's scale evaluates functional impairments based on the following two categories: reflex responses and locomotor behavior. Grasping, hopping, righting, and withdrawal reflexes due to extension, pressure, pain, and placement are evaluated (score = 0–22). In addition, gross locomotion on wide runways, narrow beams (score = 0–15), and grid runways (score = 0–20) is examined at various intervals. Finally, primates are subjected to a treadmill test at different speeds (score = 0–5) and levels of incline (score = 0–5). A total maximum score of 67 points on Babu's is considered an indicative of complete recovery. Although quite similar to the CBS for rats, Babu's scale is more detailed and includes additional criteria specific to primates.

4.4. Primate Cervical Spinal Cord Injury Model

4.4.1. Nout's Scale. Nout and colleagues [62] designed a novel rating scale for the assessment of motor function in a rhesus monkey model of cervical (C_7) SCI. Nout's scale is grossly divided into two categories: locomotion and hand function. Locomotion scores are based on general movement and trunk instability (score = 0–17), hindlimb movement, presence of weight support, presence of stepping, and extent of hindlimb (score = 0–21) and forelimb (score = 0–28) function. Due to the potential impairments associated with cervical SCI, hand function is also evaluated during object manipulation (score = 0–13), grasping, and digit movement (score = 0–8). A maximum score of 87 points on Nout's scale is considered an indicative of complete functional recovery.

Taken together, these findings indicate that accurate and unified criteria should be used to evaluate motor/sensory function in both rodent and primate models of SCI, in order to provide more objective assessments of therapeutic strategies. Such rating scales should be suitable for functional evaluation of the animal based on species and lesion type. Consistent use of such scales will lead more well-validated and effective SCI treatments.

In addition to rat/primate models, several studies have also evaluated therapeutic strategies in canine models of SCI [63, 64]. Behavioral assessments for canine models are based on the Tarlov scale [65], which was initially designed for use in rodents. This modified Tarlov scale evaluates motor coordination based on stepping behavior/regularity [64, 66].

5. Future Directions and Conclusions

In the present review, we summarized current evidence regarding animal models of SCI, cell-based therapeutic strategies, and rating scales used to evaluate motor function following SCI. Enhanced precision of SCI methods in recent years has reduced variations in the damage elicited during injury. The use of unified functional indices in conjunction with these more precise methods allows for sufficient estimation of the therapeutic effects of potential SCI treatments, without the need for additional descriptions. When the appropriate animal models and rating scales are chosen, our review suggests that the functional scores described in previous sections represent universal assessments of the animal's functional state. The use of defined animal models and suitable indices may also aid in identifying the most effective treatments and in enhancing the reproducibility of SCI research.

Conflicts of Interest

The authors declare that there are no conflicts of interest regarding the publication of this paper.

Authors' Contributions

Woon Ryoung Kim and Minjin Kang contributed equally to this work.

Acknowledgments

This research was supported by the Bio & Medical Technology Development Program (NRF-2016M3A9A5916225, Dongho Geum) and Basic Science Research Program (2016R1D1A1B03930397, Woon Ryoung Kim) of the National Research Foundation of Korea (NRF) funded by the Ministry of Education, Science and Technology and by a grant of the Korea Health Technology R&D Project through the Korea Health Industry Development Institute, funded by the Ministry of Health & Welfare, Republic of Korea (HI14C3347, Dongho Geum).

References

[1] A. Ackery, C. Tator, and A. Krassioukov, "A global perspective on spinal cord injury epidemiology," *Journal of Neurotrauma*, vol. 21, no. 10, pp. 1355–1370, 2004.

[2] A. Singh, L. Tetreault, S. Kalsi-Ryan, A. Nouri, and M. G. Fehlings, "Global prevalence and incidence of traumatic spinal cord injury," *Clinical Epidemiology*, vol. 6, pp. 309–331, 2014.

[3] S. Thuret, L. D. Moon, and F. H. Gage, "Therapeutic interventions after spinal cord injury," *Nature Reviews Neuroscience*, vol. 7, no. 8, pp. 628–643, 2006.

[4] P. Assinck, G. J. Duncan, B. J. Hilton, J. R. Plemel, and W. Tetzlaff, "Cell transplantation therapy for spinal cord injury," *Nature Neuroscience*, vol. 20, no. 5, pp. 637–647, 2017.

[5] S. I. Hodgetts, M. Edel, and A. R. Harvey, "The state of play with iPSCs and spinal cord injury models," *Journal of Clinical Medicine*, vol. 4, no. 1, pp. 193–203, 2015.

[6] B. G. McMahill, D. L. Borjesson, M. Sieber-Blum, J. A. Nolta, and B. K. Sturges, "Stem cells in canine spinal cord injury–promise for regenerative therapy in a large animal model of human disease," *Stem Cell Reviews*, vol. 11, no. 1, pp. 180–193, 2015.

[7] T. Cheriyan, D. J. Ryan, J. H. Weinreb et al., "Spinal cord injury models: a review," *Spinal Cord*, vol. 52, no. 8, pp. 588–595, 2014.

[8] D. M. Basso, L. C. Fisher, A. J. Anderson, L. B. Jakeman, D. M. McTigue, and P. G. Popovich, "Basso mouse scale for locomotion detects differences in recovery after spinal cord injury in five common mouse strains," *Journal of Neurotrauma*, vol. 23, no. 5, pp. 635–659, 2006.

[9] A. Denic, A. J. Johnson, A. J. Bieber, A. E. Warrington, M. Rodriguez, and I. Pirko, "The relevance of animal models in multiple sclerosis research," *Pathophysiology*, vol. 18, no. 1, pp. 21–29, 2011.

[10] G. C. Koopmans, R. Deumens, W. M. Honig, F. P. Hamers, H. W. Steinbusch, and E. A. Joosten, "The assessment of locomotor function in spinal cord injured rats: the importance of objective analysis of coordination," *Journal of Neurotrauma*, vol. 22, no. 2, pp. 214–225, 2005.

[11] D. M. Basso, M. S. Beattie, and J. C. Bresnahan, "A sensitive and reliable locomotor rating scale for open field testing in rats," *Journal of Neurotrauma*, vol. 12, no. 1, pp. 1–21, 1995.

[12] J. A. Gruner, "A monitored contusion model of spinal cord injury in the rat," *Journal of Neurotrauma*, vol. 9, no. 2, pp. 123–128, 1992.

[13] J. C. Gensel, C. A. Tovar, F. P. Hamers, R. J. Deibert, M. S. Beattie, and J. C. Bresnahan, "Behavioral and histological characterization of unilateral cervical spinal cord contusion injury in rats," *Journal of Neurotrauma*, vol. 23, no. 1, pp. 36–54, 2006.

[14] L. Liu, L. T. Chi, Z. Q. Tu, B. Sheng, Z. K. Zhou, and F. X. Pei, "Observation and establishment of an animal model of tractive spinal cord injury in rats," *Chinese Journal of Traumatology*, vol. 7, no. 6, pp. 372–377, 2004.

[15] Y. P. Zhang, C. Iannotti, L. B. Shields et al., "Dural closure, cord approximation, and clot removal: enhancement of tissue sparing in a novel laceration spinal cord injury model," *Journal of Neurosurgery*, vol. 100, no. 4, Supplement Spine, pp. 343–352, 2004.

[16] R. F. Heimburger, "Return of function after spinal cord transection," *Spinal Cord*, vol. 43, no. 7, pp. 438–440, 2005.

[17] L. W. Freeman, "Return of function after complete transection of the spinal cord of the rat, cat and dog," *Annals of Surgery*, vol. 136, no. 2, pp. 193–205, 1952.

[18] M. Hatami, N. Z. Mehrjardi, S. Kiani et al., "Human embryonic stem cell-derived neural precursor transplants in collagen scaffolds promote recovery in injured rat spinal cord," *Cytotherapy*, vol. 11, no. 5, pp. 618–630, 2009.

[19] H. Itosaka, S. Kuroda, H. Shichinohe et al., "Fibrin matrix provides a suitable scaffold for bone marrow stromal cells transplanted into injured spinal cord: a novel material for CNS tissue engineering," *Neuropathology*, vol. 29, no. 3, pp. 248–257, 2009.

[20] X. Li, Z. Yang, A. Zhang, T. Wang, and W. Chen, "Repair of thoracic spinal cord injury by chitosan tube implantation in adult rats," *Biomaterials*, vol. 30, no. 6, pp. 1121–1132, 2009.

[21] B. D. Watson, R. Prado, W. D. Dietrich, M. D. Ginsberg, and B. A. Green, "Photochemically induced spinal cord injury in the rat," *Brain Research*, vol. 367, no. 1-2, pp. 296–300, 1986.

[22] M. Gaviria, H. Haton, F. Sandillon, and A. Privat, "A mouse model of acute ischemic spinal cord injury," *Journal of Neurotrauma*, vol. 19, no. 2, pp. 205–221, 2002.

[23] J. X. Hao, X. J. Xu, H. Aldskogius, A. Seiger, and Z. Wiesenfeld-Hallin, "Allodynia-like effects in rat after ischaemic spinal cord injury photochemically induced by laser irradiation," *Pain*, vol. 45, no. 2, pp. 175–185, 1991.

[24] I. K. Toumpoulis, C. E. Anagnostopoulos, G. E. Drossos, V. D. Malamou-Mitsi, L. S. Pappa, and D. G. Katritsis, "Does ischemic preconditioning reduce spinal cord injury because of descending thoracic aortic occlusion?," *Journal of Vascular Surgery*, vol. 37, no. 2, pp. 426–432, 2003.

[25] R. P. Yezierski, S. Liu, G. L. Ruenes, K. J. Kajander, and K. L. Brewer, "Excitotoxic spinal cord injury: behavioral and morphological characteristics of a central pain model," *Pain*, vol. 75, no. 1, pp. 141–155, 1998.

[26] J. Das Sarma, "A mechanism of virus-induced demyelination," *Interdisciplinary Perspectives on Infectious Diseases*, vol. 2010, Article ID 109239, 28 pages, 2010.

[27] A. E. Ropper, D. K. Thakor, I. Han et al., "Defining recovery neurobiology of injured spinal cord by synthetic matrix-assisted hMSC implantation," *Proceedings of the National Academy of Sciences of the United States of America*, vol. 114, no. 5, pp. E820–E829, 2017.

[28] S. Karimi-Abdolrezaee, E. Eftekharpour, J. Wang, C. M. Morshead, and M. G. Fehlings, "Delayed transplantation of adult neural precursor cells promotes remyelination and functional neurological recovery after spinal cord injury," *The Journal of Neuroscience*, vol. 26, no. 13, pp. 3377–3389, 2006.

[29] Y. D. Teng, E. B. Lavik, X. Qu et al., "Functional recovery following traumatic spinal cord injury mediated by a unique polymer scaffold seeded with neural stem cells," *Proceedings of the National Academy of Sciences of the United States of America*, vol. 99, no. 5, pp. 3024–3029, 2002.

[30] B. L. Du, Y. Xiong, C. G. Zeng et al., "Transplantation of artificial neural construct partly improved spinal tissue repair and functional recovery in rats with spinal cord transection," *Brain Research*, vol. 1400, pp. 87–98, 2011.

[31] C. D. Pritchard, J. R. Slotkin, D. Yu et al., "Establishing a model spinal cord injury in the African green monkey for the preclinical evaluation of biodegradable polymer scaffolds seeded with human neural stem cells," *Journal of Neuroscience Methods*, vol. 188, no. 2, pp. 258–269, 2010.

[32] G. Bozkurt, A. J. Mothe, T. Zahir, H. Kim, M. S. Shoichet, and C. H. Tator, "Chitosan channels containing spinal cord-derived stem/progenitor cells for repair of subacute spinal cord injury in the rat," *Neurosurgery*, vol. 67, no. 6, pp. 1733–1744, 2010.

[33] A. Hejcl, J. Sedy, M. Kapcalova et al., "HPMA-RGD hydrogels seeded with mesenchymal stem cells improve functional outcome in chronic spinal cord injury," *Stem Cells and Development*, vol. 19, no. 10, pp. 1535–1546, 2010.

[34] K. N. Kang, J. Y. Lee, D. Y. Kim et al., "Regeneration of completely transected spinal cord using scaffold of poly(D,L-lactide-co-glycolide)/small intestinal submucosa seeded with rat bone marrow stem cells," *Tissue Engineering Part A*, vol. 17, no. 17-18, pp. 2143–2152, 2011.

[35] P. Lu, G. Woodruff, Y. Wang et al., "Long-distance axonal growth from human induced pluripotent stem cells after spinal cord injury," *Neuron*, vol. 83, no. 4, pp. 789–796, 2014.

[36] H. Nomura, T. Zahir, H. Kim et al., "Extramedullary chitosan channels promote survival of transplanted neural stem and progenitor cells and create a tissue bridge after complete spinal cord transection," *Tissue Engineering Part A*, vol. 14, no. 5, pp. 649–665, 2008.

[37] P. J. Johnson, A. Tatara, D. A. McCreedy, A. Shiu, and S. E. Sakiyama-Elbert, "Tissue-engineered fibrin scaffolds containing neural progenitors enhance functional recovery in a subacute model of SCI," *Soft Matter*, vol. 6, no. 20, pp. 5127–5137, 2010.

[38] Y. Kobayashi, Y. Okada, G. Itakura et al., "Pre-evaluated safe human iPSC-derived neural stem cells promote functional recovery after spinal cord injury in common marmoset without tumorigenicity," *PLoS One*, vol. 7, no. 12, article e52787, 2012.

[39] S. E. Nutt, E. A. Chang, S. T. Suhr et al., "Caudalized human iPSC-derived neural progenitor cells produce neurons and glia but fail to restore function in an early chronic spinal cord injury model," *Experimental Neurology*, vol. 248, pp. 491–503, 2013.

[40] A. Montgomery, A. Wong, N. Gabers, and S. M. Willerth, "Engineering personalized neural tissue by combining induced pluripotent stem cells with fibrin scaffolds," *Biomaterials Science*, vol. 3, no. 2, pp. 401–413, 2015.

[41] P. Saadai, A. Wang, Y. S. Nout et al., "Human induced pluripotent stem cell-derived neural crest stem cells integrate into the injured spinal cord in the fetal lamb model of myelomeningocele," *Journal of Pediatric Surgery*, vol. 48, no. 1, pp. 158–163, 2013.

[42] J. Ma, X. Li, B. Yi et al., "Transplanted iNSCs migrate through SDF-1/CXCR4 signaling to promote neural recovery in a rat model of spinal cord injury," *Neuroreport*, vol. 25, no. 6, pp. 391–397, 2014.

[43] J. Y. Hong, S. H. Lee, S. C. Lee et al., "Therapeutic potential of induced neural stem cells for spinal cord injury," *The Journal of Biological Chemistry*, vol. 289, no. 47, pp. 32512–32525, 2014.

[44] C. Liu, Y. Huang, M. Pang et al., "Tissue-engineered regeneration of completely transected spinal cord using induced neural stem cells and gelatin-electrospun poly (lactide-co-glycolide)/polyethylene glycol scaffolds," *PLoS One*, vol. 10, no. 3, article e0117709, 2015.

[45] A. Hurtado, L. D. Moon, V. Maquet, B. Blits, R. Jerome, and M. Oudega, "Poly (D,L-lactic acid) macroporous guidance scaffolds seeded with Schwann cells genetically modified to secrete a bi-functional neurotrophin implanted in the completely transected adult rat thoracic spinal cord," *Biomaterials*, vol. 27, no. 3, pp. 430–442, 2006.

[46] H. E. Olson, G. E. Rooney, L. Gross et al., "Neural stem cell- and Schwann cell-loaded biodegradable polymer scaffolds support axonal regeneration in the transected spinal cord," *Tissue Engineering Part A*, vol. 15, no. 7, pp. 1797–1805, 2009.

[47] J. M. Wang, Y. S. Zeng, J. L. Wu, Y. Li, and Y. D. Teng, "Cograft of neural stem cells and Schwann cells overexpressing TrkC and neurotrophin-3 respectively after rat spinal cord transection," *Biomaterials*, vol. 32, no. 30, pp. 7454–7468, 2011.

[48] E. A. Joosten, W. B. Veldhuis, and F. P. Hamers, "Collagen containing neonatal astrocytes stimulates regrowth of injured fibers and promotes modest locomotor recovery after spinal cord injury," *Journal of Neuroscience Research*, vol. 77, no. 1, pp. 127–142, 2004.

[49] S. Rochkind, A. Shahar, D. Fliss et al., "Development of a tissue-engineered composite implant for treating traumatic paraplegia in rats," *European Spine Journal*, vol. 15, no. 2, pp. 234–245, 2006.

[50] J. Zhang, X. Lu, G. Feng et al., "Chitosan scaffolds induce human dental pulp stem cells to neural differentiation: potential roles for spinal cord injury therapy," *Cell and Tissue Research*, vol. 366, no. 1, pp. 129–142, 2016.

[51] B. Shrestha, K. Coykendall, Y. Li, A. Moon, P. Priyadarshani, and L. Yao, "Repair of injured spinal cord using biomaterial scaffolds and stem cells," *Stem Cell Research & Therapy*, vol. 5, no. 4, p. 91, 2014.

[52] J. C. Gensel, D. J. Donnelly, and P. G. Popovich, "Spinal cord injury therapies in humans: an overview of current clinical trials and their potential effects on intrinsic CNS macrophages," *Expert Opinion on Therapeutic Targets*, vol. 15, no. 4, pp. 505–518, 2011.

[53] R. R. Smith, D. A. Burke, A. D. Baldini et al., "The Louisville swim scale: a novel assessment of hindlimb function following spinal cord injury in adult rats," *Journal of Neurotrauma*, vol. 23, no. 11, pp. 1654–1670, 2006.

[54] M. D. Schechter and W. T. Chance, "Non-specificity of "behavioral despair" as an animal model of depression," *European Journal of Pharmacology*, vol. 60, no. 2-3, pp. 139–142, 1979.

[55] K. Gale, H. Kerasidis, and J. R. Wrathall, "Spinal cord contusion in the rat: behavioral analysis of functional neurologic impairment," *Experimental Neurology*, vol. 88, no. 1, pp. 123–134, 1985.

[56] M. Martinez, J. M. Brezun, L. Bonnier, and C. Xerri, "A new rating scale for open-field evaluation of behavioral recovery after cervical spinal cord injury in rats," *Journal of Neurotrauma*, vol. 26, no. 7, pp. 1043–1053, 2009.

[57] A. J. Lankhorst, M. P. ter Laak, T. J. van Laar et al., "Effects of enriched housing on functional recovery after spinal cord contusive injury in the adult rat," *Journal of Neurotrauma*, vol. 18, no. 2, pp. 203–215, 2001.

[58] F. P. Hamers, A. J. Lankhorst, T. J. van Laar, W. B. Veldhuis, and W. H. Gispen, "Automated quantitative gait analysis during overground locomotion in the rat: its application to spinal cord contusion and transection injuries," *Journal of Neurotrauma*, vol. 18, no. 2, pp. 187–201, 2001.

[59] D. A. Houweling, A. J. Lankhorst, W. H. Gispen, P. R. Bar, and E. A. Joosten, "Collagen containing neurotrophin-3 (NT-3) attracts regrowing injured corticospinal axons in the adult rat

spinal cord and promotes partial functional recovery," *Experimental Neurology*, vol. 153, no. 1, pp. 49–59, 1998.

[60] A. S. Rivlin and C. H. Tator, "Effect of duration of acute spinal cord compression in a new acute cord injury model in the rat," *Surgical Neurology*, vol. 10, no. 1, pp. 38–43, 1978.

[61] R. Suresh Babu, R. Muthusamy, and A. Namasivayam, "Behavioural assessment of functional recovery after spinal cord hemisection in the bonnet monkey (*Macaca radiata*)," *Journal of the Neurological Sciences*, vol. 178, no. 2, pp. 136–152, 2000.

[62] Y. S. Nout, A. R. Ferguson, S. C. Strand et al., "Methods for functional assessment after C7 spinal cord hemisection in the rhesus monkey," *Neurorehabilitation and Neural Repair*, vol. 26, no. 6, pp. 556–569, 2012.

[63] S. H. Lee, Y. N. Chung, Y. H. Kim et al., "Effects of human neural stem cell transplantation in canine spinal cord hemisection," *Neurological Research*, vol. 31, no. 9, pp. 996–1002, 2009.

[64] N. J. Olby, L. D. Risio, K. R. Munana et al., "Development of a functional scoring system in dogs with acute spinal cord injuries," *American Journal of Veterinary Research*, vol. 62, no. 10, pp. 1624–1628, 2001.

[65] I. M. Tarlov, H. Klinger, and S. Vitale, "Spinal cord compression studies. I. Experimental techniques to produce acute and gradual compression," *A.M.A. Archives of Neurology and Psychiatry*, vol. 70, no. 6, pp. 813–819, 1953.

[66] N. J. Olby, J. H. Lim, K. Babb et al., "Gait scoring in dogs with thoracolumbar spinal cord injuries when walking on a treadmill," *BMC Veterinary Research*, vol. 10, p. 58, 2014.

Hindawi
Stem Cells International
Volume 2017, Article ID 9428176, 19 pages
https://doi.org/10.1155/2017/9428176

Review Article

Assessment of Safety and Functional Efficacy of Stem Cell-Based Therapeutic Approaches Using Retinal Degenerative Animal Models

Tai-Chi Lin,[1,2,3,4] Magdalene J. Seiler,[5,6] Danhong Zhu,[1,7] Paulo Falabella,[1] David R. Hinton,[1,7] Dennis O. Clegg,[8] Mark S. Humayun,[1,2] and Biju B. Thomas[1,2]

[1]*Department of Ophthalmology, USC Roski Eye Institute, University of Southern California, Los Angeles, CA, USA*
[2]*USC Institute for Biomedical Therapeutics, University of Southern California, Los Angeles, CA, USA*
[3]*Department of Ophthalmology, Taipei Veterans General Hospital, Taipei, Taiwan*
[4]*Institute of Clinical Medicine, National Yang-Ming University, Taipei, Taiwan*
[5]*Stem Cell Research Center, University of California-Irvine, Irvine, CA, USA*
[6]*Department of Physical Medicine & Rehabilitation, University of California-Irvine, Irvine, CA, USA*
[7]*Department of Pathology, Keck School of Medicine, University of Southern California, Los Angeles, CA, USA*
[8]*Center for Stem Cell Biology and Engineering, University of California, Santa Barbara, CA, USA*

Correspondence should be addressed to Biju B. Thomas; biju.thomas@med.usc.edu

Received 15 April 2017; Accepted 19 June 2017; Published 27 August 2017

Academic Editor: Tilo Kunath

Copyright © 2017 Tai-Chi Lin et al. This is an open access article distributed under the Creative Commons Attribution License, which permits unrestricted use, distribution, and reproduction in any medium, provided the original work is properly cited.

Dysfunction and death of retinal pigment epithelium (RPE) and or photoreceptors can lead to irreversible vision loss. The eye represents an ideal microenvironment for stem cell-based therapy. It is considered an "immune privileged" site, and the number of cells needed for therapy is relatively low for the area of focused vision (macula). Further, surgical placement of stem cell-derived grafts (RPE, retinal progenitors, and photoreceptor precursors) into the vitreous cavity or subretinal space has been well established. For preclinical tests, assessments of stem cell-derived graft survival and functionality are conducted in animal models by various noninvasive approaches and imaging modalities. *In vivo* experiments conducted in animal models based on replacing photoreceptors and/or RPE cells have shown survival and functionality of the transplanted cells, rescue of the host retina, and improvement of visual function. Based on the positive results obtained from these animal experiments, human clinical trials are being initiated. Despite such progress in stem cell research, ethical, regulatory, safety, and technical difficulties still remain a challenge for the transformation of this technique into a standard clinical approach. In this review, the current status of preclinical safety and efficacy studies for retinal cell replacement therapies conducted in animal models will be discussed.

1. Introduction

Stem cell-based therapies have shown to restore or rescue visual function in preclinical models of retinal degenerative diseases [1–5] which are built on previous data with transplantation of fetal retinal tissue sheets. This has set a standard what these optimal cells can do [6–9]. Although retinal degenerative diseases such as retinitis pigmentosa (RP), age-related macular degeneration (AMD), and Stargardt's disease differ in their causes and demographics, all of them cause RPE and/or photoreceptor destruction which can lead to blindness [1–5]. Currently, there is no clinically accepted cure for irreversible dysfunction or death of photoreceptors and RPE. Since the retina, like other central nervous system

tissue, has little regenerative potential [4, 10], stem cell-based therapies that aimed to replace the dysfunctional or dead cells remain a major hope.

In 1959, a rat fetal retina was transplanted into the anterior chamber of a pregnant rat's eye [11]. Several decades later, dissociated retinal cells or cell aggregates were transplanted into the subretinal space of rats [12–17]. In the 80s, Dr. Gouras demonstrated transplantation of cultured human retinal pigment epithelial cells into the monkey retina. The transplanted cells were identified on the Bruch's membrane by autoradiography [18]. Turner and Blair reported high survival (90–100%) and development of lamination for newborn rat retinal aggregates grafted into a lesion site of an adult rat retina [19]. Silverman and Hughes were the first one to isolate stripes of photoreceptor sheets from the postnatal and adult retina [20], and this method was modified later on by other researchers by transplanting photoreceptor sheets [21], full thickness fetal [6, 7, 22–24] or adult retina [25]. These earlier transplantation studies helped to establish "proof of concept" for future cell replacement therapies in the eye. Although the initial transplantation studies did not show any safety issues, ethical restrictions and absence of suitable animal models for preclinical evaluations delayed further progress of this approach [3]. In 2009, human embryonic stem cell- (hESC-) derived RPE cells were transplanted into Royal College of Surgeon (RCS) rats in preclinical studies [26] that eventually lead to clinical trials. Although the long-term outcomes of the preclinical investigations are not yet concluded [27–31], recent advancement in the area of induced pluripotent stem cell- (iPSC-) derived products provided a new source for transplantation. This method uses mature cells that return to a pluripotent state similar to that seen in embryonic stem cells [32–35]. Preclinical testing of iPSC-derived RPE (iPSC-RPE) cells has been established [36, 37], and human clinical trials based on iPSC-RPE have been initiated [38]. These studies indicate survival of the transplanted RPE with signs of visual functional improvement and no signs of adverse events. However, one of the first human clinical trials using autologous iPSC-RPE cells lead by Masayo Takahashi was halted for a period of time after unexpected chromosomal abnormalities were found in the second patient [39, 40]. In a different incident, severe vision loss was observed in three AMD patients after intravitreal injection of autologous adipose tissue-derived "stem cells" (https://blog.cirm.ca.gov/2017/03/15/three-people-left-blind-by-florida-clinics-unproven-stem-cell-therapy/comment-page-1/). The above report raises some concerns regarding the existing safety requirements and regulations of the use of unregulated stem cell trials [41].

In this review, current progress in stem cell-based therapies will be discussed based on safety assessments and functional evaluations conducted in various animal models of human retinal degenerative diseases.

2. Stem Cell Sources and Their Applications in the Eye

Stem cell-based therapy for RPE replacement has been initiated at various centers. Since Klimanskaya et al. developed the original protocol for hESC-derived RPE-like cells [42], various groups have used several strategies to derive RPE cells from stem cells. In earlier studies, subretinal transplantation of hESC-derived RPE (hESC-RPE) cells based on cell suspension injection was shown to rescue degenerating photoreceptors and improve vision in immunosuppressed RCS rats [26, 43]. In a more recent technique, a pregenerated RPE monolayer grown on a scaffold and transplanted in immunosuppressed RCS rats showed improved survival of hESC-RPE and better clinical outcomes [44, 45] suggesting that RPE function is dependent on polarization of the transplanted RPE cells and the monolayer morphology [44–46]. iPSCs are considered to have several advantages over hESCs including protection from immune rejection, wide variety of potential sources, and reduced ethical concerns [47]. Transplantation of iPSC-RPE [37, 48] and iPSC-derived photoreceptor precursor cells [49] has demonstrated success in different animal models. The iPSC-RPE cells were shown to have morphological and functional similarities to developing and mature RPE cells *in vitro* and *in vivo* [37, 50–52]. Although it will be advantageous to use patient-derived RPE (autologous transplants), the time requirements and production cost make allograft transplantation a desirable option [47].

Patients need to have a sufficient number of surviving, functional photoreceptor cells; otherwise, replacement of only RPE will not help to rescue vision. Therefore, stem cell-derived photoreceptors [53–56] or retinal progenitor cells (RPCs) have been used with or without RPE for transplantation experiments [3, 57–60]. Previously, several types of scaffolds made of materials having different architectures, biocompatibility, size, and stiffness have been used to enhance cell survival, migration from the scaffold pores, integration into the host retina, and in vivo differentiation [61–63].

Studies have shown that the beneficial effect of RPC transplantation is likely achieved by their differentiation into functional retinal cells and subsequent replacement of lost or dysfunctional elements [64, 65]. Other investigations suggested that success of RPC transplantation is achieved through trophic factor release rather than direct replacement of the lost cells [59, 66–68]. A major challenge in incorporating photoreceptors and other neuronal cell types is the establishment of synaptic connections with the proximal neuronal elements of the recipient retina [2, 69–71]. Using transsynaptic tracing techniques and donor cell label, synaptic connections between fetal retinal sheet transplants and the host retina have been previously reported [72–74]. Replacement therapies involving the whole retina are also in progress using retinal organoids (3D retina) [70, 71, 75, 76]. Recently, hESCs and iPSCs were differentiated into optic cups and storable stratified neural retina [77, 78]. Such 3D retinal tissue derived from iPSCs or hESCs when transplanted in rd1 mice [70, 71] and immunosuppressed retinal degeneration (RD) monkeys [75] developed a structured outer nuclear layer and showed signs of synaptic formations [70, 71, 75]. The above milestone studies highlight the new concepts of regenerative medicine in retinal therapeutics emphasizing the possibility of establishing functional connections between the transplant and the host tissue.

3. Animal Models for Stem Cell-Based Therapies

Retinal degenerate rodent models have been extensively used for biomedical research, but because of the key differences between the rodent and human eye, rodent models do not completely replicate the human disease conditions. Most importantly, the rodents do not have a fovea, and in most of the rodents, the photoreceptors are mainly rod cells. Among rodent models, there are both naturally occurring [79–83] and transgenic animal models [84–87]. Light damage [88], laser-induced choroidal neovascularization [89], and retinotoxic agents such as sodium iodoacetate [90] and N-methyl-N-nitrosourea [91, 92] have been also used to induce retinal degenerative conditions. Among this, sodium iodate (SI) has been widely used to induce outer retinal degeneration in otherwise normal animals [93–96].

Rabbits, cats, dogs, pigs, and nonhuman primates have an eye diameter more or less similar to the human eye which allows easy testing of surgical tools and procedures developed for human patients. However, in these large animal models, inducing a disease condition similar to human patients is challenging mostly because the etiology of human diseases is multifactorial, involving both genetic and environmental contributions [1, 2]. The following section summarizes the small and large animal models that are currently used in stem cell-based research.

3.1. Mouse Models. The advantage of using mouse models is their ability to express gene mutations mimicking those identified in humans. However, dissimilarities in life span and rate of disease progression between mice and humans limit the interpretation of the disease conditions. A variety of mutations in mice can cause loss of photoreceptors and reduced rod function and hence were used as AMD models [97–103]. In humans, mutations in the Abca4 gene result in Stargardt's disease, RP, cone-rod dystrophy, and the accumulation of lipofuscin granules in RPE, a characteristic of AMD [104, 105]. Therefore, Abca4 knockout mice which also show lipofuscin accumulation in RPE are considered a model for macular dystrophy conditions [106–110]. Mutations of the RPE65 gene in humans cause most frequently Leber congenital amaurosis, with a small percentage of severe early childhood onset retinal dystrophy [111]. Hence, Rpe65 knockout mice are a model for studying RPE65-mediated retinal dystrophy [112, 113]. Transgenic mice with a rhodopsin Pro23His (P23H) mutation that causes photoreceptor degeneration are highly comparable to human RP disease [99, 114, 115]. In humans, a gene responsible for the autosomal dominant form of Stargardt's disease was identified recently [116, 117]. Transgenic mice harboring this defective gene (Elovl4) are considered a good model for macular degeneration diseases because of the accumulation of high levels of lipofuscin in the RPE and subsequent photoreceptor degeneration in the central retina. This disease pattern closely resembles human Stargardt's disease and AMD [118]. Finally, there are naturally occurring mutations in mice that are used as models of RP disease inheritance [79–83]. Many of the mouse models discussed here are tested for stem cell therapies using cell suspension injections [89, 119]. In conclusion, the wide variety of gene manipulated mouse models provides a valuable tool for studies on therapeutic intervention of various forms of human RD. However, because of their small eye size, implantation of laminated sheets is found to be difficult in mice [44, 120].

3.2. Rat Models. Rats' eyes are twice the size of mouse eyes [121] which makes it easier to perform surgical procedures [121] and transplant both fetal retinal sheets [3, 9] and RPE cells grown as a monolayer [44, 45]. The RCS rat is an animal model widely used for investigating therapeutic applications in the eye [122, 123]. The dystrophic RCS rats are characterized by RPE dysfunction due to the deletion in the Mer tyrosine kinase (Mertk) receptor that abolishes internalization of shed photoreceptor outer segments by RPE cells [124]. Accumulation of debris in the subretinal space can lead to drastic photoreceptor degeneration and rapid loss of vision. In RCS rats, the degeneration progresses slowly. At one month of age, the retinal thickness remains close to the normal level [125] and near complete photoreceptor layer thickness is present [126]. Subretinal transplantation of RPE cells derived from both iPSC [127] and hESC [44, 128–130] into 21 to 28-day old RCS rats showed photoreceptor preservation and rescue of declining vision. Certain other rat models mimic the pathology and progression of RD such as the OXYS rat which spontaneously develops a phenotype similar to human aging and AMD-like pathology [131, 132]. The transgenic P23H rat (available in 3 lines with different degeneration rates), similar to P23H mouse, is frequently used as a model of studying RP diseases [85, 133]. S334ter rats carry a mutant mouse rhodopsin which leads to photoreceptor degeneration [134–136]. The five lines of this model have different characteristic rates of RD, in which S334ter line-3 and S334ter line-5 represent fast and intermediate slow degenerating models, respectively [87]. Several studies have been performed in the above rat models to assess the feasibility of retinal cell replacement therapies [3, 73, 137–141].

The advantage of using slow degeneration models is that they mimic the generally slow progression of human disease conditions. With the inner retina relatively well preserved, there is better opportunity for rescue or restoration of vision following various treatment strategies [138, 142]. However, challenges like immunological reactions and the presence of residual host photoreceptors can make it difficult to detect the transplant effects. To overcome the immunological issues, recently immunodeficient rat models (more details are provided in Section 4) are developed for testing cell-based therapies [143, 144]. In summary, rodent models are currently the leading *in vivo* tool for testing retinal cell therapies due to their affordable cost and easy availability [145].

3.3. Rabbit Models. Rabbits have an eye size comparable to humans and are considered a desirable model to examine therapeutic effects. However, the rabbit retina differs from that of human because it is rod-dominated and contains the visual streak, a horizontal band lying inferior to the optic nerve absent in humans [146, 147]. The densities of rods and cones in the visual streak are higher than elsewhere in the entire retina [146, 147]. Despite this difference, full-field

electroretinography (ERG) developed for the human eye can be used in the rabbit with reproducible results [148]. The transgenic TgP347L rabbit closely tracks human cone-sparing RP disease [86, 149]. Histopathological study in TgP347L rabbits reported that the retinal degeneration developed earlier in the visual streak than in other areas [86] along with some ERG abnormalities [150].

Previously, a dose-dependent correlation between the intravitreal injection of sodium iodate (SI) and retinal degeneration (RD) has been reported in rabbits [151]. According to the investigators, since injected SI may not be evenly distributed in the vitreous due to its uneven liquefaction characteristics, uneven retinal degeneration is caused. Another photoreceptor degeneration rabbit model produced by intravitreal injection of N-methyl-N-nitrosourea showed selective but inconsistent photoreceptor degeneration [152]. Subretinally injected hESC-RPE in immunosuppressed SI-induced RD rabbits failed to integrate into the areas that showed geographic atrophy-like symptoms [153]. This shortcoming was probably due to the unique features of the rabbit eye with a higher degree of immune rejection [153]. In summary, rabbits serve as a useful midsized animal model to study human diseases and therapeutics because they have large eyes compared to rodents.

3.4. Cat Models. Abyssinian cats with inherited rod-cone degeneration (rdAc model) are used as a model for studying retinal therapeutics [154, 155]. The genetic defect causative of retinal degeneration in Abyssinian cats has been identified as a single base pair change in intron 50 of the centrosomal protein 290 (CEP290) gene (IVS50+ 9T>G). This results in abnormalities in the transport and distribution of phototransduction and/or structural proteins through the connecting cilia resulting in photoreceptor degeneration [156]. A high prevalence of affected and carrier cats (45% and 44%, resp.) in the population was first observed in Sweden in 1983 [155]. The cause is speculated to be inbreeding [157]. In addition to have tapetum lucidum (discussed in the next section) which is different from the human eye, a major shortcoming of this model is that it does not entirely resemble the human RP diseases where the peripheral retina is strongly abnormal compared to the central area that remain relatively less damaged. No such distinction is observed in Abyssinian cats. In this model, the degeneration is evenly distributed during the early stages where normal and diseased photoreceptors are often found side-by-side [158]. In addition, this cat model manifests a very slow progression of degeneration, taking from 12 months up to four years [154, 155, 157]. Cat breeds with faster RD disease conditions are now available [159, 160]. An early onset autosomal recessive RD disease in Persian cats was virtually completed at 16 weeks of age [160]. Another cat model, the CrxRdy cats, develops retinal thinning that initially takes place in the central retina [159]. An acute, reliable, and complete photoreceptor degeneration model in cats can be achieved by ear vein injection of high-dose iodoacetic acid [161]. Retinal sheet transplantation studies conducted in Abyssinian cats showed good signs of transplant integration with the host retina and lamination of transplant photoreceptors. However, no considerable functional improvement was noticed [162].

3.5. Dog Models. A major difference in dog eyes from that of humans is the tapetum lucidum, which is a multilayered reflective tissue of the choroid. The tapetum lucidum is interposed between the branching vessels in the choroid and the single layer of the choriocapillaris beneath the retina. The RPE cells over the tapetum lucidum are normally unpigmented. The tapetum lucidum acts to amplify and reflect light back through the photoreceptor layer again in dim light conditions [163]. Tapetum degeneration called toxic tapetopathy has been described in association with the administration of several drugs in beagle dogs [164–168]. Toxic tapetopathy is the characteristic of an altered tapetal color with degeneration or necrosis of the tapetum lucidum [164, 168]. Tapetum degeneration is not observed in the eyes of animals without a tapetum lucidum (rodents, monkeys) [164, 168] and most importantly not in humans [168].

A naturally occurring canine model of autosomal dominant RP caused by a *RHO* mutation was found to strongly resemble the human RP phenotype [169]. High similarity in eye size and preretinal light transmission characteristics between dogs and humans made this model suitable for examining the genetic and environmental causes of RD diseases. Previous studies demonstrated acute retinal injury in *RHO* mutation dogs after exposure to strong light [170, 171]. By varying the dose of light exposure, its long-term consequences including fast or slow disease progression and injury repair have been examined [170]. Although there have been no reports of stem cell-based studies conducted in these animals, this dog model can be considered a suitable candidate for future preclinical studies.

3.6. Pig Models. Several transgenic pig models have been developed for RP diseases, including the Pro347Leu transgenic pig with a rhodopsin mutation [84, 172, 173], the P347S transgenic pig [174, 175], and the P23H transgenic pig, which is considered a model for autosomal dominant RP [176]. Disease progression in most of the above models is slow, making it difficult to assess therapeutic benefits.

Several reports of cell transplantation experiments conducted in pigs are available. Rhodopsin transgenic pigs have been used for transplantation of full-thickness retina [177] and retinal progenitor cell (RPC) transplantation effects [178]. A feasibility and safety study of subretinal implantation of an hESC-RPE monolayer has been reported in immunosuppressed Yucatán minipigs [179]. This study demonstrated preservation of the outer nuclear layer and photoreceptor outer segment overlying the implant. In non-immunosuppressed pigs, adaptive immune responses were activated following allogenic iPSC-RPE transplantation [180]. The above finding suggests that immunologically matched and autologous donor cells should be considered for RPE cell replacement therapies to obviate chronic immune suppression [180].

A major advantage of using pig models is that surgical tools can be developed without much adaptation from the human parameters [1]. Previous RPE cell replacement

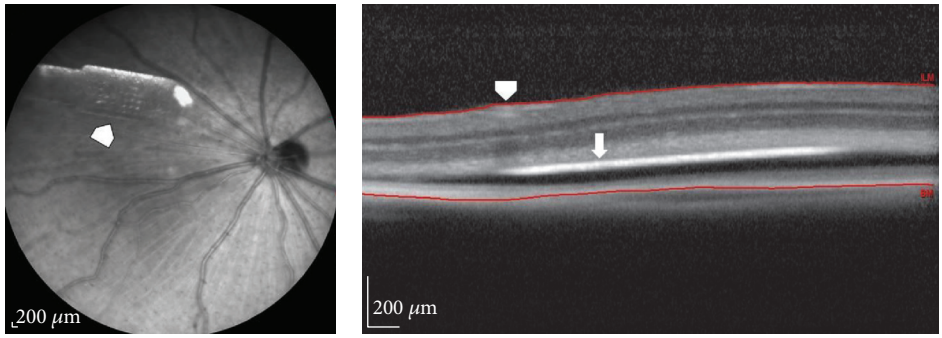

(a) (b)

Figure 1: OCT imaging to assess surgical placement of hESC-RPE implantation in rats. (a) Fundus image showing hESC-RPE implants placed inside the rat eye (arrowhead). (b) Optical coherence tomography software was used to measure the distance between the internal limiting membrane (ILM, arrowhead) and the top of the implant (arrow). The maximum and minimum values were recorded. The delta value obtained by subtracting "maximum value – minimum value" can be used to determine if the implant is placed flat or tilted relatively to the retinal surface.

therapy studies conducted in pigs were focused on testing surgical feasibility of the approach rather than testing functional improvements [1, 181]. This can be also due to the absence of a suitable pig RPE dysfunction model. Although an RPE debridement model can be developed in pigs [182, 183], it is not preferred for testing RPE cell replacement therapies presumably due to both the difficulty in creating a consistent disease pattern and the severity of the trauma that could adversely affect the study outcome.

3.7. Nonhuman Primate Models. The macula is a structure of the eye unique to humans, apes, and monkeys that plays a role as the zone of greatest visual acuity. Therefore, nonhuman primates are a potentially valuable animal model for investigating macular diseases of humans [163]. AMD-like appearance could be found in rhesus monkey (*Macaca mulatta*), cynomolgus macaque (*Macaca fascicularis*), and the Japanese macaque (*Macaca fuscata*). This suggests that the pathogenic mechanisms and associated gene variations are common between human and nonhuman primates [184–190]. Induced RD monkey models have been reported based on systemic injection of iodoacetic acid [191] and cobalt chloride [75], fiber optic light-induced retinal damage [192, 193], and focal damage by severe light exposure [193]. However, these models hold one or more adverse features including ethical issues and inability to produce adequately sized lesions [75]. Housing, maintenance, costs, and ethical concerns due to a close evolutionary relationship to humans further make the nonhuman primate models less appealing for stem cell researchers [194, 195].

Immune rejection of allogeneic iPSC-RPE transplants was studied in cynomolgus monkeys (*Macaca fascicularis*) [196]. In a recent investigation, researchers used a cobalt chloride-induced retinal degeneration RP monkey model to demonstrate possible integration of hESC-derived retinal sheets with the host bipolar cells [75]. The above finding demonstrated clinical feasibility of retina sheet transplantation approach and suggests the need for developing new strategies for future clinical applications [75].

4. Tools and Approaches for In Vivo Assessment of the Transplants and Their Functionality

The eyes are one of the few paired organs in the body where it is possible that one eye is treated while the contralateral eye will serve as control. The transparent nature of the eye makes the evaluations possible through noninvasive imaging modalities.

4.1. In Vivo Imaging of Retinal Transplants and Assessment of Disease Status. Fundus imaging and fluorescein angiography are used to record baseline and follow-up examinations after stem cell therapies. Optical coherence tomography (OCT) is a noncontact, noninvasive imaging technique widely used in the clinic. The advancement of OCT technology provided rapid assessment of transplant morphology and placement location in the eye [9, 52, 197, 198]. The use of OCT imaging to assess changes in the retinal thickness post-transplantation has been established [9, 197–201]. The above studies conducted in rat models suggested that OCT is a reliable tool for in vivo screening and evaluation of retinal transplants. In our rat experiments, we observed that OCT was helpful using a novel OCT-based screening technique developed by our team. Using OCT software (Heidelberg Spectralis's macular thickness feature), distance between the internal limiting membrane (ILM) and top of the implant was measured (Figure 1). The maximum and minimum values are recorded to determine the delta value. The delta value is obtained by subtracting the "maximum value – minimum value." Based on the delta value, it is possible to predict whether the implant is placed flat or tilted relative to the retinal surface.

Recently, Seiler et al. [9] used a Bioptigen Envisu R2200 Spectral Domain Ophthalmic Imaging System (Bioptigen, Research Triangle Park, NC, USA) to obtain SD-OCT images of the rat retina that showed similarity between OCT and histology in the lamination pattern and thickness of the transplants (Figure 2). Other techniques like scanning laser ophthalmoscopy (SLO) can generate images from retinal

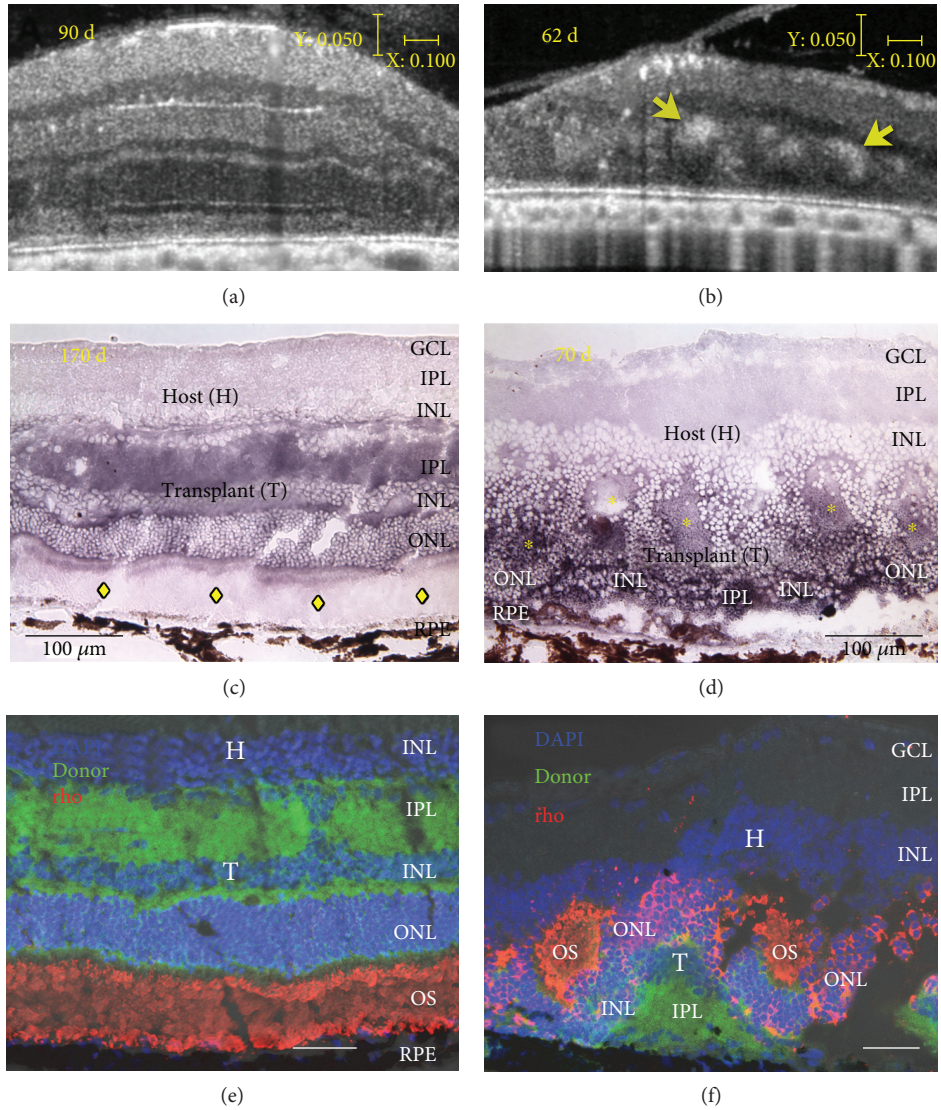

Figure 2: Correlation of live SD-OCT imaging with histology. Fetal retinas (embryonic day 19) derived from rats expressing human placental alkaline phosphatase (hPAP) in the cytoplasm of all cells were transplanted to the subretinal space of immunodeficient retinal degenerate *rho S334ter-3* rats. Transplanted rats' eyes were imaged in vivo by SD-OCT. Two transplant examples are shown. (a, b) Stretched cross-sectional B-scans of laminated (a) and rosetted (b) transplant to better distinguish different retinal layers. Rosettes are indicated by yellow arrows (b) and seen as hyperreflective orbs. (c, d) Transplant-specific histochemistry for hPAP using BCIP (purple). hPAP is expressed in the cytoplasm (not the nuclei) of donor cells. Transplant number 5 (a, c, e) has a large area of lamination parallel retinal layers with photoreceptor outer segments, indicated by yellow diamonds (c) and strong rhodopsin expression (e) in the donor outer retina. Transplant number 1 (b, d, f) is more disorganized with photoreceptors in rosettes [rosette lumens indicated by yellow asterisks in (d)]. The rhodopsin-positive outer segments face inward (f). This transplant (d) was partially placed upside down in the subretinal space. (a, b) Scale bars: vertical bar: 50 μm; horizontal bar: 200 μm; (c, d): 100 μm; (e, f) bars: 20 μm. Modified after Figure 3 of Seiler et al. vision recovery and connectivity by fetal retinal sheet transplantation in an immunodeficient retinal degenerate rat model, IOVS 2017;58:614–630. DOI:10.1167/iovs.15-19028; licensed under the Creative Commons attribution license.

reflectance, autofluorescence, and extrinsic fluorescence. With the confocal arrangement, the SLO is capable of rejecting scattered light, thereby improving image contrast and achieving moderate depth sectioning [202]. Confocal near-infrared SLO imaging was used for *in vivo* detection of subretinally placed hESC-RPE implants in rats [203]. Although the lateral resolution achieved with SLO systems is comparable to that obtained with OCT, the depth resolution was relatively poor. But the advantage of SLO is the ability to detect the presence of pigments on the hESC-RPE *in vivo* [203]. Hence, the survival and potential functionality of an RPE graft can be established. Moreover, SLO is useful when the OCT images are difficult to interpret due to the loss of retinal architecture, as in the case of advanced AMD.

4.2. Electrophysiological Assessments. Visually evoked potentials (VEPs) have been used to determine whether the photoreceptor sheet transplants to RD rats can activate the

central visual system [204]. VEPs were elicited by using strobe flash stimuli, and responses were recorded contralateral to the stimulated eye. The results showed that the reconstructed retina can produce characteristic light-evoked responses in the visual cortex [204]. Electrophysiological analysis was used to demonstrate that cortical visual function could be preserved by subretinal RPE cell grafting in RCS rats [205]. This was also established using optical imaging techniques [206]. Morphological assessments confirmed good correlation between photoreceptor survival and the extent of cortical functional preservation [206]. However, the degree of visual acuity achieved by transplants cannot be completely addressed using visually evoked cortical responses.

Electroretinography (ERG) is employed to access the diffuse electrical response of the retina. Response to flash ERG has been used to evaluate the visual functional changes in retinal degenerative animal models [43, 207, 208]. ERG assessments have revealed improved photoreceptor function in RCS rats after hESC-RPE injection [43]. A major limitation in using full-field flash ERG is that it may fail to detect signals from the comparatively small transplant area. This is because the ERG response is the cumulative effect of signals from the entire retina, whereas signal output from the transplant area may not be sufficient to generate considerable difference in the ERG wave form [9].

Focal electroretinography (fERG) is used to study a discrete region of the retina and determine if there is significantly more electrical activity in that area compared to the surrounding retina. This technique has been successfully employed in RCS rats to show photoreceptor rescue after iPSC-RPE injection [209]. Although multifocal ERG (mfERG) is also considered an equally efficient tool to analyze focal retinal changes, its application in stem cell research is still not well established. Previously, the technique has been proven to be useful in primate recordings [210] and effective in rats to show focal retinal defects [211]. However, its application in small animal studies is not very popular, presumably due to the inconsistency in the recording pattern which causes difficulties during data interpretation (unpublished observations).

Transplant functionality may be reliably assessed by means of electrophysiological mapping of the superior colliculus (SC). The SC receives direct retinal input which corresponds to the areas of the retina that are being stimulated by light [138, 212] and can provide point to point estimates of the retinal function [2]. Our previous studies have demonstrated improved SC responses in rodent models of the RD following cell-based therapies [9, 43, 137, 138, 213]. The SC mapping data can demonstrate that the quality of fetal retinal sheet transplants corresponds to the quality of the SC response [9, 214]. The transplants with more lamination shown in OCT images were later confirmed by SC electrophysiology as having better restoration of visual responses compared to those transplants that were rosetted [9] (Figure 3).

4.3. Visual Behavioral Testing. Optokinetic (OKN) testing is a noninvasive visual behavioral testing method widely used for the assessment of spatial visual acuity in rodents [3, 67, 68, 215]. The OKN response is a compensatory eye movement that reduces movement of images across the retina. Factors which affect the OKN responses are the population and distribution of surviving photoreceptors, the inner retina plasticity status, and the morphological status of subcortical visual areas of the brain like the SC [2]. The outcome of stem cell-based therapies can be assessed based on OKN responses by varying the stimulus parameters, such as grating spatial frequency and contrast sensitivity [26, 67, 68, 216]. A major advantage of the OKN testing is the ability to assess visual function without prior training of the animals. It can also enable testing of the left and right eyes independently by using a special apparatus [217] or by changing the direction of the rotation of the stimuli [218]. Previous studies demonstrated that eyes that received stem cell therapies elicit higher levels of optokinetic response compared to the control groups [43, 213, 217, 219, 220]. However, as in the case of full-field ERG, the OKN responses may be inadequate for detecting visual function from a small area showing transplant function [144]. Since the animal could see only a spot-like light from a small area in the visual field, it may fail to evoke head-tracking responses [71]. Another drawback of the OKN testing is its inability to measure higher visual processing since these responses are elicited mostly by subcortical centers. According to McGill et al. [219], since OKN responses in RD animals show conflicting results, it should be used with caution because of the subjective nature of the tests. Other techniques developed for visual behavioral testing include water maze [221, 222] and visual discrimination apparatus [223]. Although the above techniques require extensive training for the animals, they provide the opportunity to test wide variety of visual stimuli that require higher visual processing. However, these tests remain unpopular due to the training requirements, time constraints, and general concerns regarding the accuracy of two-choice tests.

5. Safety Studies for Stem Cell Transplantation Approaches

Based on some of the recent reports, the occurrence of adverse events following ocular cell replacement therapies cannot be ruled out. The first study that used autologous iPSC-RPE cells for therapy of AMD in Japan was halted after unexpected mutations were noticed in the iPSCs derived from the second patient. To overcome this issue, cord blood and samples from cord blood banks were targeted as a main source of the cells for reprogramming and a human leukocyte antigen (HLA) homozygous iPSC bank was also established [39]. The major purpose of developing this iPSC bank is to solve the issue of high cost and time consumption in processing autogenic iPSC-RPE cells [224]. There are some reports of human clinical trials based on RPE allografts that failed to survive because of immune rejection [225–227]. The degree of allografts that undergo rejection depends partly on the degree of similarity or histocompatibility between the donor and the recipient. HLA matching has great clinical impact in kidney and bone marrow transplantation but is less of a consideration in heart and lung transplantation

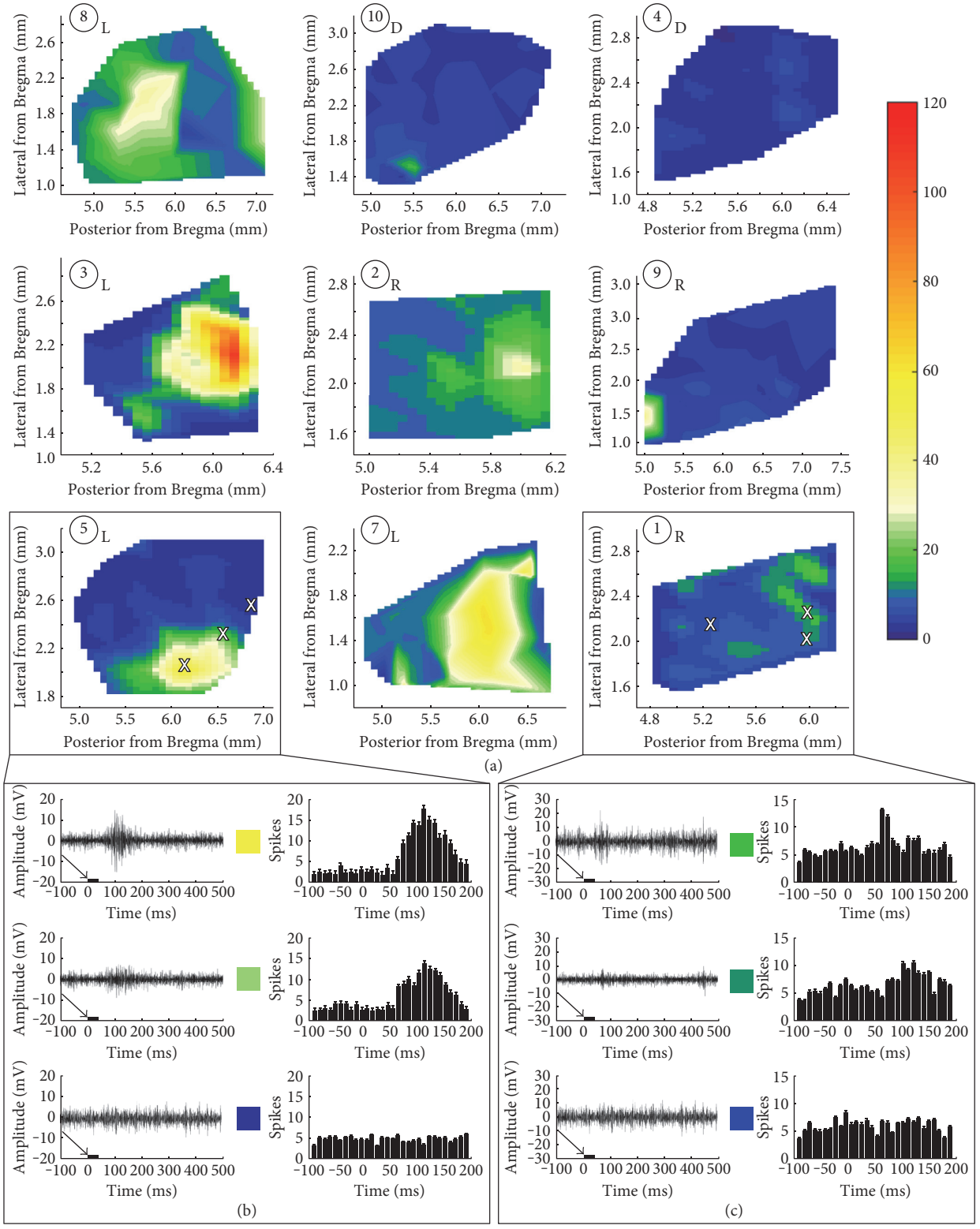

Figure 3: SC recordings from RD nude rats with retinal sheet transplants. (a) Spike count totals (heat maps) over the entirety of the region recorded in SC for all transplanted rats. L: laminated transplant; R: rosetted transplant; D: disorganized transplant. Responses were observed only in certain areas in the SC and were centered on a peak. Sample traces from areas (marked with X) with robust, intermediate, and no response for (b) transplant number 5 with strong responses and (c) transplant number 1 with weak responses. Arrows and black bars indicate the light stimulus. Taken from Figure 7 of Seiler et al., vision recovery and connectivity by fetal retinal sheet transplantation in an immunodeficient retinal degenerate rat model; IOVS 2017;58:614–630. DOI:10.1167/iovs.15-19028; licensed under the Creative Commons attribution license.

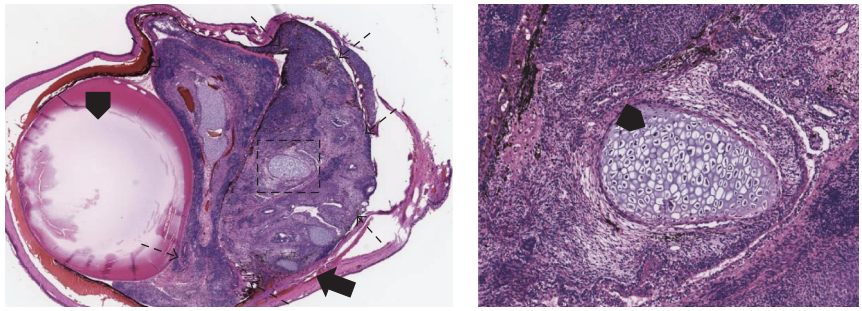

(a) (b)

Figure 4: Positive control experiments (injection of undifferentiated cells) conducted in athymic nude rats to show development of tumors in the eye. (a) Teratoma formation at about 6 weeks after injection (2 μl) of undifferentiated hESCE suspension (60,000cells/μl) shown on H&E staining (2x) (arrowhead: lens, arrow: tumor formation originated from the subretinal space, broken arrow: the margin of the tumor). (b) 10x magnification of the black square from (a). The teratoma is composed of various cell types, including cartilage cells (arrowhead).

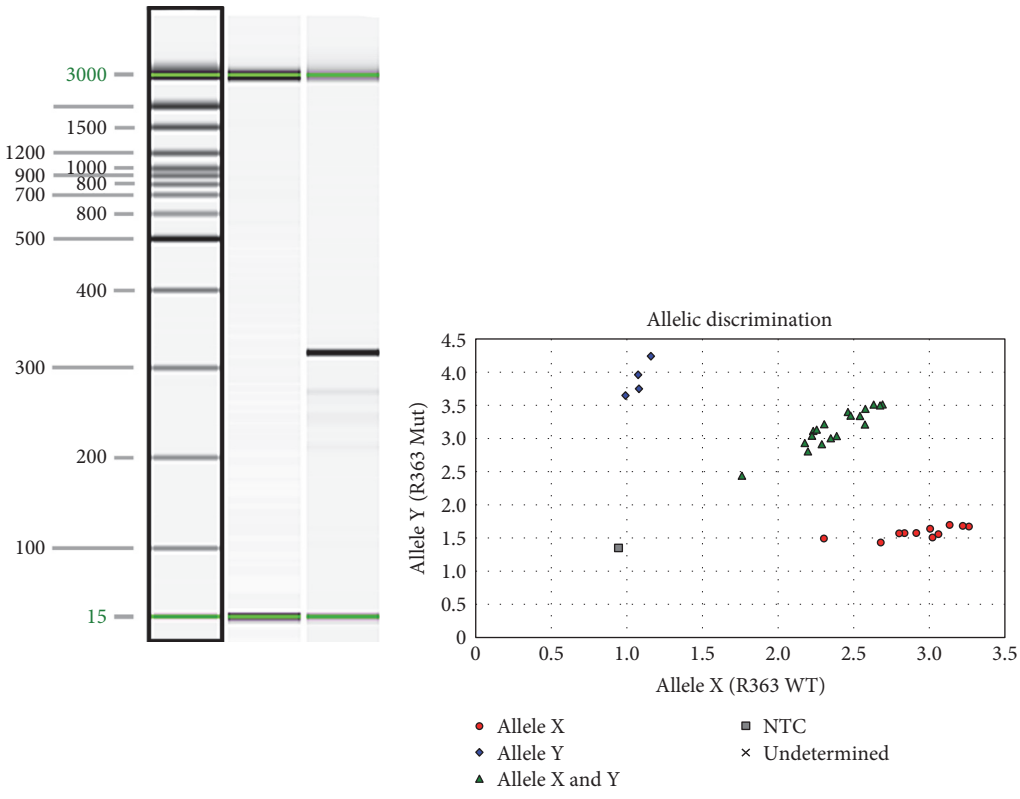

(a) (b)

Figure 5: Genotyping assays of immunodeficient S334ter-3 rats. (a) S334ter transgene genotyping assay. Lane 1 15 bp–3 kb size marker. Lane 2 transgene-negative sample. Lane 3 transgene-positive sample. Sizes in base pairs (bp) are indicated to the left of the image. An amplicon of 350 bp indicates the presence of the transgene. The 15- and 3000-bp alignment markers are present in all lanes. (b) Allelic discrimination assay plot for detection of the Foxn1rnu mutation. The fluorescence levels of VIC (wild type, allele X) and FAM (mutant, allele Y) are plotted on the *x*-axis and *y*-axis, respectively. The genotypes of each sample are represented by blue diamonds (homozygous Foxn1rnu), red circles (homozygous for the wild-type Foxn1 allele), or green triangles (heterozygous +/Foxn1rnu). The no template negative control is represented by the gray box. Reprinted from *Graefes Arch Clin Exp Ophthalmol,* vol. 252, Seiler et al., a new immunodeficient pigmented retinal degenerate rat strain to study transplantation of human cells without immunosuppression, pages 1079–1092, copyright (2014), with permission from Elsevier. DOI 10.1007/s00417-014-2638-y.

[228, 229]. Matching for HLA-B plus HLA-DR resulted in a significant correlation with graft outcome in kidney transplant patients. Grafts with no HLA-B,-DR incompatibilities had approximately 20% higher success rates at one year than grafts with 4 mismatches [230]. Sugita et al. tested all six HLA genotypes (A, B, C, DRB1, DQB1, and DPB1) and reported

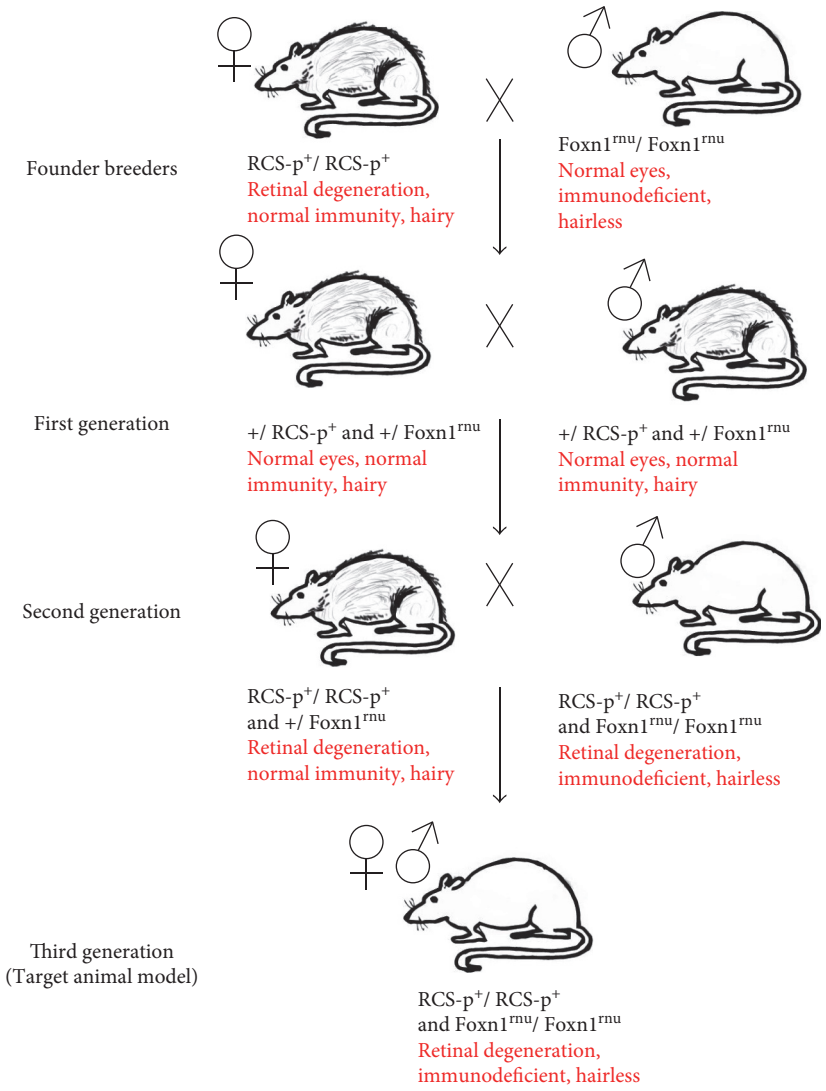

Figure 6: Breeding of immunodeficient RCS rats. Initial mating was performed between male athymic nude rats (Hsd:RH-Foxn1mu) and female dystrophic RCS rats (Mat LaVail, UCSF) to generate F1 pups. The F1 rats were further crossed to generate F2 litters. Pups that are double homozygous (homozygous for RPE dysfunction gene and immunodeficiency gene) were identified based on phenotypic and genotypic expressions.

that the effector T cells can recognize MHC molecules on the allogeneic iPSC-RPE cells, but the immune reaction caused by the T cells can be prevented after HLA blood tests [224]. Therefore, the future clinical trials can make use of allogeneic RPE cells derived from iPSC lines procured from the HLA-homozygous iPSC bank [39, 224]. Nevertheless, further detailed analysis is needed using larger sample size and long-term follow-up [224].

In a recent report, three AMD patients in Florida suffered severe vision loss after receiving injection of autologous adipose tissue-derived stem cells. In this study, adipose-derived stem cells were injected into the eye based on minimal clinical evidence of safety or efficacy. The injection caused ocular hypertension, hemorrhagic retinopathy, vitreous hemorrhage, combined traction and rhegmatogenous retinal detachment, and lens dislocation [41].

The major concern of optimum safety and purity of the cells is that the products should be free of undifferentiated cells and should demonstrate the genetic and functional signature of the desired stem cell-derived tissue. Undifferentiated pluripotent stem cells have the capacity to differentiate into all cell types of the three germ layers and may cause tumor formation. Therefore, extensive testing for the absence of tumor formation and cell migration before implantation is crucial [2]. Differentiation into nondesired cell types is a potential threat to the success of stem cell-derived cell therapies. Confirming the purity of stem cell derivations before transplantation is mandatory [231]. In one study, subcutaneous transplantation of iPSCs into immunosuppressed mice resulted in tumor formation, demonstrating the pluripotency of the injected iPSCs and its capability to evade immune detection [232]. The ability of tumor formation is often assessed using tumorigenicity studies in animal models. According to Nazari et al. [2], assessing tumorigenicity potential in immunocompetent animal models can be misleading since the absence of tumor formation might be

related to the ability of the host to reject tumorigenic cells before tumors form. However, this can be overcome by using positive controls (injection of undifferentiated cells) that are expected to develop tumors in the target area (Figure 4).

Although the eye is to a large extent regarded as an immune privileged organ, there is strong evidence for immune response to xenografts [199, 233–235]. When disease models are used for assessing functional efficacy, immunosuppressant drugs are administered to avoid immunological rejection. Most of the preclinical studies involving human-derived cells used animal models that are exposed to severe immunosuppression regimes [26, 196]. Administration of immunosuppressants in rodents is labor intensive and may cause additional pain and discomfort to the animals. A recent study demonstrated more adverse effects of immunosuppression in animal models. Cyclosporine A plus dexamethasone-administered RCS rats showed depressed scores on visual behavioral and electrophysiological testing [236]. To overcome the above issues, we have developed new immunodeficient rat models. This was accomplished by crossing between nondystrophic immunodeficient animals (NIH nude rats) and RD disease models. The double homozygous pups (immunodeficient RD) can be determined by genotyping [143, 144]. Based on this, an immunodeficient S334ter-line-3 rat colony has been established which eliminated the need for immunosuppression when transplanting xenografts [143] (Figure 5). More recently, a new immunodeficient RCS rat model has been also created [144] and is currently being tested for various stem cell-based products (Figure 6). By employing these models, it is possible to justify ethical concerns by reducing animal use and the overall study cost can be considerably lowered.

6. Conclusion

Stem cell-based therapies provide a new treatment option for retinal degenerative diseases that were previously considered incurable. Preclinical experiments conducted in animal disease models demonstrated functional efficacy and safety of ocular cell replacement therapies. Studies conducted in large animal models helped to establish the surgical techniques required for clinical trials. The above animal studies have paved the way for several clinical trials based on cell-based therapies currently in progress.

Conflicts of Interest

Magdalene J. Seiler has proprietary interest in the instrument and method for transplanting retinal sheets (Ocular Transplantation LLC). Mark S. Humayun, David R. Hinton, and Dennis O. Clegg are cofounders and consultants to Regenerative Patch Technologies (RPT). The authors declare that there is no conflict of interest regarding the publication of this paper.

Acknowledgments

This study was supported by the CIRM (Magdalene J. Seiler, Mark S. Humayun, David R. Hinton, and Dennis O. Clegg), Bright Focus Foundation (Biju B. Thomas), and Research to Prevent Blindness (USC Roski Eye Institute). The authors thank Dr. Robert Aramant (UCI, Stem Cell Research Center; Ocular Transplantation LLC, Crestwood, KY) for his helpful comments to the article and his contributions to retinal sheet transplant research. Work shown in the figures was made possible by Xiaopeng Wang (USC), Bin Lin, Ph.D., Bryce McLelland, B.S., and Anu Mathur M.S. (UC Irvine, Stem Cell Research Center).

References

[1] M. K. Jones, B. Lu, S. Girman, and S. Wang, "Cell-based therapeutic strategies for replacement and preservation in retinal degenerative diseases," *Progress in Retinal and Eye Research*, vol. 58, pp. 1–27, 2017.

[2] H. Nazari, L. Zhang, D. Zhu et al., "Stem cell based therapies for age-related macular degeneration: the promises and the challenges," *Progress in Retinal and Eye Research*, vol. 48, pp. 1–39, 2015.

[3] M. J. Seiler and R. B. Aramant, "Cell replacement and visual restoration by retinal sheet transplants," *Progress in Retinal and Eye Research*, vol. 31, no. 6, pp. 661–687, 2012.

[4] J. D. Sengillo, S. Justus, Y. T. Tsai, T. Cabral, and S. H. Tsang, "Gene and cell-based therapies for inherited retinal disorders: an update," *American Journal of Medical Genetics Part C, Seminars in Medical Genetics*, vol. 172, no. 4, pp. 349–366, 2016.

[5] M. Zarbin, "Cell-based therapy for degenerative retinal disease," *Trends in Molecular Medicine*, vol. 22, no. 2, pp. 115–134, 2016.

[6] M. J. Seiler and R. B. Aramant, "Intact sheets of fetal retina transplanted to restore damaged rat retinas," *Investigative Ophthalmology & Visual Science*, vol. 39, no. 11, pp. 2121–2131, 1998.

[7] R. B. Aramant, M. J. Seiler, and S. L. Ball, "Successful cotransplantation of intact sheets of fetal retina with retinal pigment epithelium," *Investigative Ophthalmology & Visual Science*, vol. 40, no. 7, pp. 1557–1564, 1999.

[8] N. D. Radtke, R. B. Aramant, H. M. Petry, P. T. Green, D. J. Pidwell, and M. J. Seiler, "Vision improvement in retinal degeneration patients by implantation of retina together with retinal pigment epithelium," *American Journal of Ophthalmology*, vol. 146, no. 2, pp. 172–182, 2008.

[9] M. J. Seiler, R. E. Lin, B. T. McLelland et al., "Vision recovery and connectivity by fetal retinal sheet transplantation in an immunodeficient retinal degenerate rat model," *Investigative Ophthalmology & Visual Science*, vol. 58, no. 1, pp. 614–630, 2017.

[10] A. Dahlmann-Noor, S. Vijay, H. Jayaram, A. Limb, and P. T. Khaw, "Current approaches and future prospects for stem cell rescue and regeneration of the retina and optic nerve," *Canadian Journal of Ophthalmology*, vol. 45, no. 4, pp. 333–341, 2010.

[11] P. E. Royo and W. B. Quay, "Retinal transplantation from fetal to maternal mammalian eye," *Growth*, vol. 23, pp. 313–336, 1959.

[12] M. del Cerro, H. H. Yeh, A. Marrero-Rodriguez, E. Lazar, and C. del Cerro, "Intraocular transplantation of cell layers derived from neonatal rat retina," *Brain Research*, vol. 535, no. 1, pp. 25–32, 1990.

[13] R. Aramant, M. Seiler, B. Ehinger et al., "Transplantation of human embryonic retina to adult rat retina," *Restorative Neurology and Neuroscience*, vol. 2, no. 1, pp. 9–22, 1990.

[14] M. del Cerro, J. R. Ison, G. P. Bowen, E. Lazar, and C. del Cerro, "Intraretinal grafting restores visual function in light-blinded rats," *Neuroreport*, vol. 2, no. 9, pp. 529–532, 1991.

[15] P. Gouras, J. Du, M. Gelanze, R. Kwun, H. Kjeldbye, and R. Lopez, "Transplantation of photoreceptors labeled with tritiated thymidine into RCS rats," *Investigative Ophthalmology & Visual Science*, vol. 32, no. 5, pp. 1704–1707, 1991.

[16] R. Aramant and M. Seiler, "Cryopreservation and transplantation of immature rat retina into adult rat retina," *Brain Research Developmental Brain Research*, vol. 61, no. 2, pp. 151–159, 1991.

[17] R. B. Aramant and M. J. Seiler, "Human embryonic retinal cell transplants in athymic immunodeficient rat hosts," *Cell Transplantation*, vol. 3, no. 6, pp. 461–474, 1994.

[18] P. Gouras, M. T. Flood, and H. Kjeldbye, "Transplantation of cultured human retinal cells to monkey retina," *Anais da Academia Brasileira de Ciencias*, vol. 56, no. 4, pp. 431–443, 1984.

[19] J. E. Turner and J. R. Blair, "Newborn rat retinal cells transplanted into a retinal lesion site in adult host eyes," *Brain Research*, vol. 391, no. 1, pp. 91–104, 1986.

[20] M. S. Silverman and S. E. Hughes, "Transplantation of photoreceptors to light-damaged retina," *Investigative Ophthalmology & Visual Science*, vol. 30, no. 8, pp. 1684–1690, 1989.

[21] S. Mohand-Said, D. Hicks, M. Simonutti et al., "Photoreceptor transplants increase host cone survival in the retinal degeneration (rd) mouse," *Ophthalmic Research*, vol. 29, no. 5, pp. 290–297, 1997.

[22] R. B. Aramant and M. J. Seiler, "Transplanted sheets of human retina and retinal pigment epithelium develop normally in nude rats," *Experimental Eye Research*, vol. 75, no. 2, pp. 115–125, 2002.

[23] F. Ghosh, K. Arner, and B. Ehinger, "Transplant of full-thickness embryonic rabbit retina using pars plana vitrectomy," *Retina (Philadelphia, Pennsylvania)*, vol. 18, no. 2, pp. 136–142, 1998.

[24] F. Ghosh, B. Juliusson, K. Arner, and B. Ehinger, "Partial and full-thickness neuroretinal transplants," *Experimental Eye Research*, vol. 68, no. 1, pp. 67–74, 1999.

[25] J. Wasselius and F. Ghosh, "Adult rabbit retinal transplants," *Investigative Ophthalmology & Visual Science*, vol. 42, no. 11, pp. 2632–2638, 2001.

[26] B. Lu, C. Malcuit, S. Wang et al., "Long-term safety and function of RPE from human embryonic stem cells in preclinical models of macular degeneration," *Stem Cells (Dayton, Ohio)*, vol. 27, no. 9, pp. 2126–2135, 2009.

[27] E. Lee and R. E. MacLaren, "Sources of retinal pigment epithelium (RPE) for replacement therapy," *The British Journal of Ophthalmology*, vol. 95, no. 4, pp. 445–449, 2011.

[28] B. Lu, D. Zhu, D. Hinton, M. S. Humayun, and Y. C. Tai, "Mesh-supported submicron parylene-C membranes for culturing retinal pigment epithelial cells," *Biomedical Microdevices*, vol. 14, no. 4, pp. 659–667, 2012.

[29] S. D. Schwartz, J. P. Hubschman, G. Heilwell et al., "Embryonic stem cell trials for macular degeneration: a preliminary report," *Lancet*, vol. 379, no. 9817, pp. 713–720, 2012.

[30] S. D. Schwartz, C. D. Regillo, B. L. Lam et al., "Human embryonic stem cell-derived retinal pigment epithelium in patients with age-related macular degeneration and Stargardt's macular dystrophy: follow-up of two open-label phase 1/2 studies," *Lancet*, vol. 385, no. 9967, pp. 509–516, 2015.

[31] S. D. Schwartz, G. Tan, H. Hosseini, and A. Nagiel, "Subretinal transplantation of embryonic stem cell-derived retinal pigment epithelium for the treatment of macular degeneration: an assessment at 4 years," *Investigative Ophthalmology & Visual Science*, vol. 57, no. 5, pp. ORSFc1–ORSFc9, 2016.

[32] T. Aoi, K. Yae, M. Nakagawa et al., "Generation of pluripotent stem cells from adult mouse liver and stomach cells," *Science*, vol. 321, no. 5889, pp. 699–702, 2008.

[33] J. Hanna, S. Markoulaki, P. Schorderet et al., "Direct reprogramming of terminally differentiated mature B lymphocytes to pluripotency," *Cell*, vol. 133, no. 2, pp. 250–264, 2008.

[34] K. Takahashi, K. Okita, M. Nakagawa, and S. Yamanaka, "Induction of pluripotent stem cells from fibroblast cultures," *Nature Protocols*, vol. 2, no. 12, pp. 3081–3089, 2007.

[35] K. Takahashi, K. Tanabe, M. Ohnuki et al., "Induction of pluripotent stem cells from adult human fibroblasts by defined factors," *Cell*, vol. 131, no. 5, pp. 861–872, 2007.

[36] S. Okamoto and M. Takahashi, "Induction of retinal pigment epithelial cells from monkey iPS cells," *Investigative Ophthalmology & Visual Science*, vol. 52, no. 12, pp. 8785–8790, 2011.

[37] Y. Li, Y. T. Tsai, C. W. Hsu et al., "Long-term safety and efficacy of human-induced pluripotent stem cell (iPS) grafts in a preclinical model of retinitis pigmentosa," *Molecular Medicine*, vol. 18, pp. 1312–1319, 2012.

[38] A. Garg, J. Yang, W. Lee, and S. H. Tsang, "Stem cell therapies in retinal disorders," *Cell*, vol. 6, no. 1, 2017.

[39] D. Ilic, "iPSC in the past decade: the Japanese dominance," *Regenerative Medicine*, vol. 11, no. 8, pp. 747–749, 2016.

[40] N. Wu and M. Doorenbos, "Induced pluripotent stem cells: development in the ophthalmologic field," *Stem Cells International*, vol. 2016, Article ID 2361763, 7 pages, 2016.

[41] A. E. Kuriyan, T. A. Albini, J. H. Townsend et al., "Vision loss after intravitreal injection of autologous "stem cells" for AMD," *The New England Journal of Medicine*, vol. 376, no. 11, pp. 1047–1053, 2017.

[42] I. Klimanskaya, J. Hipp, K. A. Rezai, M. West, A. Atala, and R. Lanza, "Derivation and comparative assessment of retinal pigment epithelium from human embryonic stem cells using transcriptomics," *Cloning and Stem Cells*, vol. 6, no. 3, pp. 217–245, 2004.

[43] R. D. Lund, S. Wang, I. Klimanskaya et al., "Human embryonic stem cell-derived cells rescue visual function in dystrophic RCS rats," *Cloning Stem Cells*, vol. 8, no. 3, pp. 189–199, 2006.

[44] B. Diniz, P. Thomas, B. Thomas et al., "Subretinal implantation of retinal pigment epithelial cells derived from human embryonic stem cells: improved survival when implanted as a monolayer," *Investigative Ophthalmology & Visual Science*, vol. 54, no. 7, pp. 5087–5096, 2013.

[45] B. B. Thomas, D. Zhu, L. Zhang et al., "Survival and functionality of hESC-derived retinal pigment epithelium cells cultured as a monolayer on polymer substrates transplanted in RCS rats," *Investigative Ophthalmology & Visual Science*, vol. 57, no. 6, pp. 2877–2887, 2016.

[46] S. R. Hynes and E. B. Lavik, "A tissue-engineered approach towards retinal repair: scaffolds for cell transplantation to the subretinal space," *Graefe's Archive for Clinical and Experimental Ophthalmology*, vol. 248, no. 6, pp. 763–778, 2010.

[47] K. Bharti, M. Rao, S. C. Hull et al., "Developing cellular therapies for retinal degenerative diseases," *Investigative Ophthalmology & Visual Science*, vol. 55, no. 2, pp. 1191–1202, 2014.

[48] T. Maeda, M. J. Lee, G. Palczewska et al., "Retinal pigmented epithelial cells obtained from human induced pluripotent stem cells possess functional visual cycle enzymes in vitro and in vivo," *The Journal of Biological Chemistry*, vol. 288, no. 48, pp. 34484–34493, 2013.

[49] B. A. Tucker, R. F. Mullins, L. M. Streb et al., "Patient-specific iPSC-derived photoreceptor precursor cells as a means to investigate retinitis pigmentosa," *eLife*, vol. 2, article e00824, 2013.

[50] D. E. Buchholz, S. T. Hikita, T. J. Rowland et al., "Derivation of functional retinal pigmented epithelisum from induced pluripotent stem cells," *Stem Cells (Dayton, Ohio)*, vol. 27, no. 10, pp. 2427–2434, 2009.

[51] A. J. Carr, A. Vugler, J. Lawrence et al., "Molecular characterization and functional analysis of phagocytosis by human embryonic stem cell-derived RPE cells using a novel human retinal assay," *Molecular Vision*, vol. 15, pp. 283–295, 2009.

[52] Y. Hu, L. Liu, B. Lu et al., "A novel approach for subretinal implantation of ultrathin substrates containing stem cell-derived retinal pigment epithelium monolayer," *Ophthalmic Research*, vol. 48, no. 4, pp. 186–191, 2012.

[53] D. A. Lamba, J. Gust, and T. A. Reh, "Transplantation of human embryonic stem cell-derived photoreceptors restores some visual function in Crx-deficient mice," *Cell Stem Cell*, vol. 4, no. 1, pp. 73–79, 2009.

[54] D. A. Lamba, A. McUsic, R. K. Hirata, P. R. Wang, D. Russell, and T. A. Reh, "Generation, purification and transplantation of photoreceptors derived from human induced pluripotent stem cells," *PLoS One*, vol. 5, no. 1, article e8763, 2010.

[55] B. A. Tucker, I. H. Park, S. D. Qi et al., "Transplantation of adult mouse iPS cell-derived photoreceptor precursors restores retinal structure and function in degenerative mice," *PLoS One*, vol. 6, no. 4, article e18992, 2011.

[56] D. M. Gamm and L. S. Wright, "From embryonic stem cells to mature photoreceptors," *Nature Biotechnology*, vol. 31, no. 8, pp. 712-713, 2013.

[57] B. L. Coles, B. Angenieux, T. Inoue et al., "Facile isolation and the characterization of human retinal stem cells," *Proceedings of the National Academy of Sciences of the United States of America*, vol. 101, no. 44, pp. 15772–15777, 2004.

[58] H. J. Klassen, T. F. Ng, Y. Kurimoto et al., "Multipotent retinal progenitors express developmental markers, differentiate into retinal neurons, and preserve light-mediated behavior," *Investigative Ophthalmology & Visual Science*, vol. 45, no. 11, pp. 4167–4173, 2004.

[59] J. Luo, P. Baranov, S. Patel et al., "Human retinal progenitor cell transplantation preserves vision," *The Journal of Biological Chemistry*, vol. 289, no. 10, pp. 6362–6371, 2014.

[60] D. A. Lamba, M. O. Karl, C. B. Ware, and T. A. Reh, "Efficient generation of retinal progenitor cells from human embryonic stem cells," *Proceedings of the National Academy of Sciences of the United States of America*, vol. 103, no. 34, pp. 12769–12774, 2006.

[61] B. A. Tucker, S. M. Redenti, C. Jiang et al., "The use of progenitor cell/biodegradable MMP2-PLGA polymer constructs to enhance cellular integration and retinal repopulation," *Biomaterials*, vol. 31, no. 1, pp. 9–19, 2010.

[62] S. Tao, C. Young, S. Redenti et al., "Survival, migration and differentiation of retinal progenitor cells transplanted on micro-machined poly(methyl methacrylate) scaffolds to the subretinal space," *Lab on a Chip*, vol. 7, no. 6, pp. 695–701, 2007.

[63] K. E. Kador and J. L. Goldberg, "Scaffolds and stem cells: delivery of cell transplants for retinal degenerations," *Expert Review of Ophthalmology*, vol. 7, no. 5, pp. 459–470, 2012.

[64] H. Klassen, J. F. Kiilgaard, T. Zahir et al., "Progenitor cells from the porcine neural retina express photoreceptor markers after transplantation to the subretinal space of allorecipients," *Stem Cells (Dayton, Ohio)*, vol. 25, no. 5, pp. 1222–1230, 2007.

[65] K. Warfvinge, J. F. Kiilgaard, E. B. Lavik et al., "Retinal progenitor cell xenografts to the pig retina: morphologic integration and cytochemical differentiation," *Archives of Ophthalmology*, vol. 123, no. 10, pp. 1385–1393, 2005.

[66] R. D. Lund, S. Wang, B. Lu et al., "Cells isolated from umbilical cord tissue rescue photoreceptors and visual functions in a rodent model of retinal disease," *Stem Cells (Dayton, Ohio)*, vol. 25, no. 3, pp. 602–611, 2007.

[67] R. D. Lund, P. Adamson, Y. Sauve et al., "Subretinal transplantation of genetically modified human cell lines attenuates loss of visual function in dystrophic rats," *Proceedings of the National Academy of Sciences of the United States of America*, vol. 98, no. 17, pp. 9942–9947, 2001.

[68] R. D. Lund, A. S. Kwan, D. J. Keegan, Y. Sauve, P. J. Coffey, and J. M. Lawrence, "Cell transplantation as a treatment for retinal disease," *Progress in Retinal and Eye Research*, vol. 20, no. 4, pp. 415–449, 2001.

[69] A. Gonzalez-Cordero, E. L. West, R. A. Pearson et al., "Photoreceptor precursors derived from three-dimensional embryonic stem cell cultures integrate and mature within adult degenerate retina," *Nature Biotechnology*, vol. 31, no. 8, pp. 741–747, 2013.

[70] J. Assawachananont, M. Mandai, S. Okamoto et al., "Transplantation of embryonic and induced pluripotent stem cell-derived 3D retinal sheets into retinal degenerative mice," *Stem Cell Reports*, vol. 2, no. 5, pp. 662–674, 2014.

[71] M. Mandai, M. Fujii, T. Hashiguchi et al., "iPSC-derived retina transplants improve vision in rd1 end-stage retinal-degeneration mice," *Stem Cell Reports*, vol. 8, no. 1, pp. 69–83, 2017.

[72] M. J. Seiler, B. T. Sagdullaev, G. Woch, B. B. Thomas, and R. B. Aramant, "Transsynaptic virus tracing from host brain to subretinal transplants," *The European Journal of Neuroscience*, vol. 21, no. 1, pp. 161–172, 2005.

[73] M. J. Seiler, B. B. Thomas, Z. Chen, R. Wu, S. R. Sadda, and R. B. Aramant, "Retinal transplants restore visual responses: trans-synaptic tracing from visually responsive sites labels transplant neurons," *The European Journal of Neuroscience*, vol. 28, no. 1, pp. 208–220, 2008.

[74] M. J. Seiler, R. B. Aramant, B. B. Thomas, Q. Peng, S. R. Sadda, and H. S. Keirstead, "Visual restoration and transplant connectivity in degenerate rats implanted with retinal progenitor sheets," *The European Journal of Neuroscience*, vol. 31, no. 3, pp. 508–520, 2010.

[75] H. Shirai, M. Mandai, K. Matsushita et al., "Transplantation of human embryonic stem cell-derived retinal tissue in two primate models of retinal degeneration," *Proceedings of the National Academy of Sciences of the United States of America*, vol. 113, no. 1, pp. E81–E90, 2016.

[76] D. M. Gamm, M. J. Phillips, and R. Singh, "Modeling retinal degenerative diseases with human iPS-derived cells: current status and future implications," vol. 8, no. 3, pp. 213–216, 2013.

[77] T. Nakano, S. Ando, N. Takata et al., "Self-formation of optic cups and storable stratified neural retina from human ESCs," *Cell Stem Cell*, vol. 10, no. 6, pp. 771–785, 2012.

[78] X. Zhong, C. Gutierrez, T. Xue et al., "Generation of three-dimensional retinal tissue with functional photoreceptors from human iPSCs," *Nature Communications*, vol. 5, p. 4047, 2014.

[79] M. E. McLaughlin, M. A. Sandberg, E. L. Berson, and T. P. Dryja, "Recessive mutations in the gene encoding the beta-subunit of rod phosphodiesterase in patients with retinitis pigmentosa," *Nature Genetics*, vol. 4, no. 2, pp. 130–134, 1993.

[80] C. H. Sung, C. Makino, D. Baylor, and J. Nathans, "A rhodopsin gene mutation responsible for autosomal dominant retinitis pigmentosa results in a protein that is defective in localization to the photoreceptor outer segment," *The Journal of Neuroscience*, vol. 14, no. 10, pp. 5818–5833, 1994.

[81] M. Frasson, J. A. Sahel, M. Fabre, M. Simonutti, H. Dreyfus, and S. Picaud, "Retinitis pigmentosa: rod photoreceptor rescue by a calcium-channel blocker in the rd mouse," *Nature Medicine*, vol. 5, no. 10, pp. 1183–1187, 1999.

[82] A. J. Jimenez, J. M. Garcia-Fernandez, B. Gonzalez, and R. G. Foster, "The spatio-temporal pattern of photoreceptor degeneration in the aged rd/rd mouse retina," *Cell and Tissue Research*, vol. 284, no. 2, pp. 193–202, 1996.

[83] B. Chang, N. L. Hawes, M. T. Pardue et al., "Two mouse retinal degenerations caused by missense mutations in the beta-subunit of rod cGMP phosphodiesterase gene," *Vision Research*, vol. 47, no. 5, pp. 624–633, 2007.

[84] Z. Y. Li, F. Wong, J. H. Chang et al., "Rhodopsin transgenic pigs as a model for human retinitis pigmentosa," *Investigative Ophthalmology & Visual Science*, vol. 39, no. 5, pp. 808–819, 1998.

[85] S. Machida, M. Kondo, J. A. Jamison et al., "P23H rhodopsin transgenic rat: correlation of retinal function with histopathology," *Investigative Ophthalmology & Visual Science*, vol. 41, no. 10, pp. 3200–3209, 2000.

[86] M. Kondo, T. Sakai, K. Komeima et al., "Generation of a transgenic rabbit model of retinal degeneration," *Investigative Ophthalmology & Visual Science*, vol. 50, no. 3, pp. 1371–1377, 2009.

[87] G. Martinez-Navarrete, M. J. Seiler, R. B. Aramant, L. Fernandez-Sanchez, I. Pinilla, and N. Cuenca, "Retinal degeneration in two lines of transgenic S334ter rats," *Experimental Eye Research*, vol. 92, no. 3, pp. 227–237, 2011.

[88] D. T. Organisciak and D. K. Vaughan, "Retinal light damage: mechanisms and protection," *Progress in Retinal and Eye Research*, vol. 29, no. 2, pp. 113–134, 2010.

[89] R. S. Shah, B. T. Soetikno, M. Lajko, and A. A. Fawzi, "A mouse model for laser-induced choroidal neovascularization," *Journal of Visualized Experiments*, vol. 106, article e53502, 2015.

[90] C. Graymore and K. Tansley, "Iodoacetate poisoning of the rat retina. I. Production of retinal degeneration," *The British Journal of Ophthalmology*, vol. 43, no. 3, pp. 177–185, 1959.

[91] Y. Y. Chen, S. L. Liu, D. P. Hu, Y. Q. Xing, and Y. Shen, "N -methyl- N -nitrosourea-induced retinal degeneration in mice," *Experimental Eye Research*, vol. 121, pp. 102–113, 2014.

[92] A. Tsubura, K. Yoshizawa, M. Kuwata, and N. Uehara, "Animal models for retinitis pigmentosa induced by MNU; disease progression, mechanisms and therapeutic trials," *Histology and Histopathology*, vol. 25, no. 7, pp. 933–944, 2010.

[93] A. Sorsby, "Experimental pigmentary degeneration of the retina by sodium iodate," *The British Journal of Ophthalmology*, vol. 25, no. 2, pp. 58–62, 1941.

[94] K. Kiuchi, K. Yoshizawa, N. Shikata, K. Moriguchi, and A. Tsubura, "Morphologic characteristics of retinal degeneration induced by sodium iodate in mice," *Current Eye Research*, vol. 25, no. 6, pp. 373–379, 2002.

[95] V. Enzmann, B. W. Row, Y. Yamauchi et al., "Behavioral and anatomical abnormalities in a sodium iodate-induced model of retinal pigment epithelium degeneration," *Experimental Eye Research*, vol. 82, no. 3, pp. 441–448, 2006.

[96] M. Carido, Y. Zhu, K. Postel et al., "Characterization of a mouse model with complete RPE loss and its use for RPE cell transplantation," *Investigative Ophthalmology & Visual Science*, vol. 55, no. 8, pp. 5431–5444, 2014.

[97] S. Dithmar, C. A. Curcio, Le NA, S. Brown, and H. E. Grossniklaus, "Ultrastructural changes in Bruch's membrane of apolipoprotein E-deficient mice," *Investigative Ophthalmology & Visual Science*, vol. 41, no. 8, pp. 2035–2042, 2000.

[98] J. Ambati, A. Anand, S. Fernandez et al., "An animal model of age-related macular degeneration in senescent Ccl-2- or Ccr-2-deficient mice," *Nature Medicine*, vol. 9, no. 11, pp. 1390–1397, 2003.

[99] M. Rudolf, B. Winkler, Z. Aherrahou, L. C. Doehring, P. Kaczmarek, and U. Schmidt-Erfurth, "Increased expression of vascular endothelial growth factor associated with accumulation of lipids in Bruch's membrane of LDL receptor knockout mice," *The British Journal of Ophthalmology*, vol. 89, no. 12, pp. 1627–1630, 2005.

[100] Y. Imamura, S. Noda, K. Hashizume et al., "Drusen, choroidal neovascularization, and retinal pigment epithelium dysfunction in SOD1-deficient mice: a model of age-related macular degeneration," *Proceedings of the National Academy of Sciences of the United States of America*, vol. 103, no. 30, pp. 11282–11287, 2006.

[101] J. Tuo, C. M. Bojanowski, M. Zhou et al., "Murine ccl2/cx3cr1 deficiency results in retinal lesions mimicking human age-related macular degeneration," *Investigative Ophthalmology & Visual Science*, vol. 48, no. 8, pp. 3827–3836, 2007.

[102] U. F. Luhmann, S. Robbie, P. M. Munro et al., "The drusen-like phenotype in aging Ccl2-knockout mice is caused by an accelerated accumulation of swollen autofluorescent subretinal macrophages," *Investigative Ophthalmology & Visual Science*, vol. 50, no. 12, pp. 5934–5943, 2009.

[103] Z. Zhao, Y. Chen, J. Wang et al., "Age-related retinopathy in NRF2-deficient mice," *PLoS One*, vol. 6, no. 4, article e19456, 2011.

[104] R. Allikmets, "Simple and complex ABCR: genetic predisposition to retinal disease," *American Journal of Human Genetics*, vol. 67, no. 4, pp. 793–799, 2000.

[105] F. P. Cremers, D. J. van de Pol, M. van Driel et al., "Autosomal recessive retinitis pigmentosa and cone-rod dystrophy caused by splice site mutations in the Stargardt's disease gene ABCR," *Human Molecular Genetics*, vol. 7, no. 3, pp. 355–362, 1998.

[106] R. Allikmets, N. Singh, H. Sun et al., "A photoreceptor cell-specific ATP-binding transporter gene (ABCR) is mutated in recessive Stargardt macular dystrophy," *Nature Genetics*, vol. 15, no. 3, pp. 236–246, 1997.

[107] J. Weng, N. L. Mata, S. M. Azarian, R. T. Tzekov, D. G. Birch, and G. H. Travis, "Insights into the function of Rim protein in photoreceptors and etiology of Stargardt's disease from the phenotype in abcr knockout mice," *Cell*, vol. 98, no. 1, pp. 13–23, 1999.

[108] N. L. Mata, J. Weng, and G. H. Travis, "Biosynthesis of a major lipofuscin fluorophore in mice and humans with ABCR-mediated retinal and macular degeneration," *Proceedings of the National Academy of Sciences of the United States of America*, vol. 97, no. 13, pp. 7154–7159, 2000.

[109] N. F. Shroyer, R. A. Lewis, A. N. Yatsenko, T. G. Wensel, and J. R. Lupski, "Cosegregation and functional analysis of mutant ABCR (ABCA4) alleles in families that manifest both Stargardt disease and age-related macular degeneration," *Human Molecular Genetics*, vol. 10, no. 23, pp. 2671–2678, 2001.

[110] P. Charbel Issa and A. R. Barnard, "Rescue of the Stargardt phenotype in Abca4 knockout mice through inhibition of vitamin A dimerization," *Proceedings of the National Academy of Sciences of the United States of America*, vol. 112, no. 27, pp. 8415–8420, 2015.

[111] R. G. Weleber, M. Michaelides, K. M. Trzupek, N. B. Stover, and E. M. Stone, "The phenotype of severe early childhood onset retinal dystrophy (SECORD) from mutation of RPE65 and differentiation from Leber congenital amaurosis," *Investigative Ophthalmology & Visual Science*, vol. 52, no. 1, pp. 292–302, 2011.

[112] B. Rohrer, P. Goletz, S. Znoiko et al., "Correlation of regenerable opsin with rod ERG signal in Rpe65−/− mice during development and aging," *Investigative Ophthalmology & Visual Science*, vol. 44, no. 1, pp. 310–315, 2003.

[113] S. L. Znoiko, B. Rohrer, K. Lu, H. R. Lohr, R. K. Crouch, and J. X. Ma, "Downregulation of cone-specific gene expression and degeneration of cone photoreceptors in the Rpe65−/− mouse at early ages," *Investigative Ophthalmology & Visual Science*, vol. 46, no. 4, pp. 1473–1479, 2005.

[114] J. E. Olsson, J. W. Gordon, B. S. Pawlyk et al., "Transgenic mice with a rhodopsin mutation (Pro23His): a mouse model of autosomal dominant retinitis pigmentosa," *Neuron*, vol. 9, no. 5, pp. 815–830, 1992.

[115] A. S. Lewin, B. Rossmiller, and H. Mao, "Gene augmentation for adRP mutations in RHO," *Cold Spring Harbor Perspectives in Medicine*, vol. 4, no. 9, article a017400, 2014.

[116] K. Zhang, M. Kniazeva, M. Han et al., "A 5-bp deletion in ELOVL4 is associated with two related forms of autosomal dominant macular dystrophy," *Nature Genetics*, vol. 27, no. 1, pp. 89–93, 2001.

[117] A. O. Edwards, L. A. Donoso, and R. Ritter 3rd, "A novel gene for autosomal dominant Stargardt-like macular dystrophy with homology to the SUR4 protein family," *Investigative Ophthalmology & Visual Science*, vol. 42, no. 11, pp. 2652–2663, 2001.

[118] G. Karan, C. Lillo, Z. Yang et al., "Lipofuscin accumulation, abnormal electrophysiology, and photoreceptor degeneration in mutant ELOVL4 transgenic mice: a model for macular degeneration," *Proceedings of the National Academy of Sciences of the United States of America*, vol. 102, no. 11, pp. 4164–4169, 2005.

[119] P. D. Westenskow, T. Kurihara, S. Bravo et al., "Performing subretinal injections in rodents to deliver retinal pigment epithelium cells in suspension," *Journal of Visualized Experiments*, vol. 95, article 52247, 2015.

[120] S. Arai, B. B. Thomas, M. J. Seiler et al., "Restoration of visual responses following transplantation of intact retinal sheets in rd mice," *Experimental Eye Research*, vol. 79, no. 3, pp. 331–341, 2004.

[121] S. Remtulla and P. E. Hallett, "A schematic eye for the mouse, and comparisons with the rat," *Vision Research*, vol. 25, no. 1, pp. 21–31, 1985.

[122] P. M. D'Cruz, D. Yasumura, J. Weir et al., "Mutation of the receptor tyrosine kinase gene Mertk in the retinal dystrophic RCS rat," *Human Molecular Genetics*, vol. 9, no. 4, pp. 645–651, 2000.

[123] D. Vollrath, W. Feng, J. L. Duncan et al., "Correction of the retinal dystrophy phenotype of the RCS rat by viral gene transfer of Mertk," *Proceedings of the National Academy of Sciences of the United States of America*, vol. 98, no. 22, pp. 12584–12589, 2001.

[124] E. F. Nandrot and E. M. Dufour, "Mertk in daily retinal phagocytosis: a history in the making," *Advances in Experimental Medicine and Biology*, vol. 664, pp. 133–140, 2010.

[125] G. Li, B. De La Garza, Y. Y. Shih, E. R. Muir, and T. Q. Duong, "Layer-specific blood-flow MRI of retinitis pigmentosa in RCS rats," *Experimental Eye Research*, vol. 101, pp. 90–96, 2012.

[126] T. J. McGill, R. M. Douglas, R. D. Lund, and G. T. Prusky, "Quantification of spatial vision in the Royal College of Surgeons rat," *Investigative Ophthalmology & Visual Science*, vol. 45, no. 3, pp. 932–936, 2004.

[127] A. J. Carr, A. A. Vugler, S. T. Hikita et al., "Protective effects of human iPS-derived retinal pigment epithelium cell transplantation in the retinal dystrophic rat," *PLoS One*, vol. 4, no. 12, article e8152, 2009.

[128] I. Pinilla, N. Cuenca, Y. Sauve, S. Wang, and R. D. Lund, "Preservation of outer retina and its synaptic connectivity following subretinal injections of human RPE cells in the Royal College of Surgeons rat," *Experimental Eye Research*, vol. 85, no. 3, pp. 381–392, 2007.

[129] S. Wang, B. Lu, S. Girman, T. Holmes, N. Bischoff, and R. D. Lund, "Morphological and functional rescue in RCS rats after RPE cell line transplantation at a later stage of degeneration," *Investigative Ophthalmology & Visual Science*, vol. 49, no. 1, pp. 416–421, 2008.

[130] U. C. Park, M. S. Cho, J. H. Park et al., "Subretinal transplantation of putative retinal pigment epithelial cells derived from human embryonic stem cells in rat retinal degeneration model," *Clinical and Experimental Reproductive Medicine*, vol. 38, no. 4, pp. 216–221, 2011.

[131] O. S. Kozhevnikova, E. E. Korbolina, N. I. Ershov, and N. G. Kolosova, "Rat retinal transcriptome: effects of aging and AMD-like retinopathy," *Cell Cycle*, vol. 12, no. 11, pp. 1745–1761, 2013.

[132] A. M. Markovets, V. B. Saprunova, A. A. Zhdankina, A. Fursova, L. E. Bakeeva, and N. G. Kolosova, "Alterations

of retinal pigment epithelium cause AMD-like retinopathy in senescence-accelerated OXYS rats," *Aging (Albany, New York)*, vol. 3, no. 1, pp. 44–54, 2011.

[133] N. Cuenca, I. Pinilla, Y. Sauve, B. Lu, S. Wang, and R. D. Lund, "Regressive and reactive changes in the connectivity patterns of rod and cone pathways of P23H transgenic rat retina," *Neuroscience*, vol. 127, no. 2, pp. 301–317, 2004.

[134] C. Liu, Y. Li, M. Peng, A. M. Laties, and R. Wen, "Activation of caspase-3 in the retina of transgenic rats with the rhodopsin mutation s334ter during photoreceptor degeneration," *The Journal of Neuroscience*, vol. 19, no. 12, pp. 4778–4785, 1999.

[135] A. Ray, G. J. Sun, L. Chan, N. M. Grzywacz, J. Weiland, and E. J. Lee, "Morphological alterations in retinal neurons in the S334ter-line3 transgenic rat," *Cell and Tissue Research*, vol. 339, no. 3, pp. 481–491, 2010.

[136] C. L. Zhu, Y. Ji, E. J. Lee, and N. M. Grzywacz, "Spatiotemporal pattern of rod degeneration in the S334ter-line-3 rat model of retinitis pigmentosa," *Cell and Tissue Research*, vol. 351, no. 1, pp. 29–40, 2013.

[137] B. T. Sagdullaev, R. B. Aramant, M. J. Seiler, G. Woch, and M. A. McCall, "Retinal transplantation-induced recovery of retinotectal visual function in a rodent model of retinitis pigmentosa," *Investigative Ophthalmology & Visual Science*, vol. 44, no. 4, pp. 1686–1695, 2003.

[138] B. B. Thomas, M. J. Seiler, S. R. Sadda, and R. B. Aramant, "Superior colliculus responses to light - preserved by transplantation in a slow degeneration rat model," *Experimental Eye Research*, vol. 79, no. 1, pp. 29–39, 2004.

[139] Q. Peng, B. B. Thomas, R. B. Aramant, Z. Chen, S. R. Sadda, and M. J. Seiler, "Structure and function of embryonic rat retinal sheet transplants," *Current Eye Research*, vol. 32, no. 9, pp. 781–789, 2007.

[140] K. Gregory-Evans, F. Chang, M. D. Hodges, and C. Y. Gregory-Evans, "Ex vivo gene therapy using intravitreal injection of GDNF-secreting mouse embryonic stem cells in a rat model of retinal degeneration," *Molecular Vision*, vol. 15, pp. 962–973, 2009.

[141] A. Yanai, U. O. Hafeli, A. L. Metcalfe et al., "Focused magnetic stem cell targeting to the retina using superparamagnetic iron oxide nanoparticles," *Cell Transplantation*, vol. 21, no. 6, pp. 1137–1148, 2012.

[142] A. Santos, M. S. Humayun, E. de Juan Jr. et al., "Preservation of the inner retina in retinitis pigmentosa. A morphometric analysis," *Archives of Ophthalmology*, vol. 115, no. 4, pp. 511–515, 1997.

[143] M. J. Seiler, R. B. Aramant, M. K. Jones, D. L. Ferguson, E. C. Bryda, and H. S. Keirstead, "A new immunodeficient pigmented retinal degenerate rat strain to study transplantation of human cells without immunosuppression," *Graefe's Archive for Clinical and Experimental Ophthalmology*, vol. 252, no. 7, pp. 1079–1092, 2014.

[144] B. Thomas, C. Shih, D. Zhu, J. Martinez, D. Hinton, and M. Humayun, *A new Immunodeficient Dystrophic RCS rat Model for Transplantation Studies Using Human Derived Cells Assosciation for Research in Vision and Ophthalmology; 2016*, Seattle, WA, USA, 2016.

[145] S. Veleri, C. H. Lazar, B. Chang, P. A. Sieving, E. Banin, and A. Swaroop, "Biology and therapy of inherited retinal degenerative disease: insights from mouse models," *Disease Models & Mechanisms*, vol. 8, no. 2, pp. 109–129, 2015.

[146] E. V. Famiglietti and S. J. Sharpe, "Regional topography of rod and immunocytochemically characterized "blue" and "green" cone photoreceptors in rabbit retina," *Visual Neuroscience*, vol. 12, no. 6, pp. 1151–1175, 1995.

[147] B. Juliusson, A. Bergstrom, P. Rohlich, B. Ehinger, T. van Veen, and A. Szel, "Complementary cone fields of the rabbit retina," *Investigative Ophthalmology & Visual Science*, vol. 35, no. 3, pp. 811–818, 1994.

[148] K. W. Gjorloff, F. Ghosh, S. Andréasson, and B. Ehinger, "Standardized full-field and multifocal electroretinography in rabbits," *Investigative Ophthalmology & Visual Science*, vol. 44, no. 13, p. 2695, 2003.

[149] B. W. Jones, M. Kondo, H. Terasaki et al., "Retinal remodeling in the Tg P347L rabbit, a large-eye model of retinal degeneration," *The Journal of Comparative Neurology*, vol. 519, no. 14, pp. 2713–2733, 2011.

[150] S. Ueno, T. Koyasu, T. Kominami et al., "Focal cone ERGs of rhodopsin Pro347Leu transgenic rabbits," *Vision Research*, vol. 91, pp. 118–123, 2013.

[151] B. J. Cho, J. M. Seo, H. G. Yu, and H. Chung, "Monocular retinal degeneration induced by intravitreal injection of sodium iodate in rabbit eyes," *Japanese Journal of Ophthalmology*, vol. 60, no. 3, pp. 226–237, 2016.

[152] S. Rosch, C. Werner, F. Muller, and P. Walter, "Photoreceptor degeneration by intravitreal injection of N-methyl-N-nitrosourea (MNU) in rabbits: a pilot study," *Graefe's Archive for Clinical and Experimental Ophthalmology*, vol. 255, no. 2, pp. 317–331, 2017.

[153] S. Petrus-Reurer, H. Bartuma, M. Aronsson et al., "Integration of subretinal suspension transplants of human embryonic stem cell-derived retinal pigment epithelial cells in a large-eyed model of geographic atrophy," *Investigative Ophthalmology & Visual Science*, vol. 58, no. 2, pp. 1314–1322, 2017.

[154] R. Curtis, K. C. Barnett, and A. Leon, "An early-onset retinal dystrophy with dominant inheritance in the Abyssinian cat. Clinical and pathological findings," *Investigative Ophthalmology & Visual Science*, vol. 28, no. 1, pp. 131–139, 1987.

[155] K. Narfstrom, "Hereditary progressive retinal atrophy in the Abyssinian cat," *The Journal of Heredity*, vol. 74, no. 4, pp. 273–276, 1983.

[156] M. Menotti-Raymond, V. A. David, A. A. Schaffer et al., "Mutation in CEP290 discovered for cat model of human retinal degeneration," *The Journal of Heredity*, vol. 98, no. 3, pp. 211–220, 2007.

[157] K. Narfstrom, V. David, O. Jarret et al., "Retinal degeneration in the Abyssinian and Somali cat (rdAc): correlation between genotype and phenotype and rdAc allele frequency in two continents," *Veterinary Ophthalmology*, vol. 12, no. 5, pp. 285–291, 2009.

[158] M. W. Seeliger and K. Narfstrom, "Functional assessment of the regional distribution of disease in a cat model of hereditary retinal degeneration," *Investigative Ophthalmology & Visual Science*, vol. 41, no. 7, pp. 1998–2005, 2000.

[159] L. M. Occelli, N. M. Tran, K. Narfstrom, S. Chen, and S. M. Petersen-Jones, "CrxRdy cat: a large animal model for CRX-associated Leber congenital amaurosis," *Investigative Ophthalmology & Visual Science*, vol. 57, no. 8, pp. 3780–3792, 2016.

[160] H. Rah, D. J. Maggs, T. N. Blankenship, K. Narfstrom, and L. A. Lyons, "Early-onset, autosomal recessive,

progressive retinal atrophy in Persian cats," *Investigative Ophthalmology & Visual Science*, vol. 46, no. 5, pp. 1742–1747, 2005.

[161] Y. Nan, Q. Zhang, C. Ren et al., "Functional evaluation of iodoacetic acid induced photoreceptor degeneration in the cat," *Science China Life Sciences*, vol. 56, no. 6, pp. 524–530, 2013.

[162] M. J. Seiler, R. B. Aramant, M. W. Seeliger, R. Bragadottir, M. Mahoney, and K. Narfstrom, "Functional and structural assessment of retinal sheet allograft transplantation in feline hereditary retinal degeneration," *Veterinary Ophthalmology*, vol. 12, no. 3, pp. 158–169, 2009.

[163] K. Shibuya, M. Tomohiro, S. Sasaki, and S. Otake, "Characteristics of structures and lesions of the eye in laboratory animals used in toxicity studies," *Journal of Toxicologic Pathology*, vol. 28, no. 4, pp. 181–188, 2015.

[164] G. G. Cloyd, M. Wyman, J. A. Shadduck, M. J. Winrow, and G. R. Johnson, "Ocular toxicity studies with zinc pyridinethione," *Toxicology and Applied Pharmacology*, vol. 45, no. 3, pp. 771–782, 1978.

[165] D. M. Schiavo, D. P. Sinha, H. E. Black et al., "Tapetal changes in beagle dogs. I. Ocular changes after oral administration of a beta-adrenergic blocking agent—SCH 19927," *Toxicology and Applied Pharmacology*, vol. 72, no. 2, pp. 187–194, 1984.

[166] T. Massa, G. J. Davis, D. Schiavo et al., "Tapetal changes in beagle dogs. II. Ocular changes after intravenous administration of a macrolide antibiotic—rosaramicin," *Toxicology and Applied Pharmacology*, vol. 72, no. 2, pp. 195–200, 1984.

[167] J. H. Fortner, W. B. Milisen, G. R. Lundeen, A. B. Jakowski, and P. M. Marsh, "Tapetal effect of an azalide antibiotic following oral administration in beagle dogs," *Fundamental and applied toxicology: Official Journal of the Society of Toxicology*, vol. 21, no. 2, pp. 164–173, 1993.

[168] J. E. Dillberger, R. L. Peiffer, M. J. Dykstra, M. O'Mara, and D. K. Patel, "The experimental antipsychotic agent 1192U90 targets tapetum lucidum in canine eyes," *Toxicologic Pathology*, vol. 24, no. 5, pp. 595–601, 1996.

[169] J. W. Kijas, A. V. Cideciyan, T. S. Aleman et al., "Naturally occurring rhodopsin mutation in the dog causes retinal dysfunction and degeneration mimicking human dominant retinitis pigmentosa," *Proceedings of the National Academy of Sciences of the United States of America*, vol. 99, no. 9, pp. 6328–6333, 2002.

[170] A. V. Cideciyan, S. G. Jacobson, T. S. Aleman et al., "In vivo dynamics of retinal injury and repair in the rhodopsin mutant dog model of human retinitis pigmentosa," *Proceedings of the National Academy of Sciences of the United States of America*, vol. 102, no. 14, pp. 5233–5238, 2005.

[171] S. Iwabe, G. S. Ying, G. D. Aguirre, and W. A. Beltran, "Assessment of visual function and retinal structure following acute light exposure in the light sensitive T4R rhodopsin mutant dog," *Experimental Eye Research*, vol. 146, pp. 341–353, 2016.

[172] R. M. Petters, C. A. Alexander, K. D. Wells et al., "Genetically engineered large animal model for studying cone photoreceptor survival and degeneration in retinitis pigmentosa," *Nature Biotechnology*, vol. 15, no. 10, pp. 965–970, 1997.

[173] M. O. Tso, W. W. Li, C. Zhang et al., "A pathologic study of degeneration of the rod and cone populations of the rhodopsin Pro347Leu transgenic pigs," *Transactions of the American Ophthalmological Society*, vol. 95, pp. 467–483, 1997.

[174] L. C. Shaw, A. Skold, F. Wong, R. Petters, W. W. Hauswirth, and A. S. Lewin, "An allele-specific hammerhead ribozyme gene therapy for a porcine model of autosomal dominant retinitis pigmentosa," *Molecular Vision*, vol. 7, pp. 6–13, 2001.

[175] T. W. Kraft, D. Allen, R. M. Petters, Y. Hao, Y. W. Peng, and F. Wong, "Altered light responses of single rod photoreceptors in transgenic pigs expressing P347L or P347S rhodopsin," *Molecular Vision*, vol. 11, pp. 1246–1256, 2005.

[176] J. W. Ross, J. P. Fernandez de Castro, J. Zhao et al., "Generation of an inbred miniature pig model of retinitis pigmentosa," *Investigative Ophthalmology & Visual Science*, vol. 53, no. 1, pp. 501–507, 2012.

[177] F. Ghosh, F. Wong, K. Johansson, A. Bruun, and R. M. Petters, "Transplantation of full-thickness retina in the rhodopsin transgenic pig," *Retina (Philadelphia, Pennsylvania)*, vol. 24, no. 1, pp. 98–109, 2004.

[178] H. Klassen, J. F. Kiilgaard, K. Warfvinge et al., "Photoreceptor differentiation following transplantation of allogeneic retinal progenitor cells to the dystrophic rhodopsin Pro347Leu transgenic pig," *Stem Cells International*, vol. 2012, Article ID 939801, 9 pages, 2012.

[179] M. J. Koss, P. Falabella, F. R. Stefanini et al., "Subretinal implantation of a monolayer of human embryonic stem cell-derived retinal pigment epithelium: a feasibility and safety study in Yucatan minipigs," *Graefe's Archive for Clinical and Experimental Ophthalmology*, vol. 254, no. 8, pp. 1553–1565, 2016.

[180] E. H. Sohn, C. Jiao, E. Kaalberg et al., "Allogenic iPSC-derived RPE cell transplants induce immune response in pigs: a pilot study," *Scientific Reports*, vol. 5, article 11791, 2015.

[181] C. Lane, M. Boulton, and J. Marshall, "Transplantation of retinal pigment epithelium using a pars plana approach," *Eye (London, England)*, vol. 3, Part 1, pp. 27–32, 1989.

[182] L. V. Del Priore, R. Hornbeck, H. J. Kaplan et al., "Debridement of the pig retinal pigment epithelium in vivo," *Archives of Ophthalmology*, vol. 113, no. 7, pp. 939–944, 1995.

[183] N. B. Sorensen, N. Lassota, M. V. Kyhn et al., "Functional recovery after experimental RPE debridement, mfERG studies in a porcine model," *Graefe's Archive for Clinical and Experimental Ophthalmology*, vol. 251, no. 10, pp. 2319–2325, 2013.

[184] M. G. Nicolas, K. Fujiki, K. Murayama et al., "Studies on the mechanism of early onset macular degeneration in cynomolgus (Macaca fascicularis) monkeys. I. Abnormal concentrations of two proteins in the retina," *Experimental Eye Research*, vol. 62, no. 3, pp. 211–219, 1996.

[185] M. T. Suzuki, K. Terao, and Y. Yoshikawa, "Familial early onset macular degeneration in cynomolgus monkeys (Macaca fascicularis)," *Primates*, vol. 44, no. 3, pp. 291–294, 2003.

[186] S. Umeda, R. Ayyagari, R. Allikmets et al., "Early-onset macular degeneration with drusen in a cynomolgus monkey (Macaca fascicularis) pedigree: exclusion of 13 candidate genes and loci," *Investigative Ophthalmology & Visual Science*, vol. 46, no. 2, pp. 683–691, 2005.

[187] S. Umeda, M. T. Suzuki, H. Okamoto et al., "Molecular composition of drusen and possible involvement of anti-retinal autoimmunity in two different forms of macular degeneration in cynomolgus monkey (Macaca fascicularis)," *The FASEB Journal*, vol. 19, no. 12, pp. 1683–1685, 2005.

[188] P. J. Francis, S. Wang, Y. Zhang et al., "Subretinal transplantation of forebrain progenitor cells in nonhuman primates: survival and intact retinal function," *Investigative Ophthalmology & Visual Science*, vol. 50, no. 7, pp. 3425–3431, 2009.

[189] K. K. Singh, M. Krawczak, W. W. Dawson, and J. Schmidtke, "Association of HTRA1 and ARMS2 gene variation with drusen formation in rhesus macaques," *Experimental Eye Research*, vol. 88, no. 3, pp. 479–482, 2009.

[190] C. J. Zeiss, "Animals as models of age-related macular degeneration: an imperfect measure of the truth," *Veterinary Pathology*, vol. 47, no. 3, pp. 396–413, 2010.

[191] W. K. Noell, "The impairment of visual cell structure by iodoacetate," *Journal of Cellular and Comparative Physiology*, vol. 40, no. 1, pp. 25–55, 1952.

[192] D. Fuller, R. Machemer, and R. W. Knighton, "Retinal damage produced by intraocular fiber optic light," *American Journal of Ophthalmology*, vol. 85, no. 4, pp. 519–537, 1978.

[193] J. M. Strazzeri, J. J. Hunter, B. D. Masella et al., "Focal damage to macaque photoreceptors produces persistent visual loss," *Experimental Eye Research*, vol. 119, pp. 88–96, 2014.

[194] E. W. Lankau, P. V. Turner, R. J. Mullan, and G. G. Galland, "Use of nonhuman primates in research in North America," *Journal of the American Association for Laboratory Animal Science*, vol. 53, no. 3, pp. 278–282, 2014.

[195] A. Varki and T. K. Altheide, "Comparing the human and chimpanzee genomes: searching for needles in a haystack," *Genome Research*, vol. 15, no. 12, pp. 1746–1758, 2005.

[196] H. Kamao, M. Mandai, S. Okamoto et al., "Characterization of human induced pluripotent stem cell-derived retinal pigment epithelium cell sheets aiming for clinical application," *Stem Cell Reports*, vol. 2, no. 2, pp. 205–218, 2014.

[197] B. B. Thomas, S. Arai, Y. Ikai et al., "Retinal transplants evaluated by optical coherence tomography in photoreceptor degenerate rats," *Journal of Neuroscience Methods*, vol. 151, no. 2, pp. 186–193, 2006.

[198] M. J. Seiler, B. Rao, R. B. Aramant et al., "Three-dimensional optical coherence tomography imaging of retinal sheet implants in live rats," *Journal of Neuroscience Methods*, vol. 188, no. 2, pp. 250–257, 2010.

[199] T. Ilmarinen, H. Hiidenmaa, P. Koobi et al., "Ultrathin polyimide membrane as cell carrier for subretinal transplantation of human embryonic stem cell derived retinal pigment epithelium," *PLoS One*, vol. 10, no. 11, article e0143669, 2015.

[200] C. R. Laver, A. L. Metcalfe, L. Szczygiel, A. Yanai, M. V. Sarunic, and K. Gregory-Evans, "Bimodal in vivo imaging provides early assessment of stem-cell-based photoreceptor engraftment," *Eye (London, England)*, vol. 29, no. 5, pp. 681–690, 2015.

[201] S. Al-Nawaiseh, F. Thieltges, Z. Liu et al., "A step by step protocol for subretinal surgery in rabbits," *Journal of Visualized Experiments*, vol. 115, 2016.

[202] P. Zhang, A. Zam, Y. Jian et al., "In vivo wide-field multispectral scanning laser ophthalmoscopy-optical coherence tomography mouse retinal imager: longitudinal imaging of ganglion cells, microglia, and Muller glia, and mapping of the mouse retinal and choroidal vasculature," *Journal of Biomedical Optics*, vol. 20, no. 12, article 126005, 2015.

[203] R. M. Ribeiro, A. Oregon, B. Diniz et al., "In vivo detection of hESC-RPE cells via confocal near-infrared fundus reflectance," *Ophthalmic Surgery, Lasers and Imaging Retina*, vol. 44, no. 4, pp. 380–384, 2013.

[204] M. S. Silverman, S. E. Hughes, T. L. Valentino, and Y. Liu, "Photoreceptor transplantation: anatomic, electrophysiologic, and behavioral evidence for the functional reconstruction of retinas lacking photoreceptors," *Experimental Neurology*, vol. 115, no. 1, pp. 87–94, 1992.

[205] S. V. Girman, S. Wang, and R. D. Lund, "Cortical visual functions can be preserved by subretinal RPE cell grafting in RCS rats," *Vision Research*, vol. 43, no. 17, pp. 1817–1827, 2003.

[206] C. Gias, M. Jones, D. Keegan et al., "Preservation of visual cortical function following retinal pigment epithelium transplantation in the RCS rat using optical imaging techniques," *The European Journal of Neuroscience*, vol. 25, no. 7, pp. 1940–1948, 2007.

[207] L. Q. Jiang and D. Hamasaki, "Corneal electroretinographic function rescued by normal retinal pigment epithelial grafts in retinal degenerative Royal College of Surgeons rats," *Investigative Ophthalmology & Visual Science*, vol. 35, no. 13, pp. 4300–4309, 1994.

[208] Y. Sauve, I. Pinilla, and R. D. Lund, "Partial preservation of rod and cone ERG function following subretinal injection of ARPE-19 cells in RCS rats," *Vision Research*, vol. 46, no. 8-9, pp. 1459–1472, 2006.

[209] T. U. Krohne, P. D. Westenskow, T. Kurihara et al., "Generation of retinal pigment epithelial cells from small molecules and OCT4 reprogrammed human induced pluripotent stem cells," *Stem Cells Translational Medicine*, vol. 1, no. 2, pp. 96–109, 2012.

[210] D. C. Hood, L. J. Frishman, S. Saszik, and S. Viswanathan, "Retinal origins of the primate multifocal ERG: implications for the human response," *Investigative Ophthalmology & Visual Science*, vol. 43, no. 5, pp. 1673–1685, 2002.

[211] S. L. Ball and H. M. Petry, "Noninvasive assessment of retinal function in rats using multifocal electroretinography," *Investigative Ophthalmology & Visual Science*, vol. 41, no. 2, pp. 610–617, 2000.

[212] R. Siminoff, H. O. Schwassmann, and L. Kruger, "An electrophysiological study of the visual projection to the superior colliculus of the rat," *The Journal of Comparative Neurology*, vol. 127, no. 4, pp. 435–444, 1966.

[213] T. J. McGill, G. T. Prusky, R. M. Douglas et al., "Discordant anatomical, electrophysiological, and visual behavioral profiles of retinal degeneration in rat models of retinal degenerative disease," *Investigative Ophthalmology & Visual Science*, vol. 53, no. 10, pp. 6232–6244, 2012.

[214] P. B. Yang, M. J. Seiler, R. B. Aramant et al., "Trophic factors GDNF and BDNF improve function of retinal sheet transplants," *Experimental Eye Research*, vol. 91, no. 5, pp. 727–738, 2010.

[215] A. Cowey and C. Franzini, "The retinal origin of uncrossed optic nerve fibres in rats and their role in visual discrimination," *Experimental Brain Research*, vol. 35, no. 3, pp. 443–455, 1979.

[216] B. B. Thomas, D. Shi, K. Khine, L. A. Kim, and S. R. Sadda, "Modulatory influence of stimulus parameters on optokinetic head-tracking response," *Neuroscience Letters*, vol. 479, no. 2, pp. 92–96, 2010.

[217] B. B. Thomas, M. J. Seiler, S. R. Sadda, P. J. Coffey, and R. B. Aramant, "Optokinetic test to evaluate visual acuity of each eye independently," *Journal of Neuroscience Methods*, vol. 138, no. 1-2, pp. 7–13, 2004.

[218] R. M. Douglas, N. M. Alam, B. D. Silver, T. J. McGill, W. W. Tschetter, and G. T. Prusky, "Independent visual threshold measurements in the two eyes of freely moving rats and mice using a virtual-reality optokinetic system," *Visual Neuroscience*, vol. 22, no. 5, pp. 677–684, 2005.

[219] T. J. McGill, B. Cottam, B. Lu et al., "Transplantation of human central nervous system stem cells - neuroprotection in retinal degeneration," *The European Journal of Neuroscience*, vol. 35, no. 3, pp. 468–477, 2012.

[220] S. Wang, B. Lu, S. Girman et al., "Non-invasive stem cell therapy in a rat model for retinal degeneration and vascular pathology," *PLoS One*, vol. 5, no. 2, article e9200, 2010.

[221] G. T. Prusky, P. W. West, and R. M. Douglas, "Behavioral assessment of visual acuity in mice and rats," *Vision Research*, vol. 40, no. 16, pp. 2201–2209, 2000.

[222] G. T. Prusky, K. T. Harker, R. M. Douglas, and I. Q. Whishaw, "Variation in visual acuity within pigmented, and between pigmented and albino rat strains," *Behavioural Brain Research*, vol. 136, no. 2, pp. 339–348, 2002.

[223] B. B. Thomas, D. M. Samant, M. J. Seiler et al., "Behavioral evaluation of visual function of rats using a visual discrimination apparatus," *Journal of Neuroscience Methods*, vol. 162, no. 1-2, pp. 84–90, 2007.

[224] S. Sugita, Y. Iwasaki, K. Makabe et al., "Lack of T cell response to iPSC-derived retinal pigment epithelial cells from HLA homozygous donors," *Stem Cell Reports*, vol. 7, no. 4, pp. 619–634, 2016.

[225] P. V. Algvere, "Clinical possibilities in retinal pigment epithelial transplantations," *Acta Ophthalmologica Scandinavica*, vol. 75, no. 1, p. 1, 1997.

[226] J. M. Weisz, M. S. Humayun, E. De Juan Jr. et al., "Allogenic fetal retinal pigment epithelial cell transplant in a patient with geographic atrophy," *Retina (Philadelphia, Pennsylvania)*, vol. 19, no. 6, pp. 540–545, 1999.

[227] G. A. Peyman, K. J. Blinder, C. L. Paris, W. Alturki, N. C. Nelson Jr., and U. Desai, "A technique for retinal pigment epithelium transplantation for age-related macular degeneration secondary to extensive subfoveal scarring," *Ophthalmic Surgery*, vol. 22, no. 2, pp. 102–108, 1991.

[228] S. Sheldon and K. Poulton, "HLA typing and its influence on organ transplantation," *Methods in Molecular Biology (Clifton, New Jersey)*, vol. 333, pp. 157–174, 2006.

[229] G. Opelz, T. Wujciak, B. Dohler, S. Scherer, and J. Mytilineos, "HLA compatibility and organ transplant survival. Collaborative transplant study," *Reviews in Immunogenetics*, vol. 1, no. 3, pp. 334–342, 1999.

[230] G. Opelz, "Correlation of HLA matching with kidney graft survival in patients with or without cyclosporine treatment," *Transplantation*, vol. 40, no. 3, pp. 240–243, 1985.

[231] T. Kuroda, S. Yasuda, S. Kusakawa et al., "Highly sensitive in vitro methods for detection of residual undifferentiated cells in retinal pigment epithelial cells derived from human iPS cells," *PLoS One*, vol. 7, no. 5, article e37342, 2012.

[232] K. Takahashi and S. Yamanaka, "Induction of pluripotent stem cells from mouse embryonic and adult fibroblast cultures by defined factors," *Cell*, vol. 126, no. 4, pp. 663–676, 2006.

[233] D. DiLoreto Jr., C. del Cerro, and M. del Cerro, "Cyclosporine treatment promotes survival of human fetal neural retina transplanted to the subretinal space of the light-damaged Fischer 344 rat," *Experimental Neurology*, vol. 140, no. 1, pp. 37–42, 1996.

[234] L. Berglin, P. Gouras, Y. Sheng et al., "Tolerance of human fetal retinal pigment epithelium xenografts in monkey retina," *Graefe's Archive for Clinical and Experimental Ophthalmology*, vol. 235, no. 2, pp. 103–110, 1997.

[235] K. Warfvinge, J. F. Kiilgaard, H. Klassen et al., "Retinal progenitor cell xenografts to the pig retina: immunological reactions," *Cell Transplantation*, vol. 15, no. 7, pp. 603–612, 2006.

[236] A. E. Cooper, J. H. Cho, S. Menges et al., "Immunosuppressive treatment can alter visual performance in the Royal College of Surgeons rat," *Journal of Ocular Pharmacology and Therapeutics*, vol. 32, no. 5, pp. 296–303, 2016.

Hindawi
Stem Cells International
Volume 2017, Article ID 7602951, 10 pages
https://doi.org/10.1155/2017/7602951

Review Article

Transit-Amplifying Cells in the Fast Lane from Stem Cells towards Differentiation

Emma Rangel-Huerta and Ernesto Maldonado

EvoDevo Lab, Unidad de Sistemas Arrecifales, Instituto de Ciencias del Mar y Limnología, Universidad Nacional Autónoma de México, Puerto Morelos, QROO, Mexico

Correspondence should be addressed to Ernesto Maldonado; ernesto@cmarl.unam.mx

Received 14 April 2017; Revised 23 June 2017; Accepted 11 July 2017; Published 1 August 2017

Academic Editor: Veronica Ramos-Mejia

Copyright © 2017 Emma Rangel-Huerta and Ernesto Maldonado. This is an open access article distributed under the Creative Commons Attribution License, which permits unrestricted use, distribution, and reproduction in any medium, provided the original work is properly cited.

Stem cells have a high potential to impact regenerative medicine. However, stem cells in adult tissues often proliferate at very slow rates. During development, stem cells may change first to a pluripotent and highly proliferative state, known as transit-amplifying cells. Recent advances in the identification and isolation of these undifferentiated and fast-dividing cells could bring new alternatives for cell-based transplants. The skin epidermis has been the target of necessary research about transit-amplifying cells; this work has mainly been performed in mammalian cells, but further work is being pursued in other vertebrate models, such as zebrafish. In this review, we present some insights about the molecular repertoire regulating the transition from stem cells to transit-amplifying cells or playing a role in the transitioning to fully differentiated cells, including gene expression profiles, cell cycle regulation, and cellular asymmetrical events. We also discuss the potential use of this knowledge in effective progenitor cell-based transplants in the treatment of skin injuries and chronic disease.

1. Introduction

Stem cells (SCs) possess the capacity to self-renew and at the same time to differentiate into specialized cell types. This process is essential during development to form new tissues and organs and during adulthood to replenish cellular masses or to repair damaged organs. It is an evolutionarily conserved trait in animals, and there is evidence that this process is present in Cnidarians (like hydra) [1], Sponges [2], and Ctenophores (also known as comb jellies) [3], organisms located at the base of the animal phylogenetic tree. Therefore, mechanisms regulating cell proliferation and directing the fate of SC progenitors are highly conserved [4]. It is believed that, at some point, all basal animals had adult pluripotent cells (called primordial stem cells (PriSCs)) with the ability to function as SCs or as germ cells.

One of the challenges of cell transplant-based therapies is to induce SCs to proliferate and differentiate when needed. Therefore, it is essential to identify SC genes that can activate cell division and differentiation programs, considering that while many of these genes will be shared among SCs from diverse tissues, some others will be different or will be activated at various moments. Since some SCs from adult tissue remain almost quiescent, without dividing for long periods of time, it is important to study how cell proliferation is activated and terminated. Furthermore, controlling the balance between self-renewal and differentiation requires a fine tuning in different cell functions, such as chromatin remodeling, transcription, posttranscriptional modifications and translation [5–7]. These complex processes are regulated by multiple genetic pathways acting at different levels of regulation.

A logical path in understanding how SCs work is to identify and compare the set of genes that are expressed in SC progenitors with those active in the differentiated cells they produce; however, there is another level of complexity to consider. When SCs proliferate, they divide asymmetrically generating one SC and one cell committed to differentiation; however, it has been thoroughly documented that in many tissues and organs, SCs divide into one SC and one pluripotent transit-amplifying cell (TAC). TACs proliferate rapidly, and after several rounds of cell division, they become differentiated [8]. The essential feature of this "transit" cell

population, as suggested by Loeffler and Potten [9], is their capacity to generate many maturing cells from very few cells. The cells entering the transit stage, or TACs, are capable of rapidly producing many differentiated cells, not only during development but also during regeneration.

One of the main problems in cell transplant-based therapies is the limited use of adult stem cells since these cells tend to remain almost quiescent, without dividing for long periods of time. Therefore, it is important to understand how SC progenitors are triggered to proliferate and differentiate rapidly, implying that any knowledge about TAC biology could be essential for designing new therapies. Here, we review some key aspects of TACs' characteristics and functions, with an emphasis on studies in epidermal skin cells from different organisms. First, we describe how the concept of TACs was shaped and their characteristics in cell proliferation and gene expression compared with SCs; we then present key aspects in the transition from SCs to TACs and later to differentiated cells. Finally, we summarize some information about the potential use of SCs and TACs in cell-based transplants to treat skin injuries and chronic disease.

2. Stem Cells and Transit-Amplifying Cells

Self-renewal and the capacity to differentiate into specific cells are the defining properties of SCs, as established early by McCulloch and Till in 1961, based on their experiments on "spleen colony-forming units" from bone marrow [7, 10]. At the same time, they established that SCs possess unlimited proliferative potential and pluripotency; however, in steady state conditions, SCs behave as slow proliferating cells [7]. In one attempt to define all the cell populations constituting multicellular organisms, Laszlo G. Lajtha in 1979 postulated the existence of "transit cells" that were different from SCs. These cells were produced by precursor cell populations and were short lived. The "time of transit" was defined by a maturation process limiting their proliferative capacity [11]. He also emphasized that "…amplification which occurs in transit populations originating from stem cells results in stem cells being a minority population…" [11], which predicts that proliferation rates in these transit cells will be, at some point, higher than those in SCs.

Further elaboration of the model implied that TACs were irreversibly converted in differentiated cells effectively amplifying each stem cell division and protecting the genetic pool. In addition, each TAC must have a set number of cell divisions [9, 12, 13]. While looking at cultured cells from a teratoma, Rheinwald and Green found previously unidentified epithelial cells that would grow rapidly but only in the presence of fibroblasts. Since these fibroblasts (3T3 cell line) had the capacity to enhance proliferation in keratinocyte cultures, years later, they were successfully used in the treatment of many burned patients [14]. One of the initial experiments consisted of inoculating single cells, isolated from the epidermis and placed in different culture dishes. Twelve days later, the researchers identified three distinct types of founding cells, named holoclones, paraclones, and meroclones [15].

Holoclones showed better growth potential and were believed to be SCs. Paraclones, in contrast, only grew up to 15 cell generations and were believed to be differentiated cells. Meroclones showed an intermediate growth potential. A key observation was that after subculture transfers, holoclones became meroclones, which were gradually converted to paraclones; therefore, a directional restriction in growth potential was identified [15]. Meroclones were the best candidates to possess an enriched population of TACs. These clonogenic epidermal cultures were ideal for studying the transition from SCs to TACs [16]. Some cellular markers were later identified to help distinguish holoclones (B1 integrin and keratin 14) [17] from paraclones (involucrin) [15]. However, as meroclones consist of an intermediate (transit) population of cells, it has been challenging to identify markers that distinguish them from SCs.

Epidermal SCs express a transcription factor, known as p63, that was found to be phosphorylated in TACs. Therefore, it has been used to label TACs during regeneration experiments [16, 18]. Currently, most authors recognize that TACs are a subpopulation intermediate between SCs and differentiated cells. Furthermore, TACs have the capacity to amplify the number of terminally differentiated cells that are produced from each stem cell division [19]. It is worth mentioning that some other authors believe that TACs are not part of epidermal homeostasis and tissue formation and renewal [20]. Nonetheless, TACs have been identified in multiple organisms and different organs and tissues [21-28] (see Table 1). We summarize some of the significant contributions that defined the current concept of transit-amplifying cells in Figure 1.

Table 1

Organ or tissue where TACs have been described	References
The cornea in human and mice	[26, 58]
The human mammary gland	[23]
The prostate epithelia	[27]
The mammalian epidermis	[15, 19]
The gastrointestinal tract	[28]
The skin epidermis in zebrafish	[46]
The different types of hair follicles in mammals	[25, 59]
The testis in mammals or male germline in *Drosophila*	[21, 22, 24]

3. Gene Expression in Transit-Amplifying Cells: Lessons from Hair Follicles

Essential knowledge about how TACs are regulated come from studies in mammals on the hair follicle (HF). The HF is a particularly useful system in which to study SCs and their progeny since hair growth is fueled by SCs during development, and in adults, the HFs continuously regenerate in alternate cycles of growth (anagen), destruction (catagen), and quiescence (telogen) [29]. Furthermore, mouse HFs are an ideal system to explore possible interactions and regulation between SC and TAC populations. The TACs associated with HFs are located surrounding the dermal papilla (DP) at the base of the HF; these TACs are embedded in matrix cells that enclose the DP. The DP is a specialized niche compartment,

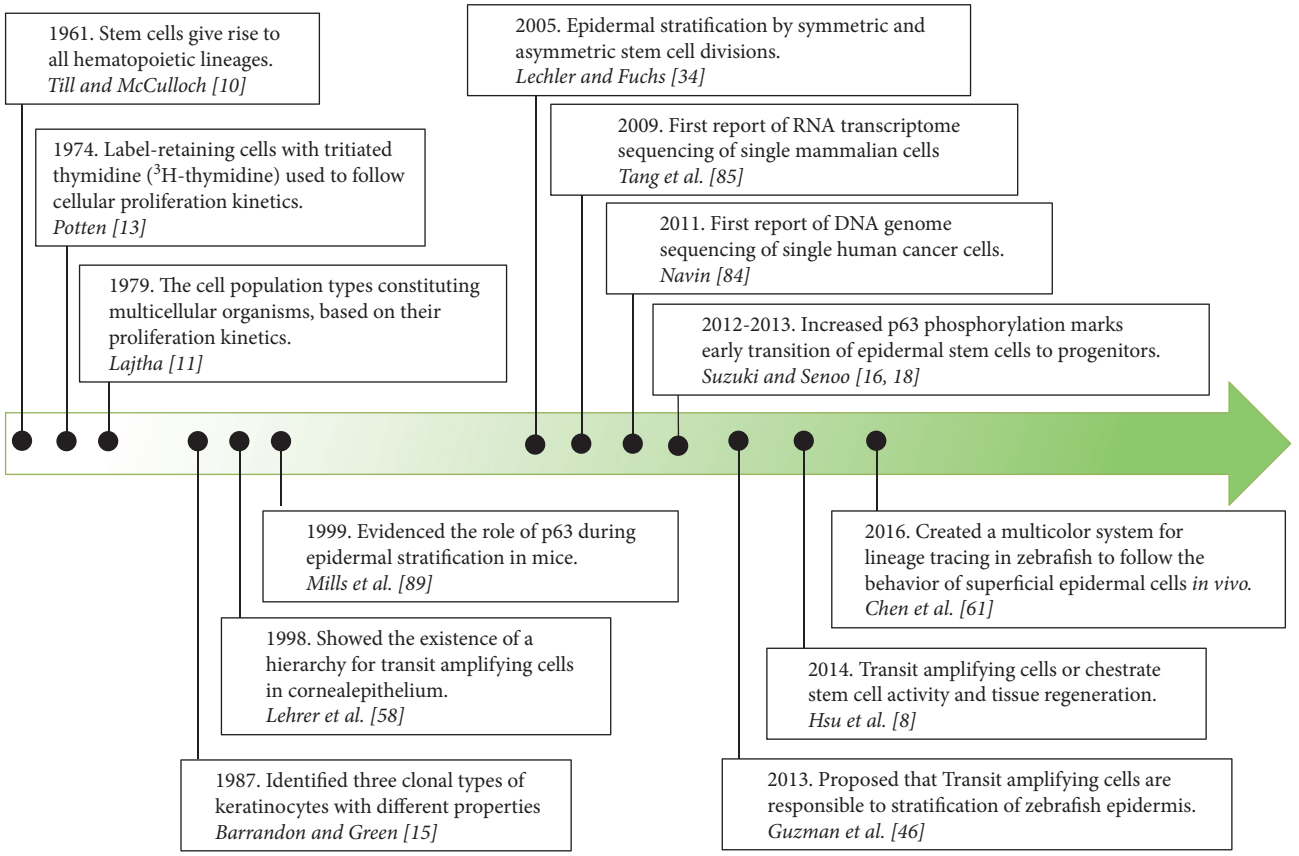

Figure 1: Time line for discoveries that shaped the current concept of Transit-Amplifying Cells.

and their signals (such as TGFB2 and FGF7) have a strong influence in regulating TAC proliferation, migration, and differentiation. At the same time, TAC signals have a role in SC regulation. For example, the TAC-secreted ligand Sonic Hedgehog (SHH) induces quiescent SCs at the HF bulge, to proliferate [8], hence promoting the anagen hair growth phase.

With the intention to describe a gene expression profile from the HF, a microarray experiment was performed in 2005, where many DP-enriched genes were identified. However, it was not possible to distinguish TAC-expressed genes from those active in other HF cell types [30]. Ten years later and taking advantage of six cell-specific transgenic reporters, it was possible to separate different cell populations in HFs during developmental stages and to perform transcriptomic analysis via next-generation sequencing [31]. More than two hundred genes were expressed by TACs, such as HOXC13, KITL, LEF1, BMP2, WNT10b, FOXP1, and GLI3, among many others (the complete list is found in http://hair-gel.net). Several of these genes are expressed in adult HF-TACs during the anagen growth phase, suggesting that there are similarities between hair growth during development and active HF proliferation cycles in mature organisms.

From the transcriptomic analysis of HF cells (outer root sheath cells, matrix cells, melanocytes, dermal fibroblasts, epidermal cells, TACs, and SCs), it was possible to build an interactome for HF signals that induce development. While epidermal populations express WNT ligands, DP cells express WNT regulators. BMP-signaling molecules are present in all HF cell types, but TACs show high expression of a TGFB pathway negative regulator called BAMBI (BMP and activin membrane-bound inhibitor). NOTCH ligands are expressed by epidermal cells, while downstream effectors of NOTCH are expressed in matrix cells and TACs. One of the conclusions of this transcriptomic analysis is that TACs are significantly involved in signaling and regulation. For example, they interact with melanocytes, outer root sheath cells, and DP cells via the KIT, EFNB2, and SHH signaling pathways, respectively [31]. Furthermore, TACs are in close communication with the DP, actively promoting TAC proliferation, with the result of efficient tissue growth. These DP-TAC interactions may modulate cell cycle frequency in primed SCs, quiescent SCs, and TACs at the HF [8].

A different approach for analyzing dynamic gene expression in TACs was to study histone modifications in adult HFs by chromatin immunoprecipitation and deep sequencing (ChiP-seq). Here, several genes were identified to be expressed in SCs but at the same time repressed in TACs [32]. This gene repression profile, in the form of H3K27-trimethylation, was mediated by Polycomb-group (PcG) proteins over genes such as SOX9, HOXA7, WNT5b, FGF18, and LGR5. At the same time, a different subset of genes, usually PcG repressed in SCs, was becoming activated in TAC progenitors, such as LEF1, BMP4, RUNX2, and WNT5a [32]. Therefore, the transition from SCs to TACs involves PcG-mediated repression of certain genes but activation of

some others. The mechanism of switching from a pluripotent state to a differentiated state may be better understood by comparing the functions of activated or repressed genes during this transition.

4. Asymmetric Cell Divisions in the Transition from Stem Cells to Transit-Amplifying Cells

Epidermis formation during development is a complex process. Lateral expansion occurs while the organism grows, and at the same time, more epidermal layers are added (stratification). As we mentioned before, SCs may divide by either symmetric cell division (SCD) or asymmetric cell division (ACD). The epidermal basal layer is formed by SCs that divide asymmetrically to produce one daughter cell, which remains at the basal layer, and another daughter TAC that will rapidly proliferate at suprabasal layers. Because of ACD, the number of SCs at the basal layer is kept constant, while the number of TACs rapidly increases, producing new epidermal layers during development [6, 33] or tissue repair [16, 18]. When stratification was initiated during mouse development, an active ACD process could be observed, since over 70% of the mitotic spindles, at the basal epidermal layer, were in a perpendicular orientation, to the basement membrane [34].

Many proteins take part in mitotic spindle reorientation during epidermal stratification by ACD. MINSC is the mouse homolog of the gene *Inscuteable* from *Drosophila melanogaster* that has been implicated in tethering apical multiprotein complexes involved in cell polarization [35]. For instance, overexpression of MINSC increased the frequency of cells with ACD [33]. One of these oligomeric complexes is formed by MINSC, PAR3 (*Partitioning defective-3*), and LGN (homolog of *Pins* from *D. melanogaster*). Once the MINSC-PAR3-LGN complex has been assembled, it recruits NuMA (*Nuclear Mitotic Apparatus*) to the apical cell cortex. The uncoupling of NuMA from MINSC-PAR3-LGN produces more cells by SCD [33]. LGN N-terminal-*TPR* repeats, and C-terminal-*Goloco* domains are essential to recruit NuMA to the complex and its apical accumulation [36]. While the *Goloco* domains bind heterotrimeric G proteins, the *TPR* domain facilitates the interaction between NuMA and MINSC [37, 38]. These multimeric complexes also recruit molecular motors, like dynein and dynactin, needed to shift the mitotic spindle orientation (Table 2) [39].

The reorientation of the mitotic spindle during ACD not only will direct the position of daughter cells but also affects the localization of cell fate determinants as well [40]. This include many cellular components, such as membrane proteins, tight junctions, and organelles that are reorganized [41]. For example, EGFR (epidermal growth factor receptor) was asymmetrically distributed after epidermal ACD [41, 42], which is particularly relevant since EGF is known to control proliferation in epidermal cells. EGFR regulates the NOTCH signaling pathway [43], explaining why blocking ACD impairs NOTCH function [44]. EGFR is also required for TACs to differentiate since it promotes keratin 5/14-expressing epidermal cells to change their expression to keratin 1/10 [45]. Control of cell division rates may also be related to ACD. During zebrafish epidermis development, higher cell proliferation rates were observed to switch from basal cells to suprabasal cells, during stratification [46]. It is clear that molecular mechanisms controlling ACD are essential for the transition from SCs to TACs during epidermis formation [41].

5. Cell Proliferation Differences between Stem Cells and Transit-Amplifying Cells

Early on, it was observed that TACs were ephemeral; they divided faster and differentiated rapidly, while SCs were almost nonproliferative in steady-state conditions [11, 15]. Indeed, SCs from adult organisms replicate very slow, as in mice where hematopoietic SCs (HSCs) replicate once every 2.5 weeks [47] or in humans where HSCs replicate every 10 months [48]. During development, SCs proliferate faster while serving as the source of cells for new organs and tissues. However, as organisms mature, SCs divide less and less, moving towards a quiescent state, which may be related to avoiding premature exhaustion and minimizing mutational events [5]. This behavior is critical for therapeutic cell transplants since low proliferation rates may limit tissue repair. In contrast, TACs are highly proliferative making cell cycle dynamics one of the main differences between SCs and TACs.

Cell proliferation rates are directly related to the duration of the G1 cell cycle phase. It is known that cyclin-dependent kinases (CDKs) are sequentially activated or repressed, modulating the duration of G1 phase. Therefore, increasing proliferation rates may involve changes in CDK expression. For example, CDK4, CDK6, and cyclins D1–3 are activated to progress from the G1 to the S phase. In the mouse pituitary gland, it was observed that TACs, but not SCs, express CDK4, suggesting that CDK4 may induce proliferation during the transition from SCs to TACs (Table 2) [49]. Opposite to the activity of cyclins and CDKs, CDKIs (cyclin-dependent kinase inhibitors) such as P21 and P27 are cell cycle regulators that inhibit the function of CDKs and lengthen G1. In P21 and P27 knockout (KO) mice, hematopoietic SCs became depleted, while there was an increase in the number of hematopoietic TACs [50, 51]. This supports the idea that after SC division, P21 is downregulated in the new TAC progenitor and CDK4 expression is activated, resulting in higher proliferation levels.

Cell cycle regulation by P21 is partially mediated by the RB protein (also known as retinoblastoma). Active cell proliferation requires that CDK2 and CDK4 phosphorylate RB (producing its inactive form). In contrast, when P21 inhibits CDK2 and CDK4, RB becomes dephosphorylated (producing the active form), and the cells are switched to a nonproliferative state. It has been observed that overexpression of P21 in cultured mammalian cells induced the depletion of the RB pool [52]. In conditional KO mice for RB, there was a substantial reduction of basal epidermal SCs, in combination with an increased cell proliferation at the suprabasal layers. At the same time, these RB-null mice showed a notorious epidermal thickening [53]. In this work, it was concluded that "RB is essential for the maintenance of the postmitotic state of terminally differentiated keratinocytes,

Table 2

Genes expressed in SCs	Genes expressed in TACs	Organ or tissue	Putative TAC function	References
GFRα1+	GFRα1−/Miwi2+/Ngn3+	Testis	Represent a novel subpopulation of undifferentiated spermatogonium. Also involved in TAC pluripotency	[24]
β1 integrins^{Hi}/α6 integrin^{Hi}/ CD71^{Low}/delta1^{Hi}/desmoglein 3^{Low}/EGFR1^{Low}/Lrig1^{Hi} MCSP +/delta1+	β1 integrins^{Low} MCSP −/delta1−	Epidermal cells	May represent a new population without any characterized function	[88–90]
Reg4	Reg4/ribosomal genes	Intestinal epithelium	TAC populations migrating upward along the intestinal crypt-villus axis	[87]
β1 integrin^{Hi}/keratin14 p63 ^{Hi}/ Pp63^{Low}	β1 integrin^{Low}/p63 ^{Low}/ Pp63^{Hi}	Clonogenic cultures and keratinocytes cultures	Increased p63 phosphorylation marks the exit from SC state and could be used to detect epidermal cell stratification	[16, 18]
Gas1+ in Bu-SCs/SHH−	Gas1−/SHH+	Hair follicle in mammals	TACs act as a signaling center between Bu-SCs and DP promoting their proliferation. TACs integrate the timing and frequency for two populations of SCs	[59]
p63/PCNA in basal cells	p63/PCNA in suprabasal cells	Zebrafish epidermis	A proliferation shift from basal to suprabasal cells marks the stratification process	[46]
Jak-STAT signaling		*Drosophila* spermatogonium	The ability of TACs to respond to signals from the SC niche and dedifferentiate into SCs	[22]
Symmetric cell division (SCD) MINSC-PAR3- and LGN-uncoupling of NuMA	Asymmetric cell division (ACD) MINSC^{Hi}, PAR3^{Hi}, LGN^{Hi} in complex with NuMA	Epidermis stratification	Asymmetric division is essential for TACs formation	[33–39]
p21^{Hi}/p27^{Hi}/RB dephosphorylated (active form)	CDK2^{Hi} CDK4^{Hi}/p21^{Low}/ RB phosphorylated^{Down} (inactive form)	Mouse pituitary gland and hematopoietic cells	Events that may trigger TAC cell proliferation	[49–51]

preventing cell cycle re-entry" [53]. Since suprabasal epidermal layers in zebrafish larvae were proposed to contain TAC progenitors [46], it is possible that P21-mediated RB inactivation may promote higher levels of cell proliferation in zebrafish epidermal TACs (Table 2).

Paired-like homeodomain transcription factor 2 (PITX2) promotes keratinocyte differentiation in the skin. PITX2 overexpression activates P21 expression in cultured keratinocytes [54]. Furthermore, microinjection of human PITX2 in zebrafish embryos thickens the epidermis and increases keratinocyte differentiation [54]. The cell cycle could be regulated at different levels. For example, the microRNA *let-7b* is a known cell cycle inhibitor [55] that is present in low amounts in epidermal SCs with high proliferation rates. When these proliferative SCs were transfected with a recombinant lentivirus expressing *miR-let-7b*, cyclin D1 and CDK4 levels were reduced and cell proliferation was halted [56]. In conclusion, the regulation of cellular division rates is a key step in the transition from SCs to TACs and later to differentiated cells.

6. The Role of Cellular Migration in the Epidermis

TACs are essential to form new layers of cells by epidermal stratification during development or in regeneration after injury [41, 46, 57]. Consequently, changes in TAC regulation could have dramatic effects on the final thickness, permeability, and appearance of the skin. For example, an increment in the number of TACs may play a role in some cellular hyperproliferative diseases, such as psoriasis [58]. Since signals from the environment may regulate the cellular behaviors of SCs and TACs [31, 59], their tissue localization could be equally important; therefore, cellular migration may also be a key aspect to consider. As we mentioned before, it has been observed, in many animal models, that SCs remain at the basal epidermal layer, while TACs are located at the basal and suprabasal layers [16, 18, 46]. Richardson et al. [60] have recently showed that reepithelialization requires long-range epithelial rearrangements, involving radial intercalations of flattened and elongated cells. Such rearrangements lead to a massive recruitment of keratinocytes from the adjacent epidermis and make reepithelization partially independent of keratinocyte proliferation [60].

A recently created zebrafish transgenic line called "skinbow" is useful for studying epidermal cell movements in an adult fish skin [61]. Using Brainbow-based multicolor, they genetically labeled each cell at the most superficial epidermal layers, also known as "superficial epithelial cells" (SECs). Under homeostatic conditions, epidermal cell replacement in SECs occurred mainly by rearrangement of neighboring

cells (78%), rather than by repopulation with newly formed cells. At this point, the authors produced epidermal injury by exfoliation (rubbing dry tissue paper over the skin). Then, they observed the contribution of cell migration from old cells in combination with reepithelization by newly formed keratinocytes. SC activity was monitored by crossing the skinbow line with an FUCCI-based sensor fish line [62]. The epidermis regenerated first by shedding large amounts of SECs and by recruiting preexisting SECs from proximal areas to the wound. After that, there was a cell proliferation burst producing new SECs that became integrated with old SECs. They concluded that the epidermis responds rapidly when suffering from injury by promoting the movement of neighboring cells to protect the remaining tissue while activating proliferation in progenitor cells [61]. In the mammalian epidermis, it is known that proliferation of TACs is activated during regeneration [16, 18, 63]; it is possible that the same is true for zebrafish.

7. Transit-Amplifying Cells and Differentiation

Transit-amplifying cells possess the capacity to rapidly amplify the pool of differentiated cells produced at each stem cell division [19]. Currently, it is not known if each TAC is committed to differentiate along one specific lineage or various lineages. In other words, their degree of pluripotency is unknown. Early on, it was suggested that TACs could be precursors of "transit populations" with different fates [11]. In the case of the hematopoietic lineage, two different populations of TACs coexist [64]. TACs from the hematopoietic system are derived from bone marrow, and their proliferation depends on "colony-stimulating factors," such as erythropoietin, to produce the erythroid lineage. Hematopoietic TACs could be divided into CFC-E (colony-forming cells) and BFC-E (erythrocyte burst-forming cells). CFC-Es require erythropoietin, for survival and proliferation while BFC-Es do not; and in the absence of erythropoietin, only CFC-Es undergo apoptosis whereas the BFC-E population remains [64].

In a different tissue, the mammalian cornea, some experimental data have suggested the existence of two distinct populations of TACs: one at the peripheral cornea and another one at the central cornea. Periphery TACs underwent two rounds of division before becoming postmitotic, while central cornea TACs only required one round of cell division. Then after cornea-induced lessons, one of the TACs remained dormant, while the other was active during reepithelization [58]. Many tissues possess two different populations of SCs, a quiescent population (qSCs) and a primed population (pSCs) that is more sensitive to activation. In the hair follicle, pSCs divides and produces TACs that express SHH that induces qSCs to proliferate [8]. If there are multiple types of SCs and different types of TACs in the same tissue, it could be important to generate a selection protocol to isolate the more proliferative progenitor cells in a tissue destined for cell-based transplants.

8. Cell-Based Transplants in the Epidermis for Therapeutic Uses

Chronic diseases, injury, cancer, and birth defects are the leading causes of organ malfunction and tissue disruption. The skin is not an exception, and because it has a prominent role as a protective barrier and in aesthetics, skin injury or chronic disease could have great impacts on a person's physical and physiological well-being. According to the CDC (Centers for Disease Control and Prevention), in 2014, close to 400,000 injuries caused by burning were reported in the US alone (www.cdc.gov). For many years now, skin graft transplants have been the lead option to help patients and heal an injured skin [65]. Skin grafting using autologous tissue is currently used to achieve partial or complete healing in acute or chronic wounds. However, one of the biggest problems in this procedure is the damage produced at the donor site. Therefore, among the things to consider is the success in reepithelialization from the grafted epidermis, the capacity of the donor site to heal, and the time required for complete healing.

To avoid damage to the donor site, in therapeutic skin grafting, it is ideal to obtain as few donor skin cells as possible for them to be used to cover larger portions of the skin. For that reason, epidermal cells are often cultured for 1 to 3 weeks and then used for treating both the wound and the donor site [14, 66]. These cells are usually cultured over commercially available matrices with collagen or with synthetic fibers used for meshing since this method helps to cover larger areas of an injured tissue. Sometimes, epidermal cells are cocultured with dermal cells [67]. Unfortunately, epidermal cultures take too long to proliferate, and after implantation, there are long-term durability issues and severe pain at the skin graft, especially when large surface areas of the body need to be restored [66]. It is worth mentioning that recent advances using epidermal cell suspensions seeded or sprayed at the wound site have shown comparable results to skin grafts [68].

Using SCs as a source for new cells, to restore damaged organs to their original condition is currently the top priority for many researchers and institutions [69-71]. Perfecting their use in cell-based therapies could close the gap towards effective wound healing or improving the quality of life in chronic disease [72, 73]. For example, mesenchymal stem cells (MSCs) can proliferate and differentiate when transplanted to different organs [74]. Notably, when MSCs were placed at the epidermis, they differentiated into epidermal cells [75]. MSCs in skin wounds induce dermal fibroblasts to respond to injury [76]; MSCs also promote vascularization [77] and improve skin and appendage regeneration, such as hair follicles or sweat glands [78]. Therefore, in some cases, MSCs could be a better option than skin grafts that do not regenerate skin appendages. Currently, there are many clinical trials to use MSCs to treat several disorders [74], but none are related to skin injuries or diseases. It is worth mentioning that adipose SCs have similar properties as MSCs in wound repair [79].

The regenerative capacity of the epidermis is related to its high cell division rates; the proliferative cells in the epidermis

consist mainly of TACs [8, 16, 18]. In theory, it would be possible to enrich the population of TACs obtained from an epidermal sample using the phosphorylated form of the transcription factor P63 [16, 18] and distinguish them from SCs based on the decreased expression of B1 integrin [17]. It is compelling to see many possibilities for future therapies in skin injury and disease treatment that could be derived from current research from SCs and transit-amplifying cells.

9. Future Directions

Bioinformatics tools have been used in the SC field of biology, such as transcriptomic analysis or RNAseq. These data have been used to describe the molecular identity of progenitor cells and to identify new marker genes [80]. Then, these marker genes could be used to label specific SC or TAC subpopulations, which can then be identified or even separated from all other cellular types. Single-cell sequencing (S-CS) [81-83] is a powerful new tool for investigating cellular diversity in several fields of biology, including cancer research. It will be of interest to understand how different cells are involved in tumor progression. Furthermore, it could have far-reaching applications in resolving intratumor heterogeneity, investigating clonality in primary tumors, tracking metastatic dissemination, deciphering the mutation rates and mutation phenotypes, and even understanding resistance to therapy [84]. S-CS has been combined with other approaches, such as cell lineage tracing, or knockout-knockdown strategies. With this interdisciplinary approach, the genotype-to-phenotype relationship was better understood for critical cancer-related genes, such as BRAF (B-rapidly accelerated fibrosarcoma), KRAS (K-RAS oncogene), P53 (P53 transcription factor), and EGFR (epidermal growth factor receptor), with relevance in cancer therapy studies [85].

RNA-seq by S-CS in combination with bioinformatics tools has also been used in developmental biology to better understand the origins of different cell types and how different cell types reach their final identity. For example, Satija et al. used reference datasets, obtained from S-CS RNA-seq profiles, to build spatial in situ gene expression patterns. With this tool in hand, they could predict the expression patterns of multiple genes during zebrafish development [86]. S-CS has also been used to identify new cell types in adult tissues; as an example, a rare type of intestinal cell was recently found. This new cell type is located at intestinal crypts, in mice, and possesses a hormone-secreting function [87]. Selected from the RNA-seq dataset, REG4 could now be used as a biomarker for this new enteroendocrine cell type that is formed by several subpopulations (Table 2). The authors suggested that one of these cell subtypes possesses a TAC-like expression profile [87].

There are several proteins that express in epidermal SCs, but not in TACs, such as B1-integrin, the NOTCH receptor DELTA1, and MCSP (melanoma chondroitin sulphate proteoglycan) (Table 2) [88, 89]. SC-S profiling was performed from single epidermal cells obtained from a human keratinocyte culture [90]. From this experiment, it was possible to detect that SCs have a high expression of LRIG1 (leucin-rich repeats and Ig-like domains 1), which is an EGF receptor antagonist. LRIG1 levels are downregulated for TAC proliferation and further differentiation to occur. SC and TAC researchers, working in different animal models, could use these markers to label and follow SC and TAC dynamics and to identify more specific markers for these essential but ephemeral cell types. One must assume that each cell has a unique transcriptome and possesses intrinsic variations that define its identity, during cell differentiation. Transcriptomic profiling offers a glimpse into the nature of cells in homeostasis and disease, including tumor cells. A better knowledge of the heterogeneity among cells, in the same tissue, would be essential in understanding the role of each cell during development or in any physiological condition [84, 91]. We have emphasized, through this review, that TAC plasticity and proliferative capacity make them worthy for exploration, offering open venues as new possibilities in cell-based transplants for therapeutic use.

Conflicts of Interest

The authors declare that there are no conflicts of interests regarding the publication of this work.

Acknowledgments

This work was supported by the Grant CONACYT Fronteras en la Ciencia-2015-1 no. 2 to Ernesto Maldonado and a graduate fellowship from CONACYT to Emma Rangel-Huerta no. 254736.

References

[1] D. A. Gold and D. K. Jacobs, "Stem cell dynamics in Cnidaria: are there unifying principles?" *Development Genes and Evolution*, vol. 223, no. 1-2, pp. 53–66, 2013.

[2] A. V. Ereskovsky, I. E. Borisenko, P. Lapébie, E. Gazave, D. B. Tokina, and C. Borchiellini, "Oscarella lobularis (Homoscleromorpha, Porifera) regeneration: epithelial morphogenesis and metaplasia," *PloS One*, vol. 10, no. 8, article e0134566, 2015.

[3] A. M. Reitzel, K. Pang, and M. Q. Martindale, "Developmental expression of "germline"- and "sex determination"-related genes in the ctenophore Mnemiopsis leidyi," *EvoDevo*, vol. 7, p. 17, 2016.

[4] A. Alie, T. Hayashi, I. Sugimura et al., "The ancestral gene repertoire of animal stem cells," *Proceedings of the National Academy of Sciences of the United States of America*, vol. 112, no. 51, pp. E7093–E7100, 2015.

[5] T. Cheng and D. T. Scadden, "Cell cycle regulators in adult stem cells," *Essentials of Stem Cell Biology*, pp. 81–87, Academic Press, UK, 2009.

[6] R. Ghadially, "25 years of epidermal stem cell research," *The Journal of Investigative Dermatology*, vol. 132, no. 3, Part 2, pp. 797–810, 2012.

[7] E. A. McCulloch and J. E. Till, "Perspectives on the properties of stem cells," *Nature Medicine*, vol. 11, no. 10, pp. 1026–1028, 2005.

[8] Y. C. Hsu, L. Li, and E. Fuchs, "Transit-amplifying cells orchestrate stem cell activity and tissue regeneration," *Cell*, vol. 157, no. 4, pp. 935–949, 2014.

[9] M. Loeffler and C. S. Potten, *Stem Cells and Cellular Pedigrees—A Conceptual Introduction*, Academyc Press, Manchester, UK, 1997.

[10] J. E. Till and E. A. McCulloch, "A direct measurement of the radiation sensitivity of normal mouse bone marrow cells," *Radiation Research*, vol. 14, pp. 213–222, 1961.

[11] L. G. Lajtha, "Stem cell concepts," *Differentiation*, vol. 14, no. 1-2, pp. 23–34, 1979.

[12] I. C. Mackenzie, "Spatial distribution of mitosis in mouse epidermis," *The Anatomical Record*, vol. 181, no. 4, pp. 705–710, 1975.

[13] C. S. Potten, "Cell replacement in epidermis (keratopoiesis) via discrete units of proliferation," *International Review of Cytology*, vol. 69, pp. 271–318, 1981.

[14] H. Green, "The birth of therapy with cultured cells," *BioEssays*, vol. 30, no. 9, pp. 897–903, 2008.

[15] Y. Barrandon and H. Green, "Three clonal types of keratinocyte with different capacities for multiplication," *Proceedings of the National Academy of Sciences of the United States of America*, vol. 84, no. 8, pp. 2302–2306, 1987.

[16] D. Suzuki and M. Senoo, "Increased p63 phosphorylation marks early transition of epidermal stem cells to progenitors," *The Journal of Investigative Dermatology*, vol. 132, no. 10, pp. 2461–2464, 2012.

[17] P. H. Jones and F. M. Watt, "Separation of human epidermal stem cells from transit amplifying cells on the basis of differences in integrin function and expression," *Cell*, vol. 73, no. 4, pp. 713–724, 1993.

[18] D. Suzuki and M. Senoo, "Expansion of epidermal progenitors with high p63 phosphorylation during wound healing of mouse epidermis," *Experimental Dermatology*, vol. 22, no. 5, pp. 374–376, 2013.

[19] F. M. Watt, "Stem cell fate and patterning in mammalian epidermis," *Current Opinion in Genetics & Development*, vol. 11, no. 4, pp. 410–417, 2001.

[20] P. H. Jones, B. D. Simons, and F. M. Watt, "Sic transit gloria: farewell to the epidermal transit amplifying cell?" *Cell Stem Cell*, vol. 1, no. 4, pp. 371–381, 2007.

[21] C. W. Bak, T. K. Yoon, and Y. Choi, "Functions of PIWI proteins in spermatogenesis," *Clinical and Experimental Reproductive Medicine*, vol. 38, no. 2, pp. 61–67, 2011.

[22] C. Brawley and E. Matunis, "Regeneration of male germline stem cells by spermatogonial dedifferentiation *in vivo*," *Science*, vol. 304, no. 5675, pp. 1331–1334, 2004.

[23] M. Cariati and A. D. Purushotham, "Stem cells and breast cancer," *Histopathology*, vol. 52, no. 1, pp. 99–107, 2008.

[24] C. Carrieri, S. Comazzetto, A. Grover et al., "A transit-amplifying population underpins the efficient regenerative capacity of the testis," *The Journal of Experimental Medicine*, vol. 214, no. 6, pp. 1631–1641, 2017.

[25] R. R. Driskell, A. Giangreco, K. B. Jensen, K. W. Mulder, and F. M. Watt, "Sox2-positive dermal papilla cells specify hair follicle type in mammalian epidermis," *Development*, vol. 136, no. 16, pp. 2815–2823, 2009.

[26] S. Kawasaki, H. Tanioka, K. Yamasaki, C. J. Connon, and S. Kinoshita, "Expression and tissue distribution of p63 isoforms in human ocular surface epithelia," *Experimental Eye Research*, vol. 82, no. 2, pp. 293–299, 2006.

[27] N. Petkova, J. Hennenlotter, M. Sobiesiak et al., "Surface CD24 distinguishes between low differentiated and transit-amplifying cells in the basal layer of human prostate," *Prostate*, vol. 73, no. 14, pp. 1576–1590, 2013.

[28] L. G. Fliervan der and H. Clevers, "Stem cells, self-renewal, and differentiation in the intestinal epithelium," *Annual Review of Physiology*, vol. 71, pp. 241–260, 2009.

[29] D. Kalaitzidis and D. T. Scadden, "Tic-TACs: refreshing hair growth," *Cell*, vol. 157, no. 4, pp. 769-770, 2014.

[30] M. Rendl, L. Lewis, and E. Fuchs, "Molecular dissection of mesenchymal-epithelial interactions in the hair follicle," *PLoS Biology*, vol. 3, no. 11, p. e331, 2005.

[31] A. Rezza, Z. Wang, R. Sennett et al., "Signaling networks among stem cell precursors, transit-amplifying progenitors, and their niche in developing hair follicles," *Cell Reports*, vol. 14, no. 12, pp. 3001–3018, 2016.

[32] W. H. Lien, X. Guo, L. Polak et al., "Genome-wide maps of histone modifications unwind *in vivo* chromatin states of the hair follicle lineage," *Cell Stem Cell*, vol. 9, no. 3, pp. 219–232, 2011.

[33] N. D. Poulson and T. Lechler, "Robust control of mitotic spindle orientation in the developing epidermis," *The Journal of Cell Biology*, vol. 191, no. 5, pp. 915–922, 2010.

[34] T. Lechler and E. Fuchs, "Asymmetric cell divisions promote stratification and differentiation of mammalian skin," *Nature*, vol. 437, no. 7056, pp. 275–280, 2005.

[35] R. Kraut and J. A. Campos-Ortega, "Inscuteable, a neural precursor gene of Drosophila, encodes a candidate for a cytoskeleton adaptor protein," *Developmental Biology*, vol. 174, no. 1, pp. 65–81, 1996.

[36] F. Yu, X. Morin, Y. Cai, X. Yang, and W. Chia, "Analysis of partner of inscuteable, a novel player of Drosophila asymmetric divisions, reveals two distinct steps in inscuteable apical localization," *Cell*, vol. 100, no. 4, pp. 399–409, 2000.

[37] N. D. Poulson and T. Lechler, "Asymmetric cell divisions in the epidermis," *International Review of Cell and Molecular Biology*, vol. 295, pp. 199–232, 2012.

[38] F. Yu, C. T. Ong, W. Chia, and X. Yang, "Membrane targeting and asymmetric localization of Drosophila partner of inscuteable are discrete steps controlled by distinct regions of the protein," *Molecular and Cellular Biology*, vol. 22, no. 12, pp. 4230–4240, 2002.

[39] L. Seldin, A. Muroyama, and T. Lechler, "NuMA-microtubule interactions are critical for spindle orientation and the morphogenesis of diverse epidermal structures," *eLife*, vol. 5, 2016.

[40] C. Juschke, Y. Xie, M. P. Postiglione, and J. A. Knoblich, "Analysis and modeling of mitotic spindle orientations in three dimensions," *Proceedings of the National Academy of Sciences of the United States of America*, vol. 111, no. 3, pp. 1014–1019, 2014.

[41] A. Muroyama and T. Lechler, "Polarity and stratification of the epidermis," *Seminars in Cell & Developmental Biology*, vol. 23, no. 8, pp. 890–896, 2012.

[42] H. RoyLe, T. Zuliani, I. Wolowczuk et al., "Asymmetric distribution of epidermal growth factor receptor directs the fate of normal and cancer keratinocytes *in vitro*," *Stem Cells and Development*, vol. 19, no. 2, pp. 209–220, 2010.

[43] C. Shang, B. Lang, and L. R. Meng, "Blocking NOTCH pathway can enhance the effect of EGFR inhibitor through targeting CD133+ endometrial cancer cells," *Cancer Biology & Therapy*, 2016.

[44] S. E. Williams, S. Beronja, H. A. Pasolli, and E. Fuchs, "Asymmetric cell divisions promote Notch-dependent epidermal differentiation," *Nature*, vol. 470, no. 7334, pp. 353–358, 2011.

[45] C. Blanpain, W. E. Lowry, H. A. Pasolli, and E. Fuchs, "Canonical notch signaling functions as a commitment switch in the epidermal lineage," *Genes & Development*, vol. 20, no. 21, pp. 3022–3035, 2006.

[46] A. Guzman, J. L. Ramos-Balderas, S. Carrillo-Rosas, and E. Maldonado, "A stem cell proliferation burst forms new layers of P63 expressing suprabasal cells during zebrafish post-embryonic epidermal development," *Biology Open*, vol. 2, no. 11, pp. 1179–1186, 2013.

[47] J. L. Abkowitz, D. Golinelli, D. E. Harrison, and P. Guttorp, "*In vivo* kinetics of murine hemopoietic stem cells," *Blood*, vol. 96, no. 10, pp. 3399–3405, 2000.

[48] S. N. Catlin, L. Busque, R. E. Gale, P. Guttorp, and J. L. Abkowitz, "The replication rate of human hematopoietic stem cells *in vivo*," *Blood*, vol. 117, no. 17, pp. 4460–4466, 2011.

[49] E. Macias, P. L. Miliani de Marval, A. Senderowicz, J. Cullen, and M. L. Rodriguez-Puebla, "Expression of CDK4 or CDK2 in mouse oral cavity is retained in adult pituitary with distinct effects on tumorigenesis," *Cancer Research*, vol. 68, no. 1, pp. 162–171, 2008.

[50] T. Cheng, N. Rodrigues, D. Dombkowski, S. Stier, and D. T. Scadden, "Stem cell repopulation efficiency but not pool size is governed by p27(kip1)," *Nature Medicine*, vol. 6, no. 11, pp. 1235–1240, 2000.

[51] T. Cheng, N. Rodrigues, H. Shen et al., "Hematopoietic stem cell quiescence maintained by p21cip1/waf1," *Science*, vol. 287, no. 5459, pp. 1804–1808, 2000.

[52] E. V. Broude, M. E. Swift, C. Vivo et al., "p21(Waf1/Cip1/Sdi1) mediates retinoblastoma protein degradation," *Oncogene*, vol. 26, no. 48, pp. 6954–6958, 2007.

[53] S. Ruiz, M. Santos, C. Segrelles et al., "Unique and overlapping functions of pRb and p107 in the control of proliferation and differentiation in epidermis," *Development*, vol. 131, no. 11, pp. 2737–2748, 2004.

[54] G. Shi, K. C. Sohn, T. Y. Choi et al., "Expression of paired-like homeodomain transcription factor 2c (PITX2c) in epidermal keratinocytes," *Experimental Cell Research*, vol. 316, no. 19, pp. 3263–3271, 2010.

[55] B. J. Reinhart, F. J. Slack, M. Basson et al., "The 21-nucleotide let-7 RNA regulates developmental timing in Caenorhabditis elegans," *Nature*, vol. 403, no. 6772, pp. 901–906, 2000.

[56] H. Lu, X. He, Q. Wang et al., "MicroRNA let-7b-regulated epidermal stem cell proliferation in hypertrophied anal papillae," *Molecular Medicine Reports*, vol. 12, no. 4, pp. 4821–4828, 2015.

[57] M. I. Koster and D. R. Roop, "Mechanisms regulating epithelial stratification," *Annual Review of Cell and Developmental Biology*, vol. 23, pp. 93–113, 2007.

[58] M. S. Lehrer, T. T. Sun, and R. M. Lavker, "Strategies of epithelial repair: modulation of stem cell and transit amplifying cell proliferation," *Journal of Cell Science*, vol. 111, Part 19, pp. 2867–2875, 1998.

[59] Y. C. Hsu, L. Li, and E. Fuchs, "Emerging interactions between skin stem cells and their niches," *Nature Medicine*, vol. 20, no. 8, pp. 847–856, 2014.

[60] R. Richardson, M. Metzger, P. Knyphausen et al., "Re-epithelialization of cutaneous wounds in adult zebrafish combines mechanisms of wound closure in embryonic and adult mammals," *Development*, vol. 143, no. 12, pp. 2077–2088, 2016.

[61] C. H. Chen, A. Puliafito, B. D. Cox et al., "Multicolor cell barcoding technology for long-term surveillance of epithelial regeneration in zebrafish," *Developmental Cell*, vol. 36, no. 6, pp. 668–680, 2016.

[62] M. Sugiyama, A. Sakaue-Sawano, T. Iimura et al., "Illuminating cell-cycle progression in the developing zebrafish embryo," *Proceedings of the National Academy of Sciences of the United States of America*, vol. 106, no. 49, pp. 20812–20817, 2009.

[63] M. Senoo, "Epidermal stem cells in homeostasis and wound repair of the skin," *Advances in wound care*, vol. 2, no. 6, pp. 273–282, 2013.

[64] H. Lodish, J. Flygare, and S. Chou, "From stem cell to erythroblast: regulation of red cell production at multiple levels by multiple hormones," *IUBMB Life*, vol. 62, no. 7, pp. 492–496, 2010.

[65] I. Herskovitz, O. B. Hughes, F. Macquhae, A. Rakosi, and R. Kirsner, "Epidermal skin grafting," *International Wound Journal*, vol. 13, Supplement 3, pp. 52–56, 2016.

[66] F. M. Wood, M. L. Kolybaba, and P. Allen, "The use of cultured epithelial autograft in the treatment of major burn injuries: a critical review of the literature," *Burns*, vol. 32, no. 4, pp. 395–401, 2006.

[67] J. Henderson, R. Arya, and P. Gillespie, "Skin graft meshing, over-meshing and cross-meshing," *International Journal of Surgery*, vol. 10, no. 9, pp. 547–550, 2012.

[68] H. Zhao, Y. Chen, C. Zhang, and X. Fu, "Autologous epidermal cell suspension: a promising treatment for chronic wounds," *Journal of Tissue Viability*, vol. 25, no. 1, pp. 50–56, 2016.

[69] I. Aharony, S. Michowiz, and N. Goldenberg-Cohen, "The promise of stem cell-based therapeutics in ophthalmology," *Neural Regeneration Research*, vol. 12, no. 2, pp. 173–180, 2017.

[70] M. E. Bernardo and W. E. Fibbe, "Mesenchymal stromal cells and hematopoietic stem cell transplantation," *Immunology Letters*, vol. 168, no. 2, pp. 215–221, 2015.

[71] E. Tsolaki and E. Yannaki, "Stem cell-based regenerative opportunities for the liver: state of the art and beyond," *World Journal of Gastroenterology*, vol. 21, no. 43, pp. 12334–12350, 2015.

[72] M. Chen, M. Przyborowski, and F. Berthiaume, "Stem cells for skin tissue engineering and wound healing," *Critical Reviews in Biomedical Engineering*, vol. 37, no. 4-5, pp. 399–421, 2009.

[73] H. Zhou, C. You, X. Wang et al., "The progress and challenges for dermal regeneration in tissue engineering," *Journal of Biomedical Materials Research. Part A*, vol. 105, no. 4, pp. 1208–1218, 2017.

[74] R. Rohban and T. R. Pieber, "Mesenchymal stem and progenitor cells in regeneration: tissue specificity and regenerative potential," *Stem Cells International*, vol. 2017, Article ID 5173732, 2017.

[75] H. Chun-mao, W. Su-yi, L. Ping-ping, and C. Hang-hui, "Human bone marrow-derived mesenchymal stem cells differentiate into epidermal-like cells *in vitro*," *Differentiation*, vol. 75, no. 4, pp. 292–298, 2007.

[76] A. N. Smith, E. Willis, V. T. Chan et al., "Mesenchymal stem cells induce dermal fibroblast responses to injury," *Experimental Cell Research*, vol. 316, no. 1, pp. 48–54, 2010.

[77] M. S. Laranjeira, M. H. Fernandes, and F. J. Monteiro, "Reciprocal induction of human dermal microvascular endothelial cells and human mesenchymal stem cells: time-dependent profile in a co-culture system," *Cell Proliferation*, vol. 45, no. 4, pp. 320–334, 2012.

[78] H. Inoue, T. Murakami, T. Ajiki, M. Hara, Y. Hoshino, and E. Kobayashi, "Bioimaging assessment and effect of skin wound healing using bone-marrow-derived mesenchymal stromal cells with the artificial dermis in diabetic rats," *Journal of Biomedical Optics*, vol. 13, no. 6, article 064036, 2008.

[79] C. Nie, G. Zhang, D. Yang et al., "Targeted delivery of adipose-derived stem cells via acellular dermal matrix enhances wound repair in diabetic rats," *Journal of Tissue Engineering and Regenerative Medicine*, vol. 9, no. 3, pp. 224–235, 2015.

[80] L. Wen and F. Tang, "Single-cell sequencing in stem cell biology," *Genome Biology*, vol. 17, p. 71, 2016.

[81] S. Joost, A. Zeisel, T. Jacob et al., "Single-cell transcriptomics reveals that differentiation and spatial signatures shape epidermal and hair follicle heterogeneity," *Cell Systems*, vol. 3, no. 3, pp. 221–237.e9, 2016.

[82] J. P. Junker and A. v. Oudenaarden, "Every cell is special: genome-wide studies add a new dimension to single-cell biology," *Cell*, vol. 157, no. 1, pp. 8–11, 2014.

[83] I. C. Macaulay, C. P. Ponting, and T. Voet, "Single-cell multiomics: multiple measurements from single cells," *Trends in Genetics*, vol. 33, no. 2, pp. 155–168, 2017.

[84] N. E. Navin, "The first five years of single-cell cancer genomics and beyond," *Genome Research*, vol. 25, no. 10, pp. 1499–1507, 2015.

[85] F. Tang, K. Lao, and M. A. Surani, "Development and applications of single-cell transcriptome analysis," *Nature Methods*, vol. 8, Supplement 4, pp. S6–11, 2011.

[86] R. Satija, J. A. Farrell, D. Gennert, A. F. Schier, and A. Regev, "Spatial reconstruction of single-cell gene expression data," *Nature Biotechnology*, vol. 33, no. 5, pp. 495–502, 2015.

[87] D. Grun, A. Lyubimova, L. Kester et al., "Single-cell messenger RNA sequencing reveals rare intestinal cell types," *Nature*, vol. 525, no. 7568, pp. 251–255, 2015.

[88] J. Legg, U. B. Jensen, S. Broad, I. Leigh, and F. M. Watt, "Role of melanoma chondroitin sulphate proteoglycan in patterning stem cells in human interfollicular epidermis," *Development*, vol. 130, no. 24, pp. 6049–6063, 2003.

[89] S. Lowell, P. Jones, I. RouxLe, J. Dunne, and F. M. Watt, "Stimulation of human epidermal differentiation by delta-notch signalling at the boundaries of stem-cell clusters," *Current Biology*, vol. 10, no. 9, pp. 491–500, 2000.

[90] K. B. Jensen and F. M. Watt, "Single-cell expression profiling of human epidermal stem and transit-amplifying cells: Lrig1 is a regulator of stem cell quiescence," *Proceedings of the National Academy of Sciences of the United States of America*, vol. 103, no. 32, pp. 11958–11963, 2006.

[91] A. A. Mills, B. Zheng, X. J. Wang, H. Vogel, D. R. Roop, and A. Bradley, "p63 is a p53 homologue required for limb and epidermal morphogenesis," *Nature*, vol. 398, no. 6729, pp. 708–713, 1999.

Hindawi
Stem Cells International
Volume 2017, Article ID 7284872, 14 pages
https://doi.org/10.1155/2017/7284872

Research Article

Tumorigenic and Differentiation Potentials of Embryonic Stem Cells Depend on TGFβ Family Signaling: Lessons from Teratocarcinoma Cells Stimulated to Differentiate with Retinoic Acid

Olga Gordeeva[1] and Sergey Khaydukov[2]

[1]*Kol'tsov Institute of Developmental Biology, Russian Academy of Sciences, 26 Vavilov Street, Moscow 119334, Russia*
[2]*Shemyakin and Ovchinnikov Institute of Bioorganic Chemistry, Russian Academy of Sciences, Miklukho-Maklaya Street 16/10, Moscow 117997, Russia*

Correspondence should be addressed to Olga Gordeeva; olgagordeeva@yandex.ru

Received 7 April 2017; Revised 1 June 2017; Accepted 13 June 2017; Published 16 July 2017

Academic Editor: Tilo Kunath

Copyright © 2017 Olga Gordeeva and Sergey Khaydukov. This is an open access article distributed under the Creative Commons Attribution License, which permits unrestricted use, distribution, and reproduction in any medium, provided the original work is properly cited.

A significant challenge for the development of safe pluripotent stem cell-based therapies is the incomplete in vitro differentiation of the pluripotent stem cells and the presence of residual undifferentiated cells initiating teratoma development after transplantation in recipients. To understand the mechanisms of incomplete differentiation, a comparative study of retinoic acid-induced differentiation of mouse embryonic stem (ES) and teratocarcinoma (EC) cells was conducted. The present study identified differences in proliferative activity, differentiation, and tumorigenic potentials between ES and EC cells. Higher expression of Nanog and Mvh, as well as Activin A and BMP4, was found in undifferentiated ES cells than in EC cells. However, the expression levels of Activin A and BMP4 increased more sharply in the EC cells during retinoic acid-induced differentiation. Stimulation of the Activin/Nodal and BMP signaling cascades and inhibition of the MEK/ERK and PI3K/Act signaling pathways resulted in a significant decrease in the number of Oct4-expressing ES cells and a loss of tumorigenicity, similar to retinoic acid-stimulated EC cells. Thus, this study demonstrates that a differentiation strategy that modulates prodifferentiation and antiproliferative signaling in ES cells may be effective for eliminating tumorigenic cells and may represent a valuable tool for the development of safe stem cell therapeutics.

1. Introduction

The cell derivatives of pluripotent stem cells are considered to be promising cell sources for regenerative therapy. Pluripotent stem cells of different origins are capable of unlimited self-renewal and differentiation into all types of somatic and germ cells in vitro and in vivo [1–9]. However, complete implementation of pluripotent potential is only possible when pluripotent stem cells are reintegrated with the blastocyst [6, 10–13]. In contrast, in vitro differentiation of the pluripotent stem cells is asynchronous and incomplete; and therefore, the residual undifferentiated cells can initiate teratoma development after transplantation into the tissues of an adult animal recipient [14–21]. This feature of pluripotent stem cells is one of the main issues for the development of safe pluripotent stem cell-based therapy.

Paradoxically, pluripotent embryonic stem (ES) and embryonic germ (EG) cells are the only types of genetically normal and nontransformed cells that can form tumors after transplantation into adult animal recipients. It is believed that genetically normal pluripotent stem cells form benign tumors that do not contain undifferentiated cells, whereas pluripotent stem cells carrying genetic aberrations give rise to malignant tumors with undifferentiated cells, similar to spontaneous teratocarcinoma tumors [22–24]. However, these correlations were found only for some human ES cell

lines with abnormal karyotypes, whereas mouse ES cells did not show a strong correlation of their karyotypes or other genetic modifications (excluding transgenic mice with E-ras overexpression) and increased tumorigenicity and malignancy [25–27]. At the same time, mouse and human teratocarcinoma (EC) cells with different genetic disorders derived from spontaneous tumors are indeed capable of forming secondary malignancies after serial transplantation into recipients [28–34]. It can be assumed that the high risk of cancer initiation after transplantation of pluripotent stem cell-derived cells can be associated with mutations in oncogenes and tumor suppressor genes. Moreover, numerous studies have shown that long-term in vitro cultivation leads to the accumulation of genetic aberrations and abnormal epigenetic changes in the genome of pluripotent stem cells, including mutations in oncogenes and tumor suppressors [27, 35–40]. This property of in vitro-maintained cells is the second major problem delaying the clinical application of cellular technologies based on pluripotent stem cells.

Thus, to assess the risks and benefits of cellular technologies for regenerative medicine, it is necessary to develop a technological platform for the reliable and reproducible assessment of the probability of cancer initiation after transplantation of stem cell derivatives that were cultured in vitro and underwent various manipulations. Undoubtedly, the use of pluripotent stem cell lines requires regular monitoring of genetic and epigenetic integrity and testing of malignant tumorigenicity using adequate animal models.

To solve the problem of residual undifferentiated cells during in vitro differentiation of pluripotent stem cells, several strategies have been proposed to eliminate undifferentiated cells via genetic modification by using "suicide" gene expression [41–44] and the cytostatic exposure [45–48] to activate the proliferation arrest and cell death, as in cancer cells. However, another promising approach aims to correct the imbalance between proliferative and differentiation processes by enhancing differentiation with different combinations of differentiation inducers; this approach promotes the transformation of malignant teratocarcinomas toward benign mature teratomas [30, 49–51]. For instance, the well-known small molecular inducer of differentiation all-trans-retinoic acid is used for the clinical treatment of acute promyelocytic leukemia, since it intensifies the differentiation of undifferentiated tumor cells [49, 51]. Considering the substantial similarity of pluripotent stem and EC cells, a comparative analysis of the mechanisms that underlie their tumorigenic and carcinogenic potentials can allow us to find the most effective way of eliminating residual undifferentiated cells.

In the present study, we conducted a comparative analysis of the dynamics of in vitro and in vivo differentiation of the mouse ES and EC cells to identify differences in the mechanisms of differentiation and tumorigenic potentials of normal pluripotent stem cells and their malignant counterparts. Based on the obtained results, we attempted to identify ways to eliminate residual undifferentiated cells that are capable of initiating tumors after transplantation into immunodeficient recipient mice.

2. Materials and Methods

2.1. Cell Line Maintenance. Mouse ES R1 cell line was kindly provided by A. Nagy (Mount Sinai Hospital, Toronto, Canada), and mouse EC F9 cell line was obtained from the Russian Cell Culture Collection (http://www.rccc.cytspb.rssi.ru/). Mouse ES R1 cells were maintained on a mouse embryonic fibroblast feeder inactivated by mitomycin C (Sigma) or in a feeder-free system in a medium containing 10 ng/ml of leukemia inhibitory factor (Sigma). The ES R1 and EC F9 cells were cultivated in DMEM supplemented with 2 mM L-glutamine, 1% nonessential amino acids (HyClone), 0.1 mM β-mercaptoethanol (Sigma), and 15% Characterized Fetal Bovine Serum (HyClone) or 15% knockout serum replacement (Invitrogen).

2.2. Induction of ES and EC Cell Differentiation with Retinoic Acid and Exposure to Activin A, BMP4, PD98059, and LY294002. The differentiation of ES R1 and EC F9 cells was stimulated with retinoic acid (10^{-6} M, all-trans-retinoic acid, RA, Sigma). At the beginning of the experiment, the undifferentiated cells were plated in a density of 10,000 cells/cm^2 and cultured overnight to facilitate adherence in a medium containing 1 mM L-glutamine, 1% nonessential amino acids, and 15% Characterized Fetal Bovine Serum (HyClone). The next day, the medium with serum was replaced with a medium supplemented with 15% knockout serum replacement and 10^{-6} M RA. Medium changes were conducted daily during experiments. After 5 days of RA stimulation, the ES R1 and EC F9 cells were dissociated using a 0.05% trypsin-EDTA solution (HyClone), transferred into new culture plates or flasks at a ratio of 1:3 and exposed to RA for the next 5 days (RA10). After 10 days of RA exposure, the cells were cultured in a standard medium without retinoic acid for 3 days (RA10 + 3).

In the next series of experiments to improve ES R1 cell differentiation, human Activin A (100 ng/ml, Invitrogen), human BMP4 (100 ng/ml, Sigma), PD98059 (50 μM, Sigma), and LY294002 (25 μM, Sigma) were added together with RA from day 5 to day 10. The differentiating ES R1 cells were then cultured in a medium without RA for 3 days.

2.3. Preparation of Cells for Transplantation. Before subcutaneous transplantation, differentiated ES R1 and EC F9 cells were dissociated using a 0.05% trypsin-EDTA solution (HyClone), and 10^6 graft cells were concentrated in 50–70 μl of Hanks solution (HyClone). For intraperitoneal transplantations, 5×10^5 cells on day 10 of RA stimulation were plated onto acetate-cellulose membranes (CA-membrane, 1.2 cm^2) and cultured in an 8-well Lab-Tek II Chamber Slide System (Nalge Nunc International) in a standard culture medium for 3 days.

2.4. Flow Cytometric Analysis of the Cell Cycle Distribution and Oct4-Expressing Cells. The cellular probes were analyzed using a Cytomics FC500 flow cytometer (Beckman Coulter). The cell suspensions (10^6/ml) were prepared using the 0.05% trypsin-EDTA (HyClone) treatment. To analyze the cell cycle distribution, the cells were fixed with cold 70% ethanol.

After fixation and triple washing with PBS the cells were incubated in PBS containing 20 μg/ml of propidium iodide (Invitrogen/Molecular Probes) and 200 μg/ml of RNAse A (Fermentas) for 30 min. After staining, the probes were analyzed immediately. The histograms were analyzed using the MultiCycle AV Software (Phoenix Flow Systems, USA).

For the flow cytometry analysis of Oct4-expressing cells, the suspensions of cells (10^6/ml) were fixed with 3% paraformaldehyde in PBS for 15 min, washed with PBS, and treated with 0.5% Triton X-100, 3% bovine serum albumin, Fraction V (Sigma), and rabbit anti-Oct4 antibodies (1 : 200, Santa Cruz Biotechnology) in PBS for 40 min. After washing, the cells were incubated in a PBS solution containing 0.5% Triton X-100, 3% bovine serum albumin, and secondary chicken anti-rabbit antibodies conjugated with Alexa-488 (1 : 1000, Molecular Probes) for 30 min. For the negative control, the cells were treated with normal rabbit IgG (sc-3888, Santa Cruz Biotechnology) and then with the same secondary antibody solution described above.

2.5. Detection of Alkaline Phosphatase Activity (ALP) and Immunostaining. The ES R1 and EC F9 cells were fixed with 2% paraformaldehyde in phosphate-buffered saline, PBS, pH 7.0, within 15 min. ALP activity was detected after incubation in a solution containing 10 ml 0.02 M Tris-HCl buffer (pH 8.7), 1 mg Naphtol-AS-B1-phospate, and 5 mg fast red dye Texas Red (all from Sigma) at 37°C for 1 h.

For immunofluorescence analysis, cells fixed in 4% paraformaldehyde in PBS for 1 h were washed and permeabilized with 0.5% Triton X-100. Nonspecific reactions were blocked by 10% chicken serum (Gibco/Invitrogen). Primary rabbit anti-Oct4 and goat anti-Gata4 antibodies (Santa Cruz Biotechnology) were used at a dilution of 1 : 100. The cells were incubated in a solution of primary antibodies in PBS-Tween 20 at 4°C overnight. Secondary chicken anti-rabbit and donkey anti-goat antibodies conjugated with Alexa Fluor 594 and Alexa Fluor 488 (Molecular Probes) were diluted at 1 : 800 in a blocking buffer and applied to the cells for 4 h at room temperature. DAPI (Molecular Probes) was applied for 15 min for nuclear staining. The cells were mounted and examined under a Leica DMRXA2 fluorescence microscope (Leica Microsystems GmbH). For negative controls, the primary antibodies were omitted, and the same staining procedure was used.

2.6. RNA Isolation and Quantitative Real-Time PCR Analysis (qRT-PCR). Total RNAs were extracted from mouse ESC and ECC samples using the TRIzol® Reagent (Invitrogen). The samples were treated with TURBO DNase (Ambion/Invitrogen) according to the manufacturer's recommendations. The RNA yield and quality were analyzed using the NanoDrop 2000 system (Thermo Scientific). cDNAs were synthesized using 1–1.5 μg of total RNA, oligo-dT18 primer, and Maxima Reverse Transcriptase (Fermentas) according to the manufacturer's protocols.

A relative quantitative analysis of gene expression was carried out using the Applied Biosystems Real-Time PCR System 7500 (Life Technologies). The probes were prepared using the qRT-PCR master mix with SYBR Green and ROX passive reference dye (Evrogen, Russia). The following amplification protocols were used: denaturation at 95°C for 5 min, followed by 40 cycles at 95°C for 15 sec and at 60°C for 1 min. All experiments were run in triplicate. The expression levels of target mRNAs were normalized to the expression of the housekeeping gene hypoxanthine guanine phosphoribosyltransferase (Hprt). The relative levels of target gene expression were calculated using the comparative $2^{-\Delta\Delta Ct}$ method (ABI Relative Quantification Study software, Applied Biosystems).

Specific primers were designed using GenBank and Ensemble data for the annotated sequences of the target genes using the Beacon Designer 8.0 software (PREMIER Biosoft, USA) and Primer 3. The primer sequences and sizes of their expected products are represented in Table S1 (Supplemental information available online at https://doi.org/10.1155/2017/7284872). The gene expression data were subjected to statistical analysis using the R v.3.2.3 software (http://www.r-project.org). The averages of the gene expression data obtained from three independent experiments were used for statistical analysis using one-way ANOVA followed by a Tukey's post hoc test.

2.7. Teratoma and Teratocarcinoma Assay. To study the development of teratomas and teratocarcinomas, 10–12-week-old immunodeficient nude mice (Nu/Nu) delivered from the Animal Breeding Facility-Branch "Pushchino" of Shemyakin and Ovchinnikov Institute of Bioorganic Chemistry, Russian Academy of Sciences (stock line was obtained from the Charles River Laboratories Inc., Wilmington, MA) were used as recipients. Nude mice were kept under pathogen-free conditions. The animal keeping and all experiments were approved by the Ethics Committee of the Institute of Developmental Biology, Russian Academy of Sciences, and performed in accordance with the Russian Federation legislation (Order of the Ministry of Health and Social Development of the Russian Federation Number 708n, August 28, 2010) based on the European Convention for the Protection of Vertebrate Animals used for Experimental and Other Scientific Purposes. Before the subcutaneous and intraperitoneal cell transplantation procedures, the animals were anesthetized with an intraperitoneal injection of 100 mg/kg ketamine (MEZ, Russia) and 10 mg/kg xylazine (Rometar, Spofa, Czech Republic). In subcutaneous transplantation experiments, differentiating ES R1 and EC F9 cells ($0.5–1 \times 10^6$ cells per mouse) were injected under the skin of the neck area of nude mice using 1 ml syringes with 27G needles (Becton Dickinson). During intraperitoneal cell transplantation, midline incisions were made in the skin and body wall to get access to the peritoneal cavity. The cells on the CA-membrane were transferred into the peritoneal cavity using tweezers.

At the end of the experiments (6–30 weeks after transplantation), the animals were sacrificed by cervical dislocation or by injection of a lethal dose of intravenous barbiturates. Autopsies were performed for all mice. The developed teratomas and teratocarcinomas were isolated and fixed with 10% paraformaldehyde (Sigma), dehydrated according to the standard method, and embedded in paraffin for sectioning. Histological preparations were stained with hematoxylin and eosin and examined under a Leica DM RXA2 microscope.

3. Results

3.1. Dynamics of RA-Induced Differentiation of ES and EC Cells. To clarify the mechanisms that regulate the balance of proliferation and differentiation processes in normal pluripotent and malignant teratocarcinoma cells, the proliferative activity and dynamics of in vitro differentiation of ES R1 and EC F9 cells were analyzed after RA stimulation (Figure 1(a)). During 10 days of RA-induced differentiation, there is a gradual decrease in the number of cells in the S-phase of the cell cycle (from 60% to 10–30%) and an increase of the number of cells in the G1/G0-phase (from 10–20% to 45–60%) in both the ES R1 and EC F9 cell populations (Figures 1(b) and 1(d)). However, the number of cells in the S-phase of the cell cycle is significantly lower in the populations of differentiating ES R1 cells than in the EC F9 cell populations on day 5 (30.7% versus 44.6%, resp.) and day 10 (10.8% versus 32.8%, resp.) of RA exposure (Figures 1(b) and 1(d)). On day 3 after RA withdrawal (RA10 + 3), the number of cells in the in the S-phase of the cell cycle is similar in both cell lines, while the number of cell in the G1/G0-phase is significantly higher in differentiating ES R1 cells (Figures 1(b) and 1(d)). Similarly, lower expression levels of C-myc are detected in the ES R1 cells than in the EC F9 cells on days 5 and 10 of RA-induced differentiation (Figure 2).

An analysis of differentiation dynamics identified a gradual decrease in the number of Oct4- and ALP-expressing cells in the ES R1 and EC F9 cell populations (Figures 1(c) and 1(e), Figure 3). However, the numbers of Oct4-expressing cells differ between the ES R1 and EC F9 cell populations on day 5 of RA-induced differentiation (52% versus 78.8%, resp.) and on day 3 after RA withdrawal (45.2% versus 2.7%, resp.). No significant differences are detected on day 10 (Figures 1(c) and 1(e)). These dynamics were confirmed by qRT-PCR analysis of Oct4 expression in differentiating ES R1 and EC F9 populations (Figure 2). Thus, during the early stages of RA stimulation, proliferation and differentiation dynamics of ES R1 and EC F9 cells are similar, but from the 5th to the 10th day of the experiment, there are significant differences in the studied cellular characteristics, which become most pronounced on day 3 after RA withdrawal.

3.2. Gene Expression Analysis of Embryonic Lineage Commitment in the Course of RA-Induced Differentiation of ES and EC Cells. To investigate early embryonic lineages during RA-induced differentiation of ES R1 and EC F9 cells, gene expression of pluripotency (Oct4 and Nanog) and lineage markers (Mvh, Gata4, Pax6, Afp, and Bry) was studied (Figures 2 and 3). Moreover, endogenous expression of TGFβ family factors (TGFβ1, Activin A, Nodal, and BMP4), which play a key role in the early lineage differentiation, was also examined (Figure 2). There is higher expression of Nanog and Mvh (germ line marker) in the ES R1 cell populations than in the EC F9 cells at all stages of RA-induced differentiation. Higher expression of Oct4 is detected in the EC F9 cells on day 5 of RA stimulation and in the ES R1 cells on day 3 after RA withdrawal (Figure 2). The expression of most somatic cell lineage markers increases significantly during the differentiation of the ES R1 and EC F9 cells (Figure 2). The strongest increase in expression is observed for markers of extraembryonic endoderm (Gata4) and neuroectoderm (Pax6) in differentiating ES R1 and EC F9 cells. Gata4 expression significantly differs between the ES R1 and EC F9 cells on day 5 of RA stimulation and on day 3 after RA withdrawal, while Pax6 expression differs between ES R1 and EC F9 cells during late stages of differentiation (RA10 and RA10 + 3). However, no significant differences in the expression of endoderm and mesoderm markers (Afp and Bry, resp.) are found between differentiating ES R1 and EC F9 populations (Figure 2).

In undifferentiated and differentiated ES R1 and EC F9 cells, endogenous expression of TGFβ family factors that initiate the corresponding signaling pathways also differs significantly. The most substantial differences are revealed in patterns of endogenous expression for Activin A and Nodal. In differentiating ES R1 and EC F9 cell populations, the expression of Activin A is upregulated, while the expression of Nodal is downregulated. Activin A is expressed at high levels in undifferentiated ES R1 cells, but the expression of this factor increases sharply and becomes higher in EC F9 cells during all stages of RA-induced differentiation (Figure 2). In contrast, Nodal is expressed at similar levels in undifferentiated ES R1 and EC F9 cells but decreases more strongly during differentiation of the ES R1 cells (Figure 2). Endogenous expression of TGFβ1 gradually increases during differentiation in both cell lines but differs significantly between ES R1 and EC F9 cells only during the final stage (RA10 + 3).

In contrast, the expression pattern of BMP4 differs from the Activin A and Nodal patterns during the differentiation of ES R1 and EC F9 cells. Endogenous expression of BMP4 is upregulated on days 3 and 5 and downregulated during the late stages of differentiation in both studied cell lines (Figure 2). These data show that differences in the endogenous expression of Activin, Nodal, and BMP that activate corresponding signaling pathways can contribute to differences in the dynamics of RA-induced lineage differentiation of ES R1 and EC F9 cells.

3.3. Tumorigenic Potential of RA-Simulated ES and EC Cells after Transplantation into Nude Mice. To evaluate tumorigenic potential, differentiating ES R1 and EC F9 cells were transplanted subcutaneously or intraperitoneally into nude mice. According to our previous data on the dynamics of tumor development [21], the formation of teratomas and teratocarcinomas was monitored in two tissue transplantation sites for 6–30 weeks (Table 1). Within 5-6 weeks, teratomas and teratocarcinomas develop in all nude mice (100%) after the transplantation of ES R1 and EC F9 cells on day 5 of RA stimulation in vitro (Figure 4, Table 1). Only teratomas develop in all mice after the transplantation of ES R1 cells on day 3 after RA withdrawal (RA10 + 3), and no teratocarcinomas form within 30 weeks after the transplantation of EC F9 cells at the same stage of in vitro differentiation (Figure 4, Table 1). The formation of tumors outside the transplantation sites is not observed after the transplantations of the studied

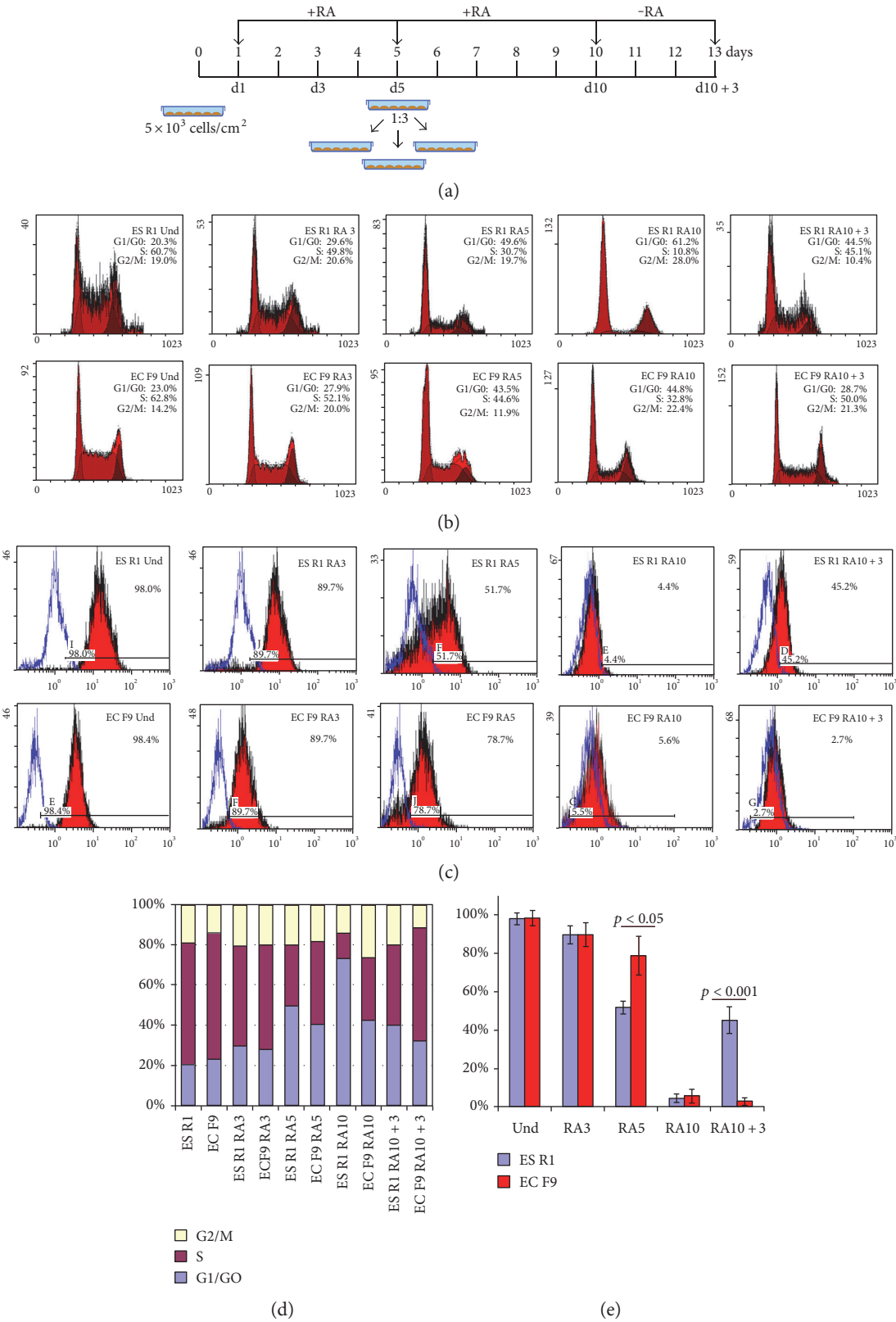

Figure 1: Proliferative activity and differentiation dynamics of ES R1 and EC F9 cells after 10 days of RA stimulation and 3 days after RA withdrawal. (a) Experimental design of RA-induced differentiation of ES R1 and EC F9 cells. (b and d) Flow cytometric analysis of the distributions of the cell cycle stages in the populations of RA-stimulated ES R1 and EC F9 cells. (c and e) Flow cytometric analysis of the number of Oct4-expressing cells in the populations of RA-stimulated ES R1 and EC F9 cells. The data are represented as the mean ± s.e., ANOVA.

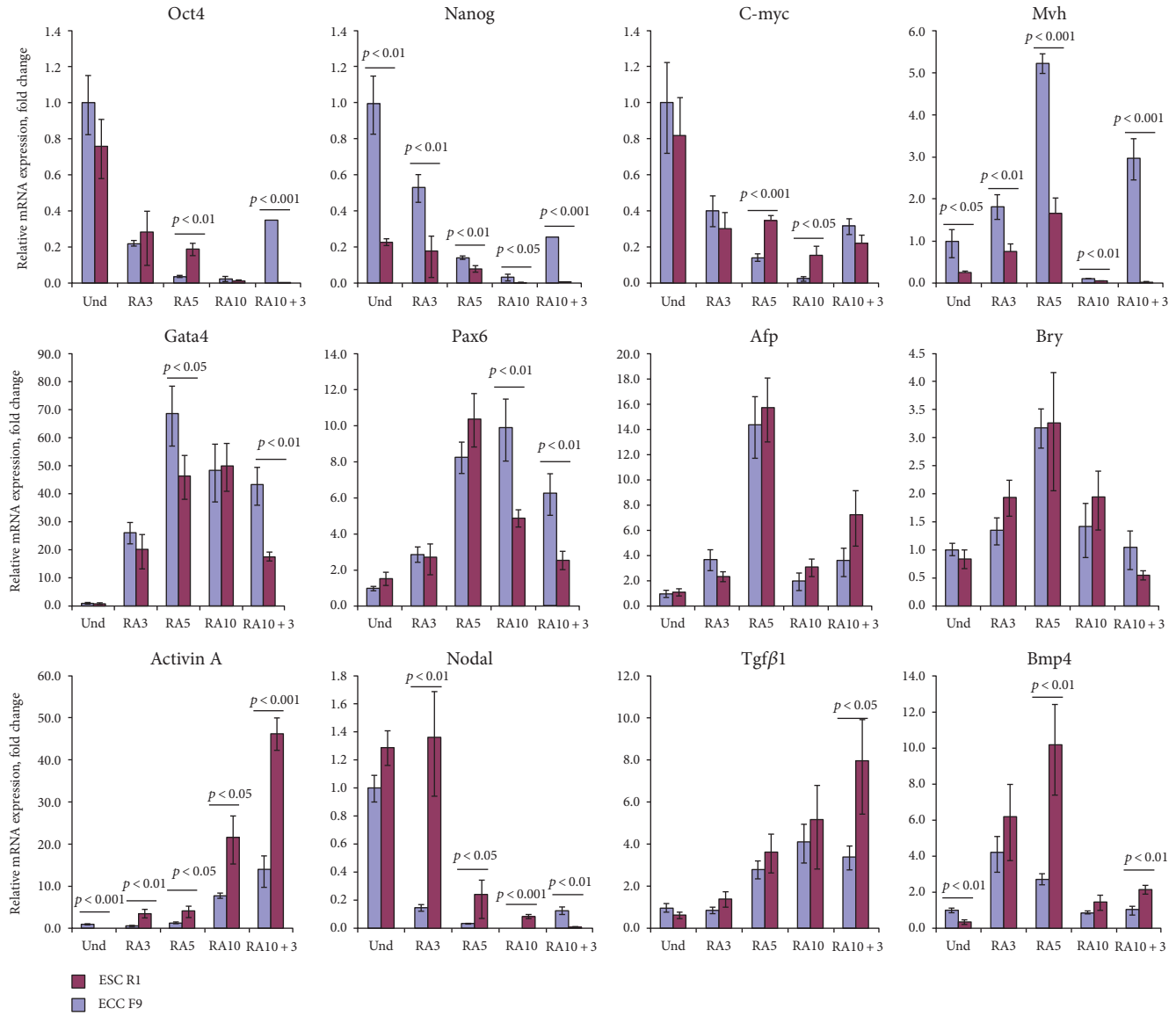

Figure 2: The gene expression patterns of pluripotency and embryonic lineage markers and TGFβ factors in the course of RA-induced differentiation of ES R1 and EC F9 cells. The gene expression levels of each gene in differentiated cells were evaluated relative to the gene expression levels in undifferentiated ES R1 cells. The data are represented as the mean ± s.d.; significant differences were estimated using ANOVA.

cells. Teratomas that develop after the transplantation of differentiating ES R1 cells contain different cell derivatives of three germ layers (Figure 4(c)). In contrast, the teratocarcinomas formed by the EC F9 cells on day 5 of in vitro RA stimulation (RA5) consist of entirely undifferentiated teratocarcinoma cells (Figure 4(c)). These experiments demonstrate different tumorigenic and differentiation potentials of the ES R1 and EC F9 cell populations after RA stimulation in vitro.

3.4. Effects of Stimulation of the Activin A/Nodal and BMP Signaling Pathways and Inhibition of the MEK/ERK and PI3K/Act Signaling Pathways on RA-Induced Differentiation of ES R1 Cells. Based on our findings concerning the differences in in vitro and in vivo differentiation of the ES R1 and EC F9 cells, we hypothesized that the tumorigenic potential of ES R1 and EC F9 cells on day 10 after RA stimulation could be associated with different activity levels of TGFβ family signaling pathways, as well as the MEK/ERK and PI3K/Act signaling cascades that counterbalance TGFβ family signaling pathways. The effects of modulation of these signaling pathways on the differentiation and tumor potential via enhancing the activity of Activin A and BMP4 signaling pathways and inhibiting of MEK/ERK and PI3K/Act signaling pathways in RA-stimulated ES R1 cells were studied in the next series of experiments. The ES R1 cells were exposed to factors (Activin A and BMP) and inhibitors (PD98059 and LY294002) from day 5 to day 10 of RA stimulation cells, because the most significant differences between differentiating ES R1 and ECF9 cells are detected during these stages. The design of the experiment is shown in Figure 5(a).

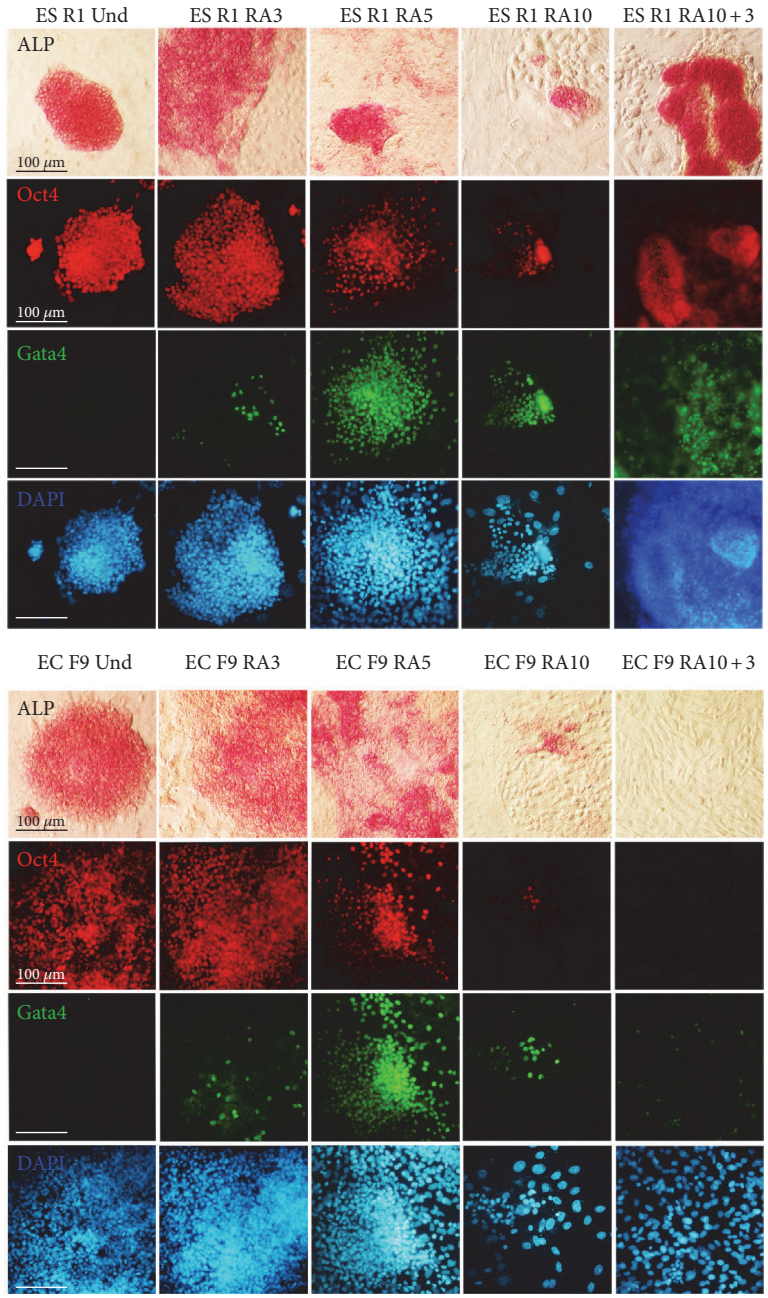

Figure 3: ALP activity and expression of Oct4 and Gata4 in differentiating ES R1 and EC F9 cells after RA stimulation for 10 days and 3 days after RA withdrawal. Nuclei were counterstained with DAPI. A significant number of the ES R1 and EC F9 cells expressed both Gata4 and Oct4 at all stages of RA-stimulated differentiation. Scale bar = 100 μm.

In all experimental variants, small numbers of Oct4- and ALP-positive cells are identified at the final stage of experiments. The numbers are similar to that observed on day 10 of RA stimulation alone (Figure 3 and Figure 5(b)). Moreover, the expression levels of Oct4, Nanog, and Mvh are significantly lower in differentiating ES R1 cell populations exposed to RA and additives than that in controls (ES R1 RA10 + 3) and are comparable to the expression levels in differentiating EC F9 cells (EC F9 RA10 + 3) (Figure 5(c)). An analysis of the tumorigenic potential of ES R1 cells differentiated with exposure to RA and additives shows that no tumors develop in either tissue site of nude mice 30 weeks after transplantation of all differentiating ES cell populations (Table 2 and Figure 6).

4. Discussion

Our study of the differentiation dynamics of normal pluripotent stem and malignant teratocarcinoma cells was conducted to answer the following questions: (i) Why do residual undifferentiated cells remain after induced in vitro differentiation of ES and EC cells? (ii) Are the residual undifferentiated cells tumorigenic and carcinogenic? (iii) What possible mechanisms underlie incomplete differentiation

Table 1: Tumor development after transplantations of RA-stimulated ES R1 and EC F9 into immunodeficient nude mice.

Transplantation sites	ES R1 + RA5	ES R1 + RA10	EC F9 + RA5	EC F9 + RA10
SC	3/3 (100%), 6 wk	4/4 (100%), 6 wk	3/3 (100%), 6 wk	0/6 (0%), 30 wk
IP	3/3 (100%), 6 wk	4/4 (100%), 6 wk	3/3 (100%), 6 wk	0/8 (0%), 30 wk

The percentage and number of animals are indicated in which tumors were found in the transplantation sites during autopsy. SC: subcutaneous transplantation; IP: intraperitoneal transplantation (the cells grown on acetate cellulose membranes).

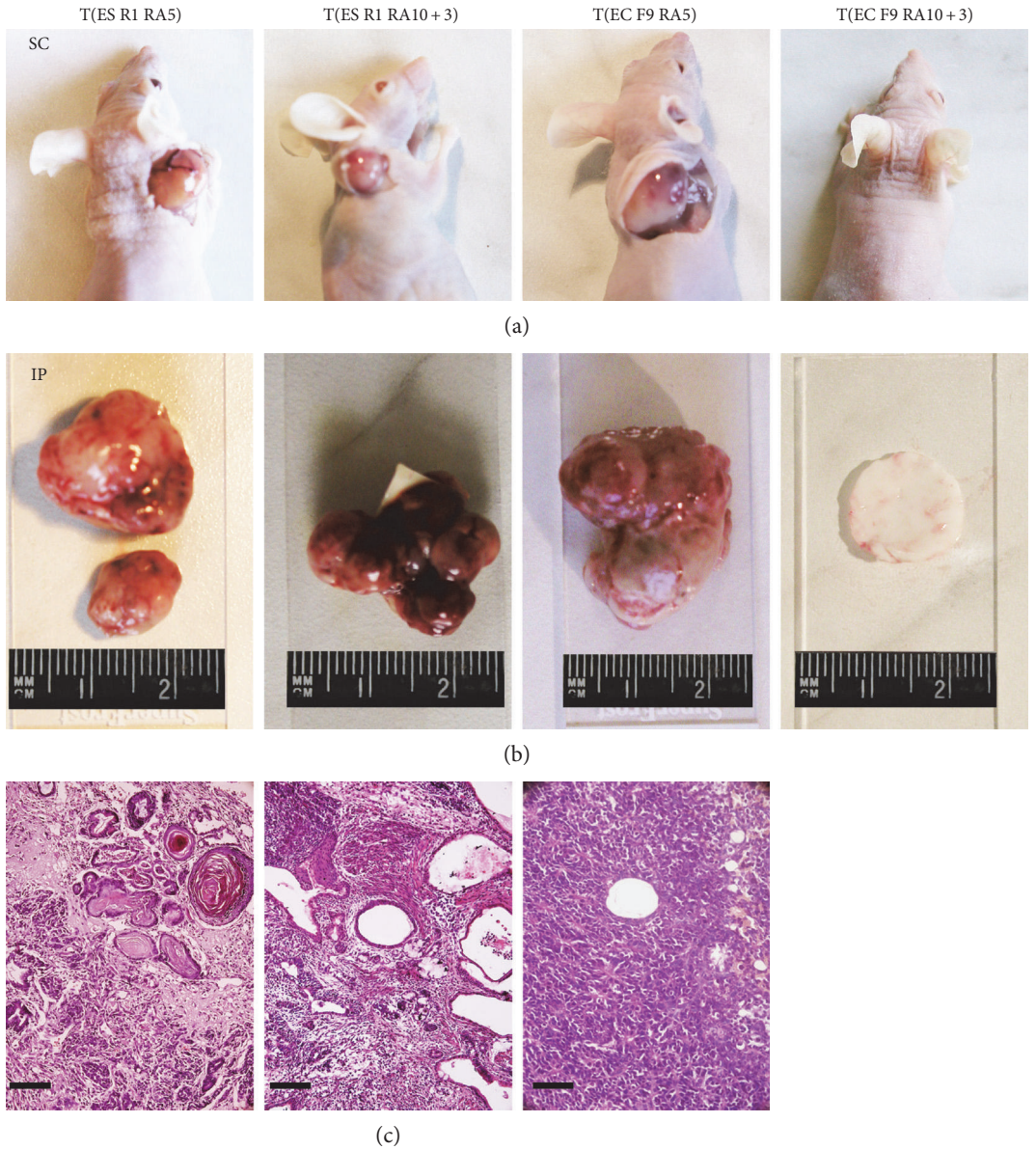

Figure 4: Tumorigenic and differentiation potential of RA-simulated ES R1 and EC F9 cells after transplantation into nude mice. (a and b) teratomas and teratocarcinomas developed in nude mice after subcutaneous (SC) and intraperitoneal (IP) transplantation of ES R1 and EC F9 cells on day 5 RA stimulation (T(ES R1 RA5), T(EC F9 RA5)) and on day 3 after RA withdrawal (T(ES R1 RA10 + 3), T(EC F9 RA10 + 3)). (c) Sections through teratomas and teratocarcinomas formed by RA-simulated ES R1 and EC F9 cells after transplantation into nude mice. The teratomas contain derivatives of three germ layers while the teratocarcinomas consisted entirely of undifferentiated cancer cells. No teratocarcinomas have formed during 30 weeks after the transplantation of EC F9 cells on day 3 after RA withdrawal (RA10 + 3). Scale bar = 100 μm.

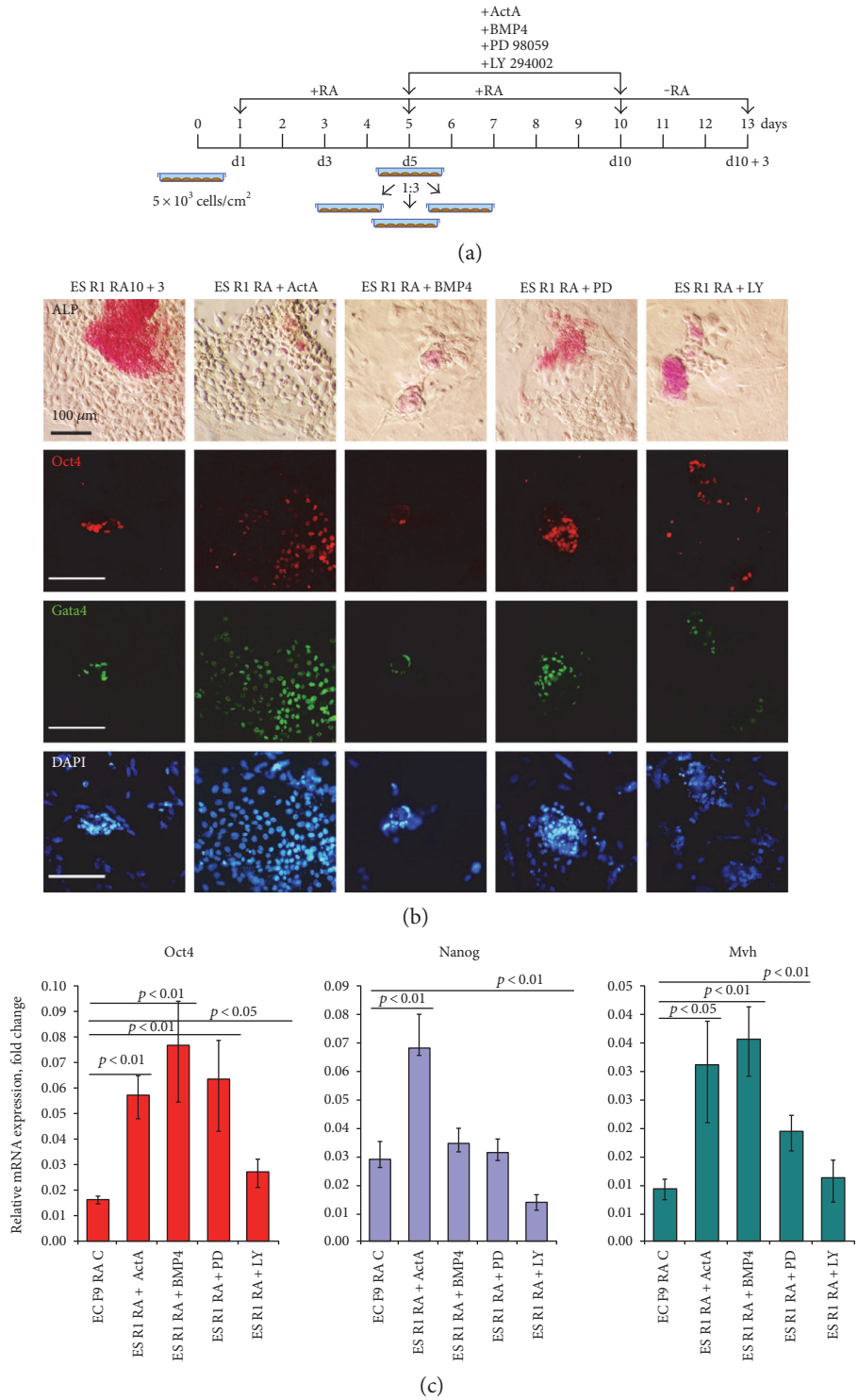

Figure 5: Stimulation of the Activin A/Nodal and BMP signaling pathways and inhibition of the MEK/ERK and PI3K/Act signaling pathways in ES R1 cells during the course of RA-induced differentiation. (a) Design of experiments on the induced differentiation of ES R1 cells with RA and exposure to Activin A, BMP4, PD98059, and LY294002. (b) ALP activity and Oct4 and Gata4 expression in differentiating ES R1 cells after exposure to RA, Activin A, BMP4, PD98059, and LY294002 on day 3 after RA and additive withdrawal. Nuclei were counterstained with DAPI. ActA: Activin A; BMP: BMP4; PD: PD98059; LY: LY294002. Scale bar = 100 μm. (c) The expression of Oct4, Nanog, and Mvh in differentiating ES R1 after exposure to RA, Activin A, BMP4, PD98059, and LY294002 on day 3 after RA and additive withdrawal. The gene expression levels of each gene in all experimental variants of differentiating ES R1 cells were calculated relative to the gene expression levels in control ES R1 cells on day 3 after RA withdrawal (ES R1 RA10 + 3) and statistically evaluated relative to the gene expression levels in control EC F9 cells on day 3 after RA withdrawal (EC F9 RA10 + 3). The data are represented as the mean ± s.d.; significant differences were estimated using ANOVA.

Table 2: Tumor development in nude mice after transplantations of ES R1 stimulated with RA in combination with Activin A, BMP4, PD98059, and LY294002.

Transplantation sites	ES R1 + RA + ActA	ES R1 + RA + BMP4	ES R1 + RA + LY	ES R1 + RA + PD
SC	0/5 (0%), 30 wk	0/5 (0%), 30 wk	0/5 (0%), 30 wk	0/5 (0%), 30 wk
IP	0/5 (0%), 30 wk	0/5 (0%), 30 wk	0/5 (0%), 30 wk	0/5 (0%), 30 wk

The percentage and number of animals are indicated in which tumors were found in the transplantation sites during autopsy. SC: subcutaneous transplantation; IP: intraperitoneal transplantation (the cells grown on acetate cellulose membranes).

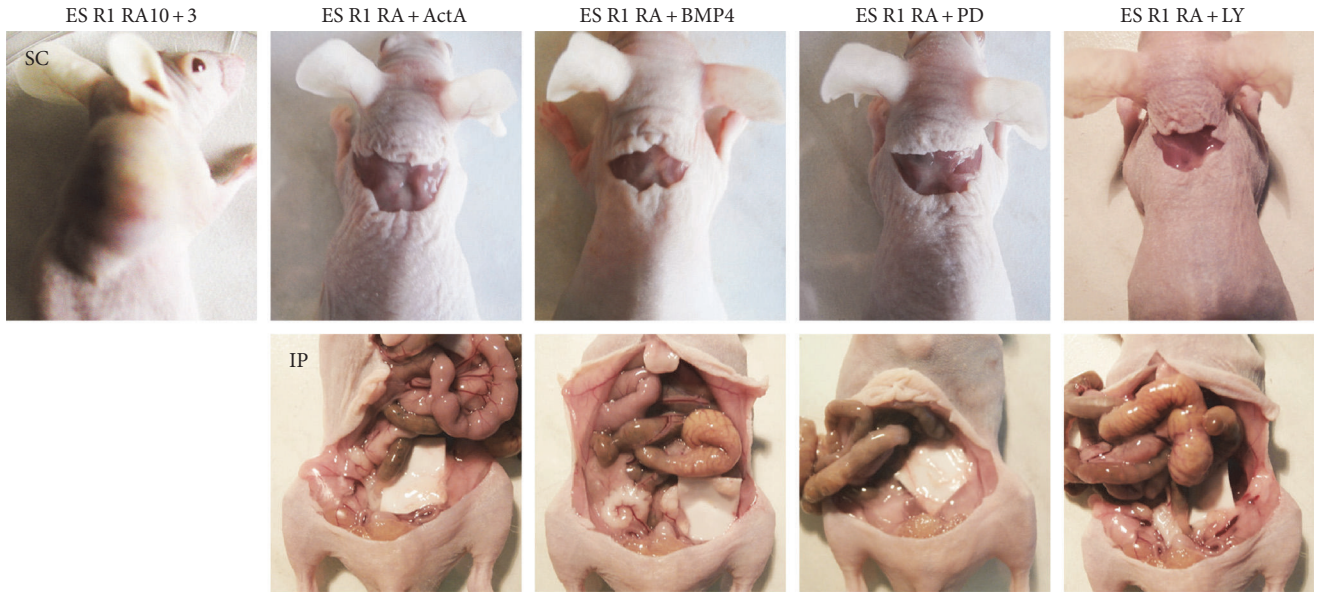

Figure 6: Assessment of the tumorigenic potential of ES R1 cells stimulated to differentiate with RA, Activin A, BMP4, PD98059, and LY294002 after transplantation into nude mice. No tumors were detected in nude mice after subcutaneous (SC) and intraperitoneal (IP) transplantation of ES R1 cells on day 3 after RA and additive withdrawal. Teratomas formed only after subcutaneous transplantation of ES R1 cells on day 3 after RA withdrawal (ES R1 RA10 + 3). ActA: Activin A; BMP: BMP4; PD: PD98059; LY: LY294002.

of ES and EC cells? And (iv) how can we reduce the number of residual undifferentiated cells in differentiating ES cell populations that are capable of forming tumors after transplantation into recipients?

The present study revealed significant differences in proliferative activity and differentiation dynamics between the ES R1 and EC F9 cells from day 5 to day 10 of RA-induced differentiation. However, despite similar numbers of residual Oct4-expressing cells in both ES and EC cell populations on day 10, the tumorigenic potential of these cells is strikingly different. Unexpectedly, differentiating ES R1 cell populations retain the ability to form tumors (teratomas), whereas the EC F9 cell populations lose tumorigenicity, as reported previously [30]. These findings indicate a different status of residual Oct4-expressing cells in differentiating ES and EC cell populations.

A gene expression analysis of pluripotent and lineage markers reveals significantly higher expression levels of Nanog and Mvh in ES R1 cells than in EC F9 cells at all stages of differentiation indicating a possible role of these genes in the maintenance of differentiation and tumorigenic potentials. Previously, we suggested that Mvh, which is a regulator of embryonic and adult germ cell development, may play a role in maintaining of the naive pluripotent state of mouse and human ES cells [52–56]. In this context, the residual undifferentiated ES cells with high expression of Oct4, Nanog, and Mvh can be considered to be the earliest precursors of germ cells, similar to primordial germ cells before their colonization of the gonadal ridges. This assumption is supported by data that demonstrate the easy in vitro conversion of primordial germ cells into EG cells, which are very similar to ES cells [55, 57–60]. Consequently, higher expression of Mvh may indicate a stronger ability of the 10-day RA-stimulated ES R1 cells to differentiate into primordial germ cells, which also easily form teratomas after transplantation into nude mice. Therefore, we propose that the ability of pluripotent stem cells to differentiate into primordial germ cells is associated with their ability to develop teratomas containing all types of embryonic cell derivatives. The residual undifferentiated ES cells cannot be considered to be cancerous because unlike EC cells, these cells are capable of differentiation into precursors of three germ layers in teratomas and even in secondary teratomas after recloning and secondary transplantation [21]. Presumably, the residual undifferentiated ES cells represent an intermediate cell type between pluripotent and primordial germ cells which are both

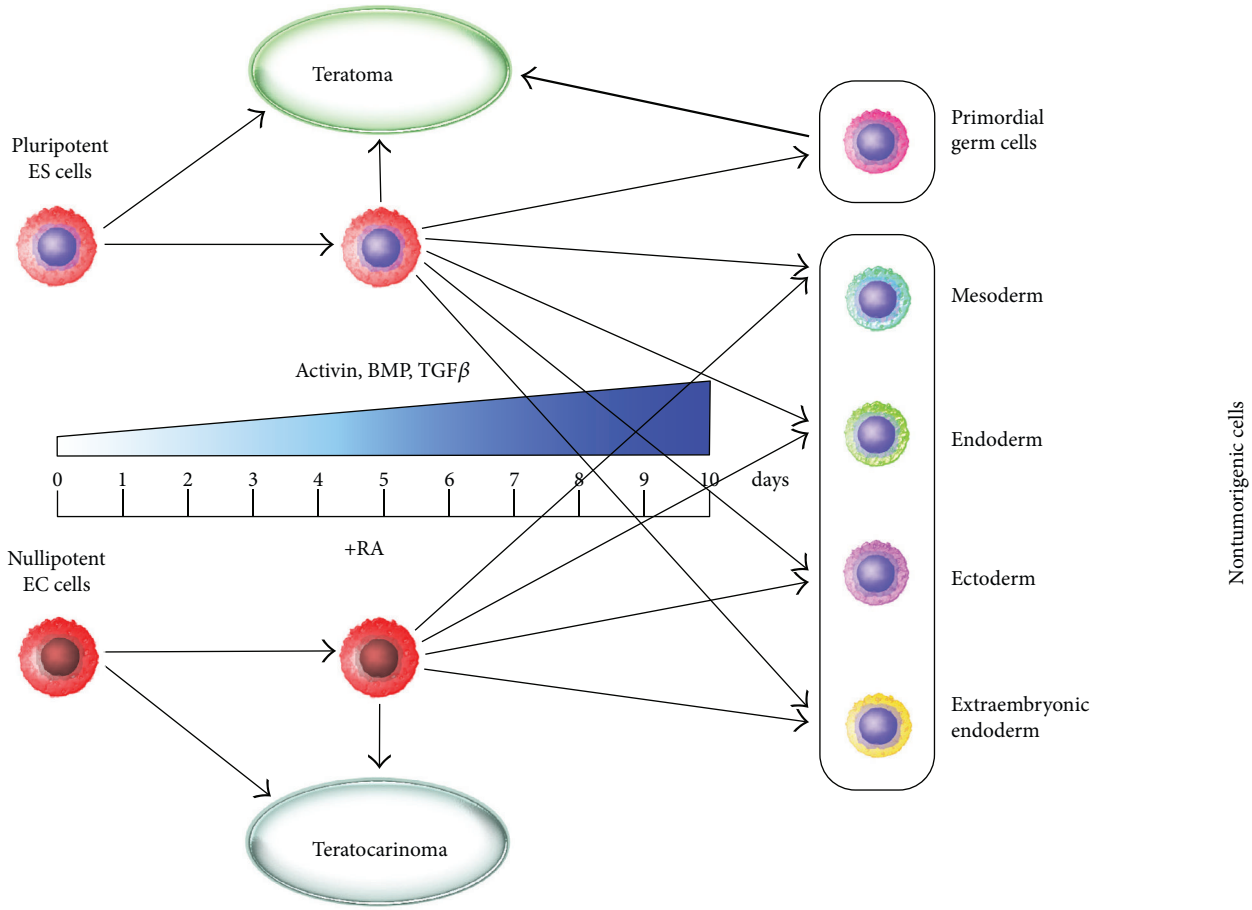

Figure 7: Tumorigenic and differentiation potentials of ES R1 and EC F9 cells during the course of RA-induced differentiation.

able to develop teratomas. In contrast, EC F9 cells expressing low levels of Mvh can differentiate after RA-stimulation only in the somatic nontumorigenic derivatives (Figure 7).

The mechanisms of RA-induced differentiation of EC and ES cells have been studied extensively [30, 49, 61–67]. To investigate the possible mechanisms underlying various tumor and differentiation potentials of ES R1 and EC F9 cells, we focused on TGFβ family factors that play a key role in the regulation of lineage fate during the early development and the earliest stages of pluripotent stem cell differentiation [68–70]. The observation that the expression levels of Activin A, Nodal, and BMP4 were higher in the EC F9 cells than in the ES R1 cells, particularly between the 5th and 10th day of RA-stimulation, led us to propose that additional stimulation of these signaling pathways might enhance the differentiation of the ES R1cells. Indeed, modulation of the Activin/Nodal and BMP signaling cascades via exposure to exogenous Activin A and BMP4 factors or by inhibiting the MEK/ERK and PI3K/Act-signaling pathways that counterbalance canonical TGFβ family factor signaling pathways resulted in reduced expression of Mvh in all experimental cell populations and a loss of tumorigenicity after transplantation into nude mice. Thus, these data show that the differentiation strategy of modulating prodifferentiation and antiproliferative signals by stimulating the Activin A/Nodal or BMP signaling pathways or inhibiting the MEK/ERK and PI3K/Act signaling pathways during the time window from 5 to 10 days of ES cell differentiation may be effective for significantly reducing of the number of cells that initiate teratoma development (Figure 7). Interestingly, this strategy is also effective for EC F9 cells, which express higher endogenous levels of Activin A and BMP4 in response to RA stimulation.

Most of the developed protocols for the in vitro differentiation of pluripotent stem cells are based on the knowledge of the molecular mechanisms that regulate the commitment and differentiation of early embryonic and extraembryonic cells during development. The modulation of the MEK/ERK, PI3K/Act, Wnt, and TGFβ family signaling pathways using various cocktails of growth factors and inhibitors, as well as small molecular inducers, for a different time of exposure is an effective approach for deriving the required differentiated cell types [68–77]. In most cases, the cell populations differentiated in vitro are heterogeneous and require cell sorting. However, the residual undifferentiated cells are a minor subpopulation; therefore, to remove these cells, negative selection methods are used that involve activating cell death in target cells via a "suicide" gene approach and chemical inducers [41–48, 78]. Nevertheless, the application of these technologies may have negative effects

on the viability of the desired differentiated cells and may cause uncontrolled genetic rearrangements due to insertional mutagenesis [43–45, 79]. Therefore, the strategy of modulating signaling pathways to enhance differentiation may be safer and more effective. Our study demonstrates the effectiveness of this strategy for inhibiting the tumorigenicity of residual undifferentiated ES cells. However, this strategy requires additive efforts to create the most effective protocols for increasing the effectiveness of directed differentiation and reducing the number of residual undifferentiated cells.

5. Conclusions

The present comparative study of RA-induced differentiation the ES R1 and EC F9 cells aimed to clarify the possible mechanisms underlying the incomplete in vitro differentiation of these cells and to determine a new approach eliminating residual undifferentiated ES cells, which can form tumors after transplantation into recipients. During 10 days of RA-induced differentiation, ES R1 and EC F9 cells were found to exhibit differences in proliferative activity and differentiation dynamics in vitro, as well as different tumorigenic potential after transplantation into nude mice. Importantly, differentiating ES R1 cell populations retain the ability to form teratomas, while the EC F9 cell populations lose tumorigenicity. Gene expression analysis revealed higher expression of Nanog and Mvh, as well as Activin A and BMP4, in undifferentiated ES R1 cells in comparison to EC F9 cells. However, the expression levels of Activin A and BMP4 increase more sharply in the EC F9 cells after RA stimulation. Moreover, the stimulation of the Activin/Nodal and BMP signaling cascades after exposure to exogenous Activin A and BMP4 factors and inhibitors of the MEK/ERK and PI3K/Act signaling pathways results in a reduction of the number of residual Oct4-expressing ES R1 cells and a loss of tumorigenicity. Thus, our study demonstrates that a differentiation strategy that enhances the Activin A/Nodal and BMP signaling pathways or inhibits the MEK/ERK and PI3K/Act signaling pathways in ES cells may be effective for reducing the number of tumorigenic cells. This approach may promote progress in the development of safe stem cell therapeutics.

Conflicts of Interest

The authors declare no financial conflict of interests.

Acknowledgments

The authors thank T. M. Nikonova for providing assistance in histological section preparation and M. Gorobets for caring for experimental animals. This work was supported by the Russian Foundation for Basic Research, Grant 11-04-00379.

References

[1] G. R. Martin, "Isolation of a pluripotent cell line from early mouse embryos cultured in medium conditioned by teratocarcinoma stem cells," *Proceedings of the National Academy of Sciences of the United States of America*, vol. 78, no. 12, pp. 7634–7638, 1981.

[2] M. J. Evans and M. H. Kaufman, "Establishment in culture of pluripotential cells from mouse embryos," *Nature*, vol. 292, no. 5819, pp. 154–156, 1981.

[3] Y. Matsui, K. Zsebo, and B. L. Hogan, "Derivation of pluripotential embryonic stem cells from murine primordial germ cells in culture," *Cell*, vol. 70, no. 5, pp. 841–847, 1992.

[4] J. A. Thomson, J. Itskovitz-Eldor, S. S. Shapiro et al., "Embryonic stem cell lines derived from human blastocysts," *Science*, vol. 282, no. 5391, pp. 1145–1147, 1998.

[5] M. J. Shamblott, J. Axelman, S. Wang et al., "Derivation of pluripotent stem cells from cultured human primordial germ cells," *Proceedings of the National Academy of Sciences of the United States of America*, vol. 95, no. 23, pp. 13726–13731, 1998.

[6] K. Takahashi and S. Yamanaka, "Induction of pluripotent stem cells from mouse embryonic and adult fibroblast cultures by defined factors," *Cell*, vol. 126, no. 4, pp. 663–676, 2006.

[7] W. E. Lowry, L. Richter, R. Yachechko et al., "Generation of human induced pluripotent stem cells from dermal fibroblasts," *Proceedings of the National Academy of Sciences of the United States of America*, vol. 105, no. 8, pp. 2883–2888, 2008.

[8] I. Park, P. H. Lerou, R. Zhao, H. Huo, and G. Q. Daley, "Generation of human-induced pluripotent stem cells," *Nature Protocols*, vol. 3, no. 7, pp. 1180–1186, 2008.

[9] M. Tachibana, P. Amato, M. Sparman et al., "Human embryonic stem cells derived by somatic cell nuclear transfer," *Cell*, vol. 153, no. 6, pp. 1228–1238, 2013.

[10] A. Nagy, E. Gócza, E. M. Diaz et al., "Embryonic stem cells alone are able to support fetal development in the mouse," *Development (Cambridge, England)*, vol. 110, no. 3, pp. 815–821, 1990.

[11] A. Nagy, J. Rossant, R. Nagy, W. Abramow-Newerly, and J. C. Roder, "Derivation of completely cell culture-derived mice from early-passage embryonic stem cells," *Proceedings of the National Academy of Sciences of the United States of America*, vol. 90, no. 18, pp. 8424–8428, 1993.

[12] K. Okita, T. Ichisaka, and S. Yamanaka, "Generation of germline-competent induced pluripotent stem cells," *Nature*, vol. 448, no. 7151, pp. 313–317, 2007.

[13] I. Polejaeva and S. Mitalipov, "Stem cell potency and the ability to contribute to chimeric organisms," *Reproduction (Cambridge, England)*, vol. 145, no. 3, pp. R81–R88, 2013.

[14] S. A. Przyborski, "Differentiation of human embryonic stem cells after transplantation in immune-deficient mice," *Stem Cells*, vol. 23, no. 9, pp. 1242–1250, 2005.

[15] M. Drukker, H. Katchman, G. Katz et al., "Human embryonic stem cells and their differentiated derivatives are less susceptible to immune rejection than adult cells," *Stem Cells*, vol. 24, no. 2, pp. 221–229, 2006.

[16] A. Brederlau, A. S. Correia, S. V. Anisimov et al., "Transplantation of human embryonic stem cell-derived cells to a rat model of Parkinson's disease: effect of in vitro differentiation on graft survival and teratoma formation," *Stem Cells*, vol. 24, no. 6, pp. 1433–1440, 2006.

[17] R. Dressel, J. Schindehütte, T. Kuhlmann et al., "The tumorigenicity of mouse embryonic stem cells and in vitro differentiated neuronal cells is controlled by the recipients' immune response," *PLoS One*, vol. 3, no. 7, article e2622, 2008.

[18] R. Dressel, "Effects of histocompatibility and host immune responses on the tumorigenicity of pluripotent stem cells," *Seminars in Immunopathology*, vol. 33, no. 6, pp. 573–591, 2011.

[19] R. Swijnenburg, S. Schrepfer, J. A. Govaert et al., "Immunosuppressive therapy mitigates immunological rejection of human embryonic stem cell xenografts," *Proceedings of the National Academy of Sciences of the United States of America*, vol. 105, no. 35, pp. 12991–12996, 2008.

[20] M. Sundberg, P. Andersson, E. Åkesson et al., "Markers of pluripotency and differentiation in human neural precursor cells derived from embryonic stem cells and CNS tissue," *Cell Transplantation*, vol. 20, no. 2, pp. 177–191, 2011.

[21] O. F. Gordeeva and T. M. Nikonova, "Development of experimental tumors formed by mouse and human embryonic stem and teratocarcinoma cells after subcutaneous and intraperitoneal transplantations into immunodeficient and immunocompetent mice," *Cell Transplantation*, vol. 22, no. 10, pp. 1901–1914, 2013.

[22] B. Blum and N. Benvenisty, "The tumorigenicity of diploid and aneuploid human pluripotent stem cells," *Cell Cycle (Georgetown, Tex.)*, vol. 8, no. 23, pp. 3822–3830, 2009.

[23] T. E. Werbowetski-Ogilvie, M. Bossé, M. Stewart et al., "Characterization of human embryonic stem cells with features of neoplastic progression," *Nature Biotechnology*, vol. 27, no. 1, pp. 91–97, 2009.

[24] U. Ben-David and N. Benvenisty, "The tumorigenicity of human embryonic and induced pluripotent stem cells," *Nature Reviews. Cancer*, vol. 11, no. 4, pp. 268–277, 2011.

[25] K. Takahashi, K. Mitsui, and S. Yamanaka, "Role of ERas in promoting tumour-like properties in mouse embryonic stem cells," *Nature*, vol. 423, no. 6939, pp. 541–545, 2003.

[26] B. Blum, O. Bar-Nur, T. Golan-Lev, and N. Benvenisty, "The anti-apoptotic gene survivin contributes to teratoma formation by human embryonic stem cells," *Nature Biotechnology*, vol. 27, no. 3, pp. 281–287, 2009.

[27] O. Hovatta, M. Jaconi, V. Töhönen et al., "A teratocarcinoma-like human embryonic stem cell (hESC) line and four hESC lines reveal potentially oncogenic genomic changes," *PLoS One*, vol. 5, no. 4, article e10263, 2010.

[28] L. C. Stevens, "Experimental production of testicular teratomas in mice," *Proceedings of the National Academy of Sciences of the United States of America*, vol. 52, pp. 654–661, 1964.

[29] L. J. Kleinsmith and G. B. Pierce, "Multipotentiality of single embryonal carcinoma cells," *Cancer Research*, vol. 24, pp. 1544–1551, 1964.

[30] S. Strickland and V. Mahdavi, "The induction of differentiation in teratocarcinoma stem cells by retinoic acid," *Cell*, vol. 15, no. 2, pp. 393–403, 1978.

[31] P. W. Andrews, "Human teratocarcinomas," *Biochimica et Biophysica Acta*, vol. 948, no. 1, pp. 17–36, 1988.

[32] I. Damjanov, "Teratocarcinoma: neoplastic lessons about normal embryogenesis," *The International Journal of Developmental Biology*, vol. 37, no. 1, pp. 39–46, 1993.

[33] S. Sell and G. B. Pierce, "Maturation arrest of stem cell differentiation is a common pathway for the cellular origin of teratocarcinomas and epithelial cancers," *Laboratory Investigation; a Journal of Technical Methods and Pathology*, vol. 70, no. 1, pp. 6–22, 1994.

[34] P. W. Andrews, "From teratocarcinomas to embryonic stem cells," *Philosophical Transactions of the Royal Society of London. Series B, Biological Sciences*, vol. 357, no. 1420, pp. 405–417, 2002.

[35] G. Caisander, H. Park, K. Frej et al., "Chromosomal integrity maintained in five human embryonic stem cell lines after prolonged in vitro culture," *Chromosome Research: An International Journal on the Molecular, Supramolecular and Evolutionary Aspects of Chromosome Biology*, vol. 14, no. 2, pp. 131–137, 2006.

[36] Y. Mayshar, U. Ben-David, N. Lavon et al., "Identification and classification of chromosomal aberrations in human induced pluripotent stem cells," *Cell Stem Cell*, vol. 7, no. 4, pp. 521–531, 2010.

[37] A. Gore, Z. Li, H. Fung et al., "Somatic coding mutations in human induced pluripotent stem cells," *Nature*, vol. 471, no. 7336, pp. 63–67, 2011.

[38] L. C. Laurent, I. Ulitsky, I. Slavin et al., "Dynamic changes in the copy number of pluripotency and cell proliferation genes in human ESCs and iPSCs during reprogramming and time in culture," *Cell Stem Cell*, vol. 8, no. 1, pp. 106–118, 2011.

[39] L. Tesarova, P. Simara, S. Stejskal, and I. Koutna, "The aberrant DNA methylation profile of human induced pluripotent stem cells is connected to the reprogramming process and is normalized during in vitro culture," *PLoS One*, vol. 11, no. 6, article e0157974, 2016.

[40] P. Simara, L. Tesarova, D. Rehakova et al., "DNA double-strand breaks in human induced pluripotent stem cell reprogramming and long-term in vitro culturing," *Stem Cell Research & Therapy*, vol. 8, no. 1, p. 73, 2017.

[41] F. Cheng, Q. Ke, F. Chen et al., "Protecting against wayward human induced pluripotent stem cells with a suicide gene," *Biomaterials*, vol. 33, no. 11, pp. 3195–3204, 2012.

[42] F. Chen, B. Cai, Y. Gao et al., "Suicide gene-mediated ablation of tumor-initiating mouse pluripotent stem cells," *Biomaterials*, vol. 34, no. 6, pp. 1701–1711, 2013.

[43] A. Bedel, F. Beliveau, I. Lamrissi-Garcia et al., "Preventing pluripotent cell teratoma in regenerative medicine applied to hematology disorders," *Stem Cells Translational Medicine*, vol. 6, no. 2, pp. 382–393, 2017.

[44] A. Bedel, F. Beliveau, I. Lamrissi-Garcia et al., "Preventing pluripotent cell teratoma in regenerative medicine applied to hematology disorders," *Stem Cells Translational Medicine*, vol. 6, no. 2, pp. 382–393, 2017.

[45] O. F. Gordeeva, "Antiproliferative and cytotoxic effects of different type cytostatics on mouse pluripotent stem and teratocarcinoma cells," *Ontogenez*, vol. 43, no. 4, pp. 268–277, 2012.

[46] U. Ben-David, Q. Gan, T. Golan-Lev et al., "Selective elimination of human pluripotent stem cells by an oleate synthesis inhibitor discovered in a high-throughput screen," *Cell Stem Cell*, vol. 12, no. 2, pp. 167–179, 2013.

[47] M. Lee, S. H. Moon, H. Jeong et al., "Inhibition of pluripotent stem cell-derived teratoma formation by small molecules," *Proceedings of the National Academy of Sciences of the United States of America*, vol. 110, no. 35, pp. E3281–E3290, 2013.

[48] L. Zhang, Y. Pan, G. Qin et al., "Inhibition of stearoyl-coA desaturase selectively eliminates tumorigenic Nanog-positive cells: improving the safety of iPS cell transplantation to myocardium," *Cell Cycle (Georgetown, Tex.)*, vol. 13, no. 5, pp. 762–771, 2014.

[49] A. I. Spira and M. A. Carducci, "Differentiation therapy," *Current Opinion in Pharmacology*, vol. 3, no. 4, pp. 338–343, 2003.

[50] S. Sell, "Stem cell origin of cancer and differentiation therapy," *Critical Reviews in Oncology/Hematology*, vol. 51, no. 1, pp. 1–28, 2004.

[51] S. Sell, "Cancer stem cells and differentiation therapy," *Tumour Biology: The Journal of the International Society for Oncodevelopmental Biology and Medicine*, vol. 27, no. 2, pp. 59–70, 2006.

[52] Y. Toyooka, N. Tsunekawa, Y. Takahashi, Y. Matsui, M. Satoh, and T. Noce, "Expression and intracellular localization of mouse Vasa-homologue protein during germ cell development," *Mechanisms of Development*, vol. 93, no. 1-2, pp. 139–149, 2000.

[53] Y. Toyooka, N. Tsunekawa, R. Akasu, and T. Noce, "Embryonic stem cells can form germ cells in vitro," *Proceedings of the National Academy of Sciences of the United States of America*, vol. 100, no. 20, pp. 11457–11462, 2003.

[54] O. Lacham-Kaplan, "In vivo and in vitro differentiation of male germ cells in the mouse," *Reproduction (Cambridge, England)*, vol. 128, no. 2, pp. 147–152, 2004.

[55] C. Eguizabal, T. C. Shovlin, G. Durcova-Hills, A. Surani, and A. McLaren, "Generation of primordial germ cells from pluripotent stem cells," *Differentiation; Research in Biological Diversity*, vol. 78, no. 2-3, pp. 116–123, 2009.

[56] O. F. Gordeeva, N. V. Lifantseva, and S. V. Khaĭdukov, "Expression patterns of germ line specific genes in mouse and human pluripotent stem cells are associated with regulation of ground and primed state of pluripotency," *Ontogenez*, vol. 42, no. 6, pp. 403–424, 2011.

[57] J. L. Resnick, L. S. Bixler, L. Cheng, and P. J. Donovan, "Long-term proliferation of mouse primordial germ cells in culture," *Nature*, vol. 359, no. 6395, pp. 550-551, 1992.

[58] G. Durcova-Hills, F. Wianny, J. Merriman, M. Zernicka-Goetz, and A. McLaren, "Developmental fate of embryonic germ cells (EGCs), in vivo and in vitro," *Differentiation; Research in Biological Diversity*, vol. 71, no. 2, pp. 135–141, 2003.

[59] L. V. Sharova, A. A. Sharov, Y. Piao et al., "Global gene expression profiling reveals similarities and differences among mouse pluripotent stem cells of different origins and strains," *Developmental Biology*, vol. 307, no. 2, pp. 446–459, 2007.

[60] M. Oliveros-Etter, Z. Li, K. Nee et al., "PGC reversion to pluripotency involves erasure of DNA methylation from imprinting control centers followed by locus-specific re-methylation," *Stem Cell Reports*, vol. 5, no. 3, pp. 337–349, 2015.

[61] J. Clifford, H. Chiba, D. Sobieszczuk, D. Metzger, and P. Chambon, "RXRalpha-null F9 embryonal carcinoma cells are resistant to the differentiation, anti-proliferative and apoptotic effects of retinoids," *The EMBO Journal*, vol. 15, no. 16, pp. 4142–4155, 1996.

[62] J. Pacherník, V. Bryja, M. Esner, L. Kubala, P. Dvorák, and A. Hampl, "Neural differentiation of pluripotent mouse embryonal carcinoma cells by retinoic acid: inhibitory effect of serum," *Physiological Research/Academia Scientiarum Bohemoslovaca*, vol. 54, no. 1, pp. 115–122, 2005.

[63] D. R. Soprano, B. W. Teets, and K. J. Soprano, "Role of retinoic acid in the differentiation of embryonal carcinoma and embryonic stem cells," *Vitamins and Hormones*, vol. 75, pp. 69–95, 2007.

[64] D. Su and L. J. Gudas, "Gene expression profiling elucidates a specific role for RARgamma in the retinoic acid-induced differentiation of F9 teratocarcinoma stem cells," *Biochemical Pharmacology*, vol. 75, no. 5, pp. 1129–1160, 2008.

[65] L. Delacroix, E. Moutier, G. Altobelli et al., "Cell-specific interaction of retinoic acid receptors with target genes in mouse embryonic fibroblasts and embryonic stem cells," *Molecular and Cellular Biology*, vol. 30, no. 1, pp. 231–244, 2010.

[66] B. S. Pickens, B. W. Teets, K. J. Soprano, and D. R. Soprano, "Role of COUP-TFI during retinoic acid-induced differentiation of P19 cells to endodermal cells," *Journal of Cellular Physiology*, vol. 228, no. 4, pp. 791–800, 2013.

[67] G. M. Kelly and M. I. Gatie, "Mechanisms regulating stemness and differentiation in embryonal carcinoma cells," *Stem Cells International*, vol. 2017, Article ID 3684178, 20 pages, 2017.

[68] T. Watabe and K. Miyazono, "Roles of TGF-beta family signaling in stem cell renewal and differentiation," *Cell Research*, vol. 19, no. 1, pp. 103–115, 2009.

[69] N. Oshimori and E. Fuchs, "The harmonies played by TGF-β in stem cell biology," *Cell Stem Cell*, vol. 11, no. 6, pp. 751–764, 2012.

[70] T. A. Beyer, M. Narimatsu, A. Weiss, L. David, and J. L. Wrana, "The TGFβ superfamily in stem cell biology and early mammalian embryonic development," *Biochimica et Biophysica Acta*, vol. 1830, no. 2, pp. 2268–2279, 2013.

[71] L. Vallier, M. Alexander, and R. A. Pedersen, "Activin/Nodal and FGF pathways cooperate to maintain pluripotency of human embryonic stem cells," *Journal of Cell Science*, vol. 118, Part 19, pp. 4495–4509, 2005.

[72] B. Greber, H. Lehrach, and J. Adjaye, "Control of early fate decisions in human ES cells by distinct states of TGFβ pathway activity," *Stem Cells and Development*, vol. 17, no. 6, pp. 1065–1077, 2008.

[73] L. Vallier, T. Touboul, Z. Chng et al., "Early cell fate decisions of human embryonic stem cells and mouse epiblast stem cells are controlled by the same signalling pathways," *PLoS One*, vol. 4, no. 6, article e6082, 2009.

[74] M. C. Nostro, F. Sarangi, S. Ogawa et al., "Stage-specific signaling through TGFβ family members and WNT regulates patterning and pancreatic specification of human pluripotent stem cells," *Development (Cambridge, England)*, vol. 138, no. 5, pp. 861–871, 2011.

[75] P. W. Burridge, G. Keller, J. D. Gold, and J. C. Wu, "Production of de novo cardiomyocytes: human pluripotent stem cell differentiation and direct reprogramming," *Cell Stem Cell*, vol. 10, no. 1, pp. 16–28, 2012.

[76] M. Bertacchi, G. Lupo, L. Pandolfini et al., "Activin/Nodal signaling supports retinal progenitor specification in a narrow time window during pluripotent stem cell neuralization," *Stem Cell Reports*, vol. 5, no. 4, pp. 532–545, 2015.

[77] C. E. Weidgang, T. Seufferlein, A. Kleger, and M. Mueller, "Pluripotency factors on their lineage move," *Stem Cells International*, vol. 2016, Article ID 6838253, 16 pages, 2016.

[78] S. Cho, S. Kim, H. Jeong et al., "Repair of ischemic injury by pluripotent stem cell based cell therapy without teratoma through selective photosensitivity," *Stem Cell Reports*, vol. 5, no. 6, pp. 1067–1080, 2015.

[79] S. Yagyu, V. Hoyos, F. D. Bufalo, and M. K. Brenner, "An inducible caspase-9 suicide gene to improve the safety of therapy using human induced pluripotent stem cells," *Molecular Therapy: The Journal of the American Society of Gene Therapy*, vol. 23, no. 9, pp. 1475–1485, 2015.

Hindawi
Stem Cells International
Volume 2017, Article ID 1479137, 7 pages
https://doi.org/10.1155/2017/1479137

Research Article

Maintenance of a Schwann-Like Phenotype in Differentiated Adipose-Derived Stem Cells Requires the Synergistic Action of Multiple Growth Factors

Alice E. Mortimer,[1] Alessandro Faroni,[1] Mahmut A. Kilic,[1,2] and Adam J. Reid[1,3]

[1]*Blond McIndoe Laboratories, Division of Cell Matrix Biology and Regenerative Medicine, School of Biological Sciences, Faculty of Biology, Medicine and Health, University of Manchester, Manchester Academic Health Science Centre, Manchester M13 9PL, UK*
[2]*Department of Biophysics, Faculty of Medicine, Adnan Menderes University, Aydin, Turkey*
[3]*Department of Plastic Surgery & Burns, University Hospitals of South Manchester, Manchester Academic Health Science Centre, Manchester, UK*

Correspondence should be addressed to Adam J. Reid; adam.reid@manchester.ac.uk

Received 7 April 2017; Accepted 16 May 2017; Published 16 July 2017

Academic Editor: Marco A. Velasco-Velazquez

Copyright © 2017 Alice E. Mortimer et al. This is an open access article distributed under the Creative Commons Attribution License, which permits unrestricted use, distribution, and reproduction in any medium, provided the original work is properly cited.

Differentiating human adipose-derived stem cells (ASCs) towards Schwann cells produces an unstable phenotype when stimulating factors are withdrawn. Here, we set out to examine the role of glial growth factor 2 (GGF-2) in the maintenance of Schwann-like cells. Following ASC differentiation to Schwann-like cells, stimulating factors were withdrawn such that cells either remained in media supplemented with all stimulating factors, GGF-2 alone, or underwent complete withdrawal of all factors. Furthermore, each stimulating factor was also removed from the growth medium individually. At 72 hours, gene (qRT-PCR) and protein (ELISA) expression of key Schwann cell factors were quantified and cell morphology was analysed. Cells treated with GGF-2 alone reverted to a stem cell morphology and did not stimulate the production of brain-derived neurotrophic factor (BDNF), regardless of the concentration of GGF-2 in the growth medium. However, GGF-2 alone increased the expression of Krox20, the main transcription factor involved in myelination, relative to those cells treated with all stimulating factors. Cells lacking fibroblast growth factor were unable to maintain a Schwann-like morphology, and those lacking forskolin exhibited a downregulation in BDNF production. Therefore, it is likely that the synergistic action of multiple growth factors is required to maintain Schwann-like phenotype in differentiated ASCs.

1. Introduction

Tissue engineering strategies have sought to harness the regenerative potential of Schwann cells (SCs) to aid peripheral nerve repair [1]. Much focus has been on the use of stem cells, particularly those derived abundantly from adipose tissue [2, 3]. Adipose derived stem cells (ASCs) differentiate into Schwann-like cells (dASC) when treated with a combination of forskolin, glial growth factor 2 (GGF-2), fibroblast growth factor (FGF-2), and platelet-derived growth factor (PDGF) [2, 3]. dASC possess many SC characteristics, including a spindle-shaped morphology, a similar secretome, and the ability to induce neurite regeneration [2–4].

Whilst rat dASCs have been used successfully in rodent in vivo models, evidence is lacking regarding the efficacy of human dASCs [4]. Given that the original differentiation protocol was developed for rat bone marrow stem cells, it is unsurprising that human dASCs revert to their stem cell phenotype upon withdrawal of stimulating factors [4]. Thus, further characterisation of dASCs is required prior to clinical translation.

GGF-2 is a soluble form of neuregulin 1 (NRG1), and in SCs, NRG1 allows for the survival of SC precursors and is involved in producing myelinating cells [5, 6]. It has recently been shown that mouse ASCs lacking GGF-2 reduce their expression of SC phenotype markers [7]. Here, we examine whether GGF-2 is sufficient alone to maintain critical Schwann-like properties by examining dASCs ability to maintain a Schwann-like morphology, produce brain-derived neurotrophic factor (BDNF), and express Krox20 (the main transcription factor involved in myelination) [5].

2. Materials and Methods

2.1. Cell Harvest, Isolation, and Differentiation. Adipose tissue was harvested from female surgical patients at the University Hospital of South Manchester, UK. Patients were fully consented, and procedures were approved by the National Research Ethics Committee (NRES 13/SC/0499). A previously described protocol was used for the isolation and differentiation of ASCs [4]. Briefly, adipose tissue was first minced with a razor blade and then underwent 60 minutes of enzymatic digestion using 0.2% (*w*/*v*) collagenase (Life Technologies, Paisley, UK). A 100 μm nylon mesh (Merck Millipore UK, Watford, UK) was then used to filter the dissociated tissue, and stromal vascular fraction (SVF) was obtained by centrifugation at 300*g* for 10 minutes. SVF was incubated for 1 minute with red blood cell lysis buffer (Sigma-Aldrich) to remove red blood cells, recentrifuged (10 minutes at 300*g*), and the resulting pellet of ASC was plated in 75 cm^2 flasks in stem cell growth medium (SCGM) consisting of alpha minimum essential medium [αMEM (Sigma-Aldrich)] supplemented with 10% (*v*/*v*) fetal bovine serum [FBS (LabTech, Uckfield, UK)], 2 mM L-glutamine (GE Healthcare UK, Little Chalfont, UK), and 1% (*v*/*v*) penicillin–streptomycin solution. For Schwann cell differentiation, subconfluent ASC cultures were supplemented with 1 mM β-mercaptoethanol (Sigma-Aldrich) for 24 hours and preconditioned for 72 hours with 35 ng/mL all-trans-retinoic acid (Sigma-Aldrich). Following preconditioning, the cell culture medium was replaced with SCGM supplemented with 14 μM forskolin (Sigma-Aldrich), 5.46 nM GGF-2 (a gift from Acorda Therapeutics, Ardsley, NY, USA), 10 ng/mL basic fibroblast growth factor [FGF-2 (Peprotech EC, London, UK)], and 5 ng/mL platelet-derived growth factor [PDGF (Peprotech EC, London, UK)] for 14 days. This same supplemented media was used for cell maintenance during culture and passaging until further experimentation.

2.2. Experimental Setup. dASCs were plated onto 12-well plates at a density of 100,000 cells per well (unless otherwise stated) and maintained in growth medium with all stimulating factors for 48 hours. Media was then replaced according to the individual experiment (see below), and cells were cultured for 72 hours, after which outcome measures described below were assessed. Experimental and technical triplicates were used throughout. Media was replaced at 48 hours with αMEM supplemented with only GGF-2 ($dASC^{-/+GGF}$) at concentrations of 0.273 nM, 2.73 nM, 5.46 nM, and 10.92 nM. Withdrawal of each factor individually ($dASC^{+/-[forskolin,\ GGF,\ FGF,\ or\ PDGF]}$) was also carried out, and in each case, a positive control of normal growth medium ($dASC^{+}$) and negative control of withdrawal of all factors ($dASC^{-}$) were used.

2.3. Morphology Analysis. Light microscopy and phalloidin staining of cells were undertaken at the experimental endpoint. Staining was carried out according to previously described methods [4]. Briefly, 5000 cells per well were plated in order to better visualize individual cell morphology. At the endpoint, cells were washed with phosphate buffer saline (PBS) solution and fixed with 4% (*w*/*v*) paraformaldehyde for 15 minutes at room temperature. Following permeabilisation with 0.2% (*v*/*v*) Triton X-100 (Sigma-Aldrich) for 20 minutes, cells were stained for 20 minutes in the dark with Alexa 488-conjugated phalloidin (1 : 40, Life Technologies, USA). After PBS washes, cells were imaged using an Olympus IX51 fluorescent microscope at 4x magnification. 15 images of cells in each experimental condition were taken, and aspect ratio (AR) for each cell (longest cell length/narrowest cell width) was determined using Image J (National Institutes of Health, USA).

2.4. Real-Time Polymerase Chain Reaction (qPCR). Cells were collected in RNAprotect reagent, and RNA was extracted using an RNeasy Plus Mini Kit according to manufacturer's instructions (Qiagen). RNA was quantified using a NanoDrop ND-100 spectrophotometer (Thermo-Fisher Scientific, USA). The RT2 First Strand kit (Qiagen) was then used to reverse transcribe RNA. RT2 qPCR SYBR Green Mastermix and a Corbett Rotor Gene 6000 real-time cycler (Qiagen) were used to perform qPCR. Primer sequences are Krox20 [forward sequence: 5′-AAC GGAGTGGCCGGAGAT-3′, reverse sequence: 5′-ATGG GAGATCCAACGACCTCT T-3′ (Sigma-Aldrich)], 18s [Qiagen (Cat number PPH05666E-200)] and BDNF [Qiagen (Cat number PPH00569F-200)]. All reactions were carried out in quadruplicate, and the following protocol was used: activation of HotStart DNA Taq polymerase by heating at 95°C for 10 minutes and followed by 45 cycles of 95°C for 15 seconds, 55°C for 30 seconds, and 72°C for 30 seconds. Melting curve analysis was performed in order to confirm specificity of primers. To analyse the qPCR data, the $\Delta\Delta$Ct method was employed, normalising data to the housekeeping gene, 18s.

2.5. Enzyme-Linked Immunosorbent Assay (ELISA). ELISA kits to detect BDNF in cell culture supernatant (RayBiotech, USA) were used according to manufacturer's instructions. Plates were read at 450 nm using an Asys UVM-340 microplate spectrophotometer (Biochrom). Protein concentrations of the samples were calculated by interpolating their absorbency values on the standard curve obtained using recombinant BDNF protein.

2.6. Statistical Analysis. One-way analysis of variance (with Tukey test) and unpaired t tests were performed

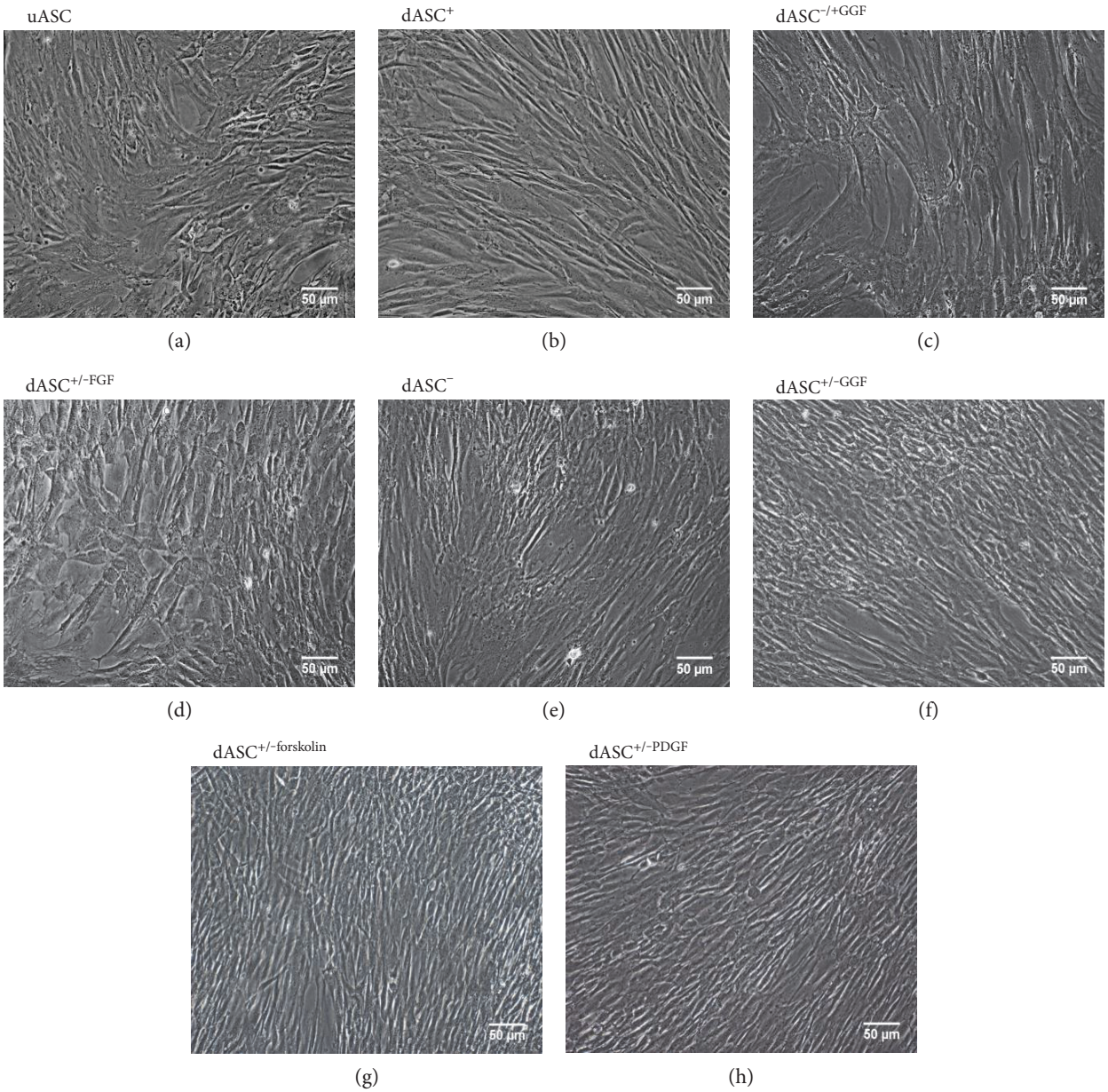

Figure 1: GGF-2 is not sufficient alone to maintain a spindle-shaped morphology, and FGF-2 is necessary to produce the Schwann-like morphology. (a) Undifferentiated cells display a flattened, fibroblast-like appearance. (b) $dASC^{+}$ elongate and take on a spindle shape. (c) $dASC^{-/+GGF}$ revert to a stem-like morphology, as do (d) $dASC^{+/-FGF}$ and (e) $dASC^{-}$, whilst (f) $dASC^{+/-GGF}$, (g) $dASC^{+/-forskolin}$, and (h) $dASC^{+/-PDGF}$ all retain a spindle-shaped appearance. All cells were photographed at 10x magnification.

using Graphpad Prism 7.0 software (Graphpad Software Inc., USA). P values of <0.05 were considered statistically significant.

3. Results

3.1. $dASC^{-/+GGF}$ Revert to a Stem Cell Morphology. Undifferentiated ASC (uASC, Figure 1(a)) stimulated to $dASC^{+}$ (Figure 1(b)) produced cells with an elongated, spindle-shaped morphology. $dASC^{-/+GGF}$ reverted to a stem cell-like morphology, as did $dASC^{+/-FGF}$ and $dASC^{-}$ (Figures 1(c), 1(d), and 1(e)), whilst $dASC^{+/-GGF}$, $dASC^{+/-forskolin}$, and $dASC^{+/-PDGF}$ retained their spindle shape (Figures 1(f), 1(g), and 1(h)).

There were more spindle-shaped $dASC^{+}$ (Figure 2(a)) compared to $dASC^{-/+GGF}$ (Figure 2(b)). $dASC^{+}$ had a significantly higher AR when compared to $dASC^{-/+GGF}$ (Figure 2(c)). The relative frequencies of cells of each AR confirm that in $dASC^{-/+GGF}$, there is a reduced frequency of cells with AR > 5 (Figure 2(d)).

3.2. $dASC^{-/+GGF}$ Have a Phenotype Similar to $dASC^{-}$. $dASC^{-/+GGF}$ upregulated Krox20 expression compared to $dASC^{+}$ (Figure 3(a)) but failed to maintain BDNF production levels regardless of GGF-2 concentration (Figure 3(b)). In

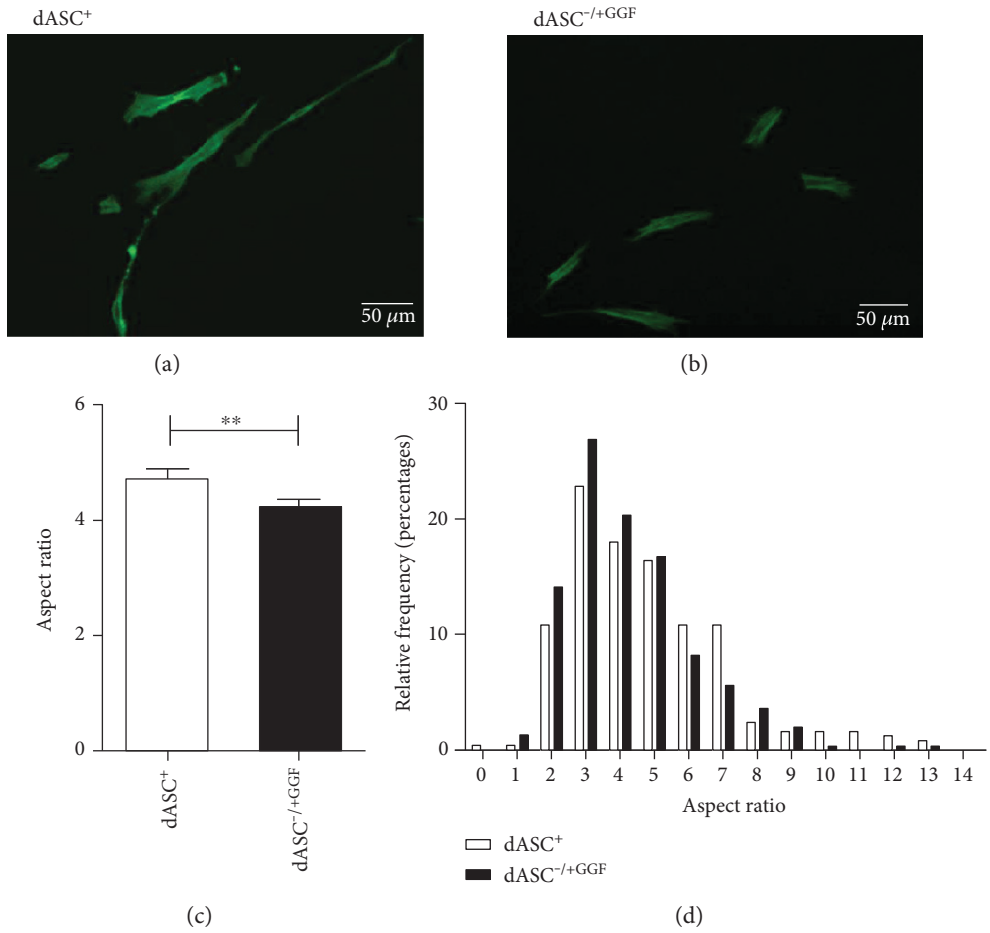

Figure 2: Cells treated with all stimulating factors have an increased aspect ratio compared to those treated with GGF-2 alone. (a) Spindle-shaped cells are clearly visible in dASC$^+$ phalloidin-stained cells. Cells were photographed at 4x magnification. (b) dASC$^{-/+GGF}$phalloidin-stained cells exhibit fewer spindle-shaped cells. (c) dASC$^+$ had a significantly higher AR when compared to dASC$^{-/+GGF}$ (4.752 ± 0.144 in dASC$^+$ versus 4.248 ± 0.107 in dASC$^{-/+GGF}$, $^{**}P < 0.01$, $n = 3$). (d) A total of 249 dASC$^+$ cells and 304 dASC$^{-/+GGF}$ cells were analysed, and the relative frequency of each AR was determined. There was a higher percentage of cells with AR < 5 in the dASC$^{-/+GGF}$ group (63% versus 53% in dASC$^+$) and a higher percentage of spindle-shaped cells (AR ≥ 5) in the dASC$^+$ group (47% versus 37% in dASC$^{-/+GGF}$).

each case, the pattern of expression was similar to that in dASC$^-$.

3.3. Forskolin Is Necessary for BDNF Production. dASC$^{+/-forskolin}$ and dASC$^{+/-PDGF}$ had significantly reduced gene expression of BDNF when compared to all other groups (Figure 4(a)). dASC$^{+/-forskolin}$ also had significantly reduced BDNF protein production compared to all other groups (Figure 4(b)).

4. Discussion

The use of ASCs in peripheral nerve injury has demonstrated real promise in experimental models [2, 3]; however, clinical translation is hindered by a rapid lack of stability in human dASCs when growth factor treatment is withdrawn [4]. Given the importance of NRG1 signalling in SC biology, we postulated that GGF-2 would be sufficient to maintain dASCs after withdrawal of other growth factors. Our results suggest that the maintenance of this phenotype is much more complex and relies on the synergistic actions of multiple growth factors. This will be crucial to understand prior to potential clinical use of this stem cell therapy for peripheral nerve injury.

We found that GGF-2 alone was unable to maintain the spindle-shaped morphology of dASCs. Interestingly, cells lacking FGF-2 also reverted to a uASC-like morphology. Stimulating rat SCs with FGF-2 in vitro induces the characteristic spindle shape, and ASCs cultured with FGF-2 maintain a spindle-shaped morphology [8, 9]. This suggests that FGF-2 may be involved in producing a Schwann-like morphology.

We found that dASC$^{-/+GGF}$ had reduced BDNF production when compared to dASC$^+$, as did dASC$^{+/-forskolin}$. We can therefore suggest that GGF-2 is not sufficient alone to produce BDNF, but that forskolin, acting synergistically with other factors may be necessary for BDNF production. Forskolin acts through intracellular cyclic adenosine

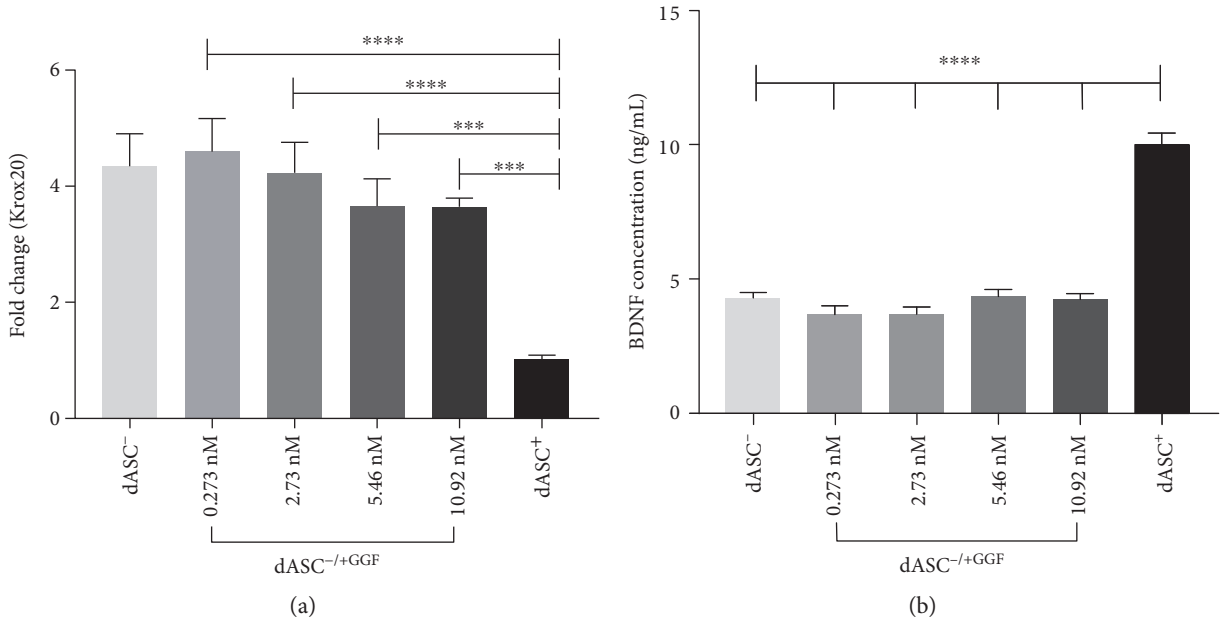

Figure 3: Krox20 gene expression and BDNF production in cells maintained in GGF-2 alone is similar to that of cells in which all stimulating factors have been withdrawn. (a) $dASC^{-}$ had a 4.351 ± 0.552-fold increase in the expression of Krox20 ($^{****}P < 0.0001$, $n = 3$, $N = 3$); $dASC^{-/+GGF\ [0.273\ nM]}$ cells had a 4.599 ± 0.568-fold increase ($^{****}P < 0.0001$, $n = 3$, $N = 3$); $dASC^{-/+GGF\ [2.73\ nM]}$ cells a 4.23 ± 0.527-fold increase ($^{****}P < 0.0001$, $n = 3$, $N = 3$); $dASC^{-/+GGF\ [5.46\ nM]}$ cells a 3.657 ± 0.468-fold increase ($^{***}P < 0.001$, $n = 3$, $N = 3$); and $dASC^{-/+GGF\ [10.92\ nM]}$ cells a 3.648 ± 0.148 ($^{***}P < 0.001$, $n = 3$, $N = 3$) in Krox20 expression compared to $dASC^{+}$ cells. There was no significant difference in expression between $dASC^{-/+GGF}$ and $dASC^{-}$. (b) $dASC^{+}$ secrete 10 ± 0.440 ng/mL BDNF compared to 4.32 ± 0.184 ng/mL in $dASC^{-}$, 3.673 ± 0.314 ng/mL in $dASC^{-/+GGF\ [0.273\ nM]}$, 3.695 ± 0.266 ng/mL in $dASC^{-/+GGF\ [2.73\ nM]}$, 4.351 ± 0.257 ng/mL in $dASC^{-/+GGF\ [5.46\ nM]}$, and 4.243 ± 0.208 ng/mL in $dASC^{-/+GGF\ [10.92\ nM]}$ ($^{****}P < 0.0001$ for all experimental groups compared to $dASC^{+}$, $n = 3$, $N = 3$).

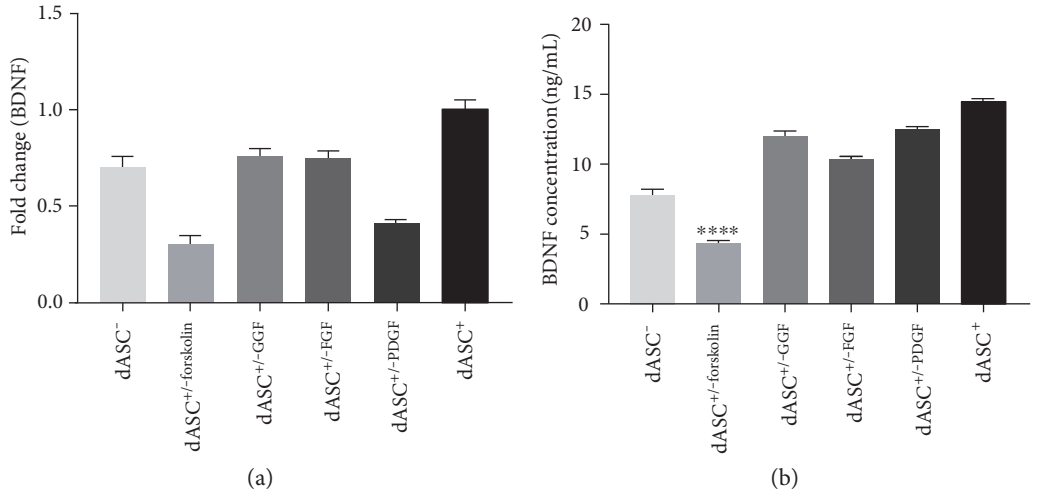

Figure 4: Forskolin may be involved in the production of BDNF. (a) PCR analysis of BDNF expression shows that both $dASC^{+/-forskolin}$ and $dASC^{+/-PDGF}$ downregulate their expression of BDNF compared to all other groups (fold change 0.705 ± 0.051 in $dASC^{-}$, 0.302 ± 0.047 in $dASC^{+/-forskolin}$, 0.761 ± 0.035 in $dASC^{+/-GGF}$, 0.749 ± 0.037 in $dASC^{+/-FGF}$, and 0.41 ± 0.017 in $dASC^{+/-PDGF}$ compared to 1 ± 0.044 in $dASC^{+}$. (b) ELISA protein analysis shows that $dASC^{+/-forskolin}$ have a large downregulation of BDNF production compared to all other groups (4.354 ± 0.120 ng/mL in $dASC^{+/-forskolin}$ versus 7.784 ± 0.413 ng/mL in $dASC^{-}$, 12 ± 0.435 ng/mL in $dASC^{+/-GGF}$, 10.33 ± 0.197 ng/mL in $dASC^{+/-FGF}$, 12.46 ± 0.158 ng/mL in $dASC^{+/-PDGF}$, and 14.48 ± 0.128 ng/mL in $dASC^{+}$; $^{****}P < 0.0001$, $n = 3$).

monophosphate (cAMP), and a recent study found that cAMP response element-binding protein (CREB) is instrumental in allowing for BDNF production by ASCs [10, 11]. The authors found that rat ASCs stimulated with forskolin rapidly increased their BDNF production and expression of phosphorylated CREB [11]. Hence, forskolin is likely to be involved in BDNF production [10, 11]; however, the mechanism in human ASCs remains to be elucidated.

NRG1 controls many aspects of myelination in SCs [6, 12, 13]. NRG1 signalling allows for myelination with low level stimulation but initiates demyelination with sustained activation [6, 14–16]. We investigated whether a similar effect would be seen in dASCs by stimulating cells with GGF-2 at increasing concentrations and quantifying Krox20 expression. $dASC^{-/+GGF}$ had a significant increase in Krox20 expression compared to $dASC^{+}$; however, there was no difference in expression between $dASC^{-/+GGF}$ and $dASC^{-}$ cells. This suggests that other growth factors may have an inhibitory action on Krox20 which requires further enquiry.

5. Conclusions

GGF-2 alone is insufficient to maintain Schwann-like properties achieved in dASCs. Cells lose their characteristic morphology and downregulate BDNF. However, we noted that cells treated with only GGF-2 increase their expression of Krox20 relative to those treated with all factors, suggesting that other factors have an inhibitory action on Krox20 expression. Forskolin appears necessary for BDNF production, and FGF-2 is likely responsible for Schwann-like morphology. Therefore, it is likely that the synergistic action of growth factors sustain the Schwann-like properties of dASC and further work in this field is required prior to clinical use of these cells.

Conflicts of Interest

The authors declare no conflicts of interest.

Authors' Contributions

Alice E. Mortimer contributed to the conception and design, collection and assembly of data, data analysis and interpretation, manuscript writing, and final approval of the manuscript. Alessandro Faroni contributed to the conception and design, financial support, provision of study materials, data analysis and interpretation, manuscript writing, and final approval of the manuscript. Adam J. Reid contributed to the conception and design, financial support, provision of study materials and patients, data analysis and interpretation, manuscript writing, and final approval of the manuscript. Mahmut A. Kilic contributed to the data analysis and interpretation, assembly of data, and final approval of the manuscript.

Acknowledgments

Alessandro Faroni and Adam J. Reid are supported by the Hargreaves and Ball Trust, the National Institute for Health Research (II-LA-0313-20003), the Academy of Medical Sciences, and the Manchester Regenerative Medicine Network (MaRMN). The authors thank the Acorda Therapeutics for kindly supplying them with recombinant GGF-2 for use in this study. The authors also thank Mr. Jonathan Duncan and Miss Siobhan O'Ceallaigh (Consultant Plastic Surgeons) and their patients at the University Hospital of South Manchester for the donation of adipose tissue.

References

[1] A. Faroni, S. A. Mobasseri, P. J. Kingham, and A. J. Reid, "Peripheral nerve regeneration: experimental strategies and future perspectives," *Advanced Drug Delivery Reviews*, vol. 82, pp. 160–167, 2015.

[2] P. J. Kingham, D. F. Kalbermatten, D. Mahay, S. J. Armstrong, M. Wiberg, and G. Terenghi, "Adipose-derived stem cells differentiate into a Schwann cell phenotype and promote neurite outgrowth in vitro," *Experimental Neurology*, vol. 207, no. 2, pp. 267–274, 2007.

[3] S. Kern, H. Eichler, J. Stoeve, H. Klüter, and K. Bieback, "Comparative analysis of mesenchymal stem cells from bone marrow, umbilical cord blood, or adipose tissue," *Stem Cells*, vol. 24, no. 5, pp. 1294–1301, 2006.

[4] A. Faroni, S. RJP, L. Lu, and A. J. Reid, "Human Schwann-like cells derived from adipose-derived mesenchymal stem cells rapidly de-differentiate in the absence of stimulating medium," *The European Journal of Neuroscience*, vol. 43, no. 3, pp. 417–430, 2016.

[5] K. R. Jessen and R. Mirsky, "Signals that determine Schwann cell identity," *Journal of Anatomy*, vol. 200, no. 4, pp. 367–376, 2002.

[6] N. Syed and H. A. Kim, "Soluble neuregulin and Schwann cell myelination: a therapeutic potential for improving remyelination of adult axons," *Molecular and Cellular Pharmacology*, vol. 2, no. 4, pp. 161–167, 2010.

[7] H. Orbay, C. J. Little, L. Lankford, C. A. Olson, and D. E. Sahar, "The key components of Schwann cell-like differentiation medium and their effects on gene expression pattern of adipose-derived stem cells," *Annals of Plastic Surgery*, vol. 74, no. 5, pp. 584–588, 2015.

[8] J. B. Davis and P. Stroobant, "Platelet-derived growth factors and fibroblast growth factors are mitogens for rat Schwann cells," *The Journal of Cell Biology*, vol. 110, no. 4, pp. 1353–1360, 1990.

[9] A. Kabiri, E. Esfandiari, B. Hashemibeni, M. Kazemi, M. Mardani, and A. Esmaeili, "Effects of FGF-2 on human adipose tissue derived adult stem cells morphology and chondrogenesis enhancement in transwell culture," *Biochemical and Biophysical Research Communications*, vol. 424, no. 2, pp. 234–238, 2012.

[10] R. H. Alasbahi and M. F. Melzig, "Forskolin and derivatives as tools for studying the role of cAMP," *Pharmazie*, vol. 67, no. 1, pp. 5–13, 2012.

[11] K. H. Tse, L. N. Novikov, M. Wiberg, and P. J. Kingham, "Intrinsic mechanisms underlying the neurotrophic activity of adipose derived stem cells," *Experimental Cell Research*, vol. 331, no. 1, pp. 142–151, 2015.

[12] C. Taveggia, G. Zanazzi, A. Petrylak et al., "Neuregulin-1 type III determines the ensheathment fate of axons," *Neuron*, vol. 47, no. 5, pp. 681–694, 2005.

[13] R. M. Stassart, R. Fledrich, V. Velanac et al., "A role for Schwann cell-derived neuregulin-1 in remyelination," *Nature Neuroscience*, vol. 16, no. 1, pp. 48–54, 2013.

[14] C. Birchmeier and D. L. H. Bennett, "Neuregulin/ErbB signaling in developmental myelin formation and nerve

repair," *Current Topics in Developmental Biology*, vol. 116, pp. 45–64, 2016.

[15] Y. Yarden and M. X. Sliwkowski, "Untangling the ErbB signalling network," *Nature Reviews. Molecular Cell Biology*, vol. 2, no. 2, pp. 127–137, 2001.

[16] I. Napoli, L. A. Noon, S. Ribeiro et al., "A central role for the ERK-signaling pathway in controlling Schwann cell plasticity and peripheral nerve regeneration in vivo," *Neuron*, vol. 73, no. 4, pp. 729–742, 2012.

Hindawi
Stem Cells International
Volume 2017, Article ID 3027520, 12 pages
https://doi.org/10.1155/2017/3027520

Review Article

In Utero Stem Cell Transplantation: Potential Therapeutic Application for Muscle Diseases

Neeladri Chowdhury[1,2,3] **and Atsushi Asakura**[1,2,3]

[1]*Stem Cell Institute, University of Minnesota Medical School, Minneapolis, MN 55455, USA*
[2]*Paul and Sheila Wellstone Muscular Dystrophy Center, University of Minnesota Medical School, Minneapolis, MN 55455, USA*
[3]*Department of Neurology, University of Minnesota Medical School, Minneapolis, MN 55455, USA*

Correspondence should be addressed to Atsushi Asakura; asakura@umn.edu

Received 28 March 2017; Accepted 26 April 2017; Published 17 May 2017

Academic Editor: Tilo Kunath

Copyright © 2017 Neeladri Chowdhury and Atsushi Asakura. This is an open access article distributed under the Creative Commons Attribution License, which permits unrestricted use, distribution, and reproduction in any medium, provided the original work is properly cited.

Muscular dystrophies, myopathies, and traumatic muscle injury and loss encompass a large group of conditions that currently have no cure. Myoblast transplantations have been investigated as potential cures for these conditions for decades. However, current techniques lack the ability to generate cell numbers required to produce any therapeutic benefit. In utero stem cell transplantation into embryos has been studied for many years mainly in the context of hematopoietic cells and has shown to have experimental advantages and therapeutic applications. Moreover, patient-derived cells can be used for experimental transplantation into nonhuman animal embryos via in utero injection as the immune response is absent at such early stages of development. We therefore propose in utero transplantation as a potential method to generate patient-derived humanized skeletal muscle as well as muscle stem cells in animals for therapeutic purposes as well as patient-specific drug screening.

1. Introduction

Skeletal muscle is the most abundant tissue in the human body, comprising 40–50% of body mass and playing vital roles in locomotion, heat production, and overall metabolism. Loss of muscle is a serious consequence of many chronic diseases including muscular diseases such as Duchenne muscular dystrophy (DMD) and aging-related sarcopenia because it leads to muscle weakness, loss of independence, and increased risk of death. In addition, traumatic muscle injury and loss caused by accident, surgery, and wartime injuries needs prolonged recovery.

Muscular dystrophies are a large and diverse group of genetic disorders that are associated with progressive loss of muscle mass and strength. The most common forms, DMD and Becker muscular dystrophy (BMD), are a result of mutations of the *DMD* gene on the X chromosome that code for the large sarcolemmal protein dystrophin. The rate of occurrence of DMD is reported to be in between 1 : 3802 and 1 : 6291 male births [1] and that of BMD is about 1 : 18,450 male births [2]. DMD is a more severe form and is caused by a complete absence of the dystrophin protein, whereas BMD is a milder form associated with lower levels of expression of dystrophin or a truncated dystrophin protein. DMD patients experience a loss of ambulation and are normally wheelchair dependent by 12 years of age followed by cardiac and respiratory failure in the second decade of life that are the main causes of death [3]. The dystrophin protein is one of the largest proteins produced in the human body containing several distinct domains. The N-terminus sequences are highly homologous to actin-binding domain responsible for interaction with the cytoskeleton. The central region consists of 24 rod-shaped spectrin-like repeats made up of triple helices. Each repeat is separated by nonhelical regions called hinges. The C-terminus region shows homology with utrophin and is responsible for binding and interacting with multiprotein dystrophin-associated protein (DAP) complex and the extracellular matrix (ECM) [4]. The large size and multiple domains of the dystrophin protein signify that it is capable of binding to multiple proteins and may perform a variety of functions. A common belief is that it acts as a spring that disperses the forces experienced by the sarcolemma during

muscle contractions and prevents membrane damage [5, 6]. The lack of dystrophin in DMD prevents this force dispersion causing excessive damage to the sarcolemma which is responsible for the progressive degeneration of the muscle fibers with age. While the skeletal muscle possesses a tremendous capacity for regeneration, this potential ultimately declines with DMD. No treatments are currently available for DMD, terminal muscle diseases.

Most organs in the body contain a population of tissue-resident stem cells that are able to proliferate and differentiate to repair the organs in the case of damage while undergoing self-renewal to maintain a constant pool of stem cells. In the skeletal muscle, this cell population is known as satellite cells due to their anatomic location between the myofiber and the basal lamina [7]. They proliferate in response to damage to give rise to muscle progenitor cells or myoblasts that then fuse to existing muscle fibers to repair the damage or give rise to new fibers [8], while myoblasts also possess adipogenic and osteogenic differentiation potential in vitro [9]. Apart from satellite cells, many atypical cell types such as side population cells, neural stem cells, hematopoietic stem cells, mesoangioblasts, pericytes, CD133+ circulating cells, and mesenchymal stem cells (MSCs) have been shown to possess myogenic differentiation potential [10–15]. One of the most promising uses for stem cells is the possibility to treat muscle diseases including those that have their origins in genetic anomalies and traumatic muscle injury and loss caused by accident, surgery, and wartime injuries.

2. Myoblast Transplantation for DMD Therapy

Due to the highly proliferative capacity of satellite cells, their transplantation has been investigated for the treatment of muscular dystrophies. In some of the earliest myoblast transplantation studies performed by Partridge in the late 1980s, they transplanted mononuclear cells isolated by disaggregation of normal neonatal muscle into nude, phosphorylase kinase- (PhK-) deficient mice. Upon harvesting the muscles and checking for PhK expression, they found that the transplanted cells contributed to the formation of new myofibers as well as fused to existing myofibers enabling them to express PhK. Different isoenzymes of glucose-6-phosphate isomerase (GPI) in donor versus recipient muscle were used to determine the animal of origin [16]. Similar experiments performed in the *mdx* mouse model for DMD showed dystrophin-positive fibers in injected muscle. Interestingly, they observed higher levels of engraftment compared to the previous study, indicating that actively regenerating muscle may be important for better engraftment of transplanted cells [17]. Experiments performed by Morgan et al. showed long-term engraftment and regenerative capacity of transplanted myoblasts. Their experiments showed better engraftment in irradiated muscle when compared to nonirradiated contralateral controls [18]. Furthermore, myoblast transplantation performed in nonhuman primates using an immunosuppressive agent (tacrolimus) showed significant levels of survival and engraftment of transplanted cells when compared to control [19]. However, the prolonged use of tacrolimus is toxic, and therefore, to reduce the effective dosage, Skuk et al. combined it with mycophenolate mofetil (MMF), another immunosuppressive, and observed fewer levels of serum antibodies and CD8+ T cells at the sites of injection in their nonhuman primate experiments [20].

The above experiments taken together provide compelling evidence for the potential of myoblast transplantation as a therapeutic technique for the treatment of muscular dystrophies in humans. These inspired multiple clinical trials in the early 90s that did not prove to be very successful due to insufficient amounts of research done in preclinical trials to determine the best protocol for myoblast transplantation [21]. Among the many reasons for the failure of the trials were the large amounts of cell death observed in the transplanted myoblasts as well as immune reactions against the donor myoblasts and fibers that were previously thought to not express the MHC class II. Furthermore, the limited migration of the transplanted myoblasts from the sites of transplantation added to the inefficiency of the procedure [22].

3. iPSC-Derived Myogenic Cells for Muscular Dystrophy Therapy

Recently, pluripotent stem cells have been investigated as sources of muscle progenitor cells for therapy due to their ability to differentiate into all three germ layers as well as their ease of expansion. The discovery of induced pluripotent stem cells (iPSCs), which enable the conversion of somatic cells to pluripotent cells by the introduction of a specific transcription factors, makes it possible to generate patient-specific stem cells, thus bypassing complications associated with immune rejection in case of transplants. Additionally, the iPSCs can be genetically corrected before transplantation, thus providing long-term cures for conditions like muscular dystrophies [15]. To overcome the problem of immune reactions and the large quantities of cells required to observe therapeutic benefits in large muscles, the use of autologous patient-derived iPSCs that can be proliferated indefinitely can be used for transplantation (Figure 1(a)). There are multiple methods including utilizing forced expression of myogenic transcription factors such as Pax3, Pax7, and MyoD and step-by-step induction methods which recapitulate embryonic myogenesis [23]. These protocols have been investigated to derive a variety of cell types having myogenic potential that has been reviewed by Darabi and Perlingeiro [24]. They identified some of the major hurdles to the use of iPSCs in therapeutic applications, such as the heavy dependence on gene overexpression to derive the myogenic precursors and the safety concerns associated with the use of these cells. However, efficient myogenic differentiation and the scale-up of myogenic differentiation remain elusive and must be developed further in order to generate effective cellular therapies. In addition, in vitro-induced myogenic cells from pluripotent stem cells only show embryonic muscle phenotypes but not mature muscle phenotype [23], limiting the use of iPSC-derived myogenic cells for clinical situation. It is therefore essential to develop alternative approaches to induce and obtain large numbers of satellite

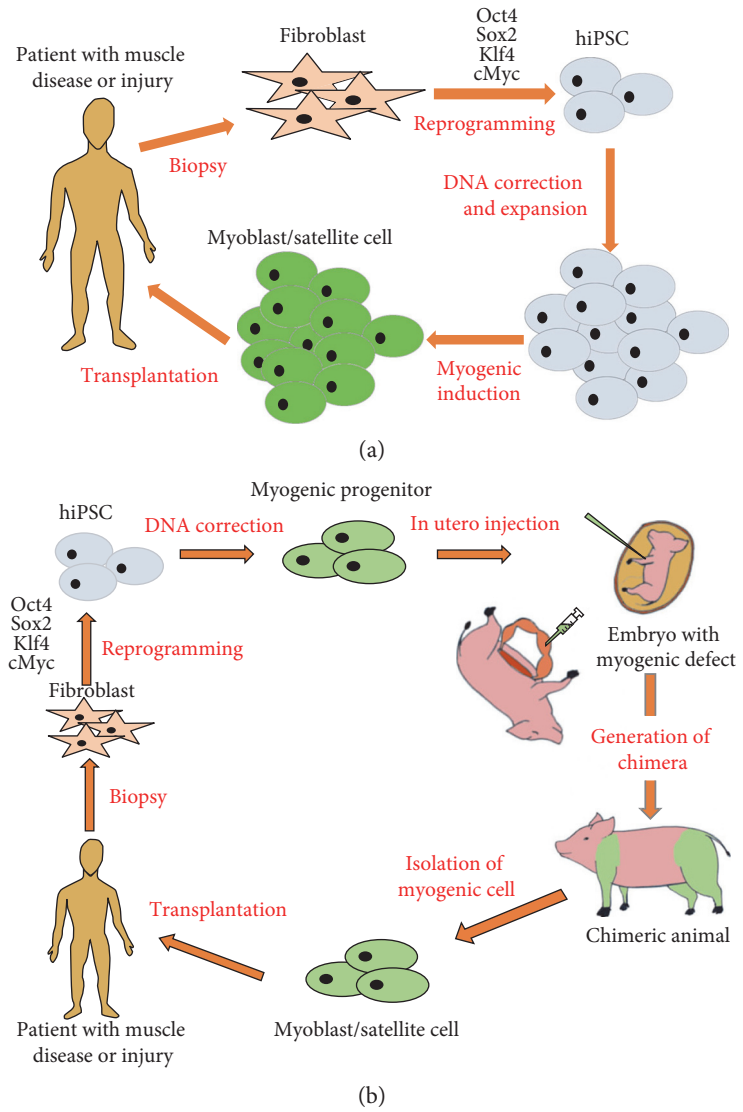

Figure 1: Current and new approaches for iPSC-derived stem cell transplantation for muscle diseases. (a) Patient-derived skin fibroblasts will be reprogramed into iPSCs by reprogramming factors. Patient-derived iPSCs will be used for DNA correction of dystrophin mutation by DNA-editing technologies. These corrected iPSCs will be induced to myogenic differentiation to generate myogenic progenitor cells which will be used for autologous cell therapy for patients suffering from muscle diseases and traumatic muscle injury and loss. (b) Patient-derived skin fibroblasts will be reprogramed into iPSCs by reprogramming factors. Patient-derived iPSCs will be used for DNA correction of dystrophin mutation by DNA-editing technologies. These corrected iPSCs will be used for myogenic progenitor cell induction followed by in utero injection into animal embryos carrying a defect of myogenic master genes such as *MyoD*, *Myf5*, and *MRF4*, allowing chimeric animal to develop human skeletal muscle. Chimeric animal-derived patient-specific myoblasts or satellite cells will be used for autologous cell therapy for muscle diseases and traumatic muscle injury and loss.

cells if the potential of myoblast transplantation as a therapeutic method is to be realized.

4. In Utero Stem Cell Transplantation (Table 1)

In utero transplantation (IUT) is based on the idea that the introduction of donor cells into a fetus at an early stage of development can result in the development of chimerism without the risk of rejection of the donor cells due to the undeveloped fetal immune system. The first evidence for this came in 1945 with Owen's observations on the blood types of bovine twins [25]. In his observations, Owen noticed that when a twin sire mated, it failed to transmit some of the antigens present on its own blood cells in any of his twenty progenies. Examination of the antigens present in his twin pointed to the possibility that these antigens could be derived from the twin. In a second observation of a case of superfecundation, he noticed that the twins possessed two antigens each that could not have been inherited from their respective sires or the dam but could have been obtained from the cosire. These observations led him to conclude that the cells containing these antigens were derived from a subset of cells that were interchanged during early embryonic development and were able to give rise to these erythrocytes throughout

Table 1: In utero cell transplantation.

Author	Year	Ref	Host animal	Donor animal	Cell type	Target tissue	Injection site	Injection stage	Disease	Duration	Number of cells	Chimerism
Fleischman et al.	1979	[29]	W/W, W^v/W^v mouse	C57Bl/6, DBA/2 mouse	Fetal liver cell (E13–E15)	Hematopoiesis	Intraplacental	E11	No	—	1×10^5	In peripheral blood is more in W/W than in W^v/W^v
Carrier et al.	1995	[30]	BALB/c, C57Bl/6 mouse	C57Bl/6 mouse	Fetal liver cell	Hematopoiesis	IP, intraplacental	E11–13	No	22–44 weeks	5×10^5	10–62% (peripheral blood, liver, and spleen)
Archer et al.	1997	[74]	Nod/Scid, C57Bl/6 mouse	C57Bl/6-Ly-5.2 mouse	BM (lin-depleted)	Hematopoiesis	IP	E13.5	No	PB analyzed 4 and 26 weeks	8×10^5	~55% (peripheral blood, spleen, BM)
Kim et al.	1999	[75]	BALB/c mouse	DBA/2 mouse	BM	Hematopoiesis	IP	E14	No	~8 weeks	—	Successful skin grafts in 2 of 3 mice
Mackenzie et al.	2002	[66]	mdx C57Bl/10 mouse	Rosa26 mouse	BM, fetal liver cell	Multiple	IP	E14	DMD	~14 months	5×10^6 BM, 1×10^6 fetal liver cell	Multiple tissues
Chou et al.	2005	[76]	BALB/c mouse	Human	MSC (BM)	Multiple	IP	E13-14	No	~5 months (postnatal)	1×10^5	~56% in multiple tissues
Frattini et al.	2005	[77]	Oc+/−C57Bl/6 mouse	Mouse CD1 CMV-GFP	BM	Hematopoiesis	IP	E14.5	Autosomal recessive osteopetrosis	~7 months	5×10^6	Improved survival
Chan et al.	2007	[68]	MF1 and mdx C57Bl/10 mice	Human	MSC (fetal)	Muscle	IP, yolk sac vein, intramuscular	E14–16	DMD	~18 weeks (postnatal)	5×10^3–1×10^6	Multiple tissues
Li et al.	2007	[78]	oim/oim mouse	Mouse	MSC (BM)	Multiple	IP	—	No	—	—	Multiple tissues
Guillot et al.	2008	[79]	oim/oim mouse	Human	MSC (fetal)	Bone	IP	E13.5–15	Osteogenesis imperfecta	E18, 1 week, 2 weeks, 4 weeks, 8 weeks, and 12 weeks	—	Multiple tissues
Kun-Yi Lin et al.	2013	[80]	Mouse	Mouse	Amniotic fluid progenitor cells	Multiple	IP	E13.5	No	3, 6, and 9 weeks (postnatal)	—	Multiple tissues
Ihara et al.	2015	[81]	MPSVII mouse	ICR/B6 actin-GFP mouse	BM (lin-depleted)	Hematopoiesis	IV in vitelline vein	E14.5	Mucopolysaccharidosis type VII	~8 weeks (postnatal)	5×10^5	Multiple tissues
Cohen et al.	2016	[52]	Mouse (W^{sh}/W^{sh})	Mouse, rat, and human	Mouse neural crest cell, mESC, riPSC, and hESC/hiPSC	Melanocyte	Intra-amniotic	E8.5	No	E10.5–E18.5, postnatal	—	Skin pigmentation
Boelig et al.	2016	[31]	C57Bl/6TgN mouse	C57Bl/6 H-2K actin-GFP mouse	BM	Hematopoiesis	IV in vitelline vein, IP, intrahepatic	E14	No	4, 24, 72 hrs, and ~6 months (postnatal)	5×10^6 IV, IP, intrahepatic, 2×10^7 IV	Multiple tissues
Munoz-Elias et al.	2004	[82]	Rat	Rat	MSC (BM)	Brain	Lateral ventricle	E15.5	No	E17.5, E19.5, and E21.5; 3 days , 1 month, and 2 months (postnatal)	—	Neuronal tissues
Chen et al.	2009	[43]	Rat	Human	MSC (placental)	Multiple	IP	E17	No	E21, 3 weeks, 12 weeks (postnatal)	—	~60% in multiple tissues
Li et al.	2012	[83]	Wistar rat	Wistar rat	BM-MSC	Neurogenesis	Lumbosacral spine	E16–18	Spina bifida aperta	E20	1–6×10^3	Neuronal tissues

Table 1: Continued.

Author	Year	Ref	Host animal	Donor animal	Cell type	Target tissue	Injection site	Injection stage	Disease	Duration	Number of cells	Chimerism
Munoz-Saez et al.	2013	[51]	Wistar rat	Wistar rat, Fischer	Fetal hepatocyte (E21)	Liver	IP	E17	No	~15 days (postnatal)	1×10^6	Multiple tissues
Li et al.	2014	[44]	Rat	Rat	MSC (BM)	Spinal cord	Spinal column	E16	Spina bifida aperta	~E20	—	Spinal cord
Burai et al.	2015	[84]	Rat	Human	Amniotic cell	Multiple	—	E18	No	1, 4, 11, and 18 days	2×10^5	Multiple tissues
Touraine et al.	1989	[40]	Human	Human	Fetal liver, thymic epithelial cell	Hematopoiesis	Umbilical vein	30 weeks	Bare lymphocyte syndrome	—	1.6×10^7	10% in lymphocyte
Wengler et al.	1996	[37]	Human	Human	T cell-depleted CD34+ BM	Hematopoiesis	IP	21 weeks	No	—	—	No GVHD, normal T cell response
Flake et al.	1996	[36]	Human	Paternal	BM (CD34+ paternal)	Hematopoiesis	IP	16–18.5 weeks	—	At birth, 3 months, 6 months (postnatal)	$1.48–2 \times 10^6$	All T cells
Gil et al.	1999	[38]	Human	Human	BM (paternal CD34+)	Hematopoiesis	IP	23 weeks and 23 weeks + 10 days	SCID	—	1.4×10^7, 6×10^6	T cells
Westgren et al.	2002	[39]	Human	Human	Fetal liver cell (10 weeks)	Hematopoiesis	IP	14 weeks	X-linked SCID	—	7×10^7	10% (24 weeks), 50% (33 weeks), all T cells/NK cells are donor origin
Le Blanc et al.	2005	[46]	Human	Human	MSC (fetal liver)	Bone	Umbilical vein	32 weeks	Osteogenesis imperfecta	—	6.5×10^6	Normal osteoblast distribution and trabeculae
Götherström et al.	2014	[85]	Human	Human	MSC (7-week, 3-day/10-week fetal liver)	Liver	Intrahepatic vein	31 weeks	Osteogenesis imperfecta	3–10 years (postnatal)	4×10^7	7.4%, healed fractures
Harrison et al.	1989	[35]	Rh monkey	Rh Monkey	Fetal liver cell (days 59–68 opposite sex)	Hematopoiesis	IP	60–62 days	No	~2 years	$1 \times 10^8–1 \times 10^9$/kg	Lymphoid, myeloid, and erythroid, no GVHD
Mychaliska et al.	1997	[34]	Monkey	Paternal	BM (T cell depleted)	Hematopoiesis	IP	61 days	No	~2 years	1×10^8/kg	<0.1%, slower progression of rejection after kidney transplants
Shields et al.	2003	[86]	Baboon/cynomolgus monkey	Baboon monkey	BM (parental, T cell-depleted B), T cell	Hematopoiesis	IP	0.34–0.38 gestation	No	~2 years	3×10^9	Peripheral blood
Asano et al.	2003	[87]	Cynomolgus monkey	Cynomolgus monkey	ESC	Multiple	IP or intrahepatic	End of 1st trimester	No	1, 3 months (posttransplantation)	$3.6–4.8 \times 10^6$	Multiple tissues, small tumor

Table 1: Continued.

Author	Year	Ref	Host animal	Donor animal	Cell type	Target tissue	Injection site	Injection stage	Disease	Duration	Number of cells	Chimerism
Crombleholme et al.	1990	[88]	Lamb	Sheep	BM (whole, T cell depleted)	Hematopoiesis	IP	—	No	—	—	18% (whole), 6% (T cell depleted), No GVHD
Zanjani et al.	1994	[89]	Sheep	Human	CD45+ cell injected with human fetal HSC	Hematopoiesis	IP	50–54 days	No	~68 weeks (postnatal)	4.9×10^6	Chimerism found in 2 of 6 sheep
Almeida-porada et al.	1999, 2000	[90, 91]	Sheep	Human	BM + stromal cell	Hematopoiesis	IP	55–60 days	No	3, 6, and 9 weeks after transplantation; 3 days, 3 months, and 1–3 years (postnatal)	5×10^4–7.5×10^5	Peripheral blood
Liechty et al.	2000	[41]	Sheep	Human	MSC (BM)	Multiple	IP	65 days, 85 days	No	2 weeks, 2 months, 5 months, and 13 months	—	Multiple tissues
Mackenzie et al.	2001	[66]	Sheep	Human	MSC	Multiple	IP	65 days, 85 days	No	—	2×10^6	Multiple tissues in 28 of 29 sheep
Emmert et al.	2013	[92]	Sheep	Human	MSC (adipose/BM)	Multiple	IP and intramyocardial	70–75 days	No	7–9 days (postnatal)	—	Multiple tissues
Jeanblanc et al.	2014	[93]	Sheep	Sheep/human (opposite sex)	BM (T cell depleted), BM (CD34+), and BM (human CD34+)	Hematopoiesis	IP	45 days, 65 days	No	10, 60, and 130 days and ~9 months (posttransplantation)	5×10^5 BM, 1.4×10^6 CD34+, and 4×10^4–5×10^5 human CD34+	In blood cells at day 65

their lives. We now know these cells to be hematopoietic stem cells (HSCs).

Following these observations, a series of experiments were performed by Billingham and colleagues in which they grafted a variety of skin combinations in between monozygotic and dizygotic twins with the aim to use this as a method to distinguish between the two types of twins [26, 27]. Their experiments were unable to find a significant difference in response to homografts between dizygotic and monozygotic twins, and they also observed varying levels of tolerance to the homografts in the dizygotic twins. These results further bolstered evidence for acquired for tolerance towards the homograft during early embryonic development. The final study that showed that exposure to antigens early in fetal development could result in the acquisition of tolerance towards those antigens was performed by Billingham et al. Here, they injected tissue homogenates from the spleen, testes, and kidneys of adult mice from A-line mice into 6 embryos of CBA mice. Five embryos survived and were grafted with the skin of A-line mice at eight weeks of age. Two of the five mice showed complete tolerance of the graft, whereas one mouse showed prolonged tolerance followed by rejection after 90 days. The two mice that showed complete tolerance were then injected with lymph nodes of CBA mice that were previously immunized against A-strain mice which resulted in rapid rejection of the previously tolerated skin grafts showing that the tolerance was due to tolerance of the graft by the mice and not due to antigenic modifications by the graft [28].

With this evidence in mind, a number of experiments were carried out to demonstrate the feasibility of IUT for therapeutic purposes. Hematopoietic stem cells (HSCs) being easy to isolate and the most well-studied stem cells were used most commonly in these studies. Moreover, tests for engraftment of HSC could be easily performed through blood draws and biopsies of the spleen, liver, and thymus to check for progeny of the transplanted cells. The first attempt to show the feasibility of IUT of HSCs (IUT-HSCs) was conducted by Fleischman and Mintz [29] who utilized W/W mice that are lethally anemic as well as W^v/W^v mice that are viably anemic. They injected C57BL/6 fetal liver HSCs into the W/W mice and DBA/2 fetal liver HSC into the W^v/W^v mice at gestational day 11. Blood tested at different time points for the type of hemoglobin in the RBCs that showed most of the RBCs were of donor origin indicating successful engraftment of the fetal liver HSCs. Engraftment of in utero-transplanted cells into normal mice was also shown in another study using PCR to detect donor cells, which proved to be a more sensitive assay [30]. They were also able to transplant allogeneic skin grafts onto the chimeric mice and observe varying degrees of tolerance towards the grafts. Further studies have shown that the mode of injection [31] is also important for improving engraftment in IUT-HSCs. IUT-HSCs have also been shown to be successful in dogs [32], sheep [33], and monkeys [34, 35]. Following these studies, IUT-HSCs have been used in a number of experimental treatments in humans to treat diseases like SCID [36–39] and bare lymphocyte syndrome [40].

IUT has also been shown to be successful for other cell types. Human MSCs have also been shown to successfully engraft in multiple tissues in sheep following in utero intraperitoneal transplantation and could be detected over a period of 13 months [41]. Similar results have been shown for fetal liver-derived MSCs in sheep and human placenta-derived MSCs in rats [42, 43]. Due to the multipotentiality of MSCs, they can possibly be used to treat a variety of conditions. In rats, MSCs injected into the spinal cord of fetuses, which were induced to have spina bifida by the administration of retinoic acid, engrafted and expressed markers of motor neurons, neurons, sensory neurons, and neural precursor cells while inducing the expression of neurotrophic factors from the surrounding tissue [44, 45]. Transplanted MSCs also showed improved bone mineralization in mouse models of osteogenesis imperfecta and could be detected in a human patient suffering from the same disease after transplantation, indicating their potential as a possible therapeutic avenue for osteogenesis imperfecta [46, 47]. Engraftment post IUT has also been shown for amniotic fluid-derived cells [48, 49] and hepatocytes [50, 51].

A recent study conducted by Cohen et al. [52] further added to the growing body of studies proving the feasibility of IUT of human stem cells. In their study, they utilized primary mouse neural crest cells (NCCs) obtained from E8.5 GFP expressing embryos from C57BL/6 background and injected these cells into a nonpigmented W^{sh}/W^{sh} *c-Kit* mutant mouse lacking endogenous melanoblasts. They then examined the coats of postnatal mice for pigmentation which would arise only from the donor cells, which was confirmed by checking for GFP. They were also able to obtain similar results from mouse ESC-derived NCCs and rat iPSC-derived NCCs. To prove that human cells could obtain similar levels of chimerism, they used hESC-derived NCCs and hiPSC-derived cells from an African American donor that were transfected with GFP. They examined the mice between E10.5 and E13.5 as well as postnatally for human chimerism and using immunohistochemistry, microscopy, and qPCR for analyzing human mitochondrial DNA. They obtained around 35% human chimerism at lower efficiencies than the mouse-mouse chimeras. However, this study highlights the potential for generating human tissue in animal models that can then be used as a model to study disease development, used to determine a cure for the condition, or used as a source of cells/tissue for transplantation.

5. Potential for Use of IUT in Treatment of Muscle Diseases

Prenatal diagnosis allows for the detection of genetic diseases early in gestation. While parental genetic screening and testing to identify carriers of mutations that can cause myopathies followed by in vitro fertilization (IVF) and preimplantation genetic screening could prevent many cases of BMD or DMD from occurring, these will only lead to a reduction and not an eradication of the disease since a third of DMD cases occur due to de novo mutations and cannot be preemptively screened for [53]. To combat this prenatal screening of fetuses could provide

an avenue to identify fetuses that carry mutations that can cause BMD or DMD. Traditionally, this is done through chorionic villus sampling (CVS) and amniotic fluid sampling which are invasive procedures and pose a 0.5% to 1% risk of embryonic death [54]. Moreover, these procedures often involve ex vivo culturing of the cells isolated to get a sufficient amount of DNA to be tested which can introduce variabilities and culture-associated abnormalities. Recent advances in these technologies however have made it easier to detect these diseases with lower risks of mortality. For example, the discovery of cell-free fetal DNA (cffDNA) present in maternal plasma enabled new noninvasive techniques of detection to be researched. Using this cffDNA and coupling it with relative haplotype dosage analysis (RHDA), Parks et al. have been able to accurately predict the occurrence of DMD and BMD [54]. In spite of the limitation of using cffDNA in the case of twins, or if the mother has been the recipient of transplants, the technique is a step forward in enabling earlier diagnoses of congenital diseases which can then be coupled with in utero interventions to cure the condition.

Naturally, the logical step following early detection of a disease-causing mutation is the early remediation of the mutation. To this end, many groups have investigated the potential of in utero gene transfer or in utero gene correction as a potential method to treat monogenic myopathies. VSV-G-, Mokola-, and Ebola-pseudotyped lentiviral vectors, adenoviral vectors, and adeno-associated viral vectors have been shown to be highly efficient in targeting cardiac muscle and skeletal muscle including satellite cells following intramuscular or intraperitoneal injections in utero [55–57]. Utilizing an equine infectious anemia virus (EIAV) of the VSV-G pseudotype, the *β-galactosidase* (*lacZ*) gene was successfully delivered to most of the respiratory muscles and limb skeletal muscle via combined intrathoracic, intraperitoneal, and intramuscular injections, and notably, no immune responses were detected towards the viral proteins for up to 5 months of age [58]. To prevent the chances of deleterious mutations due to nonspecific integration of the transgene into the genome, nonintegrating viral vectors may be a better option. The delivery of the HC-Ad adenovirus that has a large insert capacity into the muscles of E16 mouse limbs showed stable expression of lacZ up to 5 months of age and was also able to successfully deliver dystrophin cDNA and restore dystroglycan complex expression in the limbs of *mdx* mice; however, functional recovery was meagre [59, 60]. Similar results were observed utilizing AAV8 vectors carrying the minidystrophin gene [61, 62]. For a large animal model, a protocol for in utero ultrasound-guided adenoviral vector delivery to the sheep fetal muscle has been published for skeletal muscle repair. Finally, in utero delivery of oligodeoxynucleotides into *mdx* mice has been examined for dystrophin gene correction [63].

Following the success of IUT-HSCs, many groups have tried to replicate similar successes for myogenic tissue repairs. Multiple cell types have been utilized for these studies. Liechty et al. were able to show successful engraftment of normal human MSCs following in utero intraperitoneal transplantation into fetal sheep. They observed human cells in multiple organs including skeletal muscle and cardiac tissue [41, 64, 65]. Mackenzie et al. also transplanted bone marrow (BM) cells and fetal liver cells isolated from *Rosa26* donor mice (transgenic for *lacZ*) into *mdx* mouse embryos (E14) and characterized their chimerism and engraftment at 4 weeks after birth. After determining hematopoietic chimerism, they discovered the presence of donor derived myogenic cells in the diaphragm, cardiac, and skeletal muscles of the chimeric mice but were unable to show dystrophin expression due to the low levels of engraftment [66]. Utilizing a more primitive group of cell type isolated from the somites of E11.5 mice and a less invasive procedure of injection into the uterine continuation of medial circumflex femoral veins of *mdx* mice, Torrente et al. were able to show the restoration of dystrophin expression in various skeletal muscles [67]. Surprisingly, the transplanted cells were able to cross the placenta and migrate to the sites of myogenesis. More recently, human fetal MSCs have been shown to successfully differentiate into cardiac and skeletal muscle following IUT into *mdx* mice [68]. In this study, different routes of cell transplantation (intramuscular, intraperitoneal, and intravascular) were compared, and the authors identified that intraperitoneal injection allows for the most widespread distribution of the cells while intravascular injection led to complete mortality of the embryos. Intramuscular injection resulted in more localized engraftment and reduced differentiation of the cells. Although this method was not tested in the *mdx* mice, the limitation might be overcome by matching the transplanted cells to the developmental stage of the embryos.

Although IUT may not be an ideal method in the case of muscular dystrophies and myopathies due to the complexity of myogenesis and the enormity of the tissue, it could be used to generate an unlimited source of myoblasts for transplantation into patients, addressing one of the main limitations to myoblast transplantation previously discussed in this paper. The generation of humanized organs in a host animal is a potential approach for regenerative medicine to repair muscle in patients suffering from myopathic diseases. For the creation of humanized organs in animals, it is essential to selectively knock out genes in the blastocysts that are critical for organ development [69]. *MRFs*, *Pax3*, or *Lbx1* mutant mice provide an ideal model since mice carrying the gene mutation(s) display a complete absence of muscle as a whole or at the level of the limb, respectively [70–72], supplying the empty niche for myogenesis. However, since injection of human stem cells into pregastrulation embryos has an ethical issue [73], IUT of stem cells into genetically modified mouse embryos is a potential approach for generating humanized organs. The clinical significance of this approach is the production of humanized muscle using specific gene mutant mouse embryos via IUT of iPSCs, which are developmentally vacant of the limb muscle. These humanized organs created in mice will serve as an animal model to study human muscle diseases and responses to pharmacological agents. In addition, muscle engineered in these strategies holds potential as a source for muscle stem cell transplantation for patients suffering from myopathic diseases. Therefore, they can be used as a platform to develop IUT for the purposes of generating human limb muscle in these mice. Translation to large

animal models following these studies can result in the generation of patient-specific myoblasts that can then be harvested and transplanted as a possible therapeutic option (Figure 1(b)). Our preliminary results in normal mice show that transplanted myoblasts or iPSC-derived myogenic cells can survive in the developing embryo post IUT; however, their contribution to myogenesis is currently undetermined. If successful, IUT of gene-corrected iPS-derived precursors into growing fetuses of animals like pigs, sheep, or goat can be used to generate patient-specific muscle for a source of autologous myoblast transplantation.

The generation of patient-specific myogenic cells in host animals can be directly used for stem cell-based therapeutic transplantation in DMD and myopathic diseases. In addition, we can develop personalized muscle model carrying individual disease-associated mutations in the humanized animals. Potentially, such insights and developments will lead to new therapeutic interventions for myopathic diseases including DMD. With respect to expected outcomes, the work proposed in the aims of this study is collectively expected to provide new therapeutic interventions that will aid the growing number of people in this country who suffer from muscle degenerative diseases and traumatic muscle injury and loss. In addition, it is expected that the results will fundamentally advance the fields of muscle regeneration and stem cell biology.

Conflicts of Interest

The authors declare that they have no conflicts of interest.

Acknowledgments

This work was supported by the NIH R01 (1R01AR062142) and NIH R21 (1R21AR070319). The authors would also like to thank Conor Burke-Smith for a critical reading of the manuscript.

References

[1] J. R. Mendell, C. Shilling, N. D. Leslie et al., "Evidence-based path to newborn screening for Duchenne muscular dystrophy," *Annals of Neurology*, vol. 71, no. 3, pp. 304–313, 2012.

[2] K. M. Bushby, M. Thambyayah, and D. Gardner-Medwin, "Prevalence and incidence of Becker muscular dystrophy," *Lancet*, vol. 337, no. 8748, pp. 1022–1024, 1991.

[3] K. M. Flanigan, "Duchenne and Becker muscular dystrophies," *Neurologic Clinics*, vol. 32, no. 3, pp. 671–688, 2014.

[4] A. Ferlini, M. Neri, and F. Gualandi, "The medical genetics of dystrophinopathies: molecular genetic diagnosis and its impact on clinical practice," *Neuromuscular Disorders*, vol. 23, no. 1, pp. 4–14, 2013.

[5] C. Pasternak, S. Wong, and E. L. Elson, "Mechanical function of dystrophin in muscle cells," *The Journal of Cell Biology*, vol. 128, no. 3, pp. 355–361, 1995.

[6] B. J. Petrof, J. B. Shrager, H. H. Stedman, A. M. Kelly, and H. L. Sweeney, "Dystrophin protects the sarcolemma from stresses developed during muscle contraction," *Proceedings of the National Academy of Sciences of the United States of America*, vol. 90, no. 8, pp. 3710–3714, 1993.

[7] A. Asakura, "Stem cells in adult skeletal muscle," *Trends in Cardiovascular Medicine*, vol. 13, no. 3, pp. 123–128, 2003.

[8] J. Dhawan and T. A. Rando, "Stem cells in postnatal myogenesis: molecular mechanisms of satellite cell quiescence, activation and replenishment," *Trends in Cell Biology*, vol. 15, no. 12, pp. 666–673, 2005.

[9] A. Asakura, M. Komaki, and M. Rudnicki, "Muscle satellite cells are multipotential stem cells that exhibit myogenic, osteogenic, and adipogenic differentiation," *Differentiation*, vol. 68, no. 4-5, pp. 245–253, 2001.

[10] E. Gussoni, Y. Soneoka, C. D. Strickland et al., "Dystrophin expression in the mdx mouse restored by stem cell transplantation," *Nature*, vol. 401, no. 6751, pp. 390–394, 1999.

[11] R. Galli, U. Borello, A. Gritti et al., "Skeletal myogenic potential of human and mouse neural stem cells," *Nature Neuroscience*, vol. 3, no. 10, pp. 986–991, 2000.

[12] A. Asakura, P. Seale, A. Girgis-Gabardo, and M. A. Rudnicki, "Myogenic specification of side population cells in skeletal muscle," *The Journal of Cell Biology*, vol. 159, no. 1, pp. 123–134, 2002.

[13] M. Sampaolesi, Y. Torrente, A. Innocenzi et al., "Cell therapy of alpha-sarcoglycan null dystrophic mice through intra-arterial delivery of mesoangioblasts," *Science*, vol. 301, no. 5632, pp. 487–492, 2003.

[14] Y. Torrente, M. Belicchi, M. Sampaolesi et al., "Human circulating AC133(+) stem cells restore dystrophin expression and ameliorate function in dystrophic skeletal muscle," *The Journal of Clinical Investigation*, vol. 114, no. 2, pp. 182–195, 2004.

[15] F. S. Tedesco, A. Dellavalle, J. Diaz-Manera, G. Messina, and G. Cossu, "Repairing skeletal muscle: regenerative potential of skeletal muscle stem cells," *The Journal of Clinical Investigation*, vol. 120, no. 1, pp. 11–19, 2010.

[16] J. E. Morgan, D. J. Watt, J. C. Sloper, and T. A. Partridge, "Partial correction of an inherited biochemical defect of skeletal muscle by grafts of normal muscle precursor cells," *Journal of the Neurological Sciences*, vol. 86, no. 2-3, pp. 137–147, 1988.

[17] T. A. Partridge, J. E. Morgan, G. R. Coulton, E. P. Hoffman, and L. M. Kunkel, "Conversion of mdx myofibres from dystrophin-negative to -positive by injection of normal myoblasts," *Nature*, vol. 337, no. 6203, pp. 176–179, 1989.

[18] J. E. Morgan, C. N. Pagel, T. Sherratt, and T. A. Partridge, "Long-term persistence and migration of myogenic cells injected into pre-irradiated muscles of mdx mice," *Journal of the Neurological Sciences*, vol. 115, no. 2, pp. 191–200, 1993.

[19] I. Kinoshita, R. Roy, F. J. Dugre et al., "Myoblast transplantation in monkeys: control of immune response by FK506," *Journal of Neuropathology and Experimental Neurology*, vol. 55, no. 6, pp. 687–697, 1996.

[20] D. Skuk, M. Goulet, B. Roy, and J. P. Tremblay, "Efficacy of myoblast transplantation in nonhuman primates following simple intramuscular cell injections: toward defining strategies applicable to humans," *Experimental Neurology*, vol. 175, no. 1, pp. 112–126, 2002.

[21] B. Palmieri, J. P. Tremblay, and L. Daniele, "Past, present and future of myoblast transplantation in the treatment of Duchenne muscular dystrophy," *Pediatric Transplantation*, vol. 14, no. 7, pp. 813–819, 2010.

[22] D. Skuk and J. P. Tremblay, "Progress in myoblast transplantation: a potential treatment of dystrophies," *Microscopy Research and Technique*, vol. 48, no. 3-4, pp. 213–222, 2000.

[23] J. Chal, M. Oginuma, Z. Al Tanoury et al., "Differentiation of pluripotent stem cells to muscle fiber to model Duchenne muscular dystrophy," *Nature Biotechnology*, vol. 33, no. 9, pp. 962–969, 2015.

[24] R. Darabi and R. C. Perlingeiro, "A perspective on the potential of human iPS cell-based therapies for muscular dystrophies: advancements so far and hurdles to overcome," *Journal of Stem Cell Research & Therapy*, vol. 3, 2013.

[25] R. D. Owen, "Immunogenetic consequences of vascular anastomoses between bovine twins," *Science*, vol. 102, no. 2651, pp. 400-401, 1945.

[26] D. Anderson, R. E. Billingham, G. H. Lampkin, and P. B. Meda War, "The use of skin grafting to distinguish between monozygotic and dizygotic twin in cattle," *Heredity*, vol. 5, no. 3, pp. 379–397, 1951.

[27] R. E. Billingham, G. H. Lampkin, P. B. Medawar, and H. L. Williams, "Tolerance to homografts, twin diagnosis, and the freemartin condition in cattle," *Heredity*, vol. 6, no. 2, pp. 201–212, 1952.

[28] R. E. Billingham, L. Brent, and P. B. Medawar, "Actively acquired tolerance of foreign cells," *Nature*, vol. 172, no. 4379, pp. 603–606, 1953.

[29] R. A. Fleischman and B. Mintz, "Prevention of genetic anemias in mice by microinjection of normal hematopoietic stem cells into the fetal placenta," *Proceedings of the National Academy of Sciences of the United States of America*, vol. 76, no. 11, pp. 5736–5740, 1979.

[30] E. Carrier, T. H. Lee, M. P. Busch, and M. J. Cowan, "Induction of tolerance in nondefective mice after in utero transplantation of major histocompatibility complex-mismatched fetal hematopoietic stem cells," *Blood*, vol. 86, no. 12, pp. 4681–4690, 1995.

[31] M. M. Boelig, A. G. Kim, J. D. Stratigis et al., "The intravenous route of injection optimizes engraftment and survival in the murine model of in utero hematopoietic cell transplantation," *Biology of Blood and Marrow Transplantation*, vol. 22, no. 6, pp. 991–999, 2016.

[32] J. D. Vrecenak, E. G. Pearson, M. T. Santore et al., "Stable long-term mixed chimerism achieved in a canine model of allogeneic in utero hematopoietic cell transplantation," *Blood*, vol. 124, no. 12, pp. 1987–1995, 2014.

[33] A. D. Goodrich, N. M. Varain, C. M. Jeanblanc et al., "Influence of a dual-injection regimen, plerixafor and CXCR4 on in utero hematopoietic stem cell transplantation and engraftment with use of the sheep model," *Cytotherapy*, vol. 16, no. 9, pp. 1280–1293, 2014.

[34] G. B. Mychaliska, H. E. Rice, A. F. Tarantal et al., "In utero hematopoietic stem cell transplants prolong survival of postnatal kidney transplantation in monkeys," *Journal of Pediatric Surgery*, vol. 32, no. 7, pp. 976–981, 1997.

[35] M. R. Harrison, R. N. Slotnick, T. M. Crombleholme, M. S. Golbus, A. F. Tarantal, and E. D. Zanjani, "In-utero transplantation of fetal liver haemopoietic stem cells in monkeys," *Lancet*, vol. 2, no. 8677, pp. 1425–1427, 1989.

[36] A. W. Flake, M. G. Roncarolo, J. M. Puck et al., "Treatment of X-linked severe combined immunodeficiency by in utero transplantation of paternal bone marrow," *The New England Journal of Medicine*, vol. 335, no. 24, pp. 1806–1810, 1996.

[37] G. S. Wengler, A. Lanfranchi, T. Frusca et al., "In-utero transplantation of parental CD34 haematopoietic progenitor cells in a patient with X-linked severe combined immunodeficiency (SCIDXI)," *Lancet*, vol. 348, no. 9040, pp. 1484–1487, 1996.

[38] J. Gil, F. Porta, J. Bartolome et al., "Immune reconstitution after in utero bone marrow transplantation in a fetus with severe combined immunodeficiency with natural killer cells," *Transplantation Proceedings*, vol. 31, no. 6, p. 2581, 1999.

[39] M. Westgren, O. Ringden, P. Bartmann et al., "Prenatal T-cell reconstitution after in utero transplantation with fetal liver cells in a patient with X-linked severe combined immunodeficiency," *American Journal of Obstetrics and Gynecology*, vol. 187, no. 2, pp. 475–482, 2002.

[40] J. L. Touraine, D. Raudrant, C. Royo et al., "In-utero transplantation of stem cells in bare lymphocyte syndrome," *Lancet*, vol. 1, no. 8651, p. 1382, 1989.

[41] K. W. Liechty, T. C. MacKenzie, A. F. Shaaban et al., "Human mesenchymal stem cells engraft and demonstrate site-specific differentiation after in utero transplantation in sheep," *Nature Medicine*, vol. 6, no. 11, pp. 1282–1286, 2000.

[42] A. Schoeberlein, W. Holzgreve, L. Dudler, S. Hahn, and D. V. Surbek, "Tissue-specific engraftment after in utero transplantation of allogeneic mesenchymal stem cells into sheep fetuses," *American Journal of Obstetrics and Gynecology*, vol. 192, no. 4, pp. 1044–1052, 2005.

[43] C. P. Chen, S. H. Liu, J. P. Huang et al., "Engraftment potential of human placenta-derived mesenchymal stem cells after in utero transplantation in rats," *Human Reproduction*, vol. 24, no. 1, pp. 154–165, 2009.

[44] H. Li, J. Miao, G. Zhao et al., "Different expression patterns of growth factors in rat fetuses with spina bifida aperta after in utero mesenchymal stromal cell transplantation," *Cytotherapy*, vol. 16, no. 3, pp. 319–330, 2014.

[45] W. Ma, X. Wei, H. Gu et al., "Sensory neuron differentiation potential of in utero mesenchymal stem cell transplantation in rat fetuses with spina bifida aperta," *Birth Defects Research. Part a, Clinical and Molecular Teratology*, vol. 103, no. 9, pp. 772–779, 2015.

[46] K. Le Blanc, C. Gotherstrom, O. Ringden et al., "Fetal mesenchymal stem-cell engraftment in bone after in utero transplantation in a patient with severe osteogenesis imperfecta," *Transplantation*, vol. 79, no. 11, pp. 1607–1614, 2005.

[47] J. K. Chan and C. Gotherstrom, "Prenatal transplantation of mesenchymal stem cells to treat osteogenesis imperfecta," *Frontiers in Pharmacology*, vol. 5, p. 223, 2014.

[48] S. Y. Peng, Y. H. Chen, C. J. Chou et al., "Cell fusion phenomena detected after in utero transplantation of Ds-red-harboring porcine amniotic fluid stem cells into EGFP transgenic mice," *Prenatal Diagnosis*, vol. 34, no. 5, pp. 487–495, 2014.

[49] S. W. Shaw, M. P. Blundell, C. Pipino et al., "Sheep CD34+ amniotic fluid cells have hematopoietic potential and engraft after autologous in utero transplantation," *Stem Cells*, vol. 33, no. 1, pp. 122–132, 2015.

[50] J. E. Fisher, J. B. Lillegard, T. J. McKenzie, B. R. Rodysill, P. J. Wettstein, and S. L. Nyberg, "In utero transplanted human hepatocytes allow postnatal engraftment of human hepatocytes in pigs," *Liver Transplantation*, vol. 19, no. 3, pp. 328–335, 2013.

[51] E. Munoz-Saez, E. de Munck, P. Maganto, C. Escudero, B. G. Miguel, and R. M. Arahuetes, "In utero hepatocellular transplantation in rats," *Clinical & Developmental Immunology*, vol. 2013, Article ID 562037, p. 10, 2013.

[52] M. A. Cohen, K. J. Wert, J. Goldmann et al., "Human neural crest cells contribute to coat pigmentation in interspecies chimeras after in utero injection into mouse embryos," *Proceedings of the National Academy of Sciences of the United States of America*, vol. 113, no. 6, pp. 1570–1575, 2016.

[53] D. Massalska, J. G. Zimowski, J. Bijok et al., "Prenatal diagnosis of congenital myopathies and muscular dystrophies," *Clinical Genetics*, vol. 90, no. 3, pp. 199–210, 2016.

[54] M. Parks, S. Court, S. Cleary et al., "Non-invasive prenatal diagnosis of Duchenne and Becker muscular dystrophies by relative haplotype dosage," *Prenatal Diagnosis*, vol. 36, no. 4, pp. 312–320, 2016.

[55] T. C. MacKenzie, G. P. Kobinger, N. A. Kootstra et al., "Efficient transduction of liver and muscle after in utero injection of lentiviral vectors with different pseudotypes," *Molecular Therapy*, vol. 6, no. 3, pp. 349–358, 2002.

[56] S. Bouchard, T. C. MacKenzie, A. P. Radu et al., "Long-term transgene expression in cardiac and skeletal muscle following fetal administration of adenoviral or adeno-associated viral vectors in mice," *The Journal of Gene Medicine*, vol. 5, no. 11, pp. 941–950, 2003.

[57] T. C. MacKenzie, G. P. Kobinger, J. P. Louboutin et al., "Transduction of satellite cells after prenatal intramuscular administration of lentiviral vectors," *The Journal of Gene Medicine*, vol. 7, no. 1, pp. 50–58, 2005.

[58] L. G. Gregory, S. N. Waddington, M. V. Holder et al., "Highly efficient EIAV-mediated in utero gene transfer and expression in the major muscle groups affected by Duchenne muscular dystrophy," *Gene Therapy*, vol. 11, no. 14, pp. 1117–1125, 2004.

[59] R. Bilbao, D. P. Reay, E. Wu et al., "Comparison of high-capacity and first-generation adenoviral vector gene delivery to murine muscle in utero," *Gene Therapy*, vol. 12, no. 1, pp. 39–47, 2005.

[60] D. P. Reay, R. Bilbao, B. M. Koppanati et al., "Full-length dystrophin gene transfer to the mdx mouse in utero," *Gene Therapy*, vol. 15, no. 7, pp. 531–536, 2008.

[61] B. M. Koppanati, J. Li, X. Xiao, and P. R. Clemens, "Systemic delivery of AAV8 in utero results in gene expression in diaphragm and limb muscle: treatment implications for muscle disorders," *Gene Therapy*, vol. 16, no. 9, pp. 1130–1137, 2009.

[62] B. M. Koppanati, J. Li, D. P. Reay et al., "Improvement of the mdx mouse dystrophic phenotype by systemic in utero AAV8 delivery of a minidystrophin gene," *Gene Therapy*, vol. 17, no. 11, pp. 1355–1362, 2010.

[63] L. Cai, B. M. Koppanati, C. Bertoni, and P. R. Clemens, "In utero delivery of oligodeoxynucleotides for gene correction," *Methods in Molecular Biology*, vol. 1114, pp. 399–411, 2014.

[64] T. C. Mackenzie and A. W. Flake, "Multilineage differentiation of human MSC after in utero transplantation," *Cytotherapy*, vol. 3, no. 5, pp. 403–405, 2001.

[65] T. C. MacKenzie and A. W. Flake, "Human mesenchymal stem cells: insights from a surrogate in vivo assay system," *Cells, Tissues, Organs*, vol. 171, no. 1, pp. 90–95, 2002.

[66] T. C. Mackenzie, A. F. Shaaban, A. Radu, and A. W. Flake, "Engraftment of bone marrow and fetal liver cells after in utero transplantation in MDX mice," *Journal of Pediatric Surgery*, vol. 37, no. 7, pp. 1058–1064, 2002.

[67] Y. Torrente, M. G. D'Angelo, Z. Li et al., "Transplacental injection of somite-derived cells in mdx mouse embryos for the correction of dystrophin deficiency," *Human Molecular Genetics*, vol. 9, no. 12, pp. 1843–1852, 2000.

[68] J. Chan, S. N. Waddington, K. O'Donoghue et al., "Widespread distribution and muscle differentiation of human fetal mesenchymal stem cells after intrauterine transplantation in dystrophic mdx mouse," *Stem Cells*, vol. 25, no. 4, pp. 875–884, 2007.

[69] T. Kobayashi, T. Yamaguchi, S. Hamanaka et al., "Generation of rat pancreas in mouse by interspecific blastocyst injection of pluripotent stem cells," *Cell*, vol. 142, no. 5, pp. 787–799, 2010.

[70] M. A. Rudnicki, P. N. Schnegelsberg, R. H. Stead, T. Braun, H. H. Arnold, and R. Jaenisch, "MyoD or Myf-5 is required for the formation of skeletal muscle," *Cell*, vol. 75, no. 7, pp. 1351–1359, 1993.

[71] M. Tassabehji, V. E. Newton, K. Leverton et al., "PAX3 gene structure and mutations: close analogies between Waardenburg syndrome and the splotch mouse," *Human Molecular Genetics*, vol. 3, no. 7, pp. 1069–1074, 1994.

[72] M. K. Gross, L. Moran-Rivard, T. Velasquez, M. N. Nakatsu, K. Jagla, and M. Goulding, "Lbx1 is required for muscle precursor migration along a lateral pathway into the limb," *Development*, vol. 127, no. 2, pp. 413–424, 2000.

[73] I. Hyun, "Illusory fears must not stifle chimaera research," *Nature*, vol. 537, no. 7620, p. 281, 2016.

[74] D. R. Archer, C. W. Turner, A. M. Yeager, and W. H. Fleming, "Sustained multilineage engraftment of allogeneic hematopoietic stem cells in NOD/SCID mice after in utero transplantation," *Blood*, vol. 90, no. 8, pp. 3222–3229, 1997.

[75] H. B. Kim, A. F. Shaaban, R. Milner, C. Fichter, and A. W. Flake, "In utero bone marrow transplantation induces donor-specific tolerance by a combination of clonal deletion and clonal anergy," *Journal of Pediatric Surgery*, vol. 34, no. 5, pp. 726–729, 1999, discussion 729-730.

[76] M. M. Chou, J. J. Tseng, Y. C. Yi, W. C. Chen, and E. S. Ho, "Diagnosis of an interstitial pregnancy with 4-dimensional volume contrast imaging," *American Journal of Obstetrics and Gynecology*, vol. 193, no. 4, pp. 1551–1553, 2005.

[77] A. Frattini, H. C. Blair, M. G. Sacco et al., "Rescue of ATPa3-deficient murine malignant osteopetrosis by hematopoietic stem cell transplantation in utero," *Proceedings of the National Academy of Sciences of the United States of America*, vol. 102, no. 41, pp. 14629–14634, 2005.

[78] F. Li, X. Wang, and C. Niyibizi, "Distribution of single-cell expanded marrow derived progenitors in a developing mouse model of osteogenesis imperfecta following systemic transplantation," *Stem Cells*, vol. 25, no. 12, pp. 3183–3193, 2007.

[79] P. V. Guillot, O. Abass, J. H. Bassett et al., "Intrauterine transplantation of human fetal mesenchymal stem cells from first-trimester blood repairs bone and reduces fractures in osteogenesis imperfecta mice," *Blood*, vol. 111, no. 3, pp. 1717–1725, 2008.

[80] K.-Y. Lin, S.-Y. Peng, C.-J. Chou, C.-C. Wu, and S.-C. Wu, "Engraftment of mouse amniotic fluid-derived progenitor cells after in utero transplantation in mice," *Journal of the Formosan Medical Association = Taiwan Yi Zhi*, vol. 114, no. 11, pp. 1105–1115, 2015.

[81] N. Ihara, U. Akihiro, N. Onami et al., "Partial rescue of mucopolysaccharidosis type VII mice with a lifelong engraftment of allogeneic stem cells in utero," *Congenit Anom (Kyoto)*, vol. 55, no. 1, pp. 55–64, 2015.

[82] G. Munoz-Elias, A. J. Marcus, T. M. Coyne, D. Woodbury, and I. B. Black, "Adult bone marrow stromal cells in the embryonic

brain: engraftment, migration, differentiation, and long-term survival," *The Journal of Neuroscience*, vol. 24, no. 19, pp. 4585–4595, 2004.

[83] H. Li, F. Gao, L. Ma et al., "Therapeutic potential of in utero mesenchymal stem cell (MSCs) transplantation in rat foetuses with spina bifida aperta," *Journal of Cellular and Molecular Medicine*, vol. 16, no. 7, pp. 1606–1617, 2012.

[84] G. P. Burrai, E. Antuofermo, S. Farigu et al., "Target-antigen detection and localization of human amniotic-derived cells after in utero transplantation in rats," *Annals of Clinical and Laboratory Science*, vol. 45, no. 3, pp. 270–277, 2015.

[85] C. Götherström, M. Westgren, S. W. Shaw et al., "Pre- and postnatal transplantation of fetal mesenchymal stem cells in osteogenesis imperfecta: a two-center experience," *Stem Cells Translational Medicine*, vol. 3, no. 2, pp. 255–264, 2014.

[86] L. E. Shields, L. K. Gaur, M. Gough, J. Potter, A. Sieverkropp, and R. G. Andrews, "In utero hematopoietic stem cell transplantation in nonhuman primates: the role of T cells," *Stem Cells*, vol. 21, no. 3, pp. 304–314, 2003.

[87] T. Asano, N. Ageyama, K. Takeuchi et al., "Engraftment and tumor formation after allogeneic in utero transplantation of primate embryonic stem cells," *Transplantation*, vol. 76, no. 7, pp. 1061–1067, 2003.

[88] T. M. Crombleholme, M. R. Harrison, and E. D. Zanjani, "In utero transplantation of hematopoietic stem cells in sheep: the role of T cells in engraftment and graft-versus-host disease," *Journal of Pediatric Surgery*, vol. 25, no. 8, pp. 885–892, 1990.

[89] E. D. Zanjani, A. W. Flake, H. Rice, M. Hedrick, and M. Tavassoli, "Long-term repopulating ability of xenogeneic transplanted human fetal liver hematopoietic stem cells in sheep," *The Journal of Clinical Investigation*, vol. 93, no. 3, pp. 1051–1055, 1994.

[90] G. Almeida-Porada, A. W. Flake, H. A. Glimp, and E. D. Zanjani, "Cotransplantation of stroma results in enhancement of engraftment and early expression of donor hematopoietic stem cells in utero," *Experimental Hematology*, vol. 27, no. 10, pp. 1569–1575, 1999.

[91] G. Almeida-Porada, C. D. Porada, N. Tran, and E. D. Zanjani, "Cotransplantation of human stromal cell progenitors into preimmune fetal sheep results in early appearance of human donor cells in circulation and boosts cell levels in bone marrow at later time points after transplantation," *Blood*, vol. 95, no. 11, pp. 3620–3627, 2000.

[92] M. Y. Emmert, P. Wolint, N. Wickboldt et al., "Human stem cell-based three-dimensional microtissues for advanced cardiac cell therapies," *Biomaterials*, vol. 34, no. 27, pp. 6339–6354, 2013.

[93] C. Jeanblanc, A. D. Goodrich, E. Colletti et al., "Temporal definition of haematopoietic stem cell niches in a large animal model of in utero stem cell transplantation," *British Journal of Haematology*, vol. 166, no. 2, pp. 268–278, 2014.

Hindawi
Stem Cells International
Volume 2017, Article ID 6082684, 11 pages
https://doi.org/10.1155/2017/6082684

Research Article

hTERT-Immortalized Bone Mesenchymal Stromal Cells Expressing Rat Galanin via a Single Tetracycline-Inducible Lentivirus System

Ke An,[1] Hui-ping Liu,[1,2] Xiao-long Zhong,[1] David Y. B. Deng,[3] Jing-jun Zhang,[1] and Zhi-heng Liu[4]

[1]*Department of Anesthesiology, The First Affiliated Hospital of Sun Yat-sen University, Guangzhou 510080, China*
[2]*Department of Anesthesiology, The Third Xiangya Hospital of Central South University, Changsha 410013, China*
[3]*Laboratory of Research Center for Translational Medicine, The First Affiliated Hospital of Sun Yat-sen University, Guangzhou 510080, China*
[4]*Department of Anesthesiology, The First Affiliated Hospital of Shenzhen University, Shenzhen 518035, China*

Correspondence should be addressed to Ke An; anke2002wh@126.com

Received 21 November 2016; Revised 26 January 2017; Accepted 22 February 2017; Published 11 May 2017

Academic Editor: Veronica Ramos-Mejia

Copyright © 2017 Ke An et al. This is an open access article distributed under the Creative Commons Attribution License, which permits unrestricted use, distribution, and reproduction in any medium, provided the original work is properly cited.

The use of human telomerase reverse transcriptase-immortalized bone marrow mesenchymal stromal cells (hTERT-BMSCs) as vehicles to deliver antinociceptive galanin (GAL) molecules into pain-processing centers represents a novel cell therapy strategy for pain management. Here, an hTERT-BMSCs/Tet-on/GAL cell line was constructed using a single Tet-on-inducible lentivirus system, and subsequent experiments demonstrated that the secretion of rat GAL from hTERT-BMSCs/Tet-on/GAL was switched on and off under the control of an inducer in a dose-dependent manner. The construction of this cell line is the first promising step in the regulation of GAL secretion from hTERT-immortalized BMSCs, and the potential application of this system may provide a stem cell-based research platform for pain.

1. Introduction

Treatment of chronic neuropathic pain resulting from peripheral nerve injury is one of the most difficult problems in modern clinical practice. Although current treatments, such as traditional pharmacological approaches, are often effective for limited periods, these therapies have no practical significance for the progression of pain and can even induce tolerance and unacceptable systemic side effects. Diminished inhibitory neurotransmission in the superficial dorsal horn, particularly when there is an imbalance of excitatory and inhibitory systems, is the likely mechanism underlying the induction and development of neuropathic pain following nerve injury [1, 2]. Therefore, alternative methods targeting mechanisms of neuropathic pain are needed.

The use of cell lines as "biological minipumps" to chronically deliver antinociceptive molecules into the pain-processing centers of the spinal cord represents a newly developed technique for the treatment of pain [3]. Galanin (GAL) is a neuropeptide of 29 or 30 (in humans) amino acids that is proteolytically processed from the peptide precursor preprogalanin. GAL is widely distributed throughout the central and peripheral nervous system and is involved in a variety of physiological and pathophysiological activities, including pain signaling [4]. Extensive research has demonstrated that this molecule plays a gatekeeper role in the inhibition of neuropathic pain [5, 6]. Previous studies have demonstrated that immortalized astrocytes are not only easily manipulated, reproducible, and nontumorigenic but are also safe potential vehicles for the delivery of therapeutic genes (galanin) for chronic pain therapy [7–9].

However, obtaining primary neuronal cells from adult tissue is difficult and faces major ethical issues in clinical practice. Studies have increasingly focused on the potential

therapeutic effects of stem cell transplantation for neurological diseases [10]. Bone marrow stem cells, including the pluripotent hematopoietic stem cells (HSCs) and bone mesenchymal stem cells (BMSCs), are being considered as potential targets for cell and gene therapy-based approaches against a variety of different diseases. Although human HSCs as vehicles to treat metachromatic leukodystrophy (MLD) has been used to treat patients with early onset MLD in a phase I/II trial, the HSCs give rise to all different blood cell lineages, such as the myeloid and lymphoid cell lineages [11]. In contrast, BMSCs are capable of differentiating into mesenchymal lineages such as osteoblasts, chondrocytes, adipocytes, and even neurons and astrocytes [12]. BMSCs can also be engineered to secrete a variety of different proteins in vitro and in vivo that could potentially treat a variety of serum protein deficiencies and other genetic or acquired diseases [13]. Indeed, the potent pathotropic migratory properties of BMSCs and ability to circumvent both the complications associated with immune rejection of allogenic cells and many of the moral reasons associated with embryonic stem cell use suggest that BMSCs are most promising stem cells as a potential target for the clinical use of genetically engineered stem cells [14, 15]. However, BMSCs have a low proliferative ability with a finite lifespan in vitro; this limitation has been overcome via ectopic expression of human telomerase reverse transcriptase (hTERT), the catalytic component of telomerase, to produce large quantities of these cells as an attractive source for cellular transplantation [16–18].

The ability to switch on and off the expression of transgenes delivered via lentiviral vectors is desirable in a number of experimental and therapeutic situations in which the transgene product must be regulated in a timely manner. An ideal lentiviral-based system should be contained within a single vector to avoid the need for multiple transductions of the target cells with high multiplicities of infection (MOI), which would increase the risk of insertional mutagenesis [19]. The most widely studied system for gene regulation in eukaryotic cells is the tetracycline- (Tet-) regulated transgene expression system, which employs a Tn*10* Tet resistance operator derived from *Escherichia coli* [20]. The Tet-inducible system has been extensively used to control transgene expression in stem cells. Therefore, to enhance the consistent and controllable exogenous expression of the GAL gene, a new stem cell-based approach was developed by transfecting a single inducible Tet-On lentiviral vector- (LV-) mediated GAL gene delivery system into hTERT-immortalized BMSCs. We hypothesized that these newly developed stem cells will serve as efficient and controllable pools for GAL expression within the CNS for further pain study.

2. Materials and Methods

See supplemental information available online at https://doi.org/10.1155/2017/6082684 for detailed descriptions.

2.1. Ethic Statement. All procedures were conducted in accordance with the Ethical Guidelines of the International Association for the Study of Pain (1983) and approved by the Administrative Committee of Experimental Animal Care and Use of Sun Yat-sen University (permit number: 2013-A-001).

2.2. Lentiviral Vector Construction and Production. The plasmid pCI-Neo-hTERT containing hTERT cDNA was kindly provided by Professor William C. Hahn (Dana-Farber Cancer Institute, Harvard Medical School, USA). Using Gateway® Recombination Cloning Technology [21], the specific fragments of EF1α-hTERT containing the attB adaptor were PCR amplified using Phusion® high-fidelity DNA polymerase (New England BioLabs, Singapore). In the subsequent BP recombination reaction (between attB and attP sites), the PCR product containing attB was transferred to a kanamycin-resistant donor vector (pENTR). Finally, the lentiviral vector pLV.ExSi.P/Puro-EF1α-hTERT was constructed after cloning the EF1α-hTERT-specific gene into pLV.ExSi.P/Pgk-Puro expression vectors via an LR recombination reaction (between attL and attR sites) (Cyagen Biosciences Inc., Guangzhou, China) (Figures 1(a) and 1(b)). The EF1α promoter-dependent lentiviral expression vector was used instead of the more potent and widely used CMV promoter because the EF1α promoter is less prone to silencing and provides more stable long-term expression. The single Tet-inducible lentiviral vector (pLV.TetIIP-GAL-EGFP-/Ubi-TetR), expressing rat galanin, and the reporter gene EGFP with the neomycin resistance gene under the control of the TetII promoter (*P*TetIIP) was constructed from TetR-based pLV.TetIIP-EGFP-/Ubi-TetR (GV347) lentiviral backbone vector system (Genechem Co. Ltd, Shanghai, China) (Figure 2). Briefly, GAL cDNA from the construct pBS KS(+)-GAL was obtained by PCR amplification using the following primer pairs: P1: 5′-AACC GTCAGATCGCACCGGCGCCACCATGGCCAGGGGCA GCGTTATCC-3′ and P2: 5′-TCACCATGGTGGCGACC GGGGACTGCTCTAGGTCTTCTG-3′ (418 bp). Subsequently, the cDNA was cloned into the linear expression vector GV347, and the transformants were identified by PCR using the primer pair and TetIIP-F: 5′-TGTCGA GGTAGGCGTGTA-3′ and EGFP-N-R: 5′-CGTCGCCGTC CAGCTCGACCAG-3′ (532 bp).

To obtain lentiviral particles, the 293 T packaging producer cells were cotransfected with the pLV/helper packaging plasmid mix (Invitrogen Life Technologies, USA) and the expression lentivector containing ExSi.P/Pgk-Puro, ExSi.P/Puro-EF1α-hTERT, TetIIP-EGFP−/Ubi-TetR, or TetIIP-GAL-EGFP−/Ubi-TetR plasmid, respectively, using Lipofectamine™ 2000 (Invitrogen Life Technologies, USA). After 48 h, the 293 T cells were lysed and replication-incompetent lentivirus was harvested. The lentivirus was filtered using a 0.45 mm pore size filter (Corning Inc., Corning, NY, USA) and concentrated approximately 1000-fold by ultracentrifugation (Beckman Coulter Inc., USA). The titers of infectious viral particles were determined by puromycin screening with crystal violet staining (Cyagen Biosciences Inc. Guangzhou, China). The viral stocks were aliquoted and stored at −80°C until further use.

2.3. Establishment and Identification of hTERT-Immortalized Rat BMSCs. Routine in vitro maintenance cultures were

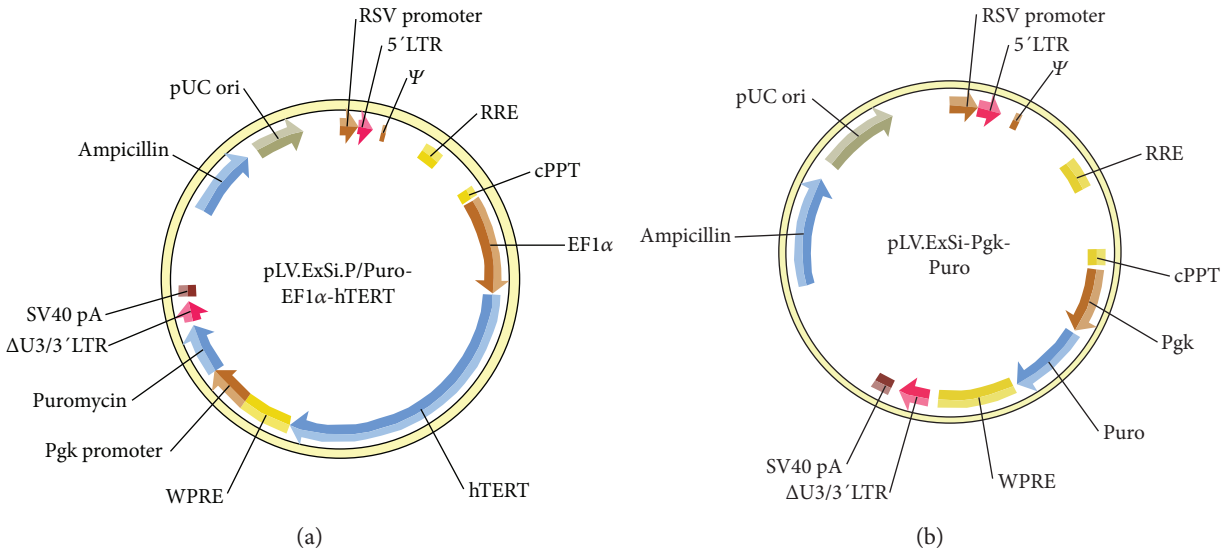

Figure 1: Plasmid profiles of the pLV.ExSi/Puro-EF1α-hTERT (a) and pLV.ExSi/ PGK-Puro (b) vectors with and without the hTERT gene, respectively, used for the immortalization of primary rat BMSCs (Cyagen Biosciences).

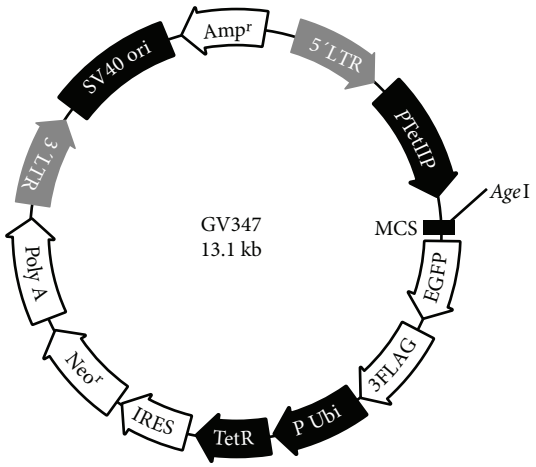

Figure 2: Plasmid profile of the single tetracycline-inducible lentiviral backbone vector system pLV.TetIIP-EGFP-/Ubi-TetR (Genechem, GV347). The system comprises an EGFP reporter gene and a tetracycline (Tet) response element under the control of separate promoters, the TetIIP and Ubi promoters. This construct drives the expression of rat galanin from transduced cells via Dox induction after cloning of the GAL gene into the multiple cloning sites (MCS).

established using sterile frozen finite-lifespan Sprague Dawley (SD) rat BMSCs (RASMX-01001) (Cyagen Biosciences Inc., Guangzhou, China). The nature of these cells was confirmed based on positivity for CD90, CD29, and CD44 and negativity for CD34, CD11b, and CD45. The cells were cultured in a humidified incubator with 5% CO_2 at 37°C in OriCell™ SD BMSC Growth Medium without a pH indicator (RASMX-90011, Cyagen Biosciences Inc.) and passaged (1 : 4) at 80% confluence. The medium was replaced at 3-day intervals. At passage 5 (P5), cultured rat BMSCs (5×10^4 cells/mL) were seeded onto a 24-well dish. The next day, lentiviral particles (ExSi/Puro-EF1A-hTERT or ExSi/PGK-Puro) were added at a MOI (multiplicity of infection) of 20 in the presence of 4 μg/mL polybrene (Sigma-Aldrich, St. Louis, MO, USA # 52495). After 8 h, the cells were washed and cultured with fresh medium containing 2 μg/mL puromycin (Gibco, USA). After 2-3 weeks of selection, the surviving clones were isolated.

Following harvest of P10-transfected and P5-untransfected BMSCs, total RNA was isolated using TRIzol reagent (Invitrogen, USA). Reverse transcriptase polymerase chain reaction (RT-PCR) was performed using the following primer pairs for hTERT and the housekeeping gene GAPDH: 5-GGCTTCAAGGCTGGGAGGAAC-3 (forward) and 5′-AGCACACATGCGTGAAACCTG-3′ (reverse) for hTERT and 5′-CCTTCCGTGTTCCTA CCC -3′ (forward) and 5′-CAACCTGGTCCTCAGTGTAG-3′ (reverse) for GAPDH. The expected amplicon sizes for hTERT and GAPDH were 164 and 150 bp, respectively.

In order to detect the telomerase activity, total RNA was extracted from P11 BMSCs and P30 hTERT-BMSCs (10^5-10^6) lysates using the TRAPeze XL Telomerase Detection Kit (Chemicon, Temecula, CA, USA) according to the manufacturer's instructions. The fluorometric telomeric repeat amplification protocol (TRAP) was used to quantify telomerase activity. Briefly, the cell lysates were mixed with TRAPeze® XL reaction mix containing Amplifluor® primers and incubated at 30°C for 30 min. The amplified telomerase products were quantified using a fluorescence plate reader (Molecular Devices, LLC, Sunnyvale, CA, USA). Telomerase activity was subsequently calculated after comparing the ratio of telomerase products to an internal standard for each lysate (ΔFL/ΔR), and each sample was examined three times [22]. Human cervical carcinoma cells (HeLa cells) were detected as a positive control, whereas heat-inactivated cells (85°C) and ExSi/PGK-Puro-transduced BMSCs (PGK-BMSCs) were used as negative controls.

Cell proliferation was detected based on the incorporation of 5-ethynyl-29-deoxyuridine (EdU) using the EdU Cell Proliferation Assay Kit (Ribobio, Guangzhou, China). Briefly, P30 hTERT-BMSCs or P14 BMSCs were seeded onto 24-well plates and incubated with 25 μM EdU for 24 h prior to fixation, permeabilization, and EdU staining according to the manufacturer's instructions. The cell nuclei were stained with Hoechst 33342 (Sigma-Aldrich, St. Louis, MO, USA) at a concentration of 10 μg/mL for 10 min at room temperature. The proportion of cells that incorporated EdU was determined by fluorescence microscopy (Olympus, Tokyo, Japan). For growth curve analysis, P30 hTERT-BMSCs, P14 BMSCs, and P14 PGK-BMSCs were seeded onto 96-well plates with 2×10^3 cells per well and grown in 200 μL culture medium respectively. Over the following 7 days, cell proliferation was measured using an MTS assay (The CellTiter 96 kit, Promega, USA) in triplicate wells each day. The spectrophotometric absorbance of each sample was measured at 490 nm using a microplate reader (Bio-Rad Laboratories, Hercules, CA, USA), with blank control wells to zero absorbance. A standard curve was obtained to display the relationship between absorbance and cell numbers. A growth curve was drawn according to the standard curve [23]. The population doubling time was calculated as $(\mathrm{PDT}) = (\log(N_n/N_{n-1}))/\log 2$ at passage n, where N is the number of counted cells. Cell cycle assays were also performed in selected cells. Briefly, the trypsinized cells were fixed in 70% ethanol, washed with PBS, and then treated with 20 mg/mL RNase (TaKaRa, Otsu, Shiga, Japan) for 15 min at 37°C. DNA was labeled with 50 μg/mL propidium iodide (PI; Sigma-Aldrich, St Louis, MO, USA) in the dark for 30 min at 4°C, and DNA content was assessed by flow cytometry with a Calibur (Becton Dickinson). Each group was analyzed in triplicate.

2.4. Phenotype and Neural Differentiation of hTERT-BMSCs. Surface molecules were detected using the monoclonal antibodies CD29, CD34, CD44, and CD45 (Becton Dickinson, USA) for the corresponding antigens of BMSCs by flow cytometry according to a standard protocol. In addition, to determine the neural differentiation of hTERT-BMSCs, the cells were removed from the flask bottom after the fourth passage, replated in 35 mm culture dishes, and induced after reaching 70–80% confluency in DMEM/F12 with B-27 supplement medium containing different epidermal growth factor (10 ng/mL) and basic fibroblast growth factor (20 ng/mL) for neuronal progenitor cell induction or glial-derived neurotrophic factor (10 ng/mL), brain-derived neurotrophic factor (10 ng/mL), and neurotrophin 3 (10 ng/mL) for neuron induction [24]. The shape of the induced cells was observed daily, and the differentiated cells were characterized by immunocytochemistry using neural-specific markers; undifferentiated hTERT-BMSCs cells were used as a control.

2.5. Tumorigenicity, Anchorage-Independent, and Karyotype Analysis. Like any genetic modification, cell immortalization may result in malignant transformation by impairing cell-cycle regulation. Thus, three four-week-old BALB/c nu/nu mice were subcutaneously injected with 0.1 mL of P40 hTERT-BMSC suspension each, and another 3 mice were injected with a human colon cancer SW480 cell suspension (ATCC, Manassas, VA, USA) as a positive control (5×10^6 cells/mL each). Animals were maintained under sterile conditions for 4 months and palpated for tumor appearance once a week. To test for soft agar colony growth capacity, hTERT-immortalized cells were plated at a density of 1×10^5 cells in 3 mL of 0.35% agarose over a 0.7% agar base in a 60 mm diameter culture dish. Cultures were fed every 3 days, and colonies with >50 cells were scored after 4 weeks in cultures under a dissecting microscope. Moreover, to determine if the abnormal karyotype resulted from ectopic hTERT, the cells were fixed using fresh stationary liquid (methanol : glacial acetic acid = 3 : 1), spread onto slides, and stained with Giemsa's solution, and the chromosome images were captured under an immersion objective using an Olympus BX51 High Class System Microscope (Olympus Corporation).

2.6. Determination of Tet-On Lentiviral Transfection Efficiency. The optimal transfection efficiency in the hTERT-BMSCs was determined based on the MOI and percentage of EGFP-positive cells using flow cytometry 2 days after LV.TetIIP-EGFP-/Ubi-TetR or LV.TetIIP-GAL-EGFP/Ubi-TetR transfection and doxycycline (Dox, Sigma-Aldrich, St. Louis, MO, USA) induction. The fraction of viral load to cell number was calculated as the MOI.

To directly observe the controllable gene expression, single Tet-on-inducible bicistronic lentiviral particles (LV.TetIIP-GAL-EGFP−/Ubi-TetR) expressing EGFP and GAL were used to infect hTERT-BMSCs, and viral supernatants at a MOI of 30 were added to fresh culture medium supplemented with 8 μg/mL polybrene and 400 μg/mL neomycin (Sigma-Aldrich, St. Louis, MO, USA). After 12 h, the cells were resuspended in fresh culture medium and then transferred to RPMI medium (Gibco, USA) containing 1 μg/mL Dox (Sigma Aldrich, St. Louis, MO, USA) and supplemented with 10% Tet system-proved FCS (BD Biosciences, Clontech, USA), an optimal tetracycline-free serum for tetracycline-controllable expression systems. EGFP expression was observed under a fluorescence microscope after 48 h.

2.7. Detection of Inducible GAL Secretion from hTERT-BMSCs/Tet-on/GAL. Subconfluent hTERT-BMSCs were exposed to freshly filtered LV.TetIIP-GAL-EGFP-/Ubi-TetR viral supernatant at MOI 30 in the presence of 8 μg/mL polybrene. After 12 h, the medium was replaced with fresh medium. At 48 h postinfection, the cells were subsequently placed in medium under neomycin selection (800 μg/mL) for 10–14 days. The resulting neomycin-resistant cell clones were separated into cultures with and without Dox (0–10000 ng/mL) induction. A total of 16 positive clones were assessed using an EGFP fluorescence assay. Clone 4 was selected for its high induction of EGFP expression in response to Dox and low leakiness (activity in the absence of Dox) and subsequently named hTERT-BMSCs/Tet-on/GAL.

The kinetics of rat GAL protein levels secreted from neuronal differentiated hTERT-BMSCs/Tet-on/GAL under different concentrations of Dox was assayed using a

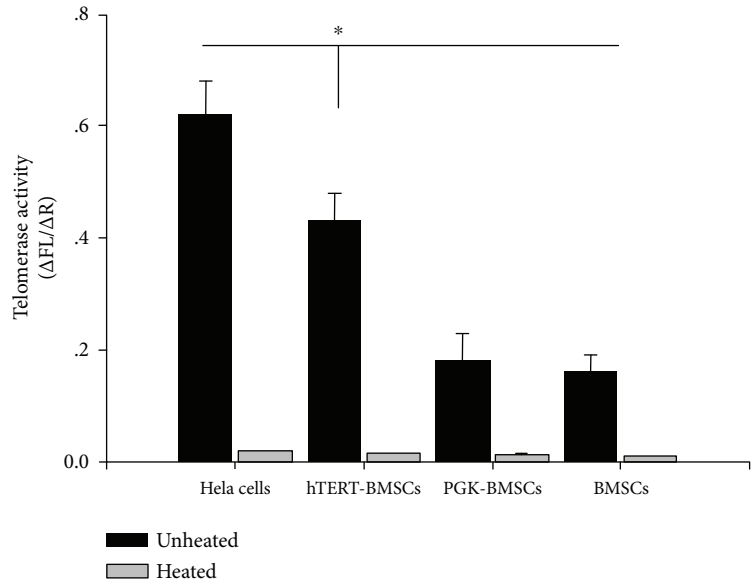

Figure 3: Telomerase activity of HeLa cells, BMSCs, PGK-BMSCs, and hTERT-BMSCs (TRAP assay) after disposed with or without heat. There was little telomerase activity in all heat-treated negative control cells; however, in unheated cells, despite extensive doublings, the immortalized cells (hTERT-BMSCs) displayed significantly higher telomerase activity than their primary counterparts and PGK-BMSCs, except the positive control cells (HeLa) and the telomerase activity of the immortalized population remained stable (assessed at P30). Significance level is $P < 0.05$, indicated by $*$.

galanin enzyme-linked immunosorbent assay (ELISA) kit (JM-E1001) according to the manufacturer's instructions (TSZ Biological Trade Co. Ltd, NJ, USA). Briefly, subconfluent neuronal differentiated hTERT-BMSCs/Tet-on/GAL (5×10^4) were incubated in the presence of Dox at 0, 10, 100, 1000, 5000, and 10000 ng/mL for 48 h or incubated for various times in 12 h intervals with the administration of 1 μg/mL Dox and removal of Dox. The supernatant from the cell culture medium was collected, centrifuged at 1000 rpm for 5 min at 4 °C, and subsequently incubated on a microplate precoated with a rat GAL monoclonal antibody for 45 min at 37°C (5 wells for each). After the second antibody conjugated with HRP was added and bound to the captured GAL, the HRP substrate TMB (tetramethylbenzidine) was added to the wells. The OD450 was measured to generate a standard curve and calculate the GAL concentration using a microplate reader (Molecular Devices, Sunnyvale, CA, USA). The secretion level was standardized and expressed in pg/mL of supernatant. hTERT-BMSCs were used as a control.

2.8. Statistical Analysis. Statistical analysis was performed using GraphPad Prism 5.01 for Windows (San Diego, CA, USA) via repeated measures one-way analysis of variance (ANOVA) followed by Bonferroni's multiple comparison test (telomerase activity) or two-way ANOVA followed by Bonferroni's posttests for evaluating the growth features and effects of Dox on GAL levels over time. Statistical significance was determined as $P < 0.05$. All data are presented as the mean ± standard error of the mean (SEM).

3. Results

3.1. Transcription of hTERT Gene and Telomerase Activity. mRNA expression of the hTERT gene was detected using RT-PCR with specific hTERT primers. For hTERT-transfected cells (hTERT-BMSCs), 164 bp-specific amplification bands of hTERT were detected, whereas for untransfected cells (BMSCs) and cells (PKG-BMSCs) transfected with the control vector, no specific band was detected (Supplemental information Figure S1(A)). Moreover, as internal reference fragments, a 150 bp-specific amplification band of GAPDH was detected in all cell groups (Supplemental information Figure S1(B)). These findings suggest that the hTERT gene was integrated into the genomic DNA of rat BMSCs and transcribed into mRNA. Subsequently, telomerase activity was also detected using TRAP for the sensitive measurement of telomerase activity. As shown in Figure 3, the immortalized population (hTERT-BMSCs) stably displayed higher telomerase activity (2.4 ± 0.5-fold) compared with their primary counterparts (BMSCs) and the negative control, even after extensive proliferation (up to 30 PDT), whereas much higher activity was observed in the positive control (HeLa cells). These results confirm the functionality of the implemented human telomerase gene in hTERT-BMSCs.

3.2. Growth Feature and EdU Proliferation Assay of hTERT-BMSCs. To confirm that rat BMSCs expressing hTERT had an extended lifespan, we monitored the growth features of the cells (i.e., hTERT-BMSCs expressing hTERT and untransfected BMSCs and PGK-BMSCs not expressing

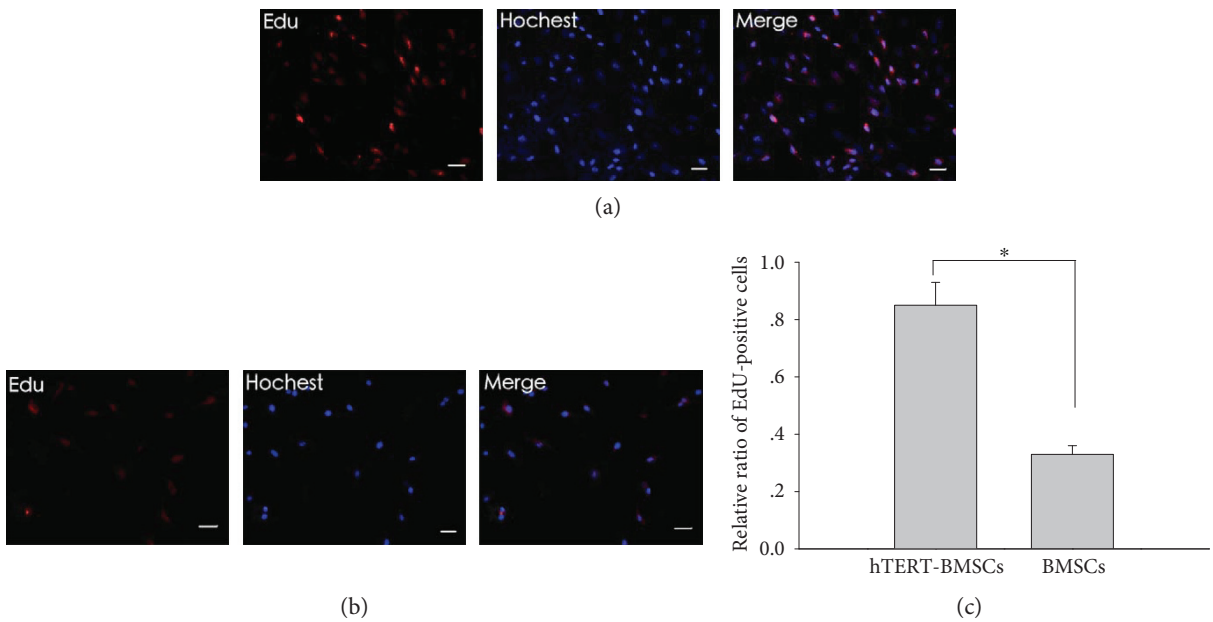

Figure 4: EdU proliferation assay of the effect of hTERT on the growth of BMSCs. The red fluorescent cells are in the S phase of mitosis, and the blue fluorescent cells represent all cells. (a) and (b) present images of P30 hTERT-BMSCs and P14 BMSCs, respectively. (c) Ratio of EdU-positive cells. Significance level is $P < 0.05$, indicated by $*$. Scale bar: 100 μm.

hTERT). The cell growth curves showed that immortalized BMSCs expressing hTERT vigorously proliferated for at least 6 days and subsequently reached a growth plateau due to inhibition of proliferation by cell-cell contact. In contrast, BMSCs and PGK-BMSCs without hTERT transduction grew slowly after plating and displayed growth retardation and senescence at 3-4 days after passage (Supplemental information Figure S2(A)). The PDT values for hTERT-BMSCs at P30, BMSCs, and PGK-BMSCs at P14 were approximately 25, 53, and 58 h, respectively. The results of flow cytometry revealed that most of the hTERT-transfected BMSCs at P30 showed a distinctive accumulation of G2/M and S phases, while, in striking contrast, untransfected or control PGK-BMSCs at P14 did not accumulate in G2/M and S phases, which implied most of cells ceased at senescence stage (see Supplementary Figure S2(B)).

To further assess the effects of hTERT on BMSCs, cell proliferation was also examined using an EdU assay, an immunochemical detection method that measures nucleotide analog incorporation into newly replicated DNA. Consistent with the results of the growth features, significantly more EdU-positive cells were observed among the hTERT-modified cells (Figures 4(a) and 4(b)), and the percentage of EdU-positive cells was significantly higher in P30 hTERT-BMSCs compared with P14 BMSCs (Figure 4(c)). These results further implied that ectogenic hTERT significantly lengthens the lifespan of cells, promoting DNA replication and telomere elongation and that hTERT immortality can favor cell proliferation. Thus, a stable hTERT-BMSC line with steady proliferation capacity was successfully generated.

3.3. Characterization of hTERT-BMSCs. In addition to becoming immortalized, the hTERT-BMSCs also retained the typical characterization of the parental cells (Figure 5). To assess cell phenotype, flow cytometry assay indicated that more than 85% of the hTERT-immortalized BMSCs were positive for typical surface markers of BMSCs (Figure 5(a)), including CD44 (85.08%) and CD29 (95.16%), whereas these cells were almost completely negative for both hematopoietic markers CD34 (0.21%) and CD45 (0.09%) (Figures 5(b)–5(e)). The cells retained a phenotype identical to that of their primary counterparts (Figure 5(f)). To assess neurogenic differentiation, the isolated hTERT-BMSCs were cultured in neuronal induction medium. Although the number of cells did not increase, the development of axon-like and dendrite-like cells indicated neuronal differentiation. To further confirm that the differentiated cells were neurogenic, the differentiated cells were detected with specific neural markers. Immunofluorescence assays demonstrated that the cells were positive for the expression of Nestin, a marker of neuronal progenitor cells, NSE, a marker of neurons, and GFAP, a marker of glial cells (Figures 5(g)–5(i)), while undifferentiated hTERT-BMSCs showed no marked expression of neural markers (data not shown).

The tumorigenicity of the hTERT-immortalized BMSC line was subsequently investigated in vivo after subcutaneous injection in the flanks of nude mice. After 2 months postinjection, the nude mice injected with SW480 cells developed tumors; in contrast, malignant transformation did not occur in mice injected with hTERT-BMSCs for up to 4 months and no colony growth in soft agar was found (data not shown). Moreover, karyotype analysis revealed that hTERT-BMSCs displayed a chromosomal pattern similar to that of the parental cells (diploid number 42), with no abnormal nuclear pattern observed after genetic modification (Supplemental information Figure S3), thus demonstrating the homogeneity and safety of the generated cell line.

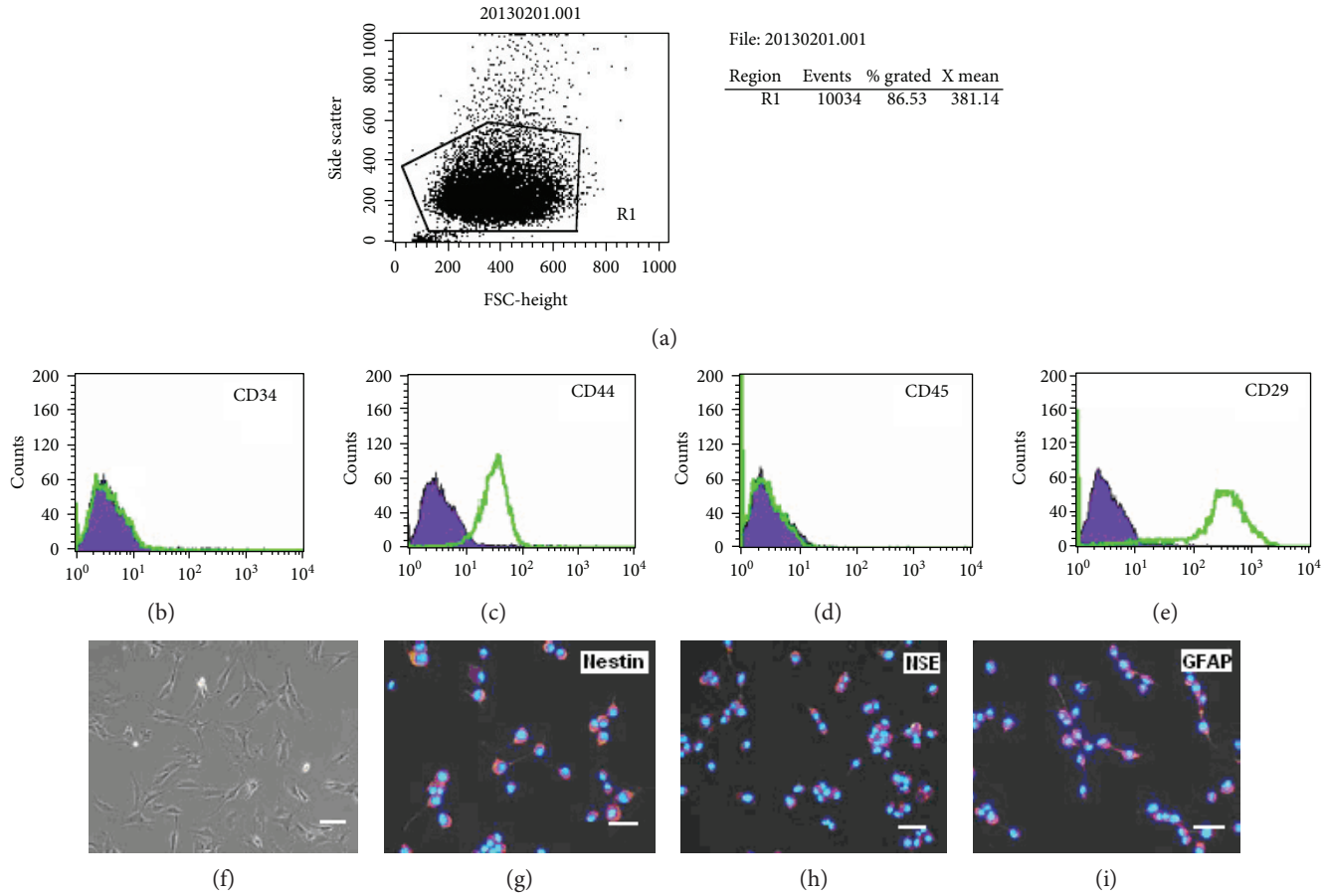

Figure 5: Identification of surface phenotype and neurogenesis of hTERT-BMSCs. (a–e) Expression of surface molecules detected using flow cytometry analysis. (f) Typical morphology was observed under an inverted phase contrast microscope. (g–i) The expression of neural specific markers on hTERT-immortalized BMSCs (note: nuclei were stained with Hoechst 33342 blue). Scale bar: 100 μm.

3.4. Construction and Transfection Efficiency of Single Tet-Inducible Lentiviral Vector. To establish a Dox-dependent GAL gene expression system with a single lentiviral vector, we inserted the expression cassettes containing the rat GAL cDNA fragment (Supplemental information Figure S4A) from the construct pBS KS(+)-GAL into the single Tet-regulated lentiviral vector system "GV347" (Figure 2). Transformants of the cloned insert were subsequently identified by PCR and electrophoresis on a 1% agarose gel. Five positive transformants with the proper orientation were detected (Supplemental information Figure S4(B)), and the sequences were confirmed by DNA sequencing.

The fraction of cells that glowed green, reflecting lentiviral gene transfer efficiency, increased dose dependently as the MOI increased from 0 to 30. The highest infection rate, approximately 78%, was obtained at an MOI of 30, and no significant increase was observed when the amount of virus increased from 30 to 75 MOI. In addition, the number of dead cells floating in the medium significantly increased. Therefore, an MOI of 30 was used in subsequent experiments.

3.5. Visualization of EGFP Fluorescence under the Dox Induction. The expression of EGFP in response to Dox was directly observed in the hTERT-BMSCs transfected with LV.TetIIP-GAL-EGFP-/Ubi-TetR (Figure 2). The expression of EGFP was induced using a Dox at concentrations of 1 μg/mL, whereas untreated cells (without Dox) exhibited little green fluorescence (Figures 6(a) and 6(b)). These results suggested that the functional tetracycline-controlled transgene can effectively be delivered with higher inducibility into mammalian cells using the developed single Tet-on vector system.

3.6. Inducible GAL Secretion from hTERT-BMSCs/Tet-on/GAL. The inducible secretion of rat GAL from hTERT-BMSCs/Tet-on/GAL by Dox after neuronal differentiation was initially confirmed by ELISA using hTERT-BMSCs as negative controls. After treatment for 48 h with different concentrations of Dox (Figure 7), low endogenous GAL secretion (20 pg/mL of supernatant) was observed in the parental hTERT-BMSCs. However, the secretion of GAL from hTERT-BMSCs/Tet-on/GAL increased in response to treatment with an increased concentration of Dox greater than 10 ng/mL in the culture medium, peaking under Dox induction at 1000 ng/mL (approximately 400 pg/mL of supernatant) (Figure 7(a)). We also assessed the reversibility of Dox induction after subjecting the hTERT-BMSCs/Tet-on/GAL to repeated on-off cycles. When Dox was added to the culture medium (1 μg/mL), GAL secretion gradually

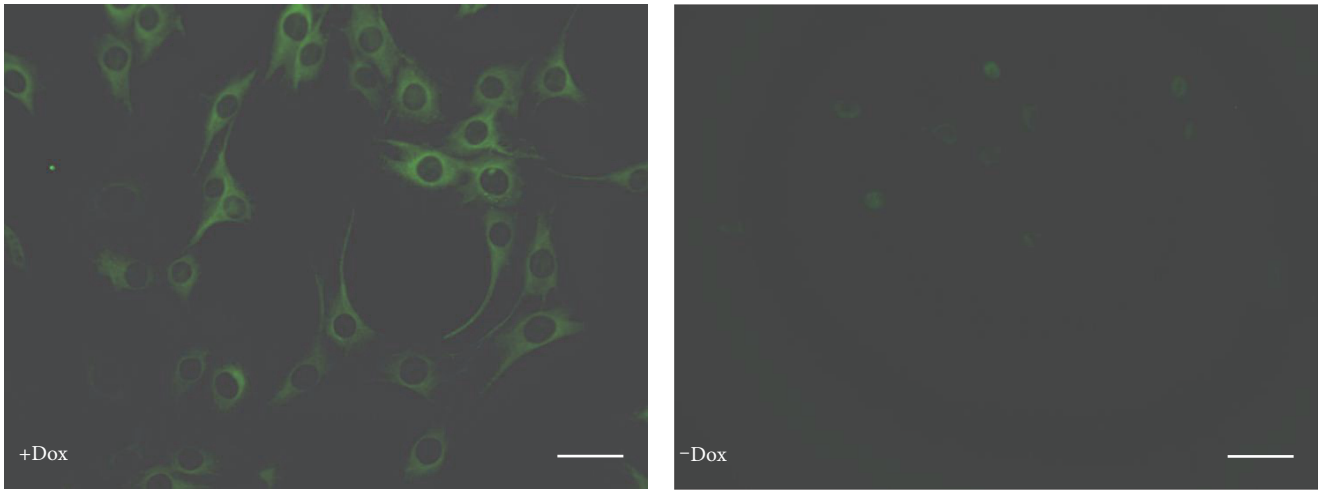

(a) (b)

Figure 6: Regulatable EGFP expression from hTERT-BMSCs/Tet-on/GAL cells in the presence and absence of Dox in vitro (×400). hTERT-BMSCs transfected with LV.TetIIP-GAL-EGFP-/Ubi-TetR showed strong green fluorescence after treatment with 1 μg/mL Dox for 48 h (a), whereas very faint fluorescence was observed without Dox induction (b). Scale bar: 200 μm.

increased to 20-fold after 48 h and subsequently returned to basal levels after Dox removal for approximately 12 h. Comparable results were obtained during the second on-off cycle (Figure 7(b)). These results suggest that GAL gene expression from these genetically modified cells (hTERT-BMSCs/Tet-on/GAL) can be regulated by the addition of Dox in vitro.

4. Discussion

To explore a novel strategy for establishing controllable expression of the exogenous GAL gene from hTERT-BMSCs for pain therapy, we constructed an hTERT-BMSCs/Tet-on/GAL line using a single Tet-on-inducible lentiviral vector. This cell line displayed low baseline activity coupled with high inducibility in the presence of low doses of the inducer Dox in vitro.

The management of neuropathic pain after nerve injury remains a major clinical challenge. The combination of ex vivo gene transfer and cell transplantation is considered a potentially useful strategy for the treatment of neurodegenerative diseases and traumatic injuries. This approach requires optimized gene delivery systems for therapeutic molecules. Several cellular vehicles have been investigated for ex vivo gene therapy of the CNS [25], and attention has focused on the therapeutic potential of BMSCs from bone marrow. BMSCs do not induce an allogenic reaction and might even suppress host T cell proliferation, suggesting that cells cultured from a single donor might be expanded to form a reserve pool that could be used for multiple recipients [26]. However, during in vitro culture, BMSCs undergo replicative senescence and lose the ability to proliferate over time, as observed in the present study. This decline has been attributed to genetic instability after critical shortening of telomeres. Lentiviral vectors have been used for the stable integration and long-term expression of transgenes. Lentiviral vectors are also favorable for biological research and gene therapy trials due to their ability to infect both dividing and nondividing cells and are particularly suitable for BMSCs [27]. Thus, in the present study, using a lentiviral system, we introduced the immortalization gene, hTERT, into primary rat BMSCs. Untransfected BMSCs without hTERT expression exhibited reduced growth associated with aging in vitro and failed to proliferate, becoming senescent after passage 14. In contrast, after transduction with hTERT, hTERT-immortalized BMSCs exhibited strong proliferation. The PDT of hTERT-BMSCs is shorter than that of nonimmortalized cells. After more than 30 passages, hTERT-BMSCs retain the potential to divide further. Similarly, significantly more EdU-positive cells were observed among the cells with ectogenic hTERT expression, indicating that hTERT-BMSCs maintained higher telomerase activity and proliferated significantly longer than wild type BMSCs. Moreover, the successive genetic modifications and extensive proliferation of these cells did not lead to an alteration of the mesenchymal phenotype, as assessed using conventional markers. The phenotype and karyotype of hTERT-BMSCs did not differ significantly from those of untransfected cells. Moreover, these cells retained the normal morphology and neuronal differentiation characteristics of stem cells when cultured in induction media. Based on the negative results of colony growth in soft agar and the lack of tumorigenicity in nude mice, our data clearly indicated that the hTERT-immortalized BMSCs did not exhibit any neoplastic transformation phenotype at least up to 4 months. Although telomerase expression is a hallmark of cancer and spontaneous tumoral transformation of MSCs expressing hTERT was reported [28], telomerase overexpression is typically nononcogenic, and hTERT-transduction has not hitherto been associated with neoplastic transformation. Many previous studies have investigated the long-term effects of forced expression of human telomerase catalytic component in

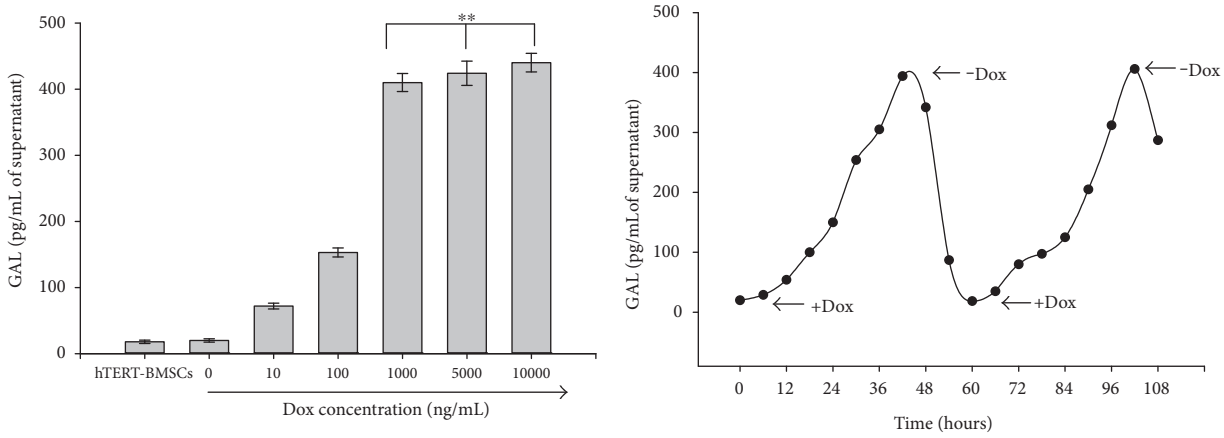

Figure 7: GAL secretion from cells after Dox induction in vitro. (a) The dose response of galanin production in cultured hTERT-BMSCs/Tet-on/GAL revealed a correlation between the Dox dose and the galanin secretion level. Significance level is $^{**}P > 0.05$, indicated by $**$. (b) Time course of galanin secretion from hTERT-BMSCs/Tet-on/GAL under the control of Dox. The arrows indicate the addition (+Dox) or removal (−Dox) of Dox from the culture medium.

normal human fibroblasts or BMSC. In vitro growth requirements, cell cycle checkpoints and karyotypic stability in telomerase-expressing cells are similar to those of untransfected controls. In addition, coexpression of telomerase, the viral oncoproteins HPV16 E6/E7 (which inactivate p53 and pRB), and oncogenic Ras does not result in growth in soft agar. Thus, although ectopic expression of telomerase in primary cells is sufficient for immortalization, it does not result in changes typically associated with malignant transformation that could be served as stem cell-based vehicles for therapeutic gene delivery in the CNS [29, 30]. But, even so, the possibility of transformation which occurs after long-term expansion of hTERT-BMSCs still need further study.

Because of the relationship of the GAL gene to galanin production and the activation of galanin through central GAL receptors in the CNS [31], we introduced the GAL gene into hTERT-BMSCs as a potential treatment for chronic neuropathic pain. Although previous studies have demonstrated that IAST genetically modified by the rat preprogalanin gene secretes higher levels of galanin in vitro and efficiently functions to relieve neuropathic pain [8], potential complications resulting from the continuous secretion of GAL appear inevitable. In most cases, the successful application of gene therapy requires the development of vectors that permit regulated control of therapeutic gene expression. Tet-regulatable systems have been successfully used to regulate transgene expression in established cell lines and transgenic animals. There are two basic variants of the tetracycline-inducible expression system: the tTA (Tet-off) system and the rtTA (Tet-on) system [32]. Typically, if a gene remains predominantly inactive and is only occasionally activated, then the Tet-on system is more appropriate than the Tet-off system. Leaky expression due to both inherent defects in Tet-based systems and promoter leakiness resulted from promoter-dependent or integration site-dependent effects compromises the desired stringent regulation of transgene expression [33]. Thus, a variety of methods for integrating Tet-inducible expression components into a single vector has recently been described to obviate the selection of a homogeneous and cotransduced population [34, 35]. In consideration of most doxycycline-responsive systems that are based on the TetR-VP16 chymeras, in these systems, the promoter is only active when the tTA or the rtTA transactivators bind the regulated promoter; the expression of the VP16 transactivators in the regulated cells can have several undesired consequences such as alteration of the promoter natural activity, activation of cellular genes, and toxicity [36]. To this end, we engineered a convenient TetR-based inducible transgene expression vector as a single Tet-inducible bicistronic lentivirus system to regulate EGFP and GAL expression in a single vector, in which EGFP under the control of the TetII promoter was used as a reporter. This system is less toxic than the rtTA since it does not have the transactivator VP16. In the present study, the inducibility and background EGFP expression of recombinant Tet-on lentiviral particles were determined after transfecting hTERT-BMSCs at an MOI of 30. As shown in Figure 6, the basal expression of EGFP was nearly absent from transfected hTERT-BMSCs without Dox, whereas treatment with Dox (1 μg/mL) resulted in marked expression of EGFP.

Although the expression of transgenes (often EGFP) can be regulated in stem cells and their differentiated progenies at an early stage, transgenes are frequently no longer expressed or regulated in mature cells, including neurons [37]. In our present study, a low level of GAL secretion from hTERT-BMSCs/Tet-on/GAL was detected in vitro in the noninduced state after neuronal differentiation, whereas an extremely low level of Dox induction (10 ng/mL) was able to activate GAL expression (see Figure 7(a)). The level of GAL secretion was controlled by Dox in an apparently dose-dependent manner, with a positive linear trend in GAL production with respect to the inducer. Additionally, as shown in Figure 7(b), kinetic

tests revealed that GAL gene activation could be repeated in on-off-on cycles, and long-term-regulated GAL expression was achieved by daily administration of Dox. These observations indicate that the Dox-based regulation of GAL secretion from hTERT-BMSCs/Tet-on/GAL was controllable, rapidly reversible, and not lost over time. Transgene regulation was also achieved in mature neurons and astrocytes after differentiation in vitro, suggesting the potential for effective function after transplantation into the CNS.

4.1. Study Limitations. Despite of significant differences in GAL secretion from transfected cells observed in the presence and absence of Dox, the weak leakage of galanin protein is problematic, and EGFP expression from hTERT-BMSCs/Tet-on/GAL was still observed in ELISA and fluorescence assays even in the off state, reflecting the unexpected translation in transduced cells in the absence of Dox [38]. Thus, the Tet-on system used in the present study still has specific limitations. Fortunately, the leaky expression of the transgenes was insignificant compared with the expression in transduced cells exposed to Dox. Therefore, unless the transgenes can affect cellular processes at an extremely low level, these vectors should be suitable for most target genes in biological research. However, an improved promoter other than TRE would enable the further reduction or even elimination of leakiness in this inducible system. Moreover, the differences in basal expression between cell lines might reflect the location of the insertion within the host genome and the influence of surrounding host genes on target gene expression. Therefore, this basal level of expression could be decreased by advanced screening for BMSCs line with low levels of expression in the off state. Thus, additional studies are needed to improve the system.

In summary, using a single tetracycline-inducible lentivirus delivery system to introduce the therapeutic GAL gene into rat hTERT-immortalized BMSCs, we generated an hTERT-BMSCs/Tet-on/GAL cell line with inducible rat GAL expression to regulate the secretion levels of GAL in vivo, which is critical for the balance of excitatory and inhibitory systems in pain-processing centers. This strategy is the first promising step toward a novel stem cell-based "biological mini pump" for potential use in pain therapy.

Conflicts of Interest

The authors have no commercial, proprietary, or financial interest in the products or companies described in this article.

Acknowledgments

The authors would like to thank Dr. David Wynick (Bristol Royal Infirmary, Bristol, England) and Professor William C. Hahn (Dana-Farber Cancer Institute, Harvard Medical School, USA) for kindly providing the constructs pBS KS(+)-GAL and pCI-Neo-hTERT-encoding rat GAL and hTERT cDNA, respectively, for the creation of the hTERT-BMSCs/Tet-on/GAL line. The authors would also like to thank Cyagen Biosciences (Guangzhou, China) for the construction of the lentiviral vectors. This work was supported by grants from the National Natural Science Foundation of China (no. 81171468) and Research Fund for the Doctoral Program of Higher Education of China (no. 20080558112). In addition, the manuscript has been edited by Wiley English Language Editing Services (950F-618E-1C95-FB30-B116).

References

[1] A. H. Dickenson, V. Chapman, and G. M. Green, "The pharmacology of excitatory and inhibitory amino acid-mediated events in the transmission and modulation of pain in the spinal cord," *General Pharmacology*, vol. 28, no. 5, pp. 633–638, 1997.

[2] E. Niederberger, H. Kühlein, and G. Geisslinger, "Update on the pathobiology of neuropathic pain," *Expert Review of Proteomics*, vol. 5, no. 6, pp. 799–818, 2008.

[3] K. A. Czech and J. Sagen, "Update on cellular transplantation into the CNS as a novel therapy for chronic pain," *Progress in Neurobiology*, vol. 46, no. 5, pp. 507–529, 1995.

[4] R. Lang, A. L. Gundlach, and B. Kofler, "The galanin peptide family: receptor pharmacology, pleiotropic biological actions, and implications in health and disease," *Pharmacology & Therapeutics*, vol. 115, no. 2, pp. 177–207, 2007.

[5] D. Wynick, S. W. Thompson, and S. B. McMahon, "The role of galanin as a multi-functional neuropeptide in the nervous system," *Current Opinion in Pharmacology*, vol. 1, no. 1, pp. 73–77, 2001.

[6] Z. Wiesenfeld-Hallin and X. J. Xu, "Neuropeptides in neuropathic and inflammatory pain with special emphasis on cholecystokinin and galanin," *European Journal of Pharmacology*, vol. 429, no. 1–3, pp. 49–59, 2001.

[7] K. An, Y. Tian, H. Yang, F. Gao, and P. Wang, "Immortalized rat astrocyte strain genetically modified by rat preprogalanin gene," *Journal of Huazhong University of Science and Technology. Medical Sciences*, vol. 25, no. 2, pp. 144–146, 2005.

[8] K. An, Y. Xu, H. Yang, H. H. Shu, H. B. Xiang, and Y. K. Tian, "Subarachnoid transplantation of immortalized galanin-overexpressing astrocytes attenuates chronic neuropathic pain," *European Journal of Pain*, vol. 14, no. 6, pp. 595–601, 2010.

[9] Y. Xu, X. B. Tian, K. An, H. Yang, and Y. K. Tian, "Lumbar transplantation of immortalized enkephalin- expressing astrocytes attenuates chronic neuropathic pain," *European Journal of Pain*, vol. 12, no. 4, pp. 525–533, 2008.

[10] J. Yoo, H. S. Kim, and D. Y. Hwang, "Stem cells as promising therapeutic options for neurological disorders," *Journal of Cellular Biochemistry*, vol. 114, no. 4, pp. 743–753, 2013.

[11] A. Biffi, E. Montini, L. Lorioli et al., "Lentiviral hematopoietic stem cell gene therapy benefits metachromatic leukodystrophy," *Science*, vol. 341, no. 6148, article 1233158, 2013.

[12] M. Guan, Y. Xu, W. Wang, and S. Lin, "Differentiation into neurons of rat bone marrow-derived mesenchymal stem cells," *European Cytokine Network*, vol. 25, no. 3, pp. 58–63, 2014.

[13] J. Reiser, X. Y. Zhang, C. S. Hemenway, D. Mondal, L. Pradhan, and V. F. La Russa, "Potential of mesenchymal stem cells in gene therapy approaches for inherited and acquired diseases," *Expert Opinion on Biological Therapy*, vol. 5, no. 12, pp. 1571–1584, 2005.

[14] D. G. Phinney and I. A. Isakova, "Mesenchymal stem cells as cellular vectors for pediatric neurological disorders," *Brain Research*, vol. 1573, pp. 92–107, 2014.

[15] R. Taran, M. K. Mamidi, G. Singh et al., "In vitro and in vivo neurogenic potential of mesenchymal stem cells isolated from different sources," *Journal of Biosciences*, vol. 39, no. 1, pp. 157–169, 2014.

[16] M. M. Bonab, K. Alimoghaddam, F. Talebian, S. H. Ghaffari, A. Ghavamzadeh, and B. Hikbin, "Aging of mesenchymal stem cell in vitro," *BMC Cell Biology*, vol. 7, no. 1, p. 14, 2006.

[17] M. A. Baxter, R. F. Wynn, S. N. Jowitt, J. E. Wraith, L. J. Fairbairn, and I. Bellantuono, "Study of telomere length reveals rapid aging of human marrow stromal cells following in vitro expansion," *Stem Cells*, vol. 22, no. 5, pp. 675–682, 2004.

[18] J. L. Simonsen, C. Rosada, N. Serakinci et al., "Telomerase expression extends the proliferative life-span and maintains the osteogenic potential of human bone marrow stromal cells," *Nature Biotechnology*, vol. 20, no. 6, pp. 592–596, 2002.

[19] I. Barde, M. A. Zanta-Boussif, S. Paisant et al., "Efficient control of gene expression in the hematopoietic system using a single Tet-on inducible lentiviral vector," *Molecular Therapy*, vol. 13, no. 2, pp. 382–390, 2006.

[20] M. Gossen and H. Bujard, "Tight control of gene expression in mammalian cells by tetracycline-responsive promoters," *Proceedings of the National Academy of Sciences of the United States of America*, vol. 89, no. 12, pp. 5547–5551, 1992.

[21] F. Katzen, "Gateway(®) recombinational cloning: a biological operating system," *Expert Opinion on Drug Discovery*, vol. 2, no. 4, pp. 571–589, 2007.

[22] M. A. Shammas, H. Koley, R. B. Batchu et al., "Telomerase inhibition by siRNA causes senescence and apoptosis in Barrett's adenocarcinoma cells: Mechanism and therapeutic potential," *Molecular Cancer*, vol. 4, no. 1, p. 24, 2005.

[23] J. Su, H. Liang, W. Yao et al., "MiR-143 and MiR-145 regulate IGF1R to suppress cell proliferation in colorectal cancer," *PloS One*, vol. 9, no. 12, Article ID e114420, 2014.

[24] J. H. Lee, W. K. Kang, J. H. Seo et al., "Neural differentiation of bone marrow-derived mesenchymal stem cells: applicability for inner ear therapy," *Korean Journal of Audiology*, vol. 16, no. 2, pp. 47–53, 2012.

[25] F. H. Gage, "Cell therapy," *Nature*, vol. 392, no. 6679, Supplement, pp. 18–24, 1998.

[26] H. Hamada, M. Kobune, K. Nakamura et al., "Mesenchymal stromal cells (MSC) as therapeutic cytoreagents for gene therapy," *Cancer Science*, vol. 96, no. 3, pp. 149–156, 2005.

[27] N. V. Sats, I. N. Shipunova, A. E. Bigil'diev, and N. I. Drize, "Stable lentiviral vector transfer into mesenchymal stem cells in vivo," *Bulletin of Experimental Biology and Medicine*, vol. 159, no. 6, pp. 764–767, 2015.

[28] N. Serakinci, P. Guldberg, J. S. Burns et al., "Adult human mesenchymal stem cell as a target for neoplastic transformation," *Oncogene*, vol. 23, no. 29, pp. 5095–5098, 2004.

[29] C. P. Morales, S. E. Holt, M. Ouellette et al., "Absence of cancer-associated changes in human fibroblasts immortalized with telomerase," *Nature Genetics*, vol. 21, no. 1, pp. 115–118, 1999.

[30] X. R. Jiang, G. Jimenez, E. Chang et al., "Telomerase expression in human somatic cells does not induce changes associated with a transformed phenotype," *Nature Genetics*, vol. 21, no. 1, pp. 111–114, 1999.

[31] R. Lang, A. L. Gundlach, F. E. Holmes et al., "Physiology, signaling, and pharmacology of galanin peptides and receptors: three decades of emerging diversity," *Pharmacological Reviews*, vol. 67, no. 1, pp. 118–175, 2015.

[32] J. Bai, J. Li, and Q. Mao, "Construction of a single lentiviral vector containing tetracycline- inducible alb-uPA for transduction of uPA expression in murine hepatocytes," *PloS One*, vol. 8, no. 4, article e61412, 2013.

[33] Z. Zhu, B. Ma, R. J. Homer, T. Zheng, and J. A. Elias, "Use of the tetracycline-controlled transcriptional silencer (tTS) to eliminate transgene leak in inducible overexpression transgenic mice," *The Journal of Biological Chemistry*, vol. 276, no. 27, pp. 25222–25229, 2001.

[34] X. Tian, G. Wang, Y. Xu et al., "An improved tet-on system for gene expression in neurons delivered by a single lentiviral vector," *Human Gene Therapy*, vol. 20, no. 2, pp. 113–123, 2009.

[35] K. Benabdellah, M. Cobo, P. Muñoz, M. G. Toscano, and F. Martin, "Development of an all-in-one lentiviral vector system based on the original TetR for the easy generation of Tet-ON cell lines," *PloS One*, vol. 6, no. 8, article e23734, 2011.

[36] M. Morimoto and R. Kopan, "rtTA toxicity limits the usefulness of the SP-C-rtTA transgenic mouse," *Developmental Biology*, vol. 325, no. 1, pp. 171–178, 2009.

[37] K. Qian, C. T. Huang, H. Chen et al., "A simple and efficient system for regulating Gene expression in human pluripotent stem cells and derivatives," *Stem Cells*, vol. 32, no. 5, pp. 1230–1238, 2014.

[38] H. Hosoda, T. Miyao, S. Uchida, S. Sakai, and S. Kida, "Development of a tightly-regulated tetracycline- dependent transcriptional activator and repressor co-expression system for the strong induction of transgene expression," *Cytotechnology*, vol. 63, no. 3, pp. 211–216, 2011.